Design and Development of LVDC Cables

Meenakshi Sundaram Ramakrishnan

November 2021

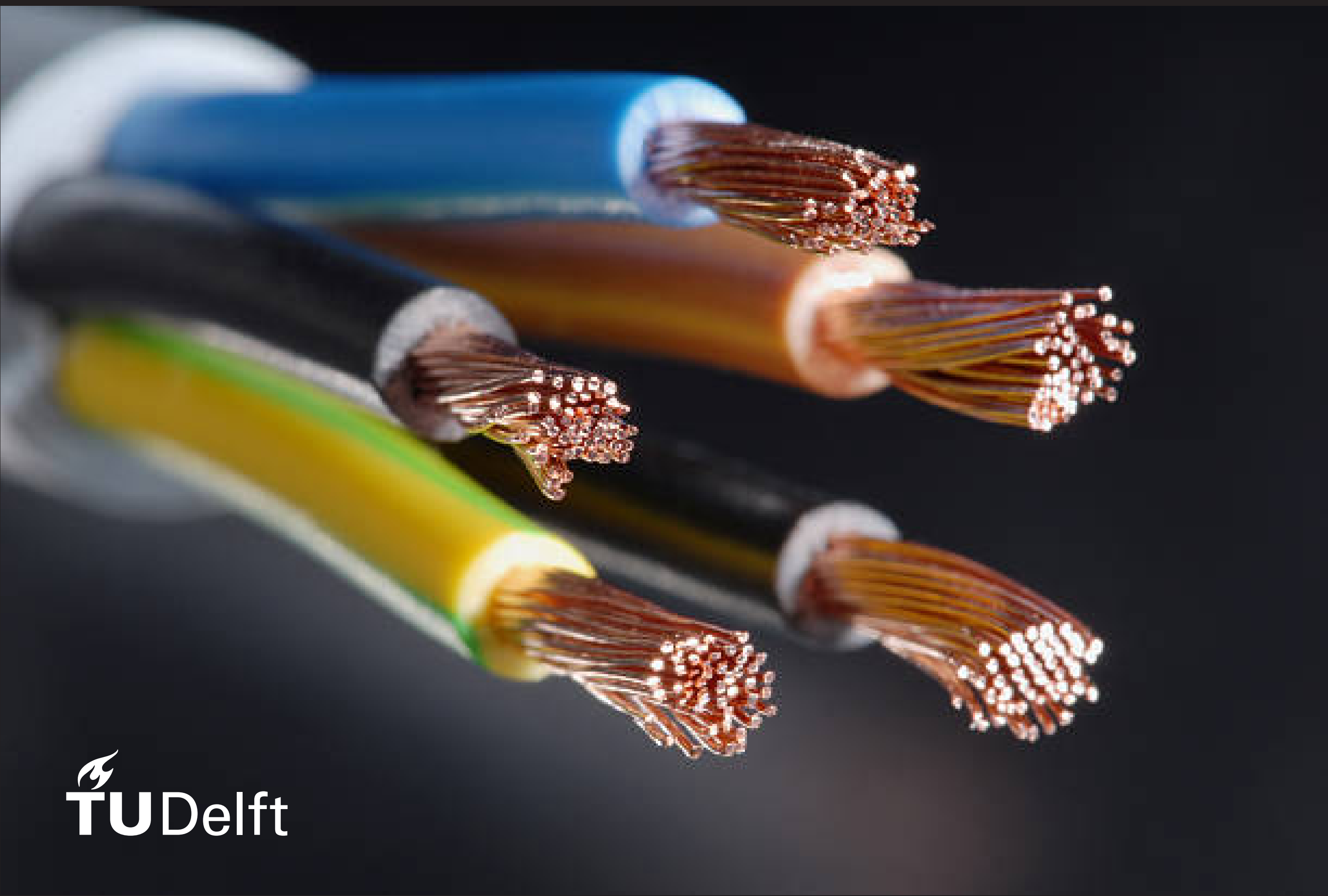

TU Delft

Design and Development of LVDC Cables

by

Meenakshi Sundaram Ramakrishnan

to obtain the degree of Master of Science
at the Delft University of Technology,
to be defended publicly on Tuesday November 30, 2021 at 10:00 AM.

Student number:	5123577	
Project duration:	December 14, 2020 – November 30, 2021	
Thesis committee:	Prof. Dr. Pavol Bauer,	TU Delft,supervisor
	Dr. Ir. Zian Quin,	TU Delft,supervisor
	Dr. Arno Smets,	TU Delft
	Ir. Sachin Yadav,	TU Delft,Daily supervisor

An electronic version of this thesis is available at http://repository.tudelft.nl/.

TU Delft

Abstract

The current energy systems with the mix of renewable and conventional sources are already working on their maximum capacity in order to meet the existing demand. In the near future to meet the burgeoning demand, the future electrical power system would be a mix of both AC and DC systems coexisting with each other. With the fast paced development of smart grids, decentralised system and micro grids, there is an increasing interest in the LVDC (Low Voltage Direct Current) distribution. Also there is increase in the loads in the residential and commercial sector side that require DC supply inherently. To tap in and realise the potential of the LVDC distribution systems, it requires the appropriate infrastructures to be developed that supports its assimilation faster. This thesis "The Design and development of LVDC cable" is a step forward in realising the potential that DC has in the LV distribution side. This research is done in collaboration between TU Delft and the Prysmian Group.

To begin with, two LVDC statespace based dynamic distribution system model namely: a neighbourhood distribution system and a ship distribution system are formed. The LVDC cables are incorporated as lines into these models. The sensitivity and stability analyses are performed by varying each of the active parameters individually, the influence that each of the active parameter has on node voltages, line currents and the stability of the system are studied and the trend is absorbed through this analysis. This analysis is set to be performed in both distribution systems under monopolar and bipolar configuration.

Subsequently, the short circuit analysis i.e the pole to pole and pole to neutral fault analysis is performed on both the neighbourhood and ship distribution system. Here the cable's active parameters that are expected to have an influence on the system performance and the line current during short circuit are taken into consideration. These active parameters are varied throughout this analysis and the resulting plots are further analysed to study their influence. These active parameters are cable resistance, cable inductance, cable capacitance, and cable length. The observations are tabulated for each of the active parameters individually. The generated results from this study would support in better assessment of cable's active parameters influence on the short circuit current and designing the LVDC cables.

The accuracy of the dynamic model are validated by breaking the distribution system model into smaller sections and forthcoming results are compared to get the model accuracy. Finally based on the results from the sensitivity stability and short circuit analyses the optimal characteristics of the LVDC cables is formulated.

Acknowledgement

This thesis was conducted in collaboration with the DC Systems, Energy Conversion & Storage (DCE&S) Research group(TU Delft) and the Prysmian group (Netherlands). Working on this project was an insightful experience for me. Through this opportunity I got a chance to improve on my research and presentation skillsets. Firstly, I would like to thank my thesis supervisors: Prof. Pavol Bauer, Prof. Prof. Zian Qin and Prof. Nils van der Blij for their guidance and constructive feedbacks during the course of this thesis. It really helped me to shape my thesis research and results better.

I would also like to thank Prof. Arno Smets for accepting to be part of my thesis committee and evaluating my thesis.

I am extremely grateful to my daily supervisor: Ir. Sachin Yadav for being always available to help me out with my silly doubts. The imperative discussions, valuable inputs and the feedbacks that he had given throughout this thesis helped me to fine tune my results and process better. I got to learn a lot from you and improve my technical skillsets.

I would like to also thank my supervision team from Prysmian : Alex Tsekmes, Luca De Rai, and Richard Van Delden for their guidance and constant inputs that they had given me during the bi- weekly meetings helped me progress better. The prompt feedback and support during the course of this thesis were extremely vital for my progress.

Special thanks to Prof. Mohamad Ghaffarian Niasar for helping me out whenever I had doubts and for the guidance he had provided throughout this thesis.

Finally I would like to thanks my parents, elder brother, whole family and my friends. They have been extremely supportive and motivating to me especially during covid times. Also thanks for taking care of me throughout my stay in the Netherlands even though we are miles apart.

Meenakshi Sundaram Ramakrishnan
Delft, November 2021

Contents

List of Figures

List of Tables

Nomenclature

Symbols

Δ_v	Voltage Drop
Γ	Incidence Matrix
C_{mat}	Capacitance Matrix
D	Identity Matrix
E	Null matrix
G_{mat}	Conductance Matrix
I_l	Line Current
I_n	Current flowing through node
L_{mat}	Inductance Matrix
P_{trans}	Maximum transmissible power
R_{mat}	Resistance matrix
rpm	revolutions per minute
u	Input matrix
U_n	Node voltage
V_{pn}	Pole to neutral voltage
V_{pp}	pole to pole voltage
x	State vector matrix

Abbreviations

AC	Alternating Current
DC	Direct Current
$HVAC$	High Voltage Alternating Current
$HVDC$	High Voltage Direct Current
LE	Lumped Element
LV	Low Voltage
$LVAC$	Low Voltage Alternating Current
$LVDC$	Low Voltage Direct Current
OC	Open Circuit
PEC	Power Electronic Converter
PN	Pole to Neutral
PP	Pole to Pole
SC	Short Circuit
TL	Transmission Line

1 Introduction

The electricity demand is rising at a rapid pace with the expected global electricity demand for the year 2050 is set to be increased by 57% with respect to the 2017 demand [1]. The rise in global electricity demand from 2017 till 2050 is expected to be more than 2% annually [1] . The current energy system with the mix of renewables and conventional sources are already working on their maximum capacity to meet the existing demand [2]. So, there is an increasing need to quickly increase the generation capacity at a gradual pace along with the demand in order to avoid overloading of existing energy network. As the conventional sources are likely to be depleted and also due to its polluting nature, it can't be used to meet the increase in demand. Then the non-conventional (renewable) sources will be in forefront to balance this increase in demand and could also support in meeting the emission targets set in the Paris agreement. The distributed renewable sources like solar and wind are predominantly used Renewable Energy Technologies (RET). If the power transmission from these Renewable Energy Sources (RES) are done in DC condition through DC grids then there is decrease in losses (Lack of skin and proximity effect)[3], so increase in power delivered to the receiving end in comparison to AC conditions. [4] [5].Also DC requires less number of conductors,less voltage drop for long distance transmission and many more advantages that will be explained in the upcoming chapters.

The solar arrays inherently produce DC power, so it requires only a DC- DC converter in order to connect it to the DC grid. The wind farms, microturbines and tidal sources are integrated to the AC grid through a AC/DC/AC conversion system [6], but now connecting to a DC grid would require a AC/DC converter. In the near future there is high probability of both the transmission and distribution grids to transition from AC to DC[7]. Already for long range transmission, HVDC grids are preferred, and there is a good chance to realise this change in distribution grids too [8]. In order to realize it in the LV(Low Voltage) distribution side the infrastructure and the load that supports this grid transition needs to be available. The significant infrastructure that is required is the formulation of LV Cables, specifically designed to operate in DC conditions will be vital in leading this grid transition.

There is an increasing interest in the LVDC (Low Voltage Direct Current) distribution with the growth of decentralised and microgrid systems supporting the tail end of the power networks. The LV Cables designed specifically for DC condition will play an important part in taking this transition forward and realising it. Currently LVAC (Low Voltage Alternating Current) cables are utilized in the DC conditions too, as the LV cables specifically designed for DC conditions is still in the formulation phase [9]. The LVAC cables operating in DC conditions, are not optimal as there is a string of advantages in utilising appropriate LVDC cables in low voltage DC conditions like better power transfer with less losses, longevity of the cable and less material wastage [9]. The LVAC cable operating at DC peak voltage experiences absolute losses leading to lesser transmissible power compared to LVDC cables and also heat generation within the cable causing faster ageing of the LVAC cable [9]. Continuous working at this DC peak voltage will lead to faster degradation of the insulation layer leading to shorter life span of the LVAC cable.

Now it is the right time to test the capabilities of the LVDC Distribution system with the formulation of appropriate LVDC cables. As nowadays in the residential and commercial sector many electrical loads in the distribution side inherently need DC supply. For example, loads like advanced lighting systems (CFL, LEDs), Multimedia appliances (TVs, Speakers), administrative appliances (laptops, PCs, scanners, printers) and communication appliances (Mobile phones, modems) are inherently DC loads [6]. The future generation might be dominated with RET which are inherently DC, to balance the energy network during shortage (due to intermittency of RET) batteries would be utilized that are inherently DC and the loads in the distribution side are also available in DC. So, it is not always appropriate to have AC systems as the best possible solutions in every level of the electrical grid system network mainly in the transmission and distribution network[10]. With the introduction of smart grids, decentralised system and micro grids, the future electrical power systems would be a mix of both AC and DC systems coexisting with each other. In order to realise the potential of the DC systems it needs the right infrastructures to be developed and put up in place. This research collaboration between TU Delft and the Prysmian Group on ”The Design and development of LVDC cable” is a step forward in realising the potential that DC has in the LV distribution side.In this thesis, through different analysis and simulations a comprehensive set of guidelines are formed to design the LVDC cables.

1.1. Research Objectives

The main objective of this research is to formulate the optimal characteristics for the LVDC cables by looking closely in to the results of different analysis and simulation conducted through this thesis. The aim of this thesis is achieved by working on the following research objectives step by step:

1. Choose an appropriate DC distribution system modelling method and then formulate the DC distribution system models for a neighbourhood and ship distribution system.
2. Find the influential parameters that could affect the performance of the LVDC Cable by simulating different scenarios in the models.
3. Study how the variation in active parameters affects distribution system’s stability and cable performance.
4. Carry out short circuit analysis to study the system stability and the limits of the cable.
5. Validate the accuracy of the distribution system model through which different analyses were carried out.

By following these steps, ultimately leads to forming a set of characterstics guidelines for designing an optimal LVDC cable based on the outcomes of the studies carried out. These guidelines would give more in detail description of the LVDC cable formulation.

1.2. Research Methodology

As for most of the LVDC application the LVAC cables are utilized and it seems to work fine. So there is not a lot of research that is available based on LVDC cable formulation and also there is no standardisation of cable design for the LVDC cable as of now [11]. The most of LVDC cable that are designed now are based upon the behaviour of the LVAC cables under DC conditions. In order to formulate the optimal characteristics for the LVDC cables, a comprehensive approach is set up. The intended approach utilized for the thesis is enumerated below:

1. In the literature review the intended approach for the thesis was identified by analysing and studying about the characteristics of low voltage distribution system and the low voltage cables. Also from the approaches available for modelling the LVDC distribution system, the state space approach is deemed to be suitable for designing the LVDC distribution and in reaching the objectives set.

2. Designing the dynamic models of LVDC distribution system for both neighbourhood and ship through the state space approach and simulation the behaviour of LVDC cables in them.

3. Simulating different scenarios in the models in order to detect the influential parameters that could affect the performance of the LVDC Cable.

4. Conducting the sensitivity and stability analysis on the distribution system models by varying the influential cable and system parameters and assess its influence on the stability and system performance.

5. Performing short circuit analysis on the distribution system models in order to analyse the limits of the cables. Also to get a better outlook of cable parameter's influence on the magnitude of the peak short circuit current formed.

6. Finally validate the accuracy of the model by breaking the distribution system model into smaller sections and simulating it and comparing the results obtained.

By following this approach it is intended to aid in reaching the main objective that is formulating the optimal characteristics for the LVDC cables based on the outcomes of the different analyses performed during the thesis. These results from the sensitivity, stability and short circuit analyses form the base for formulating the optimal characteristics of the LVDC cables. The set objectives of this thesis can be achieved by answering the following research questions:

1. How does the performance and the stability of the LVDC neighbourhood and ship distribution systems gets influenced when each of the active cable and system (system parameters which has influence on the cable parameters are varied individually?

2. How influential are each of the cable‘s active parameters on limiting the effect of the short circuit in the distribution systems modelled?

3. How should the optimal LVDC cable's active parameters look in order to provide the ideal performance expected by the users? Also comment on the accuracy of the dynamic models utilised for the simulation.

1.3. Thesis organisation

The thesis report is structured as follows. Firstly, Firstly in chapter 1 a brief introduction about this thesis with its approach and the limitation involved are described. Then in chapter 2, the back ground of LVDC distribution system, different system model configurations available, active parameters and challenges in formulation of LVDC cables are discussed. Followed by the description of dynamic modelling approaches for the LVDC distribution system is outlined in chapter 3. Chapter4 deals with explaining the LVDC distribution system and electronic power converter models that are involved in this thesis. Next in chapter 5, different analyses that are performed on the formulated LVDC distribution system models are explained. In chapter 6, the short circuit studies that were performed on the neighbourhood and ship distribution system models are described in depth. The results and the key findings from all the analysis performed in the model are discussed in chapter7. Finally, the 8 chapter deals with the concluding set of optimal characterstics to design the LVDC cables and the future scope of the thesis.

1.4. Limitations

The first limitation is that the dynamic distribution system model based on the state space approach is valid only when the wavelength of the system signals are larger than the length of the distribution lines in the system[12] [13]. This limitation needs to be satisfied in order to have a valid model design of any DC distribution system utilizing this approach explained in chapter 3. The wavelength of the system signal is calculated using equ (1.1), shown below [12]. Where c is the speed of light, f is the frequency of the signal, μ_r and ϵ_r are the relative permeability and relative permittivity of the distribution line.

$$\lambda = \frac{c}{f\sqrt{\epsilon_r \mu_r}} \tag{1.1}$$

The second limitation is that as the modelling approach taken is through a non transient model with a lumped element representation of the distribution line parameters. These models neglect and don't consider the frequency dependent effects and propagation delay present in the system [14] . The distribution line parameters such as resistance, inductance, conductance and capacitance are considered to be constant in the selected approach, but they are frequency dependent parameters which are not always constant. However several literature [12][15][16] states that the propagation delay can be neglected, if the length of the distribution lines in the system are smaller than the signal wavelength.

The third limitation is the accuracy of the model utilized to perform different analysis. As the models utilized are non transient based and they are neglecting the influence of frequency dependent effects on the distribution line parameters in the model[16]. In general the transient models have higher accuracy compared to the non transient models. But realizing the DC system through these transient models is difficult as they are far more complex and the simulation requires more computational power and time to compile the simulation. So that's the main reason for modelling the DC distribution system in the state space dynamic approach method, more explanation about the methodology used is explained in Chapter 3. The analysis of the model accuracy is also part of the research objectives, so the state space dynamic model's accuracy will be analysed deeply, more on this in chapter 5.

1.5. Summary

In this chapter a brief introduction about the thesis, the research objectives and the methodology used were described. Also the thesis outline with the limitations of the dynamic models utilized in this thesis was explained in this chapter.

2
Framework

The discussions in this chapter will give the background information on the LVDC distribution systems and LV cables. Section 2.1 deals with the structure of LV distribution system. Followed by section 2.2, which presents the detailed characteristic assessment of LVAC and LVDC cables. Then, in section 2.3, the design of LV cables is discussed. Section 2.4 deals with the active parameters of LV cables. Next in section 2.5, the challenges that are present in formulating LVDC cable is discussed. Finally in section 2.6, a complete summary of chapter2 is presented.

2.1. Low voltage distribution systems

The tail end of the power system network constitutes the low voltage distribution system that is responsible to deliver electricity to the consumers. In accordance to the IEC 's international standard the voltage rating of the low voltage distribution system is below 1500 V in DC conditions and under 1000V in AC conditions[17]. The low voltage distribution can be done in two ways: through DC or AC. Each of them has their own pros and cons that will be discussed in this chapter with primary focus given to LVDC distribution.

In order to learn and analyse the characteristics of the LVDC cables, first the distribution system in which the cables are situated must be known better. So the top down approach is taken and from the system level to element level progression will be made. In this section only the power transmission capabilities and the advantages of each of the LVDC distribution system configurations will be discussed. The modelling and the theory regarding it would be discussed in chapter 3. The power system layout consists of different structural levels, in regard to low voltage distribution the main focus is on the LV distribution power grid. The LV distribution grid contains lines from the MV/LV transformers and its connected to the household feeders[18]. The three-phase distribution system with a return path is the most preferred distribution layout in Europe [19]. The detailed explanation of different layout configurations that are present in distribution level will be discussed in upcoming sections.

In the distribution power grid, three configurations one associated with AC and the other two associated with DC are analysed. The Layout configurations of distribution power grid that were assessed are:

- Three phase AC system
- DC Monopolar System
- DC Bipolar system

The favourable layout configurations in the distribution power grid were analysed by calculating their respective transmissible power [20] [21] [22][23] [24]. Through the transmissible power calculation for each of the layout configurations allows us to view the maximum transmissible power delivered by each of the configuration listed above. For simplicity in the calculating the transmissible power delivered by different configuration, it is assumed that for the AC system line reactance, skin and proximity effect are neglected.

2.1.1. Distribution Grid configuration

In this section a brief description about the transmissible power calculation[23] [20] done for the different configuration of the LV distribution grid is explained. Three different distribution grid configuration layouts, one associated with AC and other two associated with DC are compared based on their transmissible power delivered (Ptrans). The DC monopolar configuration is not utilized in the current trend [18][19], but still its performance in comparison with other configurations is beneficial for further DC studies. For the AC based distribution power grid: AC three-phase with return conductor configuration is considered and for the DC based distribution power grid, DC bipolar and DC monopolar configurations are considered. The transmissible power is calculated for a total cable cross section of $500mm^2$ for all the system configuration and the length of the cable is varied along to find the power transfer capabilities for longer range[23] [20] .

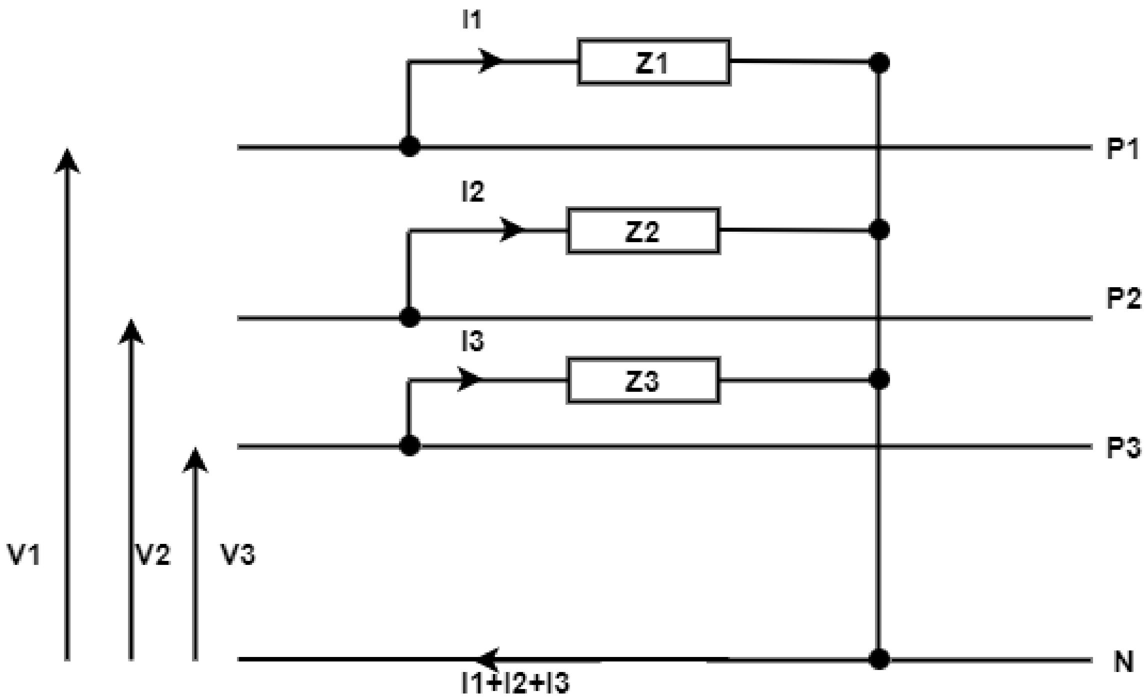

Figure 2.1: AC three phase with Return Conductor configuration

Firstly, AC three-phase with return conductor configuration is analysed, and the diagrammatic representation of this configuration is shown in Fig 2.1. This configuration is the most widely used in the European distribution grid [19]. The AC three phase with neutral conductor contain 4 conductors: each of the 3 phases has one conductor each and the neutral conductor takes one(configuration 1). The three phase system is considered to be a balanced three phase system, so no current flow through the neutral conductor. The maximum transmissible power calculation is done with respect to the voltage drop in the cable and the ampacity limit of the cable. The equations which will govern the maximum transmissible power of this AC system are shown in equ(2.1) and (2.2)[23]. The maximum transmissible power calculation with respect to the cable ampacity (Imax1)is shown in equ (2.1). Where Vp-n is the rms line to neutral voltage, Z is the line impedance present in the cable and cos ϕ is the power factor. The line impedance (Z) is a combination of resistance (R) and reactance (X) as said earlier the reactance of cable or line is neglected and the power factor is taken as 1[23]. The maximum transmissible power calculation with respect to the voltage drop limitation (ΔV) is shown in equ (2.3)[23]. The minimum value calculated by these two maximum transmissible power equations will take precedence and will dominate the system by being the maximal transmissible power as shown in equ (2.4)[23]. As there are four conductors (including the neutral) present, so for each of the cable the cross section is taken as $125mm^2$. The cable ampacity for this configuration is taken as 264 A[23].

$$P1_{Imax} = 3(V_{pn} - ZI_1)I_1 cos\phi \tag{2.1}$$

$$R(L) = \rho \frac{2L}{A} \tag{2.2}$$

$$P1_{\Delta V} = 3(V_{pn} - \Delta V)\frac{\Delta V}{R} cos\phi \tag{2.3}$$

$$P_{trans,1} = min(P1_{Imax}, P1_{\Delta V}) \tag{2.4}$$

Secondly, the Monopolar DC configuration is analysed, and the diagrammatic representation of this configuration is shown in Fig 2.2. This configuration has only a positive pole and a return conductor present in it and that makes it less efficient in comparison to the three phase AC and Bipolar DC configurations. But still its costs the least among the grid configurations compared in this analysis as only one conductor and a return are present. The maximal transmissible power is calculated based on the voltage drop in the cable and the ampacity limit of the cable as shown in equ (2.5)and (2.6)[23]. In equ (2.5), the maximum transmissible power is calculated based on the cable ampacity limit where $\hat{V}_{pn}$ is the peak pole-neutral voltage, R_2 is the per conductor resistance of the cable in the unipolar configuration and I_2 is the cable ampacity limit for this configuration and it is calculated to be 392 A[23]. The resistance is calculated similarly using equ(2.2) and the cross section for this two conductor system (including the return) is taken as $250mm^2$ for each of the cable. The maximum transmissible power calculation with respect to the voltage drop limitation ($\Delta\hat{V}$) is calculated using equ(2.6)[23].

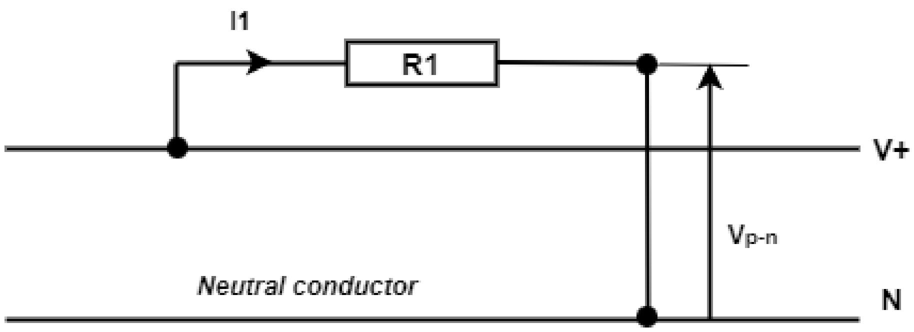

Figure 2.2: DC Monopolar configuration

$$P2_{Imax} = (\hat{V}_{pn} - 2R_2I_2)I_2 \tag{2.5}$$

$$P2_{\Delta\hat{V}} = (\hat{V}_{pn} - \Delta\hat{V})\frac{\Delta\hat{V}}{2R_2} \tag{2.6}$$

Lastly the Bipolar DC configuration is analysed, and the diagrammatic representation of this configuration is shown in Fig2.3. As seen in figure this configuration has positive, negative and a neutral conductor. In the DC bipolar system, the cable insulation must be designed for twice the pole to neutral voltage[23]. In this configuration the load can be connected to the system based on their load requirements as the pole to neutral connection provides $\hat{V}_{pn}$ and the pole to pole connection provides 2 $\hat{V}_{pn}$. The bipolar DC configuration is the most efficient configuration in comparison with the other two configurations. In equ(2.7), the maximum transmissible power is calculated based on the cable ampacity limit[23] where R_3 is the per conductor resistance of the cable in the Bipolar configuration and I_3 is the cable ampacity limit for this configuration and it is calculated to be 314 A. The resistance is calculated similarly using equ(2.2) and the cross section for this three conductor system is taken as $167mm^2$

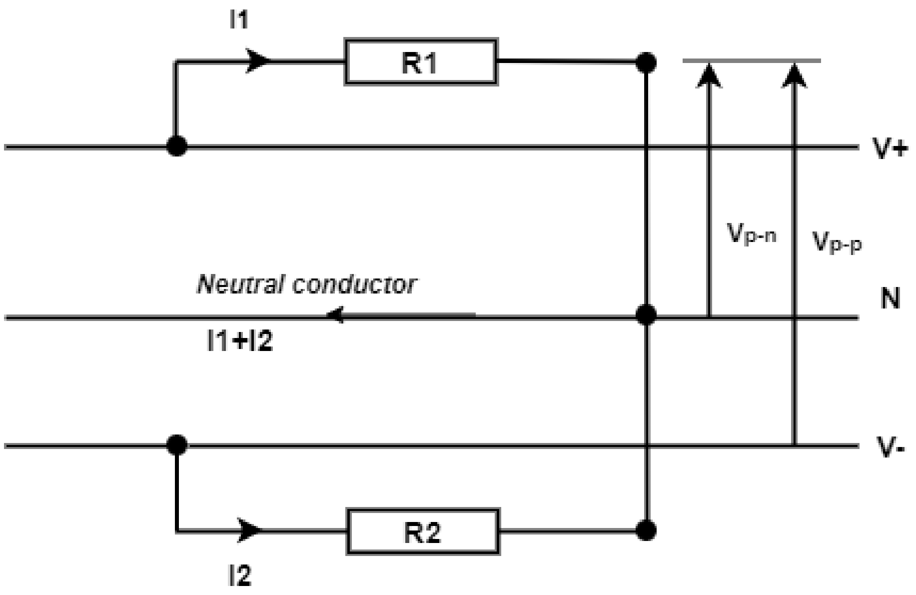

Figure 2.3: DC Bipolar configuration

for each of the cable. The maximum transmissible power calculation with respect to the voltage drop limitation ($\Delta\hat{V}$) is calculated using equ(2.8) [23].

$$P3_{Imax} = 2(\hat{V}_{pn} - R_3 I_3) I_3 \tag{2.7}$$

$$P3_{\Delta\hat{V}} = 2(\hat{V}_{pn} - \Delta\hat{V}) \frac{\Delta\hat{V}}{R_3} \tag{2.8}$$

2.1.2. Transmissible Power Comparison

The transmissible power for all the three different distribution power grid configurations is compared with the load distance and it is plotted in the graph shown in Fig2.4. The three phase AC configuration's power factor is maintained at 1 for the best case and for the worst case it is taken as 0.8. From the graph it is visible that the voltage drop in the bipolar DC configuration is clearly lower than that of AC three-phase configuration [18][21][23]. Even after neglecting the line reactance, skin and proximity effect in the AC systems, transmissible power is reduced as the load distance increases is mainly because the rms current limits the power transfer capabilities for the AC configurations [18] [19][20][23]. Based on the graph shown in Fig2.4, the bipolar DC configuration achieves the maximum transmissible power followed by three phase AC and then the unipolar DC configurations. When DC distribution takes upper hand in the distribution grid then bipolar configuration could be looked upon as a replacement to the three phase AC configuration which is currently used in the existing AC distribution grids [19][21][9]. So with all the advantages that DC distribution has over AC in terms of greater transmissible power, lower voltage drop, lower losses and greater efficiency if the reliable supporting infrastructure is introduced, then at an instant LV DC distribution can over take AC [22][24][9][14][25].

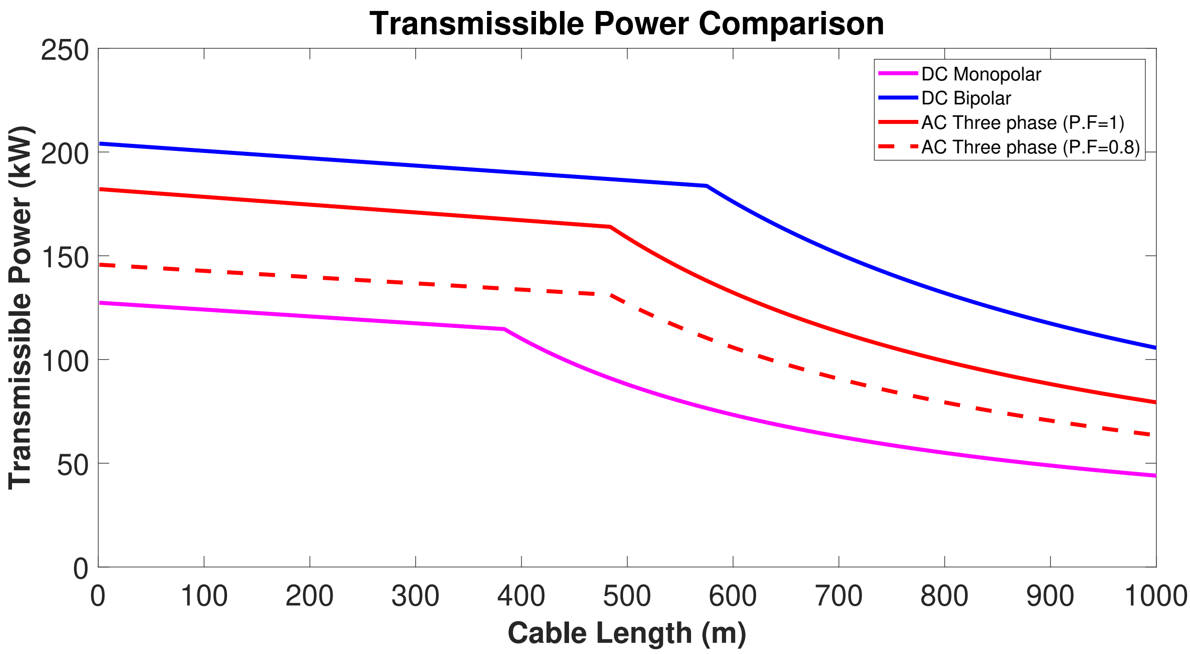

Figure 2.4: Transmissible power at different cable length for different distribution power grid configurations

2.2. Characteristics of LV cables

The characteristics of LV cables utilized in the LV system is analysed both under LVAC and LVDC conditions. This is mainly done to understand the cable behaviour better, so that more efficient LV cables could be modelled based on the existing ones. As the LVDC cables are still in their formulation phase it is necessary to get more info on the behaviour of these cable under DC conditions. In this chapter, sec2.2.1 deals with the characteristics of LV cables under AC conditions. Followed by describing the characteristics of LV cable under DC condition in sec2.2.2.

2.2.1. LVAC Cables

The existing AC LV distribution network utilizes LVAC cables for the distribution purpose. The LV cables that are currently formulated are predominantly for AC condition. As the distribution side both in the household and distribution power grid side are dominated by AC. Majorly in Europe, the underground cables are mostly used in LV distribution network and they usually contains 3 or 4 cores in their cables. These cables have an insulation layer and the commonly used materials for this purpose are XLPE (Cross-linked polyethylene), EPR (Ethylene Propylene Rubber), and PVC (Polyvinyl chloride)[22][9][26][27]. More details about the insulation material's properties are discussed in the upcoming sections. A LVAC cable requires three conductors to carry power as they operate in three phase system. The three-core XLPE cable are widely used in the LVAC distribution network [23][28][29] and a pictorial representation of it is shown in Fig2.5. Under AC conditions the cable used will deliver less power to the receiving end user due to the cable reactance, skin and proximity effects. The skin and proximity effects are absent under LVDC conditions[18][19][14][30] So the transmissible power for the LV cable under LVDC is higher compared to LVAC conditions.

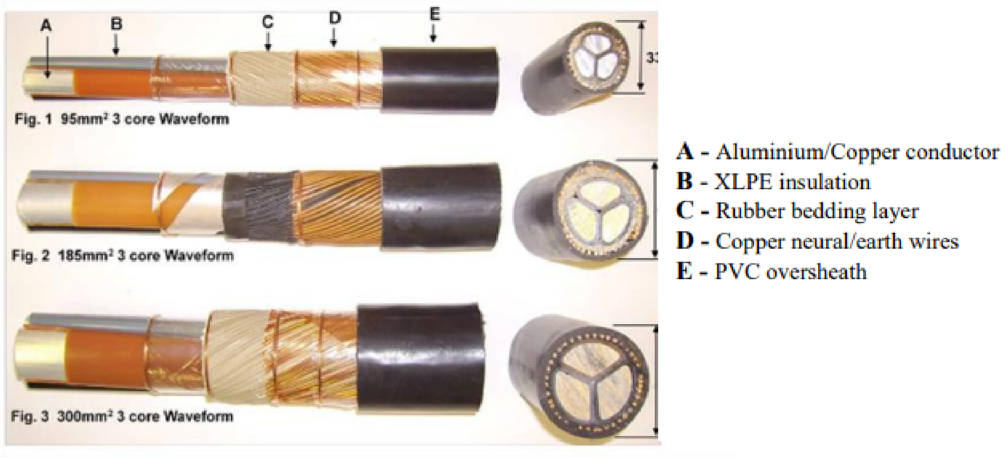

Figure 2.5: Three core XLPE cable [31]

Secondly, ageing and the lifetime of the cables under AC conditions are affected due to the thermal breakdown and electrical treeing [25][32][33][32]. The thermal breakdown occurs when excessive currents more than rated flow through the cable due to voltage transients or harmonics present in the AC system and also it could be due to environmental factors (Elevated temperatures and Flooding)[32]. These conditions for the AC cables will reduce the lifetime of the cable by more than half and these shortcomings needs to be considered during the design phase in order to be rectified. Also the electrical treeing occurs due to the manufacturing defects such as voids and the contaminants present in the cable. These cable defects present in the AC system causes high electrical stress that would eventually lead to insulation layer erosion and decrease in dielectric strength[31][34].

Finally, the effects of temperature on the LV cables under AC condition is explained. It was seen that on three phase 230 V system, the temperature difference across the cable was raised insteps of 5 °C[33] [32] [9]. The electric field was seen to be rising in near the sheaths of the cable uniformly and it doesn't cause any adverse effect on the system performance due to the polarity reversal that takes place in AC. But the result in the LVDC condition was seen to be different and affecting the cable.

2.2.2. LVDC Cables

The LVDC cable are not a common occurrence in the distribution network as it is dominated by the AC distribution. The DC cables are usually utilized for longer range high voltage transmission but due to the advantages seen in LV DC distribution, slowly the distribution side is transitioning towards LVDC distribution. As said before, the LVDC cables are not available everywhere, it is necessary to understand and improve the working of LVDC cable by analysing the behaviour of LVAC cables. The HVDC cable design is not taken into consideration for the design of LVDC cable since they both operate at different voltage levels and the breakdown mechanism for the cable is completely different[28]. So, the LVAC cables working well in LVDC and LVAC conditions are looked upon for the LVDC cable design.

In DC condition, the power losses in the conductor due to the presence of skin and proximity effect doesn't occur. The main reason for skin effect occurrence is due to the presence of back emf. The rate of change of flux is zero in DC thus back emf is zero. So the current is uniformly distributed across the conductor leading to no skin effect in DC. The LV cable utilized in LVDC condition seems to have increased power transfer capabilities compared to LVAC, up to 2 times and in some cases 3.5 times higher power transfer than the LVAC condition [22][4] [5]. This mainly is due to absence of skin, proximity effect and the dielectric losses leading to lower losses in the system. The space charge accumulation is a big problem in HVDC condition as it would increase the losses, but in low DC field the space charge accumulation in solid insulation need not be considered, as it is assumed to be insignificant. The electric field distribution under cable insulation in DC voltage is dependent on the electrical conductivity of the material[25].

Secondly, ageing and the lifetime of the cables under DC conditions are affected due to the thermal breakdown and sheath corrosion [25][34][33][32]. The electrical treeing is not a major factor affecting the lifetime of the LVDC cable in comparison to AC. The thermal breakdown occurs when the cable are working under elevated temperatures, the DC conductivity increases and that increases the current through the insulation, leading to heat generation[32]. This leads to reduction in the cable lifetime significantly; this could be avoided by properly analysing and improving the thermal design of the cable. Similar to the AC, the chemical treeing has become a major contributor in causing cable breakdown in LVDC too. The chemicals and contaminants in the soil directly cause corrosion in the sheath layer and this ultimately leads to insulation breakdown as the days progress. Then the cable failure occurs, so it is important to have the anti-corrosion coating over the insulation layers utilized in order to be protected against certain corrosive chemicals[31][34].

Finally, the effect of temperature on the LV cables under DC condition is looked into. In the DC Bipolar system of 325 V, the temperature difference across the cable was raised insteps of 5 °C[33][32][9]. The electric field was seen to be constantly rising near the sheaths to higher levels non-uniformly leading to insulation failure and cable breakdown[35]. This is mainly due to DC conductivity being increased at elevated temperature, in order to solve this better thermal design of the cable needs to be done.

2.3. Design of LV cables

In this section, different structural layers that forms the low voltage cable are explained and it is pictorially represented in Fig 2.6. The structural importance of each of the cable layer with their material consideration that will support in LV conditions are described briefly.

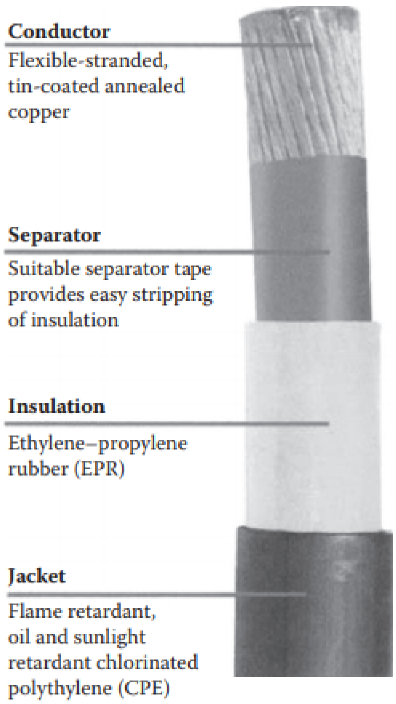

Figure 2.6: Structural diagram of a LV Cable [34]

Table 2.1: Resistivity of prominent metal conductors [31]

Metal	Ohm-mm2 /m × 10−8	Ohm-cmil/ft × 10−6
Silver	1.629	9.80
Copper, annealed	1.724	10.371
Copper, hard drawn	1.777	10.69
Copper, tinned	1.741–1.814	10.47–10.91
Aluminium, soft, 61.2% cond	2.803	16.82
Aluminium, 1/2 hard to full hard	2.828	16.946
Sodium	4.3	25.87
Nickel	7.8	46.9

2.3.1. Conductor

The conductor layer is one of the most important layers inside a cable. The purpose of having the conductor is to provide a conducting path for the current to pass through. For a LVDC system at low voltage (75 to 1500V) the conductors are not subjected to high electric stress. The most preferred conductor materials for the LVDC cable are Aluminium and Copper. For different situation different conductor material could be chosen. There are several low resistivity materials (High conductivity) available that could be used as the conductor. The values of resistivity of conductor metal is tabulated in table 2.1. But comparing the resistivity values and the cost of the material then copper and Aluminium is the most obvious choices. They are the most dominant metal used in the power cable industry[36][34].

Not only the value of resistivity is important but the physical and chemical properties of the selected conductor material should be also within the favourable limits. Based on the resistivity, Silver has good levels of resistivity, but its high cost and weak physical strengths are the main reasons for neglecting it. The comparison of physical and mechanical properties of Copper and Aluminium is shown in table 2.2. The factors that influence the conductor selection between Copper and Aluminium is enumerated below[37]

- Aluminium metal has been relatively less expensive compared to copper.
- For equivalent ampacity condition, the Aluminium has lower mass compared to copper that makes it easier to handle large cable sizes.
- For terminations the Aluminium conductor requires special treatment and Copper doesn't require a special termination treatment.
- For equivalent ampacity condition, copper conductor is smaller and can be easily installed in smaller raceways and it is flexible in nature as well.

Table 2.2: Comparison of physical and mechanical properties of Copper and Aluminium [31]

Property	***Unit***	***Copper, Annealed***	***Alum, Hard Drawn***
Density at 20°C	Pounds/in3	0.3211	0.0975
Density at 20°C	Grams/cm3	8.890	2.705
Linear Temp. Coef.	per °F	9.4 × 10−6	12.8 × 10−6
of Expansion	per °C	17.0 × 10−6	23.0 × 10−6
Melting Point	°F	1981	1205–1215
Melting Point	°C	1083	652–657

2.3.2. Insulation layer

The second most influential layer in the LV cable is the Insulation layer. Insulation is used to protect the conductor from local environment by isolating it from other objects and also at the same time ensure that the current flow path remains constant. The insulation layer is expected to fulfil its functions for both dry and wet conditions. The key properties that characterize good insulating polymer at stress condition are: Dielectric Constant (k), volume resistivity (VR) , Polarisation and dissipation factor(DF). VR can be defined as the electrical resistance between opposite faces of a cube of interest, when measured at a set temperature and pressure. DF is a measure of lost energy as heat instead of being transmitted as electrical energy. It can also be denoted as the power factor (P.F). K is the measure of how well the insulation holds a charge. For a good insulation material, the value of K and DF must be low [34].

For the LVDC cable the suitable insulation materials are XLPE (Cross-linked polyethylene), EPR (Ethylene Propylene Rubber), and PVC (Polyvinyl chloride)[9]. The material properties of each of this material is tabulated in table 2.3. From the table it is clearly seen that the XLPE insulation material has better insulation properties compared to the EPR and PVC. The XLPE material also has higher voltage break down strength and the most resistant to chemicals[27]. This insulation is perfectly suitable for LVDC underground cable as it can resist chemical corrosion and increase the longevity of the cable. Few of the insulation material are used as the insulation in the cable for specific purpose and environment condition.

Table 2.3: Material properties of suitable insulation material [38]

Condition	***EPR***	***XLPE***	***PE***	***PVC***
Max Continuous Operating Temperature °C	90	90	75	60
Emergency and Overload °C	130	130	95	100
Short Circuit (Max 5 seconds) °C	250	250	150	150
Volume Resistivity (ohm-cm)	>10^15	>10^16	>10^16	>10^12
Dielectric Constant	3.5	2.3	2.3	4
Power Factor	1.5	<0.2	<0.2	>4
Tensile Strength (kgf/mm2)	min 0.5	min 1.27	min 1	min 1
Elongation (%)	min 300	min 350	min 350	min 150

The EPR insulations are utilized by the cable which are set to be installed in rough and flame prone areas. As EPR insulation has good level of toughness and flame resistant it is more suitable to that environment than XLPE. But in normal condition it is not preferred over XLPE because of its thermal conductivity and ampacity is lower than XLPE. The PVC insulation ‘s main advantage over the other two insulation material is that it’s the cheapest among the three. So for lower cost projects the PVC insulated cables are widely used. Also it is used as jacketing layer for many LVDC cables, improving the strength of the cable. For inner power station wiring, the PVC insulated cables are avoided because when fire accidents take place the smoke generated during the burning of the cable causes severe respiratory problem. The residue from the burnt cable is a corrosive mixture which cause extensive damage to the whole system. So, based on the environmental condition the cable insulation is selected. For normal conditions and high investment projects the XLPE insulation is usually preferred[33]. It is also more important to check the compatibility between the insulation layer used and the conductor material. If the insulation layer is not compatible, then it might cause extensive corrosion towards the conductor layer and ultimately led to cable failure. So, it is important to check the conductor compatibility before installing them [27] [29].

2.3.3. Sheath layer

The third level of influential layer in a LV cable is the sheath and the Jacket layer. They represent the same portion of the cable, but they are named different based on the metallic or non-metallic component over the insulation layer of the cable. The non-metallic coverings are called jacket and the metallic coverings are called sheaths. They are mainly utilized in LV cable to overcome the effect of electro statics, electromagnetic fields, it also acts as mechanical protective layer and moisture barrier [39] [34].

The sheath layer wraps around the outside of the cable, it's primary functionalities are to protect the conductor of the cable and to isolate vital areas of the cable from external environment [40]. The metals like Aluminium, Bronze, Copper, Lead is usually used as sheath in LV and MV cables [31]. In general, for LV cables most predominantly Lead and Aluminium metals are used as sheath layers [34]. The constrains for assessing the precedence of metal used as sheath layer is categorized by their cost, ampacity requirements of the system during fault and the compatibility with other materials [32] [31].

Lead metal has been constantly used as the sheath material for the cables. With favourable material properties having low melting point, softness and it can also be easily extruded over the cable allowing it to protect the cable from moisture and harsh chemicals. The metal also doesn't get corroded that easily even though the mechanical strength of the material is poor. These material properties allow lead to even act as metallic screen to divert short circuit if its required. The one disadvantage of using lead sheath is that it can get easily damaged due to mishandling of the cable. When the cable is mis handled by bending and unbending this leads to causing fatigue of the lead sheaths and ultimately the sheath layer fails. With the introduction of XLPE as insulation material and it being quickly integrated into being major part of the LV cable design has caused the omission of lead as sheath material. This mainly due to its incompatibility with XLPE and its carcinogenic nature [34].

Nowadays, Aluminium sheath are being widely utilized in cables as it has better mechanical strength and electrical properties compared to the other preferred range of metals [34] [41]. The DC resistance of aluminium being low allows it to even act shielding material for the cable. Also as the cable is already mechanically strong, it doesn't require any added mechanical protection in the form of armour. The only disadvantage that the aluminium sheath layer has, is that it easily gets corroded. So in order to avoid corrosion, it needs an addition of an anti-corrosive layer such as bitumen followed by thermo plastic covering. This combination is being widely used in LV cables [39].

2.3.4. Jacket layer

Jackets are the non-metallic coverings found on the outer layer of the cables. The functionality of the jacket layer is to serve as electrical and mechanical protection to the cable materials. Based on the type of jacket material included in the structure of the cable, it increases physical toughness, chemical and flame resistance of the cable. There are two different categories of jacket material available one is thermo plastic and the other is thermo setting jacket material. The thermo setting jacket material is not used in the underground distribution cables and they are widely used in the industrial and power plant application. As the LV cables are usually underground cables [11], so the thermo setting jacket materials are not focussed in this section.The summary of material properties of different jacket material is tabulated in table2.4.

The thermo plastic jacket materials that is widely used as jacket material in the cables are Polyvinyl chloride, Polyethylene, and Chlorinated Polyethylene[34] [31].The PVC is the most widely used jacketing material, this was mainly due to its low cost. The other favourable properties of PVC are its easy processability and an excellent combination of fire and chemical resistance. In the LV cables PVC are utilized as a single layer of material that functions as both insulation and a jacket material. But based on material properties of PVC it is know that PVC cannot withstand high temperature[35]. So during fault current situations PVC insulations could be permanently damaged by melting or it could emit plasticizers and become brittle and stiff within a period of time. Due to this, PVC jackets were avoided in high temperature conditions[26]. Also, under DC conditions in wet environment, the PVC cable (PVC jacket and insulation) have frequently known to fail in these conditions due to moisture ingress [34] [26]. Based on these responses, PVC is not preferred for underground power cables.

Table 2.4: Comparison of material properties of jacket materials

Property	PVC	PE	CPE
Heat resistance	Excellent	Good	Excellent
Sun resistance	Good	Good	Excellent
Flame resistance	Excellent	Poor	Excellent
Water resistance	Fair	Excellent	Good
Low temperature	Poor	Good	Fair

Polyethylene has been used as jacket material for the underground cable mainly due to moisture resistance characteristics. Polyethylene are usually compounded with carbon black that enables polyethylene to be used a s jacket material and the carbon black addition also provides the polyethylene with sunlight protection. For instances where moisture resistance is a requirement in the cable design[39], then polyethylene is the perfectly suitable for it as it has the best moisture resistance capabilities compared to other non-metallic jacket materials and good ageing properties when operated within its temperature limits [35]. They are extremely difficult to bend at low temperature due to their stiffness. The one major disadvantage of using polyethylene as jacket material is that it has poor flame resistance properties. High Density Polyethylene (HDPE) is extensively utilized as jacket material in low voltage cables that are used in rough environment as it increases the toughness of the cables [42].

Chlorinated polyethylene (CPE) is considered usually as a thermo plastic material, although thermoset version of it is also available. Thermo plastic CPE has excellent heat, water and flame resistance properties compared to the other jacket materials[43]. This allowed the thermo plastic version have a better reach and it is more commonly used as jacket material in the LV cable industry due to its favourable properties [44].

2.4. Active parameters of the LV cables

In this section the active parameters of the LV cable, that could affect the system and cable performance are described. These active parameters are chosen based on the previously available literatures studies. These active parameters give us an idea about the things to take consideration of while formulating the LVDC cable design. Each of them has a trend in affecting or improving the system performance when increased or decreased. This trend that's mentioned in the literature is described in this section.

First, the active parameters of the cable that could have an influence in the system performance and stability is discussed. The cable parameters that are described to have an influence on the system performance and stability are inductance, capacitance, cross section (resistance) and the length of the cable. The cable or line inductance value when it is increased this leads to the eigenvalue calculated to analyse the stability of the system to decrease. This decrease in the eigenvalue would lead to the roots lie closer to the real axis and this would mean the stability margin of this distribution system is decreasing. So it can be concluded that the increase in inductance would lead to decrease in the stability of the system with the magnitude of the eigenvalue decreasing[45][46]. Then with the decrease in the cable cross section value, it leads to increase in the cable resistance and the eigenvalue. The increase in cable resistance is said to have a positive effect in the stability of the system. This increase in the resistance leads to slight decrease in the voltage and increase in the current delivered by the cables. The decrease in cable cross section would increase the resistance that will lead to better stability due to improved damping and performance from the system[47].

When the cable capacitance is increased, it said to be increasing the magnitude of the eigenvalue. With the increase in the magnitude, the roots of the system tend to lie on the imaginary axis further away from the real axis and this leads to improved stability of the system with less oscillations. So the increase in capacitance leads to better system stability. But during the analysis, the results seems to contradict this inference. Then finally with the increase in the cable length is said to increase all the admittances and impedances value associated with the cable. So this is said to be affecting the stability of the system as the length increase [48][46]. The roots of the eigen values of the system tends to be positioned closer to the real axis as the cable length increases.

These active parameters of the LVDC cable mentioned above are said to be having an influence in the stability and performance of the cable. These cable parameters will be closely looked upon and more concrete inferences would be collected by conducting different analysis during the thesis. Also not only the cable parameters many system parameters are said to be influencing the performance and stability of the LVDC distribution system. These system parameter would be also mentioned, with the influence it has on the system performance and stability in the upcoming chapters.

2.5. Challenges

There are challenges in formulating a LVDC cable based on its simulation behaviour under a LVDC distribution system. A detailed description of few of these challenges that were found based on the literature review are enlisted in this section.

Firstly, the cable fault detection under a DC system is a bit more difficult than the AC system as there is no natural zero crossing and the system operate within the normal current and voltage level making it hard to distinguish a fault from normal operation[49]. The power electronic device present in a LVDC system are influencing the current behaviour in the system and this makes it hard in interrupting the DC fault currents[30]. When a fault occurs in the cable, the network which experiences it gets disconnected from the system, this affected network could be reconnected and time taken for that majorly depends on the speed in locating the fault in order to clear it[50]. But a longer wait to detect and clear the fault mainly due to recurring disturbances could lead to a possible blackout. The intermittent fault in LV cables are even more difficult to locate, with numerous joints and connections these faults are more prone to occur in LV systems[51]. Also, the DC fault currents have high di/dt that makes detecting the fault location and isolating it more difficult.

The second challenge is the lack of standardisation in LVDC Systems. There are no universal voltage standards as different voltage levels are utilized for different LVDC application [52]. Due to this the LVDC cables are also not formulated in a standardised way that could be utilized for all kinds of LVDC application, they are being designed conceptually for very specific applications.But, in the Netherlands there are standards for bipolar system with the system voltage level need to be 350 or 700V. Now most researchers are converging towards 350-380 V to be the standardised voltage levels for LVDC application[53][54]. This voltage level was chosen because it matches the voltage levels of consumer electronics used in household appliances[55][56]. But still, these voltage levels are not officially approved by any research or government organisation, so it would be need to be done quickly to standardise the LVDC side of the network. This delay in standardisation is mainly due to the lack of small DC grids being present in distribution side and this shortage of DC grids is mainly caused due to lack of DC devices present in the consumer side[53][24]. So as each of them are being interdependent on each other, both the DC grid and DC devices expansion is not taking shape in the consumer side.

The last challenge is the research based on LVDC cables. As the availability of LV cables to work specially under DC Condition is limited in the cable industry. For most of the LVDC application the LVAC cables are utilized. There is not a lot of research that is available based on LVDC cable formulation and there is no standardisation of cable design for the LVDC cable as of now[57]. The most of LVDC cable that are designed now, are based upon the behaviour of the LVAC cables under DC conditions. The HVDC cables are not involved in the LVDC cable design that is mainly because of the working conditions of the cable under different voltage levels and the break down mechanism of the HVDC cable is completely different to the LVDC cables [28]. So there is limited research available that is useful and also utilized to validate the research findings that is going to be done during this thesis.

2.6. Summary

In this framework chapter the structure of the LVDC distribution system, LV cables and the design of the cables were discussed. Also the active parameters and the challenges involved with formulating LV cable was explained in detail in this chapter.

3
Modelling

The DC distribution system modelling is a vital part in formulating the LVDC cable, as the behaviour of the cable designed is assessed by simulating it in a LV distribution system environment. Based on the outcomes received through simulations, will help in better understanding of the DC distribution system and it would lead to better designing of the LVDC cables.

The DC distribution system could be modelled by three different modelling methods, each of the methods utilized has a specific purpose that it satisfies. The three methods which could be utilized for modelling the DC distribution system are steady state, dynamic and transient modelling. The steady state modelling is preferred when the system that is modelled is set to be in steady state operating condition and the variables considered in the simulation are expected to be constant with respect to time [58].The transient modelling is preferred when the propagation delays and the frequency dependent effects needs to be considered for the system modelled [46]. This modelling gives a clear viewpoint on the evolution of the variable and circuit parameters with respect to time[15][59]. The dynamic modelling is preferred when the dynamic behaviour of the capacitances, inductances and discrete elements present in the system needs to be continuously assessed for the system modelled [60][46].The dynamic modelling method is the most comprehensive approach compared to the other modelling methods[61]. The DC distribution system for this thesis also needs to be modelled dynamically, as the behaviour of discrete and the energy storage elements present in the system needs to be assessed continuously in order to ideally formulate the LVDC cables. In the forthcoming section more details on the different approaches of the dynamic modelling is presented.

3.1. Dynamic Modelling

As mentioned earlier, in dynamic modelling the dynamic behaviour of the discrete elements and the energy storage elements like the capacitance and the inductance present in the system are continuously assessed for the distribution system modelled. The dynamic modelling of the distribution system could be done in three different ways namely through the transfer function of the system, through the state space approach and lastly through the transient simulation[62]. All these approaches of dynamic modelling are further explored in the upcoming section.

3.1.1. Transfer Function

The dynamic modelling of a distribution system could be also done by deriving the transfer function of the model. A dynamic model is a mathematical representation of the inputs and the outputs that are present in the dynamic system. The dynamic system models are usually represented in the form of a differential equation. Also, the dynamic system models could be either linear or non linear. A linear model obeys both the principle of superposition and homogeneity and the non linear models do not obey the principles of superposition and homogeneity[63].

The transfer function is the polynomial function that defines the relationship between the inputs and the outputs of the dynamic models. This includes the capacitance, inductance and discrete elements present in the system needs to be continuously assessed for the dynamic system modelled[64]. After deriving the transfer function of the dynamic model, based on the transfer function various studies could be carried out in order to understand the dynamic system better. The nature of the system could be explored even more by finding the limits of the system by utilizing the dynamic nature of the inputs and the output functions[65]. The transfer function also provides with a complete description of the dynamic characterisation of the system. For any configuration of the DC distribution system, once the transfer function of that distribution system is derived then the eigen value of the system could be assessed from the transfer function[66]. The eigen value denotes the dominant pole movements, from that the stability of the distribution system could be analysed. This shows the importance of the transfer function based dynamic modelling as it provides a pathway to analyse the stability of the distribution system through an algebraic analysis[67].

3.1.2. Transient Simulation

The transient simulation based dynamic models are the most accurate models dynamic model as they take in to account the propagation delays present in the system[16]. These dynamic models are far more complex to implement and the simulation take more computational power and time. Due to the complexity involved the DC distribution system designed doesn't permit to take the conductance involved in the system to account. So usually non transient models are frequently utilized for dynamic modelling of the DC distribution system. These models lack the flexibility and the ease that the non transient models. Also these models cannot be extended and they are not flexible in order to accommodate different distribution system models with varying design[59].

The transient simulation can be done in the PSCAD-EMTDC, EMTP, and ATP environments. The results provided for short circuit analysis implemented in distribution system models take into account the propagation delays and this aid in far more accurate results[68]. The line elements in these system are modelled based on lumped elements or travelling wave model[16][69].

3.1.3. State Space Approach Based Dynamic Modelling

One of the most prominent method for conducting the dynamic modelling of distribution system is through the state space approach [70][71] [72]. The state space model solves many of the limitations that were found in classical control theory in which transfer functions were used. The state space model describes the behaviour of the dynamic distribution system as a set of first order ordinary differential equation [72].

The state space approach is defined by two sets of equation namely the state equation and the output equation. Firstly, the state equation is represented by equ(3.1). In this equation $\dot{x}$ is the derivative of x, A is the state matrix, B is the input matrix, x is the state vector and U is the input vector. The number of state variables x present in the state space model is equal to the highest order of ODE present in describing the dynamic distribution system[73]. The state variable (x) could also be defined as the set of independent variables that completely describes the system. The variables set is not completely different and they may be defined as physical variable that could be measured or by variables that cannot be measured directly[73][72].

$$\dot{x} = A \cdot x + B \cdot u \tag{3.1}$$

The general representation of each of the variable present in the state equation is given as:

$$x = \begin{Bmatrix} x_1 \\ x_2 \\ \cdots \\ x_n \end{Bmatrix}_{n\times 1} \tag{3.2}$$

$$u = \begin{Bmatrix} u_1 \\ u_2 \\ \cdots \\ u_m \end{Bmatrix}_{m\times 1} \tag{3.3}$$

$$A = \begin{bmatrix} a_{11} & a_{12} & \dots & a_{1n} \\ a_{21} & a_{22} & \dots & a_{2n} \\ \dots & \dots & \dots & \dots \\ a_{n1} & a_{n2} & \dots & a_{nn} \end{bmatrix}_{n\times n} \tag{3.4}$$

$$B = \begin{bmatrix} b_{11} & b_{12} & \dots & b_{1m} \\ b_{21} & b_{22} & \dots & b_{2m} \\ \dots & \dots & \dots & \dots \\ b_{n1} & b_{n2} & \dots & b_{nm} \end{bmatrix}_{n\times m} \tag{3.5}$$

Secondly, the output equation given by equ3.6. In this equation Y denotes the output variable, D is the output matrix and finally E is the direct transmission matrix. Collectively ABDE matrixes are called as state space matrices [71][74].

$$y = D \cdot x + E \cdot u \tag{3.6}$$

$$y = \begin{Bmatrix} y_1 \\ y_2 \\ \cdots \\ y_p \end{Bmatrix}_{p\times 1} \tag{3.7}$$

$$D = \begin{bmatrix} d_{11} & d_{12} & \dots & d_{1m} \\ d_{21} & d_{22} & \dots & d_{2m} \\ \dots & \dots & \dots & \dots \\ d_{p1} & d_{p2} & \dots & d_{pm} \end{bmatrix}_{p\times m} \tag{3.8}$$

$$E = \begin{bmatrix} e_{11} & e_{12} & \dots & e_{1n} \\ e_{21} & e_{22} & \dots & e_{2n} \\ \dots & \dots & \dots & \dots \\ e_{p1} & e_{p2} & \dots & e_{pn} \end{bmatrix}_{p\times n} \tag{3.9}$$

As the general outlook of the state space approach is now familiar, next the working of this approach in dynamic modelling is explained. The dynamic behaviour of the discrete elements and the energy storage elements like the capacitance and the inductance present in the lines are taken in to account for the distribution system modelled [71] [75]. Firstly the distribution system for which the state space approach based dynamic modelling is said to be done, need to be represented like the line model representation. After the representation the state space approach can be implemented on the model. The state space approach starts with first choosing the state variable for the model, usually for DC distribution system modelling the current in each distribution line and the voltage at each node are chosen [70] [73]. This method is most widely preferred method for dynamic modelling of DC distribution system as it has a highly flexible model and it is highly accurate with its results [70] [73] [75]. So finally based on the literature research, the state space approach method would be perfectly suitable to realize and assess the dynamic behaviour of the DC distribution system modelled in this thesis.

3.2. Distribution System Modelling

The LVDC distribution system as said in the previous section is said to be modelled through the dynamic based state space approach[46]. The state space approach utilized to represent a DC distribution system takes into account the dynamic nature of the system elements present in the distribution grid. The dynamic based state space approach utilised to model the LVDC distribution system is based on [46]. In this section, detailed explanation about each of the different levels of the distribution system's representation in the state space approach is given.

3.2.1. Grid elements

The DC distribution grid can be represented by the number of nodes (N), number of distribution lines (L) and the number of phase conductors (M) present in the system. The lines contain the cables between the nodes. This information is completely necessary in order to form the state space equation and matrices of the distribution system. After the above system information is known, the first step in the state space approach is the formation of incidence matrix of the selected DC distribution grid. The state space approach described can be utilized to form any DC distribution system by following the implementation methodology used in this section. The state space approach is implemented on a three node two line bipolar system. The bipolar system consists of three conductors in comparison to the monopolar system which has just one conductor. At each of the node, there is a power electronic converter connected to it. The state space approach is implemented in a bipolar system mainly because it is slightly complex to define compared to the monopolar system, the influence of mutual inductance is taken into consideration and knowing the approach in the bipolar system makes it easier to implement in the monopolar system.

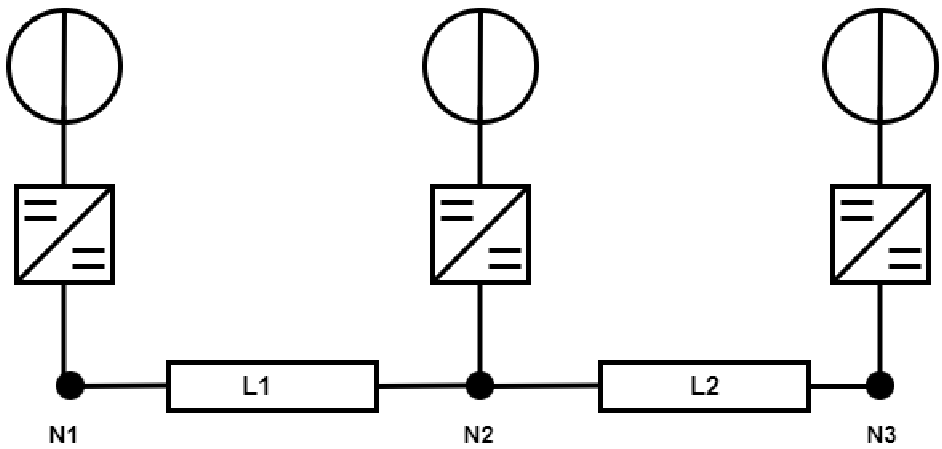

Figure 3.1: 3 Node 2 Line DC Monopolar Distribution System

The incidence matrix is the algebraic representation of the interconnection present between the lines and the nodes of the distribution system. The rows of the incidence matrix represent the lines present in the system and the nodes of the distribution system are represented by the columns of the incidence matrix. The system considered here is a bipolar system containing three conductors, so it contains L*M rows and N*M columns as the size of the incidence matrix. The incidence matrix of the bipolar configuration of the system shown in Fig 3.1, is given by equ(3.10)[46]. The bipolar distribution system contains 3 nodes, 2 lines and 3 conductors so the size of the incidence matrix is 6*9. When the current is flowing from the node to a line, it is represented as 1 and when the current is flowing from the line to a node then it is represented as-1 in the incidence matrix. The direction of current flow is made through assumptions here and the sign denoted in the matrix could be opposite[46]. If the incidence matrix is formulated for a monopolar system the size of it is reduced by three as it has only one conductor.

$$\Gamma = \begin{bmatrix} 1 & 0 & 0 & -1 & 0 & 0 & 0 & 0 & 0 \\ 0 & 1 & 0 & 0 & -1 & 0 & 0 & 0 & 0 \\ 0 & 0 & 1 & 0 & 0 & -1 & 0 & 0 & 0 \\ 0 & 0 & 0 & 1 & 0 & 0 & -1 & 0 & 0 \\ 0 & 0 & 0 & 0 & 1 & 0 & 0 & -1 & 0 \\ 0 & 0 & 0 & 0 & 0 & 1 & 0 & 0 & -1 \end{bmatrix}_{L\times M, N\times M} \tag{3.10}$$

3.2.2. System elements

The modelling of the distribution system is done through the state space approach, after deriving the incidence matrix the state variables which defines the distribution system needs to be chosen. In this case it is chosen to be the node voltage and the line currents present in the distribution system. The amount of nodes and lines present in the system has a say in the computational speed of the system with lesser state variable leads to higher computational speed. The KCL and KVL are applied on the distribution system in order to derive the statespace equation in terms of the state variable chosen.

First the KCL is applied on the 3 node, 2 line Bipolar Distribution system, the monopolar version of the model is shown in Fig 3.1 in order to derive the state equation for the node voltages. An extended and elaborate version of Fig 3.1 can be seen in Appendix A. Applying KCL at node 1+ , the resultant equation is shown in equ (3.11). Where I_{n1+} is the current flowing through node 1+,I_{l1+} is the current flowing through the positive conductor of distribution line 1,C_{1+} is the capacitance connected only to the positive conductor of node1, C_{1+-} is the capacitance connected between positive and negative conductor of node 1, similarly G_{1+} is the conductance connected only to the positive conductor of node 1, G_{1+-} is the conductance connected between positive and negative conductor of node 1, U_{n1+} is the voltage at node 1+ and $\dot{U}_{n1+}$ is the time derivative of node voltage denoted with a dot notation.

$$\begin{aligned} I_{n1+} = {} & C_{1+}\dot{U}_{n1+} + C_{1+N}(\dot{U}_{n1+} - \dot{U}_{n1N}) + C_{1+-}(\dot{U}_{n1+} - \dot{U}_{n1-}) + G_{1+}U_{n1+} \\ & + G_{1+N}(U_{n1+} - U_{n1N}) + G_{1+-}(U_{n1+} - U_{n1-}) + I_{l1+} \end{aligned} \tag{3.11}$$

Similarly KCL is applied at other nodes (node 1N and node 1-) within node 1 and then it is carried on to other nodes present in the system. Extended step by step derivation of the statespace approach applied on this DC distribution is given in Appendix A. The general form of the KCL applied on each of the nodes, rearranged in terms of state variable- node voltage is given by the equ (3.12)[46].Where Γ is the incidence matrix that is multiplied with the current through the distribution line is mainly done to denote the difference current flowing between two nodes. This equation shows the voltage across the capacitance is equal to the difference between the current flowing through the node injected by the converter, the current flowing through the distribution lines and the current leaked through the conductance.

$$C\dot{U}_n = I_n - \Gamma^T I_L - GU_n \tag{3.12}$$

Secondly the KVL is applied to the distribution system, in order to derive the state equation for the line currents. Applying KVL between Node 1+ and Node 2+, the resultant equation is shown in equ (3.13). Where R_{l1+} is the resistance present in line 1, L_{l1+} is the inductance connected to line 1, M_{1+N} is the mutual inductance induced between positive and neutral conductor of node 1, M_{1+-} is the other mutual inductance induced between positive and negative conductor, I_{l1+} is the current flowing through the positive conductor of distribution line 1 and $\dot{I}_{l1+}$ is the time derivative of the current flowing through the positive conductor of distribution line 1 denoted with a dot notation. The rest of the elements are the same as described in the above equations. Similarly, KVL is applied between node 1N and node 2N, and node 1- and node 2-. Then it is carried on to other nodes present in the system.

The extended version of the derivation is available in the appendix A. As the whole derivation is not explained here, the general form of the KVL applied between each of the nodes, rearranged in terms of state variable - (line current) is given by the equ (3.14)[46]. Also this equation shows the current through the line inductance is equal to the difference between the node voltages and the voltage drop across the resistances present in the nodes. Here L is the inductance matrix which contains also the mutual inductances present in the system.

$$U_{n1+} - R_{l1+}I_{l1+} - L_{l1+}\dot{I}_{l1+} - U_{n2+} - M_{1+N}\dot{I}_{l1n} - M_{1+-}\dot{I}_{l1-} = 0 \tag{3.13}$$

$$L\dot{I}_l = \Gamma U_L - RI_l \tag{3.14}$$

The general form of the equations present in equ(3.12)and (3.14) are re-arranged to form the states-space equations of the system[46]. These equations are represented in the form of first order ODE and it is given by equ (3.15) and (3.16).

$$\dot{U}_n = C^{-1}I_n - C^{-1}\Gamma^T I_L - C^{-1}GU_n \tag{3.15}$$

$$\dot{I}_l = L^{-1}\Gamma U_L - L^{-1}RI_l \tag{3.16}$$

The KCL and KVL equations found through by applying it on each of the nodes present in the distribution system is converted in to matrix form separately. After the conversion the equations are arranged interms of their state variable as shown in equ (3.15) and (3.16). Then both the KCL and KVL equations are combined together to form the statespace equation of the system in their matrix form shown in equ (3.17)[46]. Where $\dot{U}_n$ is the matrix containing the time derivative of node voltages, $\dot{I}_l$ is the matrix containing the time derivative of the line currents[46], R,L,C,G are the individual matrix containing the Resistance, Inductance, Capacitance and Conductance present in the distribution system and finally $I_{n,N,C}$ (N and C represents number of nodes and conductors) is the matrix containing the node currents injected by the converters. Extensive description of this equ(3.17) with complete elaboration of each of the matrix elements is given in Sec 3.2.3.

$$\begin{bmatrix} \dot{U}_n \\ \dot{I}_l \end{bmatrix} = \begin{bmatrix} -C^{-1}G & -C^{-1}\Gamma^T \\ L^{-1}\Gamma & L^{-1}\mathrm{R} \end{bmatrix} \begin{bmatrix} U_n \\ I_l \end{bmatrix} + \begin{bmatrix} -C^{-1} \\ \emptyset \end{bmatrix} \begin{bmatrix} I_{n,1,1} \\ I_{n,N,M} \end{bmatrix} \tag{3.17}$$

This equ (3.17) is converted into the state space form by utilizing the state space equation shown in equ (3.1) and (3.6). By converting in terms of state space equation we can define x,u and the statespace matrices as shown in equ(3.18)-(3.23) below[46]. Here state vector matrix x consists of all the node voltages and line currents present in the system, n, l and c represents the number of nodes, lines and conductors. The input vector u consists of all the node currents injected/ extracted by the converter present in the system [46]. The state space matrix D is an identity matrix and E is a null matrix in the output equation formed. Then the line elements present in the state space matrices are defined elaborately in the forthcoming section 3.2.3.

$$x = \left[U_{1,1} \cdots U_{n,c}, I_{1,1} \cdots I_{l,c}\right] \tag{3.18}$$

$$u = \left[I_{n,1,1} \cdots I_{n,N,C}\right] \tag{3.19}$$

$$A = \begin{bmatrix} -C^{-1}G & -C^{-1}\Gamma^T \\ L^{-1}\Gamma & L^{-1}R \end{bmatrix} \tag{3.20}$$

$$B = \begin{bmatrix} -C^{-1} \\ \emptyset \end{bmatrix} \tag{3.21}$$

$$D = I \tag{3.22}$$

$$E = \emptyset \tag{3.23}$$

3.2.3. Line elements

In this section the line or cable elements (R,L,C,G) present in the distribution system 's matrix representation in the state space approach is described. First the model that is used to define the cable elements is the lumped element pi model of the bipolar distribution system shown in Fig 3.2. In this representation, the mutual inductance, capacitance and conductance present between the multiple conductors of the bipolar system are considered, as they could have a significant impact on the system performance. It can be seen that the admittance of the line or cable (G and C) are distributed between the nodes that its connected to, each of the node considered are set to have half of the capacitance and the conductance of the distribution line due to the pi model representation.

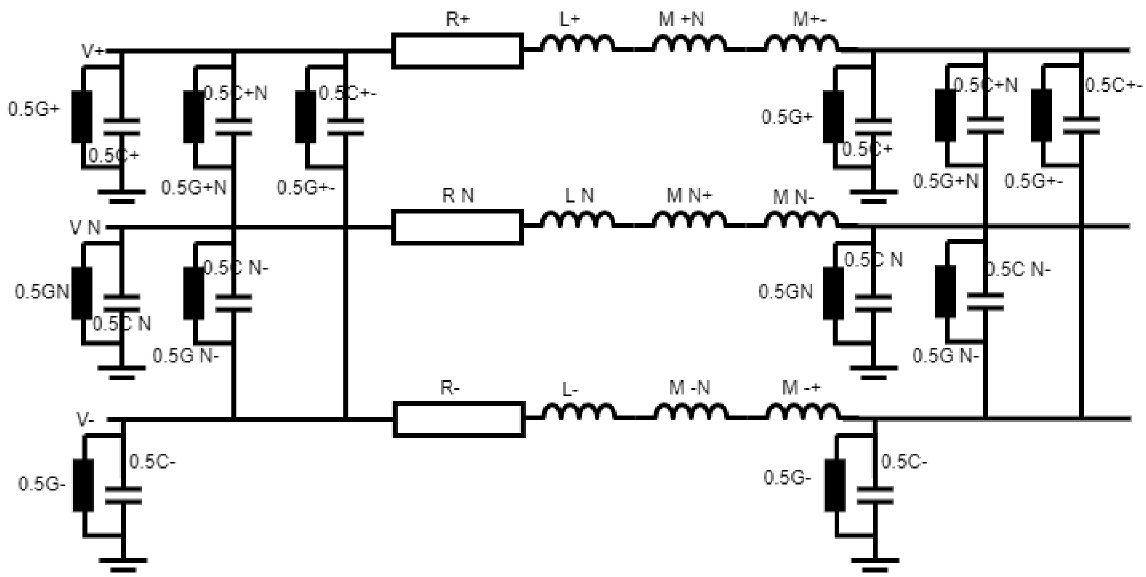

Figure 3.2: Bipolar distribution system 's Lumped element Pi model representation

The matrix definition of the cable elements (R,L,C,G) is done in two steps, first the cable elements are defined in terms of the lines and in the second step all the cable elements are defined in terms of the nodes present in the distribution system [46]. First the cable elements are defined in terms of the lines and the number of conductors (C) present in the distribution system is shown in equ(3.24)-(3.27). Here in the matrix the cable elements are defined in terms of its connections present between the phase conductors of each distribution line present in the distribution system.

$$R_{L,l} = \begin{bmatrix} R_1 & 0 & \cdots & 0 \\ 0 & R_2 & \ddots & 0 \\ \vdots & \ddots & \ddots & 0 \\ 0 & \cdots & 0 & R_C \end{bmatrix} \tag{3.24}$$

$$L_{L,l} = \begin{bmatrix} L_{11} & M_{12} & \cdots & M_{1C} \\ M_{21} & L_{22} & \ddots & M_{2C} \\ \vdots & \ddots & \ddots & M_{(C-1),C} \\ M_{m1} & \cdots & M_{C,(C-1)} & L_{CC} \end{bmatrix} \tag{3.25}$$

$$C_{L,l} = \begin{bmatrix} \sum_{p=1}^{C} C_{1p} & -C_{12} & \cdots & -C_{1M} \\ -C_{21} & \sum_{p=1}^{C} C_{2p} & \ddots & -C_{2M} \\ \vdots & \ddots & \ddots & -C_{(C-1),C} \\ -C_{C1} & \cdots & -C_{C,(C-1)} & \sum_{p=1}^{C} C_{Cp} \end{bmatrix} \tag{3.26}$$

$$G_{L,l} = \begin{bmatrix} \sum_{p=1}^{C} G_{1p} & -G_{12} & \cdots & -G_{1M} \\ -G_{21} & \sum_{p=1}^{C} G_{2p} & \ddots & -G_{2M} \\ \vdots & \ddots & \ddots & -G_{(C-1),C} \\ -G_{C1} & \cdots & -G_{C,(C-1)} & \sum_{p=1}^{C} G_{Cp} \end{bmatrix} \tag{3.27}$$

Now for the second step, the cable elements are defined in terms of their nodes and this representation is the one that is utilized by the state equations formed before. As the pi model is used to represent the distribution lines, the admittance matrix are defined differently. The capacitance and conductance of the node are found by summing the half of the capacitance and conductance of each distribution line connected to that specific node. As shown in the equ(3.28) and (3.29) [46], the incidence matrix Γ is utilized as it gives the connection between the lines and the nodes of the distribution system. The final representation of the cable element's matrix in terms of their nodes is defined by the equ(3.30)-(3.33)[46]. This representation is only utilized for solving the state equation defined above.

$$C_{N,n} = \frac{1}{2}\left|\Gamma^T\right| \sum_{q=1}^{l} C_{L,q} \tag{3.28}$$

$$G_{N,n} = \frac{1}{2}\left|\Gamma^T\right| \sum_{q=1}^{l} G_{L,q} \tag{3.29}$$

$$R_{mat} = \begin{bmatrix} R_{L,1} & 0 & \cdots & 0 \\ 0 & \ddots & \ddots & \vdots \\ \vdots & \ddots & \ddots & 0 \\ 0 & \cdots & 0 & R_{L,l} \end{bmatrix} \tag{3.30}$$

$$L_{mat} = \begin{bmatrix} L_{L,1} & 0 & \cdots & 0 \\ 0 & \ddots & \ddots & \vdots \\ \vdots & \ddots & \ddots & 0 \\ 0 & \cdots & 0 & L_{L,l} \end{bmatrix} \tag{3.31}$$

$$C_{mat} = \begin{bmatrix} C_{N,1} & 0 & \cdots & 0 \\ 0 & \ddots & \ddots & \vdots \\ \vdots & \ddots & \ddots & 0 \\ 0 & \cdots & 0 & C_{N,n} \end{bmatrix} \tag{3.32}$$

$$G_{mat} = \begin{bmatrix} G_{N,1} & 0 & \cdots & 0 \\ 0 & \ddots & \ddots & \vdots \\ \vdots & \ddots & \ddots & 0 \\ 0 & \cdots & 0 & G_{N,n} \end{bmatrix} \tag{3.33}$$

3.3. Summary

In this modelling chapter, the different dynamic modelling approaches for DC distribution system were explained. Along with the detailed discussion about the grid, system and line elements present in the distribution system's representation in the state space approach was presented in this chapter.

4

LVDC Distribution System

Two LVDC distribution systems are modelled namely: a neighbourhood distribution system [46] and a Ship distribution system[76]. The cables are incorporated as lines into these models. Different analyses focussed on cables are carried out in both these distribution system models mainly to check the cable performance in different distribution system under different conditions.Also, the results generated from the analyses performed in both distribution system is compared, to get a better and far more reliable outlook on designing the LVDC cable. The power simulation scenario that has been utilized for the analysis has both positive and negative load imbalances present and it is structured in a way to meet the equilibrium system conditions that is present during the start of the simulation. Simulating the system in different scenarios will definitely aid in a better assessment of the cable and its performance. This chapter will provide a detailed description of the different LVDC distribution system models that has been modelled with its respective power simulation scenario. Also the Power electronic converters models that is utilized during different analysis are explained in detail.

4.1. Neighbourhood Distribution System

The LVDC neighbourhood distribution system modelled consists of 5 nodes and 8 lines. For the monopolar configuration of this distribution system, it has 1 conductor and for the bipolar configuration it has 3 conductors. In the bipolar configuration it consist of positive negative and a neutral (acting as metallic return) conductor. The neutral conductor is used to avoid the direct injection of DC Current to the ground causing corrosion. The neutral conductor provides a return path for these currents and also it improves the reliability of the distribution system. The analyses are carried out in both these configurations to figure out the differences present in the results. The Monopolar representation of the neighbourhood distribution system is shown in Fig 4.1. There are five power electronic converters present in the system, each of the power electronic converter is connected to a node[46]. The power electronic converter connected to node 1 is droop controlled. The source converter is connected to node 2 and 4. The load converter is connected to node 3 and 5. The power electronic converters specified are operated as Bidirectional DC- DC interleaved converters as it provides better efficiency compared to other converter models due to reduction in switching losses and output voltage ripples[77]. The cable length of all cables utilized in this system is taken as 100 meters. The nominal voltage level of the bipolar system is ±350 V_{DC}[46].

The power simulation scenario considered for this distribution system is shown in table4.1[46]. The power flow through each of the node at a particular time period is tabulated below. At node 1 as the droop-controlled converter is connected, so there is no variation in the output power[46]. But in the other nodes, the source and the load power converters are allowed to change their respective power output at different time period. The source converters are connected to node 2 and 4, as the power is flowing into the system through the nodes it is given a positive sign. The load converters are connected to node 3 and 5, as the power is taken out from the system through the nodes it is given a negative sign.At t=0ms there is no power flowing through the system. First the source converter connected at node 2 is turned on and the rest of the nodes are maintained at zero at t= 10ms. The load at Node 5 is turned on at t=20ms. At t=30 ms the load at node 3 in addition to the load at node 5 is turned on. At t=40 and 50ms all the source and the load nodes are turned on.

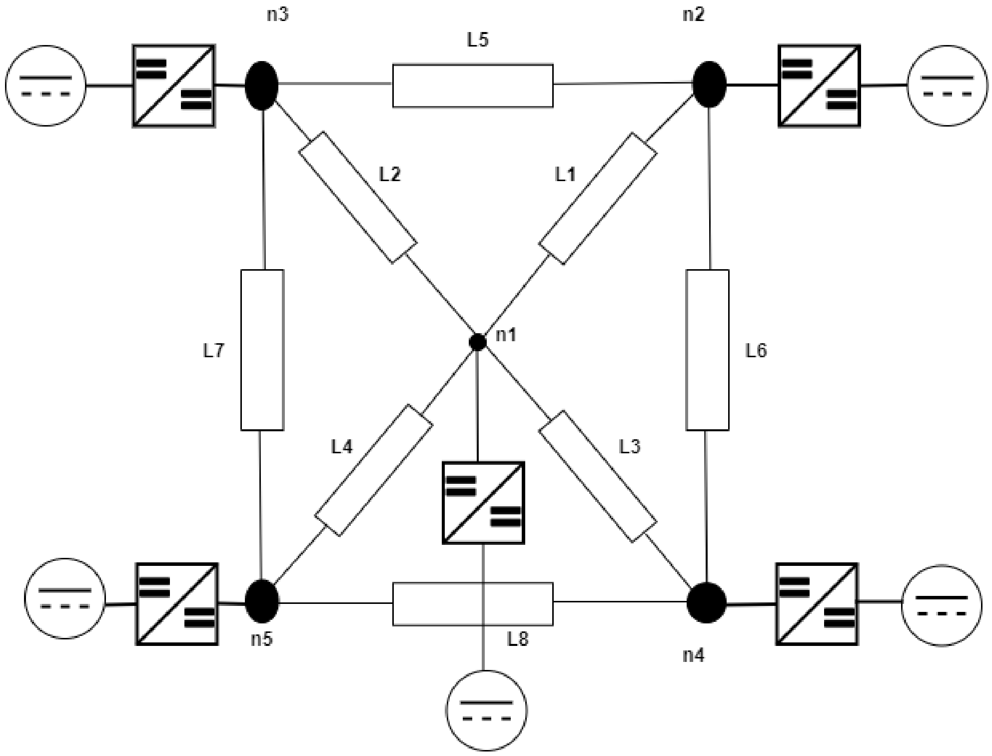

Figure 4.1: Monopolar DC Neighbourhood distribution system

All the capacitors are considered to be fully charged to ±350 V_{DC}, which is the nominal voltage of the distribution system. As said before, the power simulation scenario values are predefined in a way to accommodate both the positive and negative load imbalances in the system. This is done in order to be able to assess the cable's performance better as it is put through different situations. The specific line or cable parameter values used for the neighbourhood system are described in the forthcoming section 5.3. A smaller version of the neighbourhood system is modelled here to carry out different analysis and produce definitive results at a faster pace. By using the state space approach even larger extensive models with any number of lines, nodes and conductors under different system arrangement and simulation scenario can be easily done. But the simulation would take longer to execute and produce results of different analysis as the system equation would take longer to solve.

Table 4.1: Power simulation scenario of the neighbourhood distribution system

Time(ms)	P1(W)	P2(W)	P3(W)	P4(W)	P5(W)
0	0	0	0	0	0
10	0	1500	0	0	0
20	0	1500	0	0	-1500
30	0	1500	-3000	0	-1500
40	0	1500	-3000	2250	-1500
50	0	1500	-3000	2250	-1500

4.2. Ship Distribution System

The ship distribution system modelled consists of 12 nodes and 11 lines[76]. This ship design layout is formulated based on a basic electric ferry ship design. Similar to the neighbourhood distribution system the ship distribution system is also analysed under Monopolar and Bipolar configuration. The ship is powered by 6 batteries, each with a nominal capacity of 30.5 kWh. The voltage level of the bipolar ship distribution system is ±331 VDC [76]. The monopolar representation of the ship distribution system is shown in Fig 4.2. The loads that are connected to this system are propulsion motors, service loads and bow thruster motor. The two propulsion motors are connected at Node 8 and Node 11. The bow thruster motor is connected at Node12. The service loads are connected at Node 9 and 10[76]. The bow thruster motor is rated at 24 KW and 2000 rpm motor speed. Then the propulsion motor connected at port side is rated at 140 KW and 700 rpm motor speed. The second propulsion motor connected at star board side is rated at 100KW and 1000rpm motor speed. The line length of all the cables or lines present in this system is shown in table 4.3[76].

Table 4.2: Power simulation scenario of the Ship distribution system in kW

Time(ms)	P1	P2	P3	P4	P5	P6	P7	P8	P9	P10	P11	P12
0	0	0	0	0	0	0	0	0	0	0	0	0
20	0	0	0	0	0	0	0	0	-10	-5	0	0
40	0	35	35	0	0	0	0	-70	-10	-5	0	0
60	0	35	35	35	35	35	0	-70	-10	-5	-70	-25
80	0	0	0	0	0	0	0	0	-10	-5	0	0
100	0	0	0	0	0	0	0	0	0	0	0	0

As shown in the figure, the Bidirectional DC- DC interleaved converters are connected to the batteries at the front end of the distribution system. The power electronic converter connected to node 1 is droop controlled. The DC-AC converters are connected to the loads at the tail end of the distribution system. Similar to the previous distribution system droop controlled converter is connected at node 1 and all the capacitors are considered to be completely charged to the nominal voltage of the distribution system. The power at Node 7 is taken as zero for all instances because it acts as a common node with no source or load connected to it. The line parameter's of the cables utilized in the ship distribution system is explained extensively later in the section 5.3.

The power simulation scenario is constructed with both positive and negative load imbalances in the system and is structured in a way to meet the equilibrium system conditions that is present during the start of the simulation. First at t=20ms the service loads are turned on and these load's needs are satisfied by the droop controlled converter connected to the battery at Node 1. At t=40 ms the two battery connected source converter at node 2 and node 3 are turned on, also the propulsion motor at the port side is turned on. Then the battery connected source converters at node 4,5,6 are also turned on with the propulsion motor on the star board side at T= 60ms[76].All the loads excluding the service loads are turned off and only the droop controlled source converter is turned on during t= 80ms. At t=100ms all the loads and sources are turned off. The power simulation scenario considered for this distribution system is shown in table4.2.

Table 4.3: Line length data

Line	Length (m)
Line1-6	5
Line7,10	15
Line 8,9	7
Line11	10

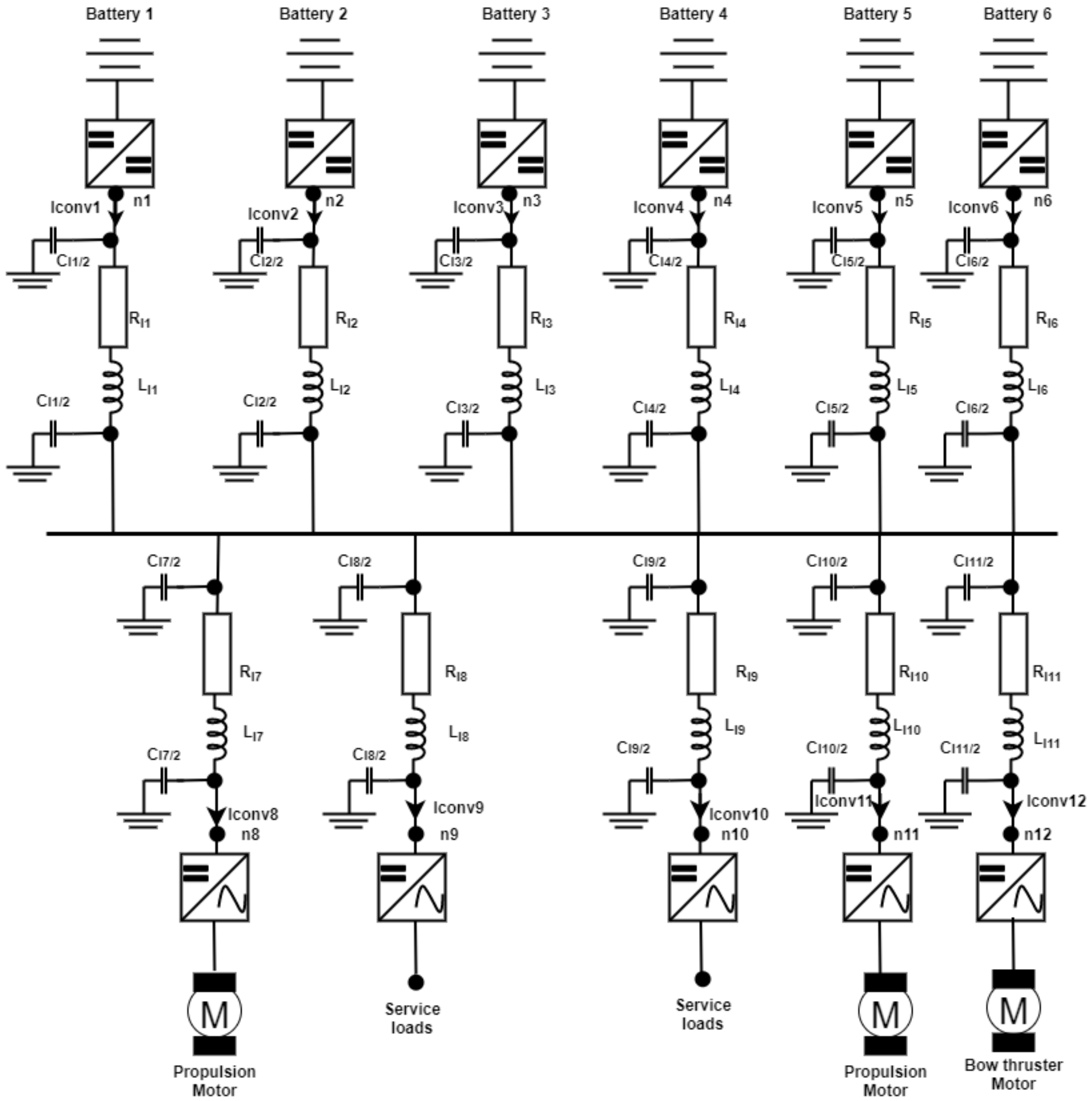

Figure 4.2: Monopolar DC Ship distribution system

4.3. Electronic power converters models

In this section the different electronic power converter models that are used in the distribution system are extensively explained in detail. The large signal converter models describe the non linear behaviour of the distribution system more accurately. But for larger DC distribution systems using large signal models for the converters and deriving stability is quite complicated [78][79]. For that reason small signal is preferred over large signal models. The small signal models also linearize the power electronic converter that is accurate in time frames longer than semiconductor's switching period. Also the converter instantaneously react to the disturbance in the system as their bandwidth is lower than one tenth of the switching frequency[80].

The Norton equivalent small signal model is used for modelling the power electronic converters. This small signal model in their linearized version usually consists of shunt capacitance (C_C), impedance (Z_C) and injected/extracted converter current (I_C)[46].The pictorial representation of the Norton equivalent power electronic converter model is shown in Fig4.3. The constant current converters is implemented by making the impedance reach infinity, and the constant impedance converter is implemented by making the current reach zero. In the upcoming section the droop controlled and constant power converter's linear and idealized model representation would be discussed. The converters can be modelled in two ways namely the linearized and idealised models. Each of these type of models are utilized during certain instances and these will be explained in the forthcoming sections.

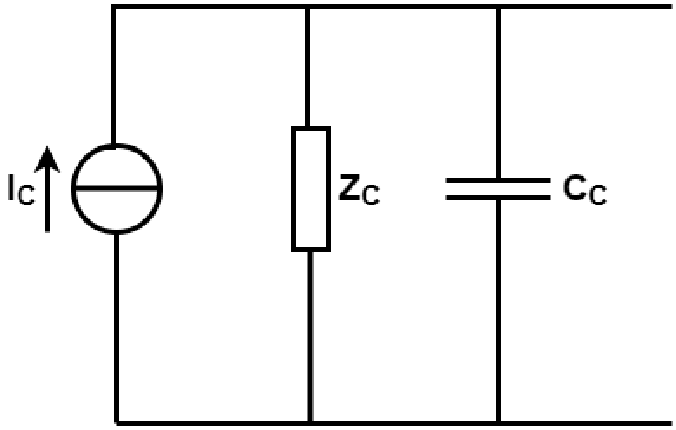

Figure 4.3: Norton small signal model representation of the power electronic converter

4.3.1. Idealized converter model

The state space approach that's been utilized to design DC distribution system uses the idealized converter models for deriving its results. As there are two converter types that have been used in the distribution system namely droop and constant power controlled converters. The droop controlled converter is mainly used in both the distribution system models as it assists in the voltage regulation of the system. The droop control helps the system regulate the system voltage in relations to the power demanded from or supplied to the system. For the rest of the sources and loads are assumed to be attached to the constant power converter in the distribution system models. As in this state space dynamic models it is assumed that the power electronic converters spontaneously reacts inside their control bandwidths limit. So the power electronic converters are modelled in terms of their idealized Norton equivalent circuit[46]. This converter model's idealized version is shown in Fig 4.4 below.

In the idealised power electronic converters models the generalised form of current flowing through or taken from the droop and constant power controlled converters is shown below in equ (4.1)and (4.2) [46].

$$I_{droop} = \frac{U_{ref} - U_N}{Z_{droop}} \tag{4.1}$$

$$I_{conv} = \frac{P_{conv}}{U_N} \tag{4.2}$$

Here U_{ref} is the reference output voltage, U_N is the voltage at the node in which converter is connected, Z_{droop} is the impedance of the droop controlled converter and P_{conv} is the power flowing through/ taken out from the converter. The reference voltage is set in accordance to the monopolar and bipolar distribution system taken. The droop impedance is taken as 1(Ω) in both the cases and the power flowing through the converter from the source is taken as positive and the power flowing out of the converter to the load is taken as negative. So the converter current is positive for the source node and negative for the load node of the positive conductor. All the formula shown above is for the monopolar system and for the bipolar system it is defined differently and more explanation about this is given in sec 5.3.

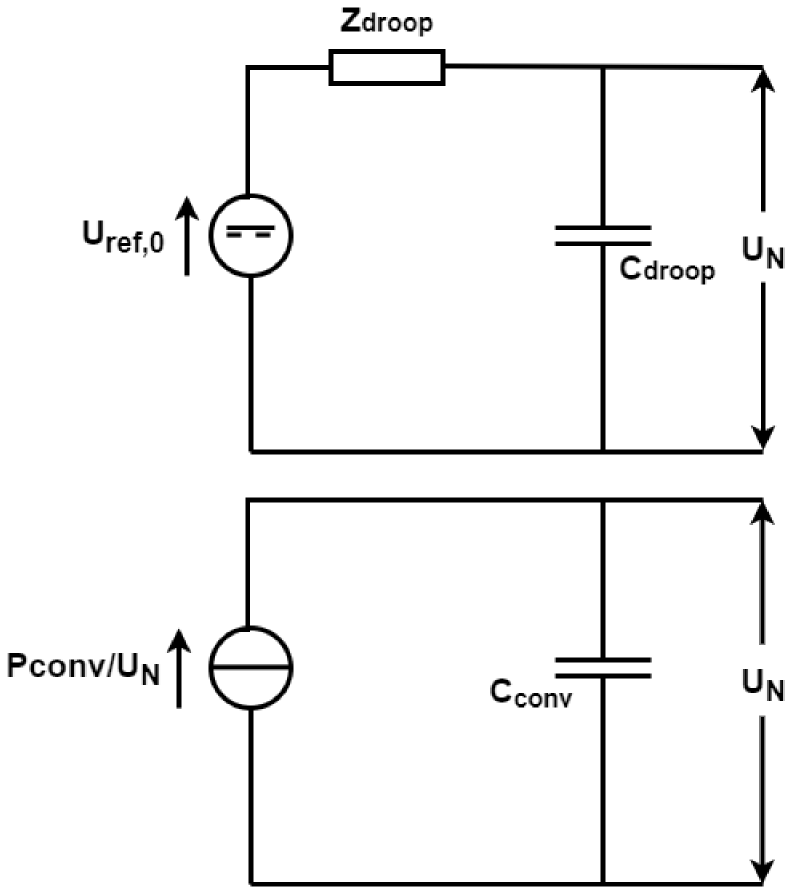

Figure 4.4: Ideal droop and constant power converter models

4.3.2. Linearized converter model

The linearized converter model is mainly utilized during the distribution system's stability analysis. As the stability of the distribution system is analysed with respect to the converter impedance, so the idealised models aren't utilized for the stability analysis [81][82]. A new linearized converter model is established with proper impedance representation in the droop and constant power converters. The linearized model of the power electronic converters is shown in Fig4.5. In comparison to the idealised converter models it can be seen that in the linearized models of both the converters, a constant current source is used, the impedance and the capacitance of the converters are connected in the shunt position.

In the linearized power electronic converters models [46] the generalised form of current flowing through or taken from the droop and constant power controlled converters is shown below in equ(4.3) and (4.4).

$$I_{\text{droop}} = \frac{U_{\text{ref}}}{Z_{\text{droop}}} - \frac{U_N}{Z_{\text{droop}}} = I_{\text{droop, }o} - \frac{U_N}{Z_{\text{droop}}} \tag{4.3}$$

$$I_{conv} = I_{conv,o} - \frac{U_{conv}}{Z_{conv}} \tag{4.4}$$

Here ($I_{droop,0}$) is the linearized droop converter's output current, (Z_{conv}) is the converter impedance and ($I_{conv,0}$) is the linearized converter output current [46]. The constant power converters are linearized around a set voltage limit and also an equivalent impedance is added in the linearized power converter model. The formula shown above is for the monopolar system and for the bipolar system it is defined differently and the more explanation about this is given in sec 5.3.

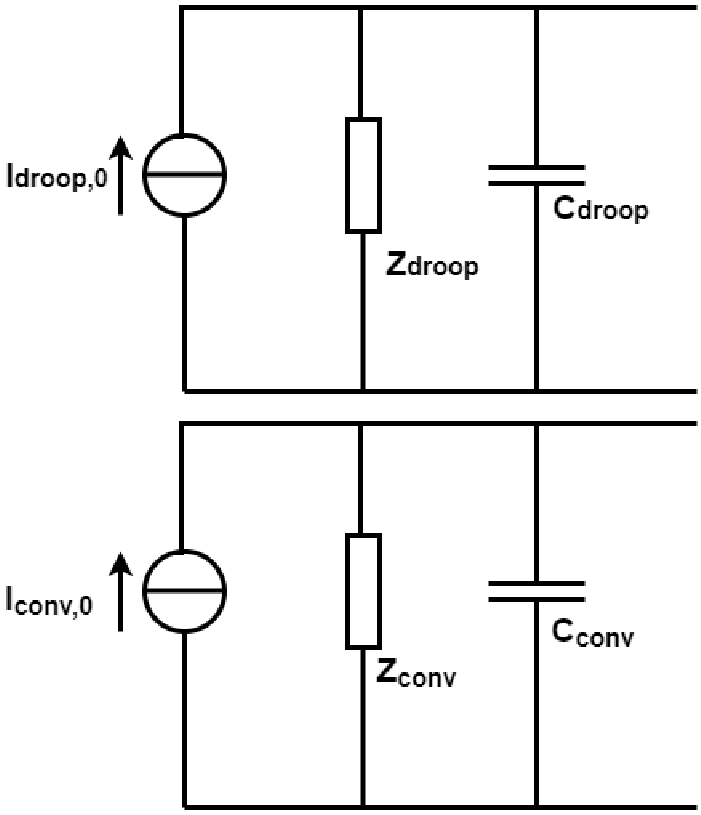

Figure 4.5: Linearized droop and constant power converter models

4.4. Summary

In this LVDC distribution system chapter, the LVDC distribution system model utilized for the upcoming analysis were explained in detail with their respective power simulation scenario.Also the electronic power converter models that are used in the distribution system models were discussed extensively in this chapter.

5 Analysis

In this chapter the different analyses, that's been carried out in the thesis is explained in detail. Short circuit analysis is not explained in this chapter as it is separately explained in chapter 6. The analyses that are carried out are namely the sensitivity, stability and the methodology utilised for varying the active cable parameters is explained in this chapter. The stability analysis is conducted through the eigenvalue approach. The sensitivity analysis is carried out by varying the system, cable parameters and the influence this has on node voltages, line currents and the stability of the system is studied. As the state-space approach is used to model the distribution system the voltages at each node and the current at each distribution line are obtained, as they are chosen as the state variables of the distribution system. These state variables are represented in the state-space equation, and by solving this state-space equation the node voltages and line currents present in the system are obtained[69][81].The sensitivity and stability analysis are implemented in a combined way and the default case results are also presented in this chapter. In the forthcoming sections, a detailed description of the analysis that are carried out will be explained.

5.1. Stability analysis

The stability analysis is done by using the eigenvalue approach. This analysis is mainly done due to the constant power converters that are connected to the loads, it shows negative impedance behaviour that could make the system unstable[83][24]. So it is vital to analyse the stability of the distribution system with respect to the converter impedance. In the state-space approach, the converter model utilized is idealized. But in the eigenvalue analysis the converter model utilized need to be linearised[81][46]. So linearized converter models are utilized for this analysis, the pictorial representation of these converters is shown in Fig 4.4. Now the generalised form of current flowing in/ taken out from the linearised converter is given by equ(4.3) and (4.4).

Combining equ(4.3),(4.4) with the state equations of the DC distribution system shown in equ(3.15),(3.16). The resultant equation's matrix form is shown below in equ (5.1) [46]:

$$\begin{bmatrix} \dot{U}_N \\ \dot{I}_L \end{bmatrix} = \begin{bmatrix} -C^{-1}Z^{-1} & -C^{-1}\Gamma^T \\ L^{-1}\Gamma & -L^{-1}R \end{bmatrix} \begin{bmatrix} U_N \\ I_L \end{bmatrix} + \begin{bmatrix} C^{-1} \\ \emptyset \end{bmatrix} I_{N,\mathbf{0}} \tag{5.1}$$

Where A, B are the new state matrices, x is the state variable matrix consisting of node voltage and line current present in the system. u is the input matrix that contains the node current to/from power converters present in the system. The new representation of state matrix A is used in the stability analysis of the system and it is shown in equ (5.2).

$$A = \begin{bmatrix} -C^{-1}Z^{-1} & -C^{-1}\Gamma^T \\ L^{-1}\Gamma & -L^{-1}R \end{bmatrix} \tag{5.2}$$

$$B = \begin{bmatrix} -C^{-1} \\ \emptyset \end{bmatrix} \tag{5.3}$$

$$x = \begin{bmatrix} U_{1,1} & U_{1,2} & \cdots & U_{N,C} & I_{1,1} & I_{1,2} & \cdots & I_{l,C} \end{bmatrix} \tag{5.4}$$

$$u = \begin{bmatrix} I_{n,1,1} & I_{n,1,2} & \cdots & I_{n,N,C} \end{bmatrix} \tag{5.5}$$

The Stability of the DC distribution system can be analysed by solving the characteristic equation of the system and deriving the roots of the system. These roots depict the poles of the distribution system, based on the positioning of these poles in the jω- axis, the stability of DC distribution system is analysed[84]. The characteristic equation of the system is given by equ(5.6). Where A is the state-space matrix and I is the identity matrix.

$$|\lambda I - A| = 0 \tag{5.6}$$

The poles of the distribution system are found by solving the characteristic equation. The system is considered to be stable, only if the poles found have negative real part present and the poles should lie on the left-hand side of the jω -axis. The oscillations present in the distribution system can also be assessed through the eigenvalue analysis. The amplitude of oscillation is set to be high when the poles of the distribution system lie closer to the jω axis and the amplitude of oscillation is set to be low when the poles of the distribution system lie farther away from the jω axis[82].

The impedance is assumed to be connected between the positive or negative and the neutral pole in the power electronic converter. There is no impedance directly connected between the positive and negative pole in bipolar configuration. The impedance is calculated through equ(5.7) shown below. The impedance is calculated based on the node voltage and the power extracted/ injected by the power electronic converter. Where V_{p-n} is the pole to neutral voltage and P is the power from the converter delivered to the load or generated by the source connected between pole and neutral conductor. In order to analyse the system stability in a more well defined way, the system stability is analysed at the lowest operating point (lowest equilibrium node voltage) achieved by the distribution system. The droop converter‘s impedance is set as $1(\Omega)$.The impedance connected in the rest of the converters is calculated based on the below equation, will be negative for the loads and positive for the sources connected in the system.

$$Z = \frac{(V_{p-n})^2}{P} \tag{5.7}$$

5.2. Sensitivity Analysis

The sensitivity analysis is carried out to analyse the DC distribution performance and stability when the active parameters are varied. The sensitivity of the distribution system towards the variation of each of the active parameters is seen and they are extensively analysed through this analysis. First a parameter is called an active parameter, when the variation of the set parameter influences the distribution system performance and stability. Then only the set parameter is identified as active parameter. The active parameters are identified as cable inductance, cable capacitance, cable cross-section (indirectly proportional to cable resistance), droop impedance and the source and load converter capacitance. These active parameters are expected to have an influence on the system performance and the stability of the system. So in this sensitivity analysis, these active parameters are varied and their influence on the stability, node voltage, system oscillation and line currents of the system are observed. This analysis is done in both the distribution system under monopolar and bipolar configuration. As per the description of this analysis, it can be seen that the sensitivity and stability analysis is combined together to analyze how the variation in the active parameters influences the system. In the result sections, more details about the range of the active parameters utilized and the influence it has on the system will be discussed in detail.

For the idealised converter model, the governing equation that will denote the converter current injected/extracted by the droop and constant power converters under bipolar configuration is explained below. Also, the formulas involved with the cable parameter's rating chosen for the analysis is explained in this section. First the droop converter's input current is calculated through equ(5.8) for the bipolar configuration's positive pole or conductor. As in the bipolar configuration there are three conductors present, so the reference voltage is the bipolar voltage level of the system that is twice the pole-neutral voltage of the monopolar system. For example in the neighbourhood system the reference voltage is taken as 350 V under monopolar configuration and in the bipolar configuration as positive and negative conductors are individually operating at 350 V so the reference output voltage is taken as 700V. The small difference in the droop controlled converter current equation for the bipolar configuration is that the node voltage is calculated based on the pole- pole voltage. Again for the constant power controlled converter the input current is calculated through equ(5.9) for the bipolar configuration's positive pole [46]. Here also the node voltage is calculated based on the pole to pole voltage .As the system is balanced , the converter input current through the negative pole or conductor is taken as equal in magnitude but opposite in sign to the positive pole converter input current. The neutral pole‘s converter input current is given by the sum of positive and negative pole‘s converter input currents, ultimately its zero as the system is balanced. Only during faults or short circuit the current flows through neutral and the system becomes unbalanced.

$$I_{droop(+p)} = \frac{2U_{ref} - (U_{+p} - U_{-p})}{Z_{droop}} \tag{5.8}$$

$$I_{conv(+p)} = \frac{P_{conv}}{(U_{+p} - U_{-p})} \tag{5.9}$$

Then the resistance of the cable is calculated based on equ(5.10). Where ρ is the resistivity of the wire material, l is the length of the cable and A is the cross section area of the cable. The resistivity of copper wire is taken as 1.67* 10^{-8} ohm-m, the length and cross section area of the cables are assumed to be different for different distribution system models, more explanation on this is given in Sec 5.3. The rest of the cable parameters (Capacitance, inductance, conductance) are given in terms of their per KM values based on their cable length. The converter capacitance is taken as 400μF, as it is within the industrial converter's capacitance range (300μF-700μF)[85]. The rest of the cable parameters are extensively explained in Sec 5.3.

$$R = \frac{\rho * l}{A} \tag{5.10}$$

5.3. Default case analysis

In the default case simulation, the values that are taken for different system and cable parameters are considered to be default. The results found through the default case analysis would be vital, as it is used to compare with other active parameter analysis results. This comparison helps in figuring out significant differences that are present in the results found through the certain analysis and the default case. This default case simulation will be carried out for both the ship and neighbourhood distribution system, as they make the base for these studies to be carried out. In the next sub-sections, a detailed description of both the neighbourhood and ship distribution system‘s default case analysis will be explained. Here in this analysis the resulting node voltages and line currents of the positive pole or conductor are only discussed. As the negative pole quantities tend to be equal in magnitude but opposite in sign to the positive pole and the neutral quantities is zero due to the system being in balanced condition. So, in order to get better clarity of the results found only positive pole quantities are plotted in the node voltage and line current graphs.

5.3.1. Neighbourhood Distribution system

The default case analysis of the neighbourhood distribution system with 5 nodes and 8 lines, first its monopolar configuration is simulated. The parameter values utilized for this system simulation is presented in table 5.1 shown below. As said before the positive pole quantities are only plotted in the node voltage and line current graphs. The stability analysis through the eigenvalue approach is also carried out for this default case. Through the state-space approach, the node voltages and line currents are obtained for the dynamic model simulated. The resulting positive pole quantities of the node voltages and line currents are plotted in Fig 5.1 and 5.2. The poles of this DC neighbourhood distribution found through the eigenvalue analysis are shown in Fig5.3.

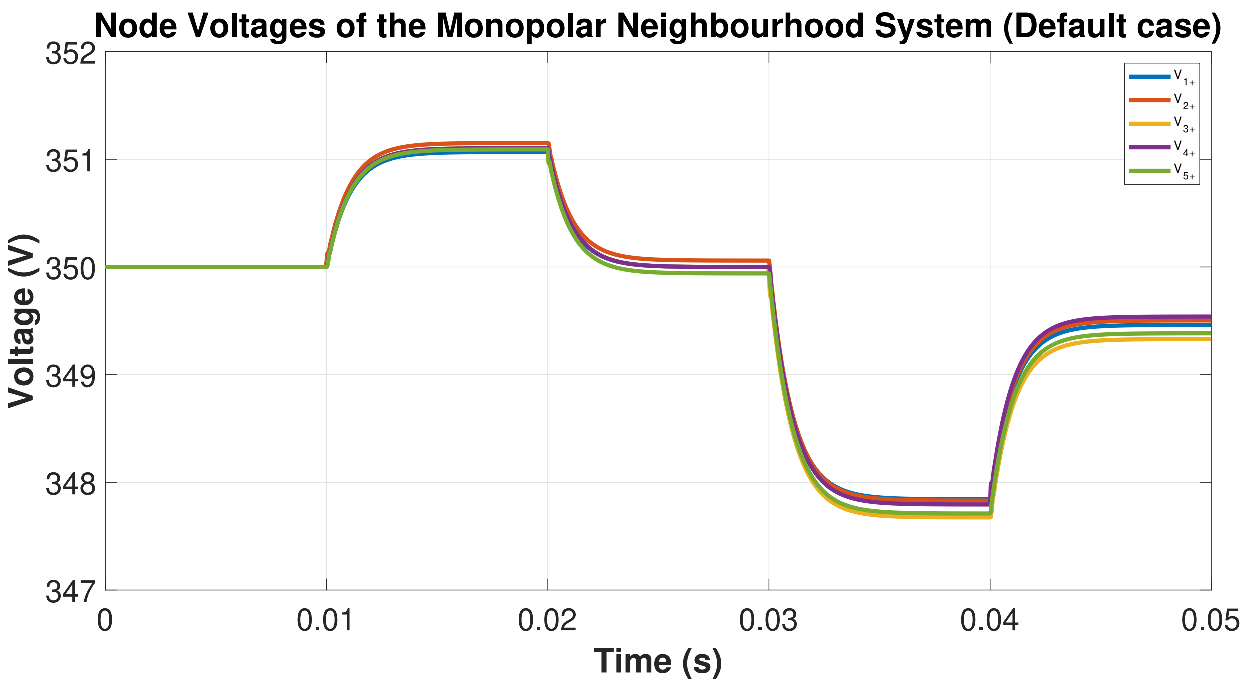

Figure 5.1: Node voltages of the Monopolar neighbourhood distribution system for default case analysis

Table 5.1: Default case parameter values

Parameters	Value (unit)
Line-length	100(m)
Inductance	32(μH/Km)
Capacitance	45(nF/Km)
Source converter capacitance	400(μF)
Load converter capacitance	400(μF)
Conductance	0
Cable cross section	20 (mm^2)
Droop Impedance (Conv)	1(Ω)

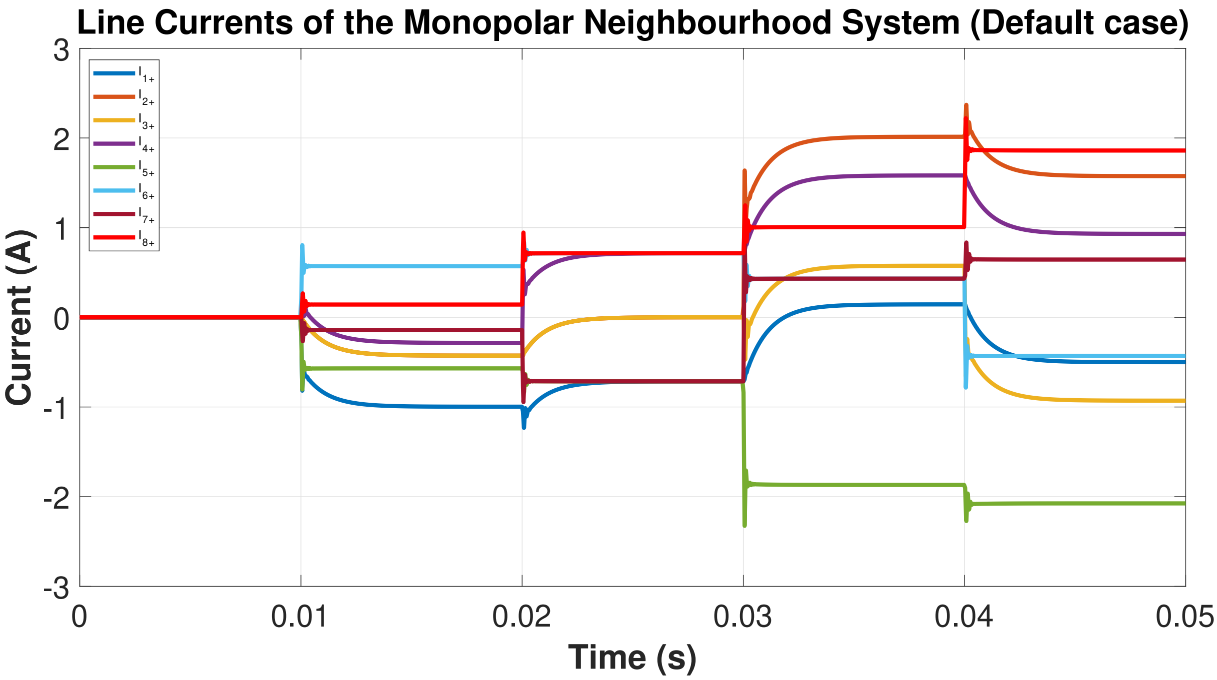

Figure 5.2: Line currents of the Monopolar neighbourhood distribution system for default case analysis

First, from the node voltages plot, it is seen that the neighbourhood distribution system is stable and the power exchange in the system takes place in accordance with the power simulation scenario presented before for the neighbourhood distribution system. Also,small signs of oscillation can be seen in the node voltages of this system. The presence of droop control aid in the system voltage level being closely regulated by it[23][46]. It takes into consideration the power simulation scenario that's been simulated for that time instance and regulates the system voltage based on that. The equilibrium voltages are reached when the state derivatives become zero. The general trend could be seen where the equilibrium voltage of the nodes gets increased when there is a positive load imbalance present and the equilibrium voltage tends to decrease when there is a negative load imbalance present.

Secondly, from the line currents plot, it is also seen that the system is stable, but the oscillations present in the system is more prevalent now. This initial oscillation that is present at each load change is mainly due to the interaction between the cable inductance and the converter capacitance that is present in the system[46]. The negative currents that are seen in the positive pole quantities plotted in the line current graph, is due to the current direction that is defined in the incidence matrix.

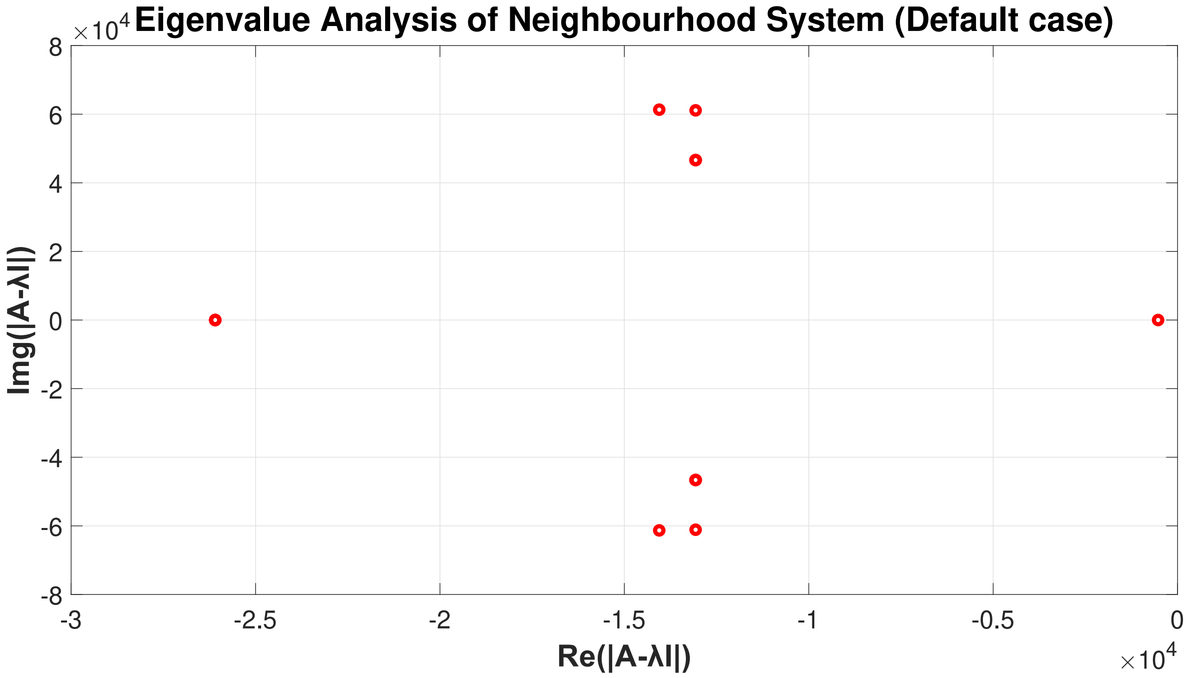

Figure 5.3: Poles of the Monopolar neighbourhood distribution system for default case analysis

Finally, from the eigenvalue analysis plot of the neighbourhood distribution system, it is seen that all the poles derived from the roots of the characteristic equation have only negative real parts present. So, all the poles of the system lie on the left-hand side of the jω-axis, so the system is considered to be stable. As already discussed, the proximity of the poles of the system to the jω-axis is directly proportional to the amplitude of oscillations present in the system. The pole that is present closest to the jω–axis is related to the droop controlled converter present in the system. This pole has a greater impact on the stability of the system, as the droop impedance of the converter is increased this makes the poles go even closer to the jω–axis.

The calculations involved in the bipolar neighbourhood default case, is already discussed in Sec 5.2. As the bipolar neighbourhood system also produces similar results of the positive pole node voltages and line currents in comparison to the monopolar configuration. So to avoid repetition the node voltages and the line currents graphs of the default case bipolar neighbourhood system are presented in the B.

5.3.2. Ship distribution system

The default case analysis of the ship distribution system with 12 nodes and 11 lines, its monopolar configuration is simulated. As mentioned before the cable length value of the line is considered to be different for this system as shown in table 4.3. The parameter values utilized for this system simulation is presented in table 5.2. The positive pole quantities of the ship distribution system are only plotted in the node voltage and the line currents plot. The node voltages and the line currents of this dynamic model are obtained through the state space approach. Their respective plots are shown in Fig 5.4 and 5.5. The poles of this DC ship distribution system are shown in Fig 5.6.

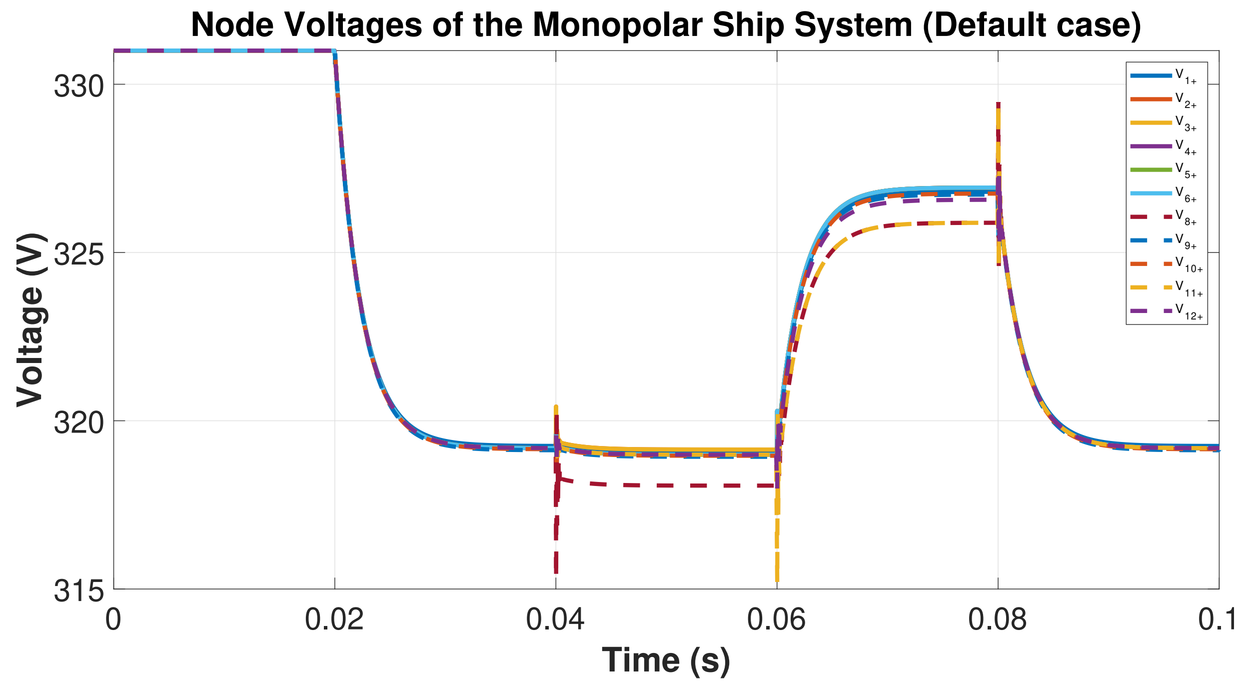

Figure 5.4: Node voltages of the Monopolar ship distribution system for default case analysis

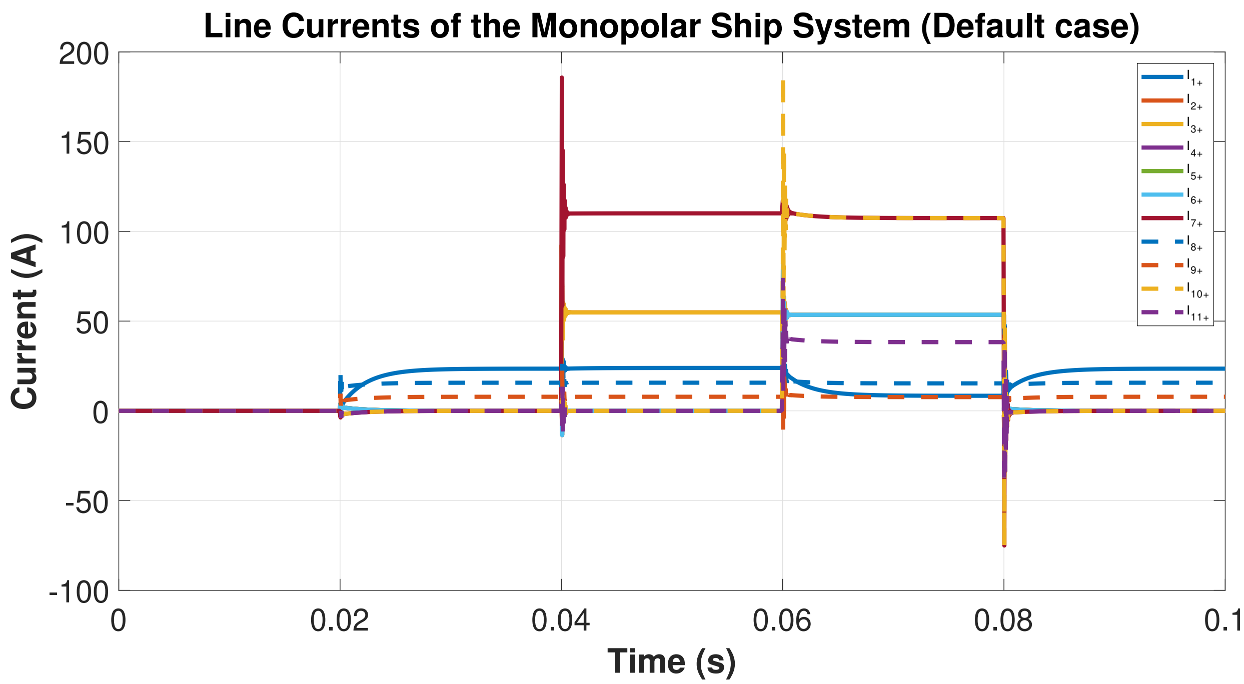

Figure 5.5: Line currents of the Monopolar ship distribution system for default case analysis

From the node voltages plot, it can be seen that the ship distribution system is stable and the power exchange in the system takes place in accordance with the power simulation scenario presented before for the ship distribution system. It can be seen that the oscillations are present in the node voltages plot of the ship distribution system. Again, the converter present in node 1 is droop controlled, so it helps in regulating the system voltage level. Here it takes note of the power simulation scenario that's been taken for that time instance and regulates the system voltage for that time instance. The equilibrium voltage of the nodes is reached when the state derivatives become zero[76]. A similar general trend seen in the neighbourhood system for the node voltages increase and decrease can be also seen in the ship distribution system. As node 7 is a common node present in the system, so it is not considered nor plotted in the node voltages plot as it does not contribute to the study.

From the line currents plot seen in Fig5.5, it can also be said that the system is stable. But the oscillations are also present in the ship distribution system. These oscillations are present due to the interactions between the cable inductances and the converter capacitances that are present in the system. The negative currents that are present in the line currents plot are because of the negative current direction assumed in the incidence matrix.

Table 5.2: Default case parameter values

Cable parameters	Value (unit)
Inductance	$32(\mu\mathrm{H/Km})$
Capacitance	$45(\mathrm{nF/Km})$
Source converter capacitance	$400(\mu\mathrm{F})$
Droop converter capacitance	$400(\mu\mathrm{F})$
Conductance	0
Cable cross section	30 (mm^2)
Droop Impedance (Conv)	$1(\Omega)$

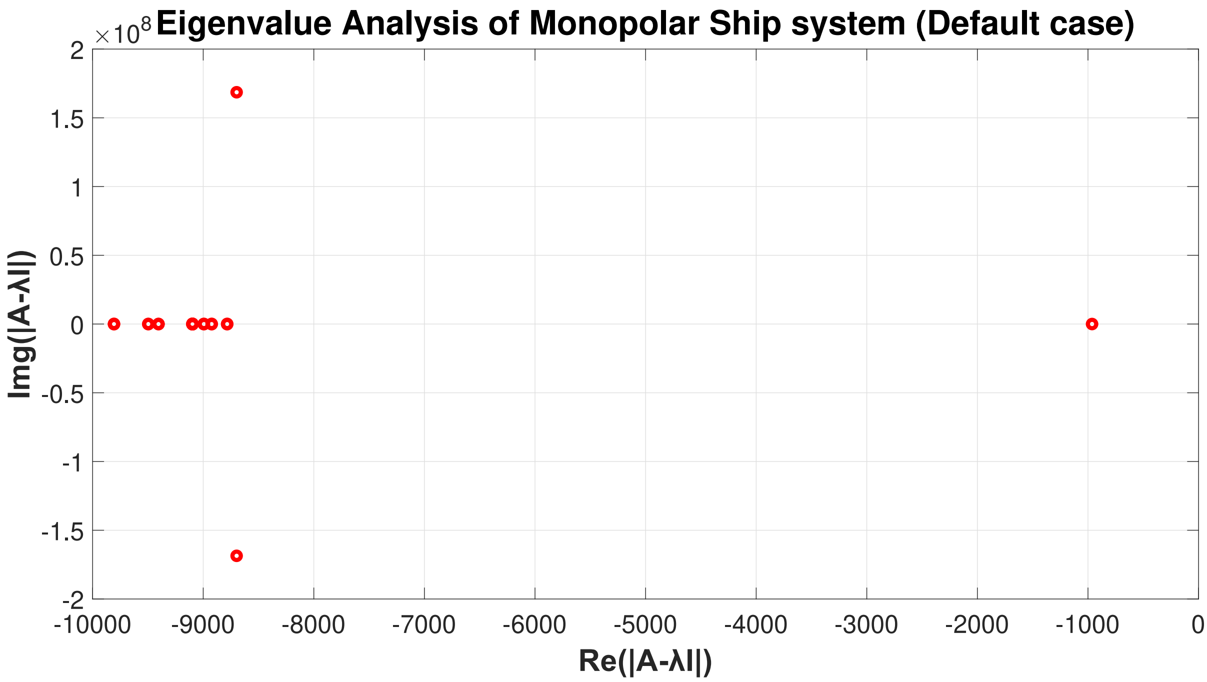

Figure 5.6: Poles of the Monopolar ship distribution system for default case analysis

In the eigenvalue analysis plot of the ship distribution system, it is seen that more number poles are present in comparison with the neighbourhood system. This is mainly because of the greater number of nodes and lines present in the ship distribution system. The poles of this system derived from the roots of the characteristic equation have only negative real parts present, so the system is considered to be stable. The poles are present away from the jω axis so the amplitude of oscillations experienced by the ship system would be less[76]. The pole that is present closest to the jω–axis is related to the droop controlled converter present in the system. Increasing the droop impedance of the converter makes the poles go even closer to the jω–axis. This default case analysis of both the distribution system forms the base with which the resulting plots generated after the analysis are compared with.

This is done in order to be able to get proper inference about the system performance when each of the active parameters is varied. Similarly, the resulting graphs of the positive pole node voltages and line currents of the Bipolar ship distribution are identical to the monopolar results. The node voltages and line currents graph of the Bipolar ship distribution system is presented in Fig A.4-5.

5.4. Variation of Active cable parameters

In this research each of the active parameters(R,L,C) of the cable are individually increased or decreased during the analysis. This is done to assess each of the cable's active parameter's individual influence on the system performance and stability through the sensitivity, stability and the short circuit analysis. Through the results that are obtained from these analyses would form the base for the LVDC cable formulation that would be presented in chapter8. As the cable utilized by the distributions systems could be a single core or multiconductor cables based on the system configuration (Monopolar or Bipolar). These cables have a solid round conductor. So, in this section the description is provided for the basis through which each of the active cable parameters values of LV single core cables or multiconductor cables are individually varied without affecting other cable parameters. The formula described in this sections are defined in terms of its per unit length of the cable.

5.4.1. Cable resistance

The cable resistance for each conductor present in the single core and multi-conductor cables are calculated through equ (5.11) shown below[86]. The resistance of the cable can be increased or decreased by varying the resistivity of the conductor material (ρ) used in the cable. As ρ is directly proportional to the resistance of the cable, using different conductor with increased resistivity leads to the resistance of the cable to be increased [86]. The length and the area of the conductor are maintained the same due to cable capacitance and inductance are directly or indirectly dependent on it. Varying the length and the area of conductor will induce changes in the cable capacitance and inductance. So, only the resistivity of the conductor that is independent to the cable capacitance and inductance variation is used.

The cable resistance is increased by increasing only the resistivity of the conductor material. This done by, firstly utilising different conductor material that has greater resistivity value compared to the conductor material utilized previously. Secondly by using annealed type of the same conductor material that was previously used, the annealed version of conductor material has higher resistivity compared to the normal conductor [31]. Thirdly by adding impurities to the conductor material and increasing the resistivity value to the level required to match the cable resistance value taken for simulation. Also the cable resistance value could be decreased, by utilising pure conductor material without any impurities, this reduces the resistivity of the conductor material[8]. Also different conductor material having resistivity lower than that previously utilised conductor material could be used. For ex when cable utilising Copper conductor (resistivity is 1.68e-8 Ω/m)[31] is replaced by silver conductor (resistivity is 1.56e-8 Ω/m)[31], this reduces the cable resistance.

$$R(perconductor) = \frac{\rho * l}{A} \tag{5.11}$$

5.4.2. Cable Capacitance

Secondly, the cable capacitance variation is discussed. The cable capacitance for the single core and multiconductor cable are calculated through equ(5.12) and (5.13)[8][12]. In equ(5.12) ϵ denotes the permittivity of the insulation material used in the cable, R is the radius of the external sheath and r is radius of the cable conductor[8]. For the multiconductor cable the pole to pole capacitance is calculated through equ(5.13)[12]. Here S denotes the spacing between the conductors (all the conductor present in the cable are equidistant from each other), r1 and r2 are the radius of conductor 1 and conductor 2 of the cable[12]. In equ (5.14) [12]ϵ_0 denotes the permittivity of vacuum and ϵ_r denotes the relative permittivity of the cable insulation material. In both the cable configuration the cable capacitance is individually varied by utilising the relative permittivity of the insulation material ϵ_r[12]. The relative permittivity of the insulation material is independent and doesn't affect the cable inductance or cable resistance when it is varied.

The capacitance of the cable is directly proportional to the relative permittivity of the insulation material ϵ_r.so using different cable insulation material having increased relative permittivity of the insulation (ϵ_r), increases the cable capacitance. Also increasing the sheath radius and decreasing the distance between conductors will increase the cable capacitance value[86]. But these variation in sheath radius and the conductor spacing will have its effect on the cable inductance and the resistance as the geometry of the cable is changed when varying the above set parameters. So only way to increase the capacitance of the cable is by using the different insulating material having different relative permittivity of the insulation material ϵ_r [31]. Varying this relative permeability of insulation material used in cable is the pathway to reach closer to the cable capacitance value used in the simulation.

$$C = \frac{2 * \pi * \varepsilon}{\ln \frac{R}{r}} \tag{5.12}$$

$$C(\text{ pole } - \text{ pole }) = \frac{2 * \pi * \varepsilon}{\cosh^{-1} * \frac{S^2 - r_1^2 - r_2^2}{2 r_1 r_2}} \tag{5.13}$$

$$\varepsilon = \varepsilon_0 \epsilon_r \tag{5.14}$$

5.4.3. Cable Inductance

Thirdly the cable inductance variation is discussed. The cable inductance formula for the single core and multiconductor cable are calculated through equ (5.15) and (5.16)[86]. In these equations,μ_0 is the permeability of free space, R is the radius of external sheath, r is radius of the conductor, D is the distance between conductor(equidistant for this case)and GMr is the geometric radius of the conductor[86].

For both the cable configuration, the inductance of the cable cannot be varied individually without affecting the cable capacitances and resistance [31]. As the variables utilised for calculating the inductance of single core and multi conductor cable are interdependent directly or indirectly with the cable capacitance and resistance. In order to vary the cable inductance, in single core cable the radius of the external sheath and for muticonductor cable the distance between conductors variables are varied [31]. Varying these parameters is done by changing the geometry of the cable that would in turn change the cable capacitance and resistance. They shouldn't be influenced but here the capacitance and resistance are varied. So for cable capacitance, the insulation material is changed based on their relative permittivity of the insulation material ϵ_r and previously defined cable capacitance (before geometrics changes) is brought back even though the geometry of the cable is changed. The cable resistance is brought back to its previously defined cable resistance (before geometrics changes) even though the geometry of the cable is changed. This is done through selecting the right conductor material whose resistivity of the conductor material (ρ) value would support in bringing back the previously defined cable resistance value (before geometrics changes). Through these ways the cable inductance variation is done without affecting the cable resistance and cable capacitance, even though the geometry of the cable is changed.

$$L = \frac{\mu 0}{2\pi} \ln \frac{R}{r} \tag{5.15}$$

$$L(per\ \mathrm{cond}) = \frac{\mu 0}{2\pi} \ln \frac{D}{GMr} \tag{5.16}$$

By following the stated way described above, each of the active parameters(R,L,C) of the cable can be individually increased or decreased for the analysis. The cable's active parameter's individual influence on the system performance and stability is now studied further through the different analyses carried out further through this thesis.

5.5. Summary

In this chapter the different analyses, that's been carried out in the thesis were explained in detail with the procedure followed for each of them. The default case sensitivity and stability analyses results were also presented in this chapter.This default case analysis of both the distribution system forms the base with which the resulting plots generated after the analysis are compared with.This is done in order to be able to get proper inference about the system performance when each of the active parameters is varied.

6 Short circuit analysis

The calculation of the magnitude of peak current flowing through the LVDC system during short circuit are essentially required to incorporate appropriately rated protective equipments into the system and protect the distribution system from severe outages. The short circuit studies conducted could also aid in designing of LVDC cable, as the increase or decrease in ratings of the cable parameters are found to have an effect on the magnitude of peak short circuit current reached by the Bipolar LVDC system after the fault occur[87][88]. So the short circuit studies are conducted on the dynamically modelled LVDC distribution system to comprehend the effect that the cable parameters has on the peak short circuit current reached. Also the results of the default case analysis will be discussed in detail in this chapter.

6.1. Approach

There are many comprehensive approaches to calculate the short circuit current of the DC system available. Mostly, the transient approaches are utilized for the DC systems namely the summation method, where the short circuit current of the sources present are individually calculated and summed. The other method calculates the short circuit current based on the ratio of the system voltages to the pre-fault equivalent resistance of the system and its multiplied by the transient decay time constant. As the distribution system modelled in this thesis is through the state space approach, this model continuously assesses the dynamic behaviour of the discrete elements and energy storage elements present in the system. It doesn't take propagation delay into account, which is considered in the transient approach. So the short circuit analysis method that's utilized needs to suit the model's dynamic requirements. Where the discrete elements and energy storage element's (C,L) variation will have an effect on the magnitude of short circuit peak reached by the system. Finally to suit the system‘s requirements the fault current injection method is formulated for the short circuit analysis. Though this method both the symmetrical (pole-pole) and asymmetrical fault (pole-neutral) are analysed to get a better outlook of cable parameter's influence on the magnitude of the peak short circuit current.

In the fault current injection method, the magnitude of short circuit current is calculated and the fault current calculated is allowed to flow in to the system by injecting it through the converter connected in the faulted node at the specific time instance when the fault occurs. When this fault current flows through the converter, it helps set the node voltage and line currents of the system as the system response to this short circuit situation. Usually in normal case the current injected from the converter is given by (4.2). As we cannot assess the power injected/extracted from the converter during short circuit condition, it is necessary to convert (4.2) in to justifiable form. So the power is converted and given by combining watts and ohms law. The short circuit current that's injected through the converter is after simplifying is given by equ(6.1). Where VN is the faulted node‘s voltage at the time instance in which fault occurs and Requ is the calculated equivalent resistance of the system. This would give us closest approximation of the fault current flowing, due to this faulted converter current helps set the node voltage and line current of the system. The system short circuit response is seen visually through the current flowing in the faulted line connected to the faulted node. The peak short circuit current magnitude achieved by the faulted line depends on the dynamic behaviour of the discrete elements and energy storage elements present in the system too. This formulated fault current injection method perfectly suits the dynamic distribution system model and would support in properly analysing the short circuit fault. Also the fault current injected through the converter shown in equ (6.1) would take different form for pole-pole and pole- neutral fault. More on this would be explained in the forthcoming sections.

$$I_f = \frac{V_n}{R_{equ}} \tag{6.1}$$

6.2. Implementation

In this section, more explanation is given about the implementation of fault current injection method on the short circuit fault analysis. It is implemented differently for the pole-pole and pole- neutral fault analysis. Each of them will be explained in detail in upcoming sections. The short circuit analysis is set to be performed on the bipolar distribution system models of neighbourhood and ship distribution system. Also based on the results that are obtained during short circuit, the node voltage, line currents and the oscillation present in these plots are deeply analysed to form the inference on different cable parameter's influence. The cable parameters whose variation's influence on the magnitude of the short circuit current are looked upon are cable resistance, cable cross section area, cable capacitance and cable length.

6.2.1. Pole to pole fault

First in the pole to pole fault, the positive and negative pole of a particular node present in the bipolar system is considered to be shorted together. Here this fault is a balanced fault and the system remains symmetrical after the fault has occurred. For the neighbourhood system it is considered that the pole-pole fault occurs on load node 3 at t=40ms. In the ship distribution system it is considered that the pole-pole fault occurs on load 10 at t=80ms. The pole to pole fault is implemented in these distribution systems by utilizing the concept of fault current injection method discussed above. Here the fault current injected by the converter connected in the faulted node through the positive and negative pole is given by equ(6.2) shown below. Where V_{f+} is the node voltage at the faulted node's positive and V_{f-} is the node voltage at the faulted node's negative and Requ is the equivalent resistance of the system. The maximum magnitude of fault current flowing through the positive pole when the pole-pole fault occurs is given by equ(6.2). Similarly fault current injected at the negative pole is given as the opposite to the magnitude of current flowing in the positive pole. The current flowing through the neutral would be zero as the system is balanced.

$$I_{f+} = \frac{V_{f+} - V_{f-}}{Requ} \tag{6.2}$$

The cable's active parameter influence on the magnitude of the short circuit formed is analysed during the analysis. The cable's active parameters that are looked at during this analysis are: Inductance, Capacitance, Length and cross section area of the cable. For each of the active parameter's variation the positive pole node voltages and line currents plots are deeply analysed to provide conclusive inferences about the influence that each of the cable's active parameter has on the magnitude of the short circuit current. Also the oscillations present in the node voltage and line currents plots are analysed. The negative pole is not taken into considerations as the system is balanced and they are opposite signed equal in magnitude compared to the positive pole. For the neighbourhood system as the fault occurs at node 3, the positive pole node voltage at node3 in the node voltage plots and then in the line current plots the positive pole quantities at line 2,5 and 7 (lines connected to node 3)are analysed further. For the ship system as the fault occurs at node 10, the positive pole node voltage at node 10 in the node voltage plots and the in the line current plots the positive pole quantities at line 9(line connected to node 10) are further analysed.

6.2.2. Pole to neutral fault

In the pole to neutral fault, the positive and neutral pole of a particular node present in the bipolar system is considered to be shorted together. Here this fault is an unbalanced fault and the system becomes asymmetrical after the fault has occurred. For the neighbourhood system it is considered that the pole-neutral fault occurs on load node 3 at t=40ms. In the ship distribution system it is considered that the pole-neutral fault occurs on load 10 at t=80ms. Here the fault current injected by the converter connected in the faulted node through the positive and neutral pole is given by equ (6.3) shown below. Where V_{fn} is the node voltage at the faulted node's neutral. The maximum magnitude of fault current flowing through the positive pole when the pole-pole fault occurs is given by equ (6.3). Similarly fault current injected at the neutral is given as the opposite to the magnitude of current flowing in the positive pole. The current flowing through the negative pole would be zero as it is given by the negative sum of positive and neutral pole fault currents.

$$I_{f+} = \frac{V_{f+} - V_{fn}}{Requ} \tag{6.3}$$

Again for each of the active parameter's variation the positive pole node voltages and line currents plots are deeply analysed to provide conclusive inferences about the influence that each of the cable's active parameter has on the magnitude of the short circuit current. Also the oscillations present in the node voltage and line currents plots are analysed. The positive and neutral pole quantities are taken into considerations. The neutral quantities are further analysed due to the system being unbalanced as large currents flow through the neutral and the fault effect not being identical as the pole-pole fault. For the neighbourhood system as the fault occurs at node 3, the positive pole and neutral node voltage at node3 in the node voltage plots and then in the line current plots the positive pole and neutral quantities at line 2,5 and 7 (lines connected to node 3)are analysed further. For the ship system as the fault occurs at node 10, the positive pole and neutral node voltage at node 10 in the node voltage plots and the in the line current plots the positive pole and neutral quantities at line 9(line connected to node 10) are further analysed.

6.3. Equivalent resistance

The equivalent resistance calculation is important for assessing the magnitude of short circuit current injected into the system. The equivalent resistance is calculated by considering all the resistance connections present in each of the equipment utilized in the system. The equivalent resistance calculation is done for the ship distribution system. As it is a radial system, the equivalent resistance is calculated by assessing the pathway of currents flowing through the system during short circuit. Also, considering all the resistance connections present in each of the equipment utilized in the ship system. But the neighbourhood system as it is meshed, the equivalent resistance is calculated through a code. Where Kirchhoff's voltage laws are applied at each node and select two points A and B where you want to measure the equivalent resistance. Than arrange the voltage distribution in such a way that it creates 1A current coming from A and exiting at point B. The voltage difference between A and B is the equivalent resistance.

All the source nodes are connected with a battery and all the load nodes are connected with motor as the load unless specified. The resistance ratings considered for both the distribution system is summarised in the table6.1 below. The clevapower batteries with rated nominal voltage: 384V, current:40Ah is utilized for the neighbourhood system[89]. The motor utilized as load here has power rating:3Kwh nominal voltage:220V. For the ship distribution system , the clevapower battery utilized has a nominal voltage: 384V, current:80Ah[89]. The motor utilized as load here has power rating:70Kwh nominal voltage:440V. As the service loads are not energy producing there will be no return flow of current during short circuit so it is avoided in the calculation. For both the systems the droop source impedance is taken as 1 Ω. The final equivalent resistance values calculated for both the distribution system for pole to pole and pole to neutral fault are shown in table6.2:

Table 6.1: Resistance rating of different electrical equipment utilized in the distribution system

Equipment	Neighbourhood System	Ship System
Droop source	$1(\Omega)$	$1(\Omega)$
Battery	$700(\ \mathrm{m}\Omega)$	$375(\ \mathrm{m}\Omega)$
Motor	$1(\Omega)$	$0.1(\Omega)$
Converter Switches	$100(\ \mathrm{m}\Omega)$	$100(\ \mathrm{m}\Omega)$

Table 6.2: Equivalent resistance calculated for different faults

Fault	Equivalent Resistance (Ω)
Neighbourhood Pole-pole	0.8194
Neighbourhood pole-Neutral	0.727
Ship pole-pole	0.0473
Ship Pole -neutral	1.1134

6.4. Default case analysis

In the default case analysis,the values considered for this short circuit analysis is same as the previously considered default case analysis utilized for the sensitivity and stability analysis. Again, the results found through the default case analysis would be vital, as it is used to compare with other active parameter variations results. This default case simulation will be carried out for both the Bipolar ship and neighbourhood distribution system, as they make the base for the short circuit studies to be carried out. Through this analysis, the resulting node voltages and line currents of the positive pole (Pole-Pole fault) and positive and neutral pole (Pole-Neutral fault) are only discussed. As the negative pole quantities tend to be equal in magnitude but opposite in sign to the positive pole, they are not further discussed in the line current plots (Pole-Pole fault). The parameter values utilized for this system simulation is the same as the one previously presented in table 5.1and 5.2.

6.4.1. Pole to pole fault

In the pole to pole fault, the default case analysis is performed on both the bipolar neighbourhood and ship distribution system. The pole to pole fault is set to occurs at t=40ms at load node 3 in the neighbourhood system. For the ship system the pole to pole fault set to occur at t=80ms at load node 10. The node voltages and line currents are plotted for both the distribution system for this short circuit analysis.

First, the node voltages plots of the neighbourhood and ship distribution system are shown in Fig1 and 3 below. It can be seen from the node voltages plots that till the fault instance the distribution system are stable and the power exchange in the system takes place in accordance with the power simulation scenario presented before. After the fault occurs in both the distribution system, there is a sharp decay in the positive pole node voltage curve and then after a few more milliseconds the equilibrium is reached.

The equilibrium node voltage reached by these nodes after the fault mainly depends on the magnitude of the short circuit current reached by the system. The higher magnitude short circuit current reached the lower the equilibrium node voltage is set by the droop. It can be seen through the plots that the equilibrium node voltage achieved by the faulted node(Node 3 for neighbourhood and Node 10 for ship system) is the lowest among the other nodes present in the system. Also for reference the node voltage plots of the negative pole are also plotted. It shows inherently opposite curve trend to the positive pole quantities as the negative pole quantities tend to be equal in magnitude but opposite in sign to the positive pole.

Secondly from the line currents plots of the neighbourhood and ship distribution system are shown in Fig2 and 4 below. The negative currents that are seen in the positive pole quantities plotted in the line current graph, is due to the current direction that is defined in the incidence matrix. It can be seen that the system is stable, but the oscillations present in the system are more prevalent after the fault instance. After the fault occurs at a particular node, the lines connected to it reaches peak short circuit current magnitude to satisfy the higher load demand of that faulted node. So, it is seen in the graphs too, that the lines connected to the faulted node at the neighbourhood (lines2,5 and 7) and ship distribution system(Line 9) reaches higher peak magnitude of oscillating short circuit current after the fault occurs for a few milliseconds. The peak magnitude of short circuit current reached by the lines during pole to pole fault is greater than the pole to neutral fault. Then the equilibrium is attained for the rest of the time. These peak magnitudes of the short circuit current reached by these lines are also set to be influenced by the active parameters of the cables. To comprehend this better, through this short circuit analysis each of the active cable parameter's values are varied and the influence this has on the peak short circuit currents and the node voltages are thoroughly analysed and compared with this default case.

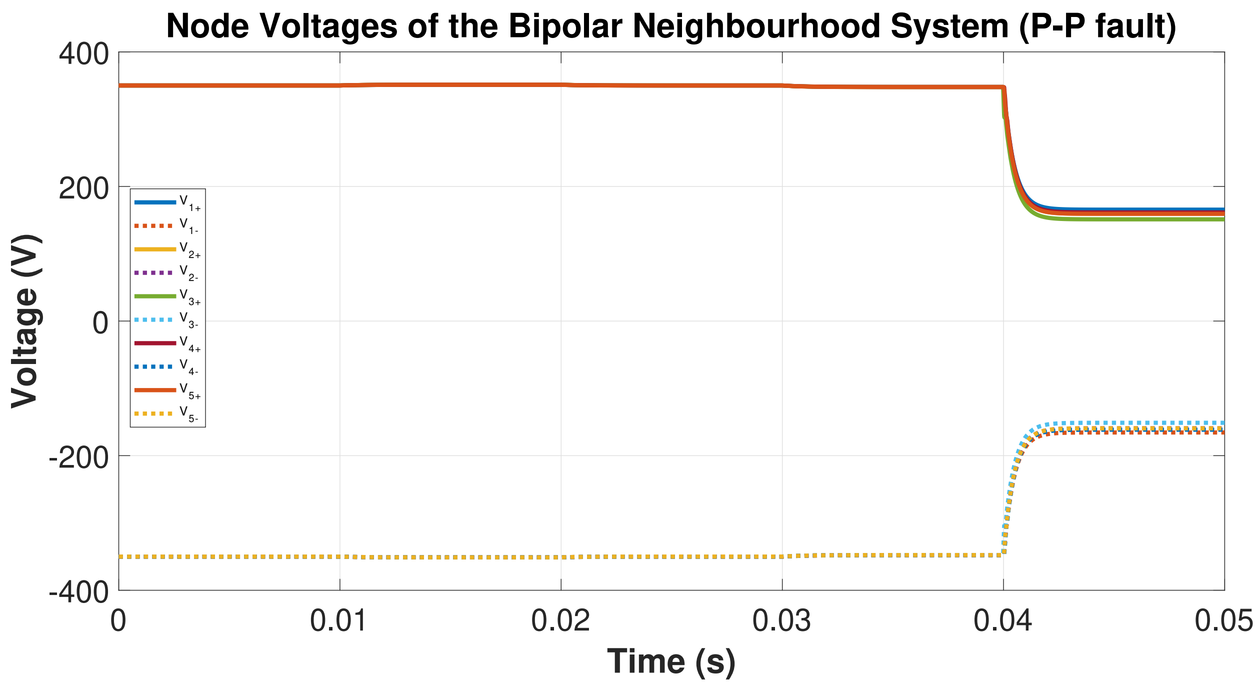

Figure 6.1: Pole to pole fault node voltages plot of Bipolar Neighbourhood system

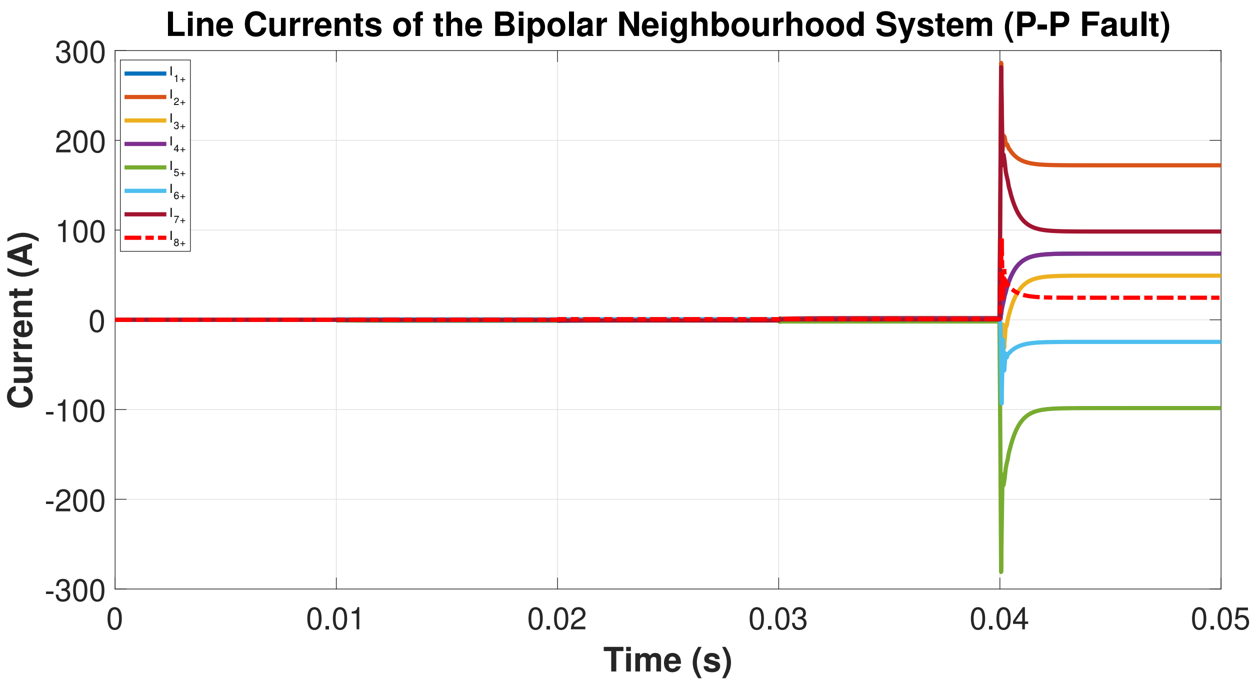

Figure 6.2: Pole to pole fault Line currents plot of Bipolar Neighbourhood system

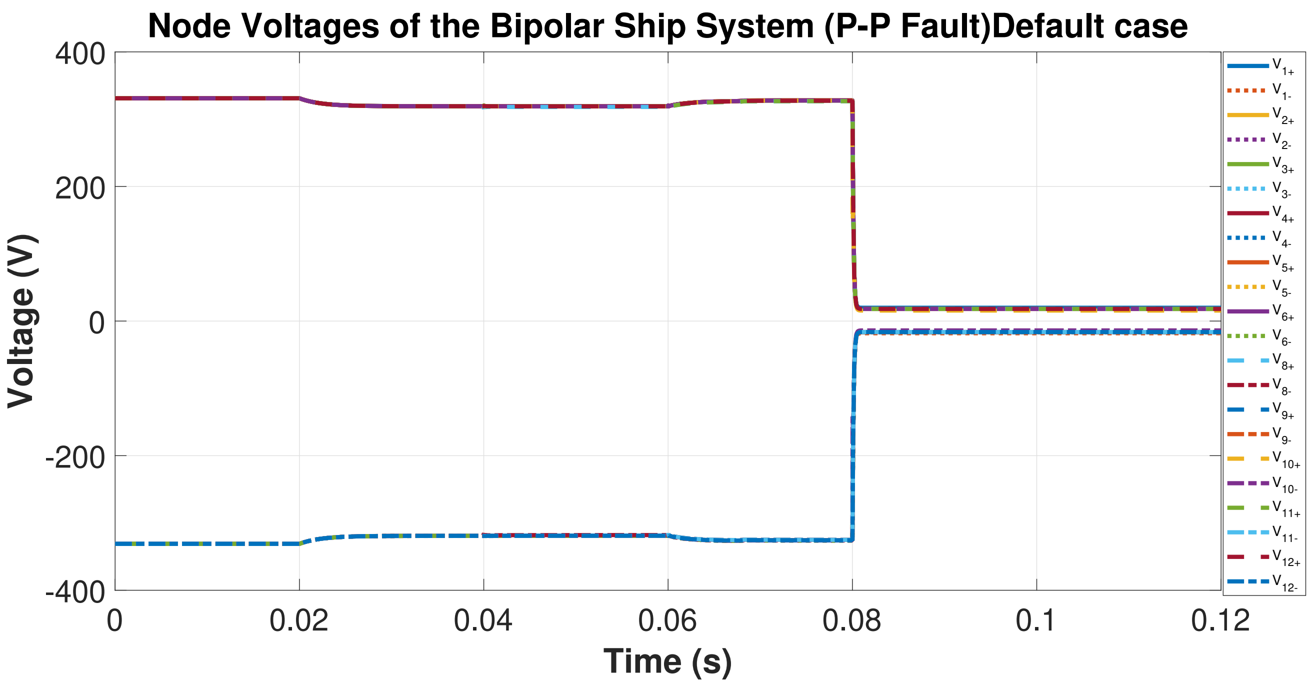

Figure 6.3: Pole to pole fault node voltages plot of Bipolar Ship system

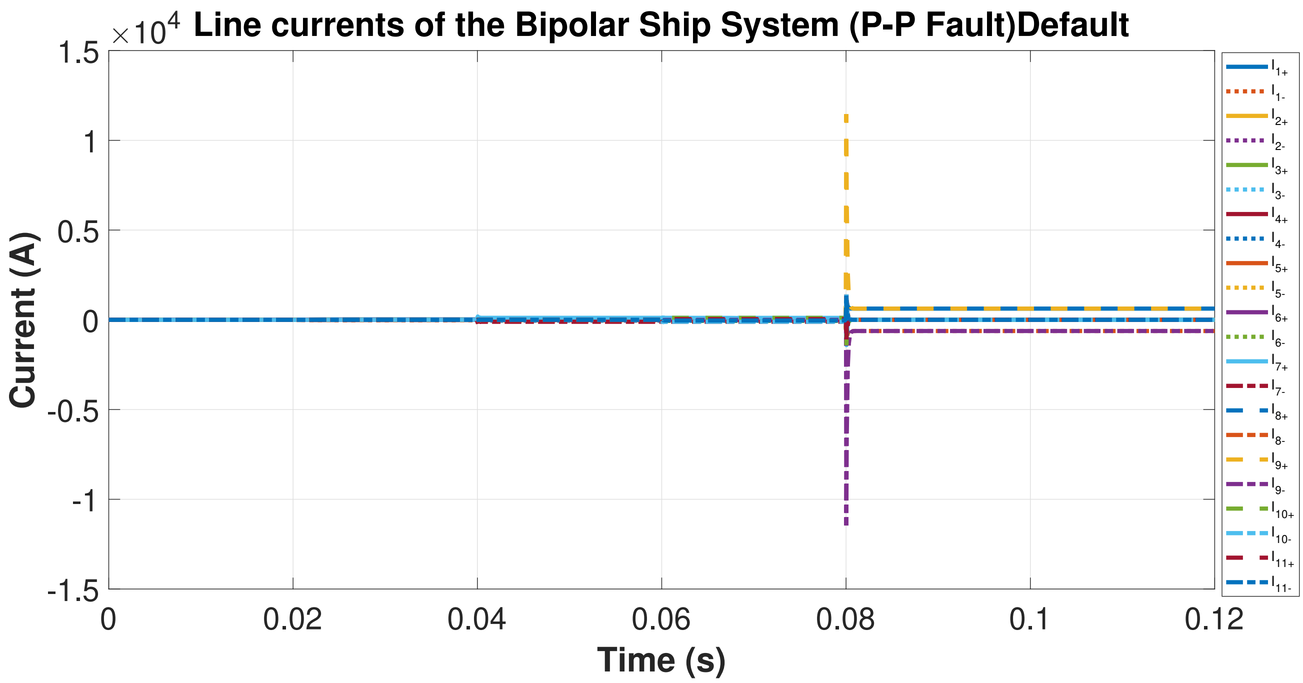

Figure 6.4: Pole to pole fault line currents plot of Bipolar Ship system

6.4.2. Pole to neutral fault

In the pole to neutral fault, the default case analysis is performed on both the bipolar neighbourhood and ship distribution system. The pole to neutral fault also set to occurs at t=40ms at load node 3 in the neighbourhood system. For the ship system the pole to neutral fault set to occur at t=80ms at load node 10. The node voltages and line currents are plotted for both the distribution system for this short circuit analysis. Here in the analysis, both the positive and neutral pole quantities are plotted as it is asymmetrical fault.

First, the node voltages plots of the neighbourhood and ship distribution system are shown in Fig5 and 7 below. It can be seen from the node voltages plots that till the fault instance the distribution system are stable and the power exchange in the system takes place in accordance with the power simulation scenario presented before. After the fault occurs in both the distribution system, there is a sharp decay in the positive pole node voltage curve, there is a sharp rise in neutral node voltage curve and then after a few more milliseconds the equilibrium is reached. The equilibrium node voltage reached by the positive pole of the nodes after the fault mainly depends on the magnitude of the short circuit current reached by the system. The higher magnitude short circuit current reached the lower the equilibrium node voltage is set by the droop. It can be seen through the plots that the equilibrium node voltage achieved by the faulted node (Node 3 for neighbourhood and Node 10 for ship system) is the lowest among the other nodes present in the system. As there are large return currents flowing through the neutral after the asymmetrical fault occurrence, the neutral conductor comes in contention. So the positive and neutral pole quantities are further analysed during this short circuit analysis.

Secondly from the line currents plots of the neighbourhood and ship distribution system are shown in Fig6 and 8 below. The negative currents that are seen in the positive pole quantities plotted in the line current graph, is due to the current direction that is defined in the incidence matrix. It can be seen that the system is stable, but the oscillations present in the system are more prevalent after the fault instance. It is seen in the graphs too, that the lines connected to the faulted node at the neighbourhood (lines2,5 and 7) and ship distribution system(Line 9) reaches higher peak magnitude of oscillating short circuit current after the fault occurs for a few milliseconds. The peak magnitude of short circuit current reached by the lines during pole to neutral fault is lesser than the pole to pole fault. The equilibrium is not achieved after the fault occurrence because of the continuous discharge by the energy storage elements connected between the pole and neutral conductors present in the system. These peak magnitudes of the short circuit current reached by these lines are also set to be influenced by the active parameters of the cables. To comprehend this better, through this short circuit analysis each of the active cable parameter's values are varied and the influence this has on the peak short circuit currents and the node voltages are thoroughly analysed and compared with this default case.

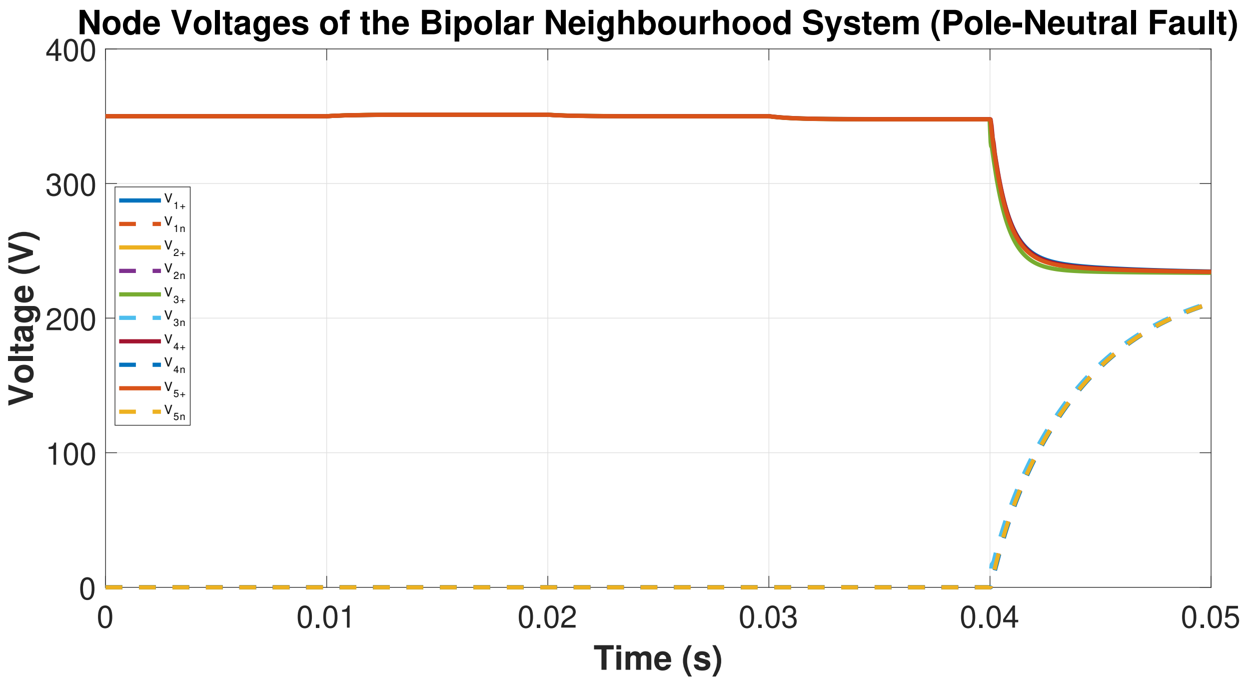

Figure 6.5: Pole to neutral fault node voltages plot of Bipolar Neighbourhood system

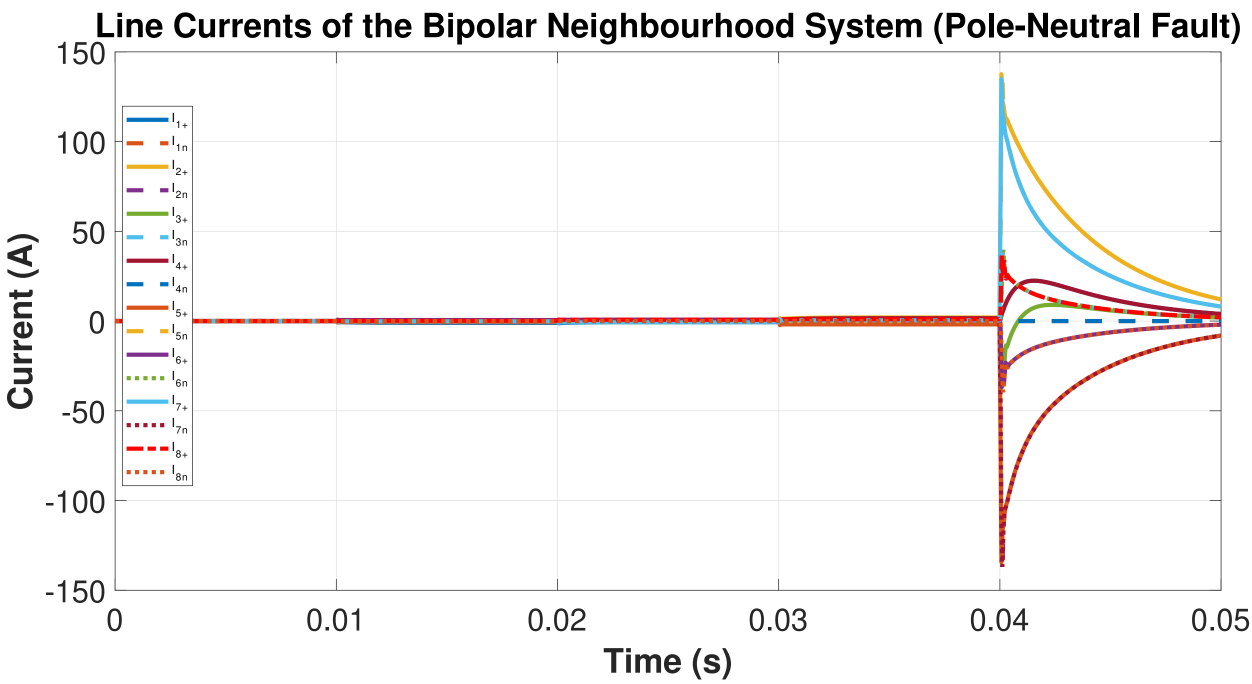

Figure 6.6: Pole to neutral fault Line currents plot of Bipolar Neighbourhood system

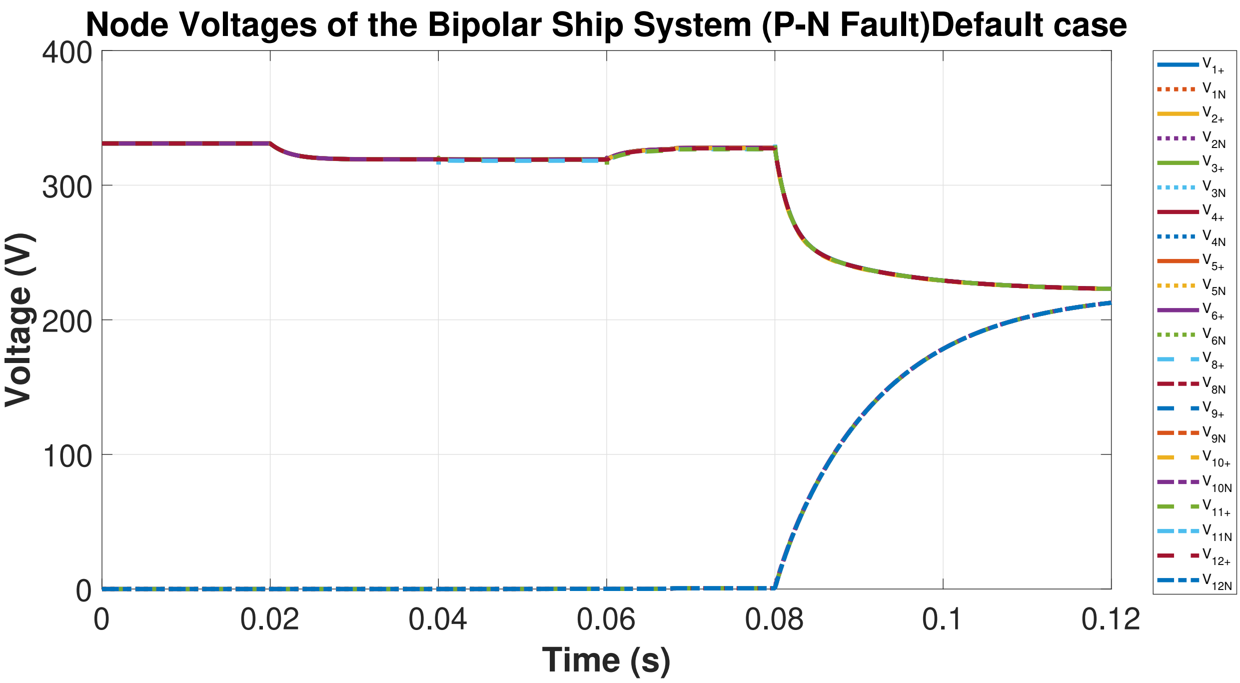

Figure 6.7: Pole to neutral fault node voltages plot of Bipolar Ship system

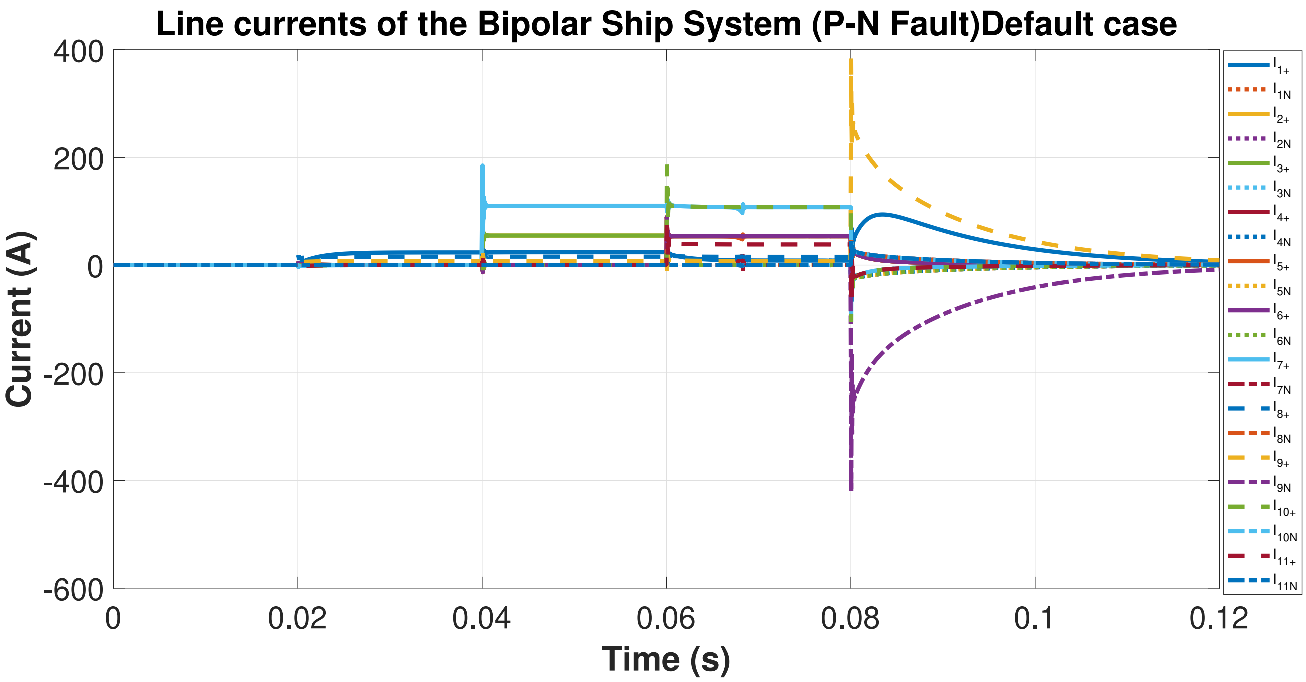

Figure 6.8: Pole to neutral fault Line currents plot of Bipolar Ship system

6.5. Summary

In this chapter, the short circuit analysis that is performed on the distribution system is explained in detail. Both Pole to pole and pole to neutral faults are conducted in this model to analyse the active cable parameter's influence on the peak short circuit current reached by the system. The procedures followed for both the type of faults were described extensively. The equivalent resistance calculations done for both the systems and the resistance ratings taken for each of the system elements were discussed. Also the default case short circuit analysis was performed on both the distribution system for the pole to pole and pole to neutral faults.

7

Results and Discussion

In this results section, the sensitivity, stability, short circuit and accuracy analysis that is performed in both neighbourhood and ship distribution system will be discussed. Here in this analysis the resulting node voltages and line currents of the positive pole quantities are only discussed. As the negative pole quantities tend to have a similar magnitude compared to the positive pole but in the opposite sign and the neutral quantities are zero due to the system being in balanced condition for the pole to pole systems. So, in order to get better clarity of the results found, only positive pole quantities are plotted in the node voltage and line current graphs for pole to pole systems.For the bipolar systems during pole to neutral fault analysis, as the system becomes unbalanced both the pole and neutral quantities are plotted. The generated results from all these analyses mentioned above would surely help in better assessment and designing of the LVDC cables, as all the active parameters are varied to get this comprehensive outlook. The results found through the analysis carried out on the active parameter variation would be compared with the default case analysis.

7.1. Sensitivity and stability analysis:Monopolar Configuration

In this analysis, the active parameters that are expected to have an influence on the system performance and the stability of the system are considered and varied. These active parameters are cable inductance, cable capacitance, cable cross-section(indirectly resistance),cable length, droop impedance and the source and load converter capacitance. The sensitivity and stability analysis are performed by varying the active parameters. The influence this has on node voltages, line currents and the stability of the system are studied through this analysis. This analysis is set to be performed in both distribution systems under monopolar and bipolar configuration.

In the neighbourhood distribution system and ship distribution system, the sensitivity and stability analysis are carried out. In this analysis, each of the active parameter's values is set to be varied individually. The general trend of the system performance and stability due to this variation is observed. This observation is tabulated for each of the active parameters individually. During this analysis, few active parameters values are varied above and below the rated/permissible values for a LV cable. This is done in order to deeply assess the general trend and influence each of the active parameter has on the cable performance and the stability of the system. The generated results from this study would surely help in better assessment and designing of the LVDC cables as all the active parameters are involved in it. This comprehensive study will also support in understanding the influence that active parameters have on system performance and stability.

7.1.1. Cable inductance

In this analysis, first the inductance of the cable is varied, the rest of the active parameter's values are maintained as it is in the default condition. This inductance value is varied in both the ship and neighbourhood monopolar distribution system. The default case inductance value is taken as 32(μH/Km) for both the distribution system. To get the general trend of how the inductance variation would affect the system performance, the inductance value is increased and decreased with respect to the default case value. The inductance value that is taken for this analysis are 1.2,12, and 100(μH/Km). For these set inductance values the node voltages, oscillations, line currents and stability of the system are analysed separately.

Major variation can be seen in the stability analysis plots shown in Fig7.1 and Fig7.2. Here the poles derived through roots of the characteristic equation of both the distribution system can be seen plotted away from the jω-axis as the inductance value is decreasing. As said before the amplitude of oscillation present in the system tends to increase as the poles of the system lie closer to the jω axis. These oscillations directly affect the stability of the distributions system and need to be taken into account. The influence of the inductance variation in node voltages and the line currents plots can be seen in the appendix B. From both these sets of plots, there is a certain trend that can be deducted as the inductance value is increased. The trend is that there are more visible oscillations present in both line current and node voltage plots of the distribution system as the cable inductance value is increased. Also, the equilibrium node voltage and line current are reached with fewer oscillations when the cable inductance value is decreased. So, it is inferred through these plots, that as the cable inductance value is decreased this leads to the distribution systems become more stable and fewer oscillations are present. This inductance variation has no distinct effect on the equilibrium node voltage and line current achieved by the distribution system[31]. A summary table of the findings from the stability and sensitivity analysis carried out for the cable inductance variation is shown in table7.1 below.

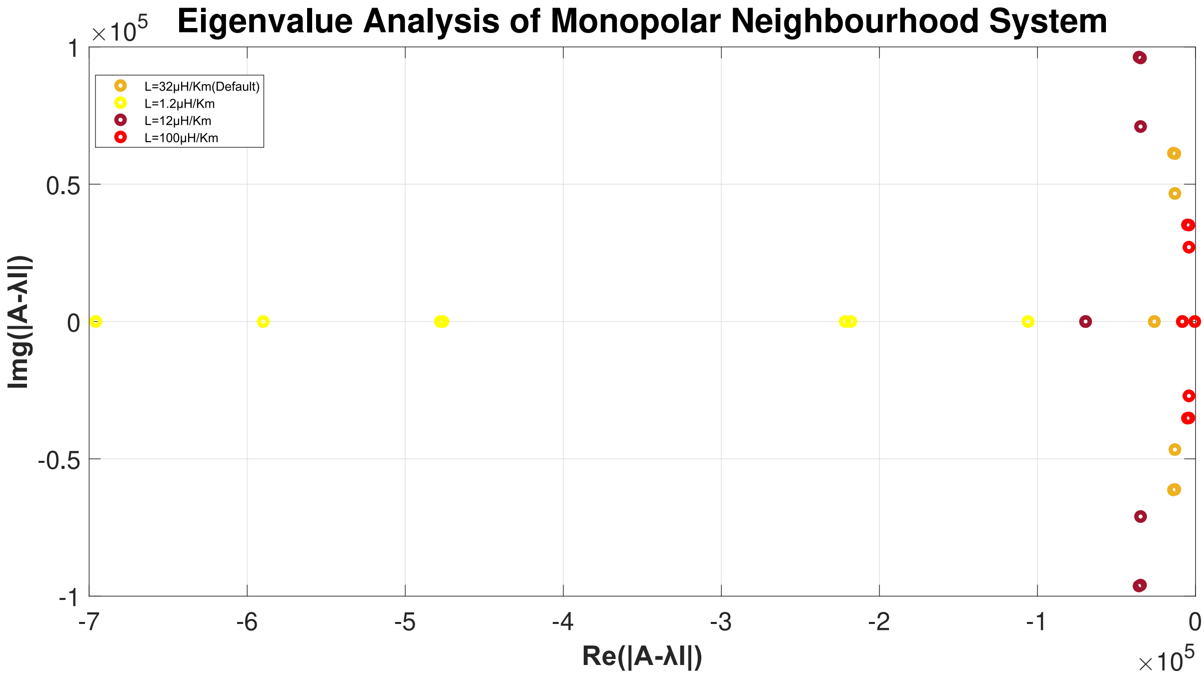

Figure 7.1: Influence of cable inductance variation in the eigenvalue plots of neighbourhood system

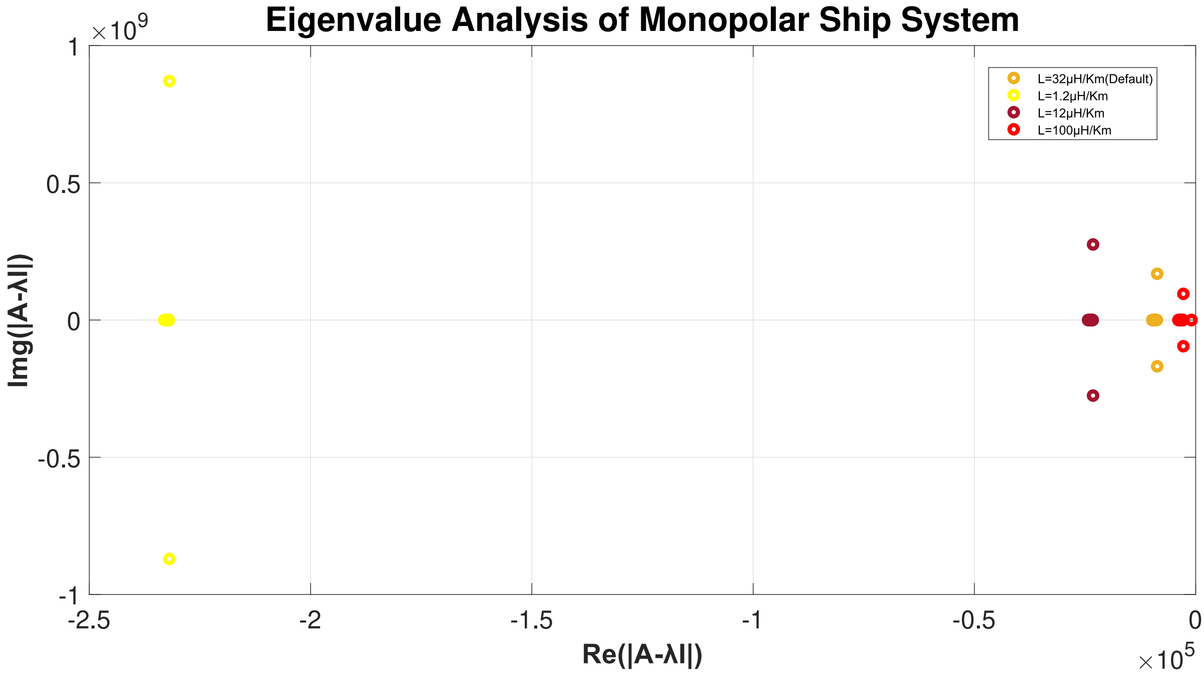

Figure 7.2: Influence of cable inductance variation in the eigenvalue plots of ship system

Table 7.1: Inference from the analysis carried out for the cable inductance variation

Inductance (μH/Km)	Stability	Node Voltage	Line current	Oscillation
L=1.2	**Most stable compared -all cases**	**Not affected**	**Not affected**	**Least oscillation compared -all cases**
L=12	**Increased stability compared- case 3**	**Not affected**	**Not affected**	**Increased oscillation compared - case 1**
L=100	**Decreased stability compared- all cases**	**Not affected**	**Not affected**	**Most oscillation compared- all cases**

7.1.2. Cable capacitance

The capacitance of the cable is varied, the rest of the active parameter's value is maintained as it is in the default condition. This stability and sensitivity analysis carried out for the cable capacitance variation in both ship and neighbourhood monopolar distribution systems. The default case line capacitance or cable capacitance value is taken as 45(nF/Km) for both the distribution system. The general trend of how the capacitance variation would affect the system performance, when the cable capacitance value is varied above and below the default case value is analysed.

The capacitance value that is taken for this analysis is 20,100, and 300(nF/Km). For these set capacitance values the node voltages, oscillations, line currents and stability of the system are analysed. As seen in Fig A.10 and Fig A.11, there is no variation in the stability analysis plots as the capacitance value is changed. Also, the capacitance variation also has no effect on the node voltages and line currents shown in Fig A.12- A.15.This is mainly because the ratings of converter capacitance value (400μF) are far greater than the line capacitance(45nF/Km) ratings. So, it is inferred through these plots that the variation of line capacitance has no effect in influencing the stability, node voltage and line current achieved by the monopolar distribution system. But the line capacitance variation is seen to have an effect in the bipolar distribution system, more on this in the upcoming sections. A summary table of the findings from the stability and sensitivity analysis carried out for the cable capacitance variation is shown in table 7.2 below.

Table 7.2: Inference from the analysis carried out for the cable capacitance variation

Capacitance (nF/Km)	Stability	Node Voltage	Line current	Oscillation
C=20	No changes	No changes	No changes	No changes
C=100	No changes	No changes	No changes	No changes
C=300	No changes	No changes	No changes	No changes

7.1.3. Cable cross section

In this analysis, now the cable cross-section is varied and the rest of the active parameter's value is maintained as it is in the default condition. As the resistance of the cable is calculated using the formula shown in (5.10), it shows that the cable resistance is inversely propositional to the cross-section area of the cable (A). So varying the cross-section area of the cable is indirectly varying the cable resistance. The cable cross-section value is varied in both the ship and neighbourhood monopolar distribution system. The default case cross-section value is taken as 20(mm^2) for neighbourhood and 30(mm^2) for the ship distribution system respectively. The cross-section value that is taken for this analysis is 5,100, and 400(mm^2). For these set cross-section values, the variation in node voltages, oscillations, line currents and stability of the system is analysed.

The first difference can be seen in the stability analysis plots, that is shown in Fig 7.3 and Fig 7.4. In these plots, it shows that the poles of the distribution system derived from their characteristic equation lie closer to the jω axis as the cross-section value is increased. This increase in the cross-section area leads to a decrease in the cable resistance and the stability of the system tends to decrease due to this trend[34]. The amplitude of oscillation present in the system increases and these oscillations directly affect the stability of the distributions system. The influence of the cross-section variation in node voltages and the line currents plots can be seen in Fig 7.5,7.6 and in the appendix B. The equilibrium node voltage achieved by the system also tends to decrease as the cross section area increases and the line resistance of the cable decreases.The equilibrium line current achieved by the system, doesn't show any variation to the cross section variation. There is more visible oscillation present, the positive peak amplitude and the negative peak amplitude of oscillation in both the node voltage and line currents plots is seen to be increasing as the cable cross-section value is increased. So, it is inferred through these plots, that as the cable cross-section value is decreased the cable resistance increases and this leads to the distribution systems become more stable, node voltage decreases and fewer oscillations are present. A summary table of the findings from the stability and sensitivity analysis carried out for the cable cross-section variation is shown in table 7.3 below.

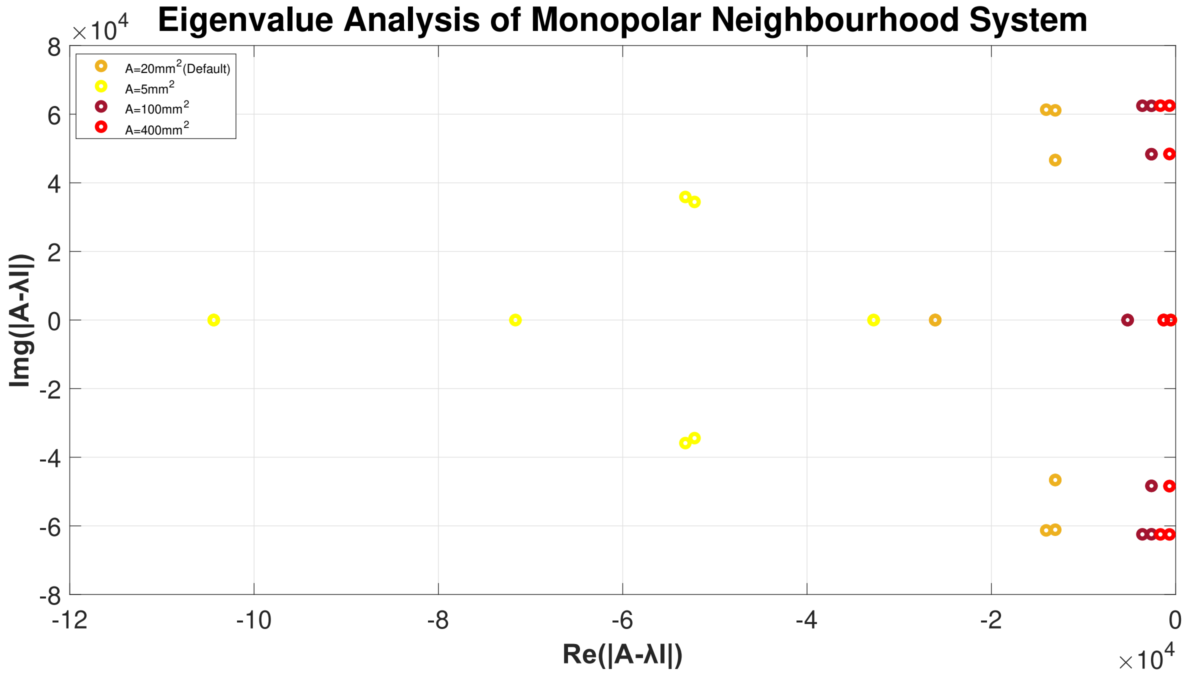

Figure 7.3: Influence of cable cross section variation in the eigenvalue plots of neighbourhood system

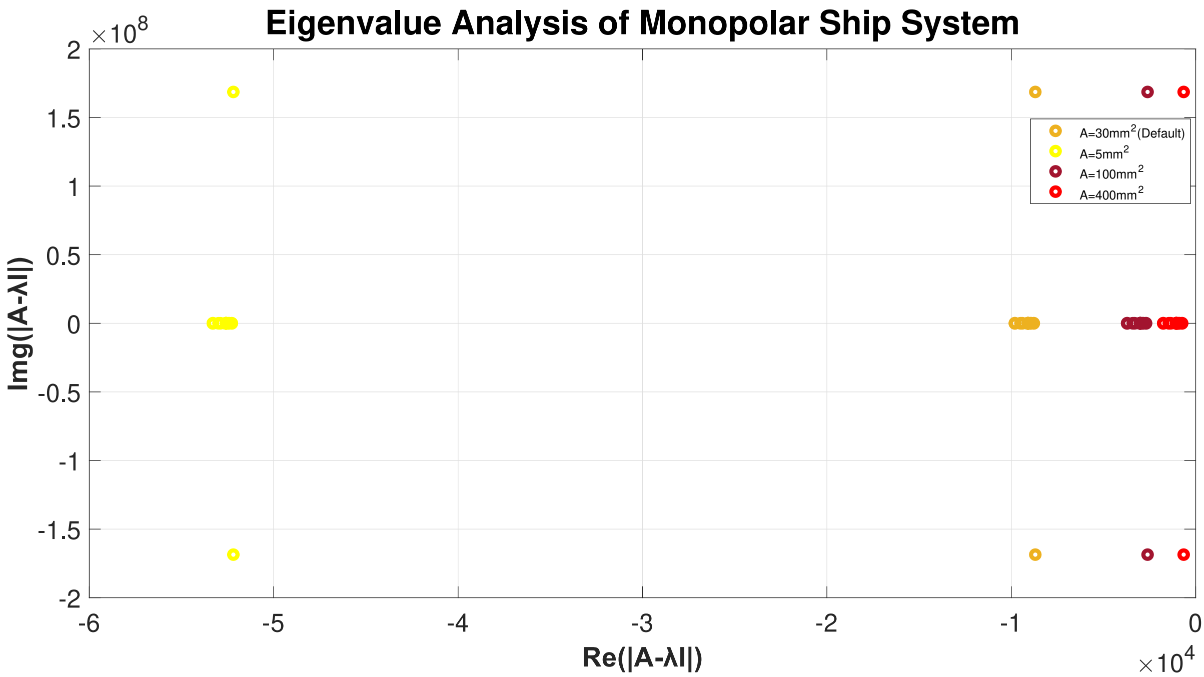

Figure 7.4: Influence of cable cross section variation in the eigenvalue plots of ship system

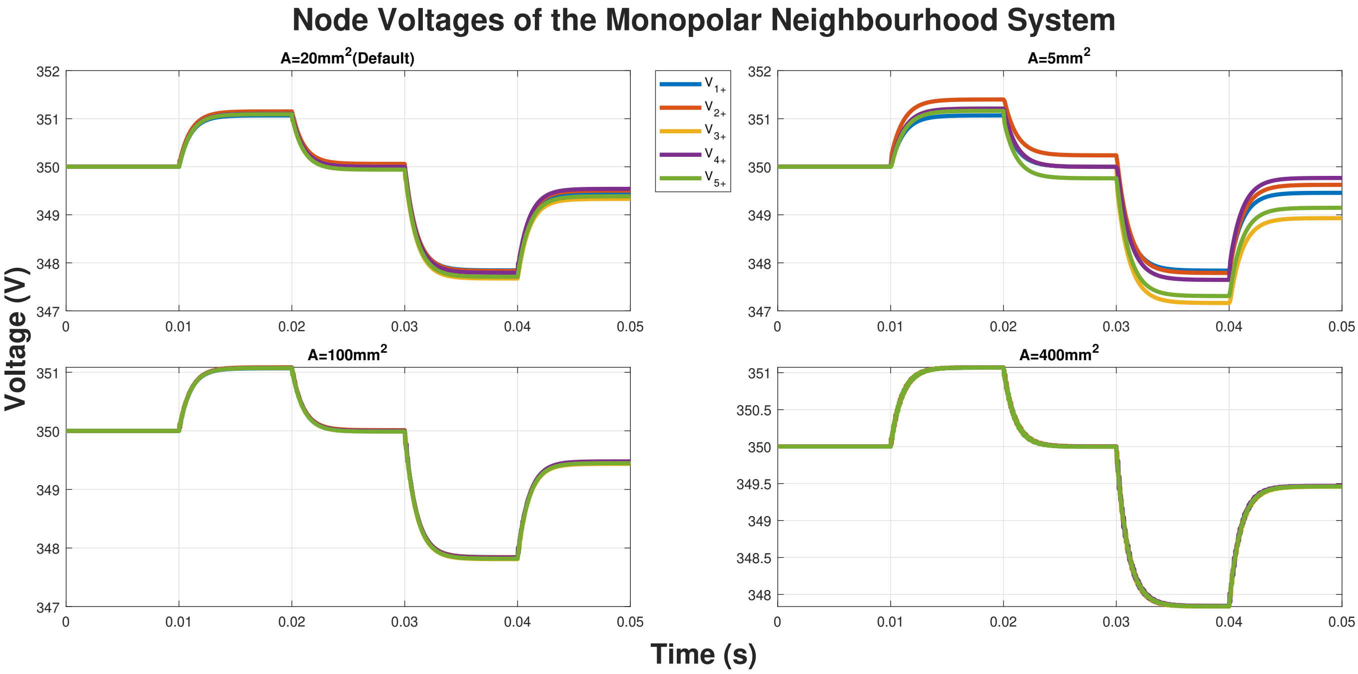

Figure 7.5: Influence of cable cross section variation in the nodevoltages of neighbourhood system

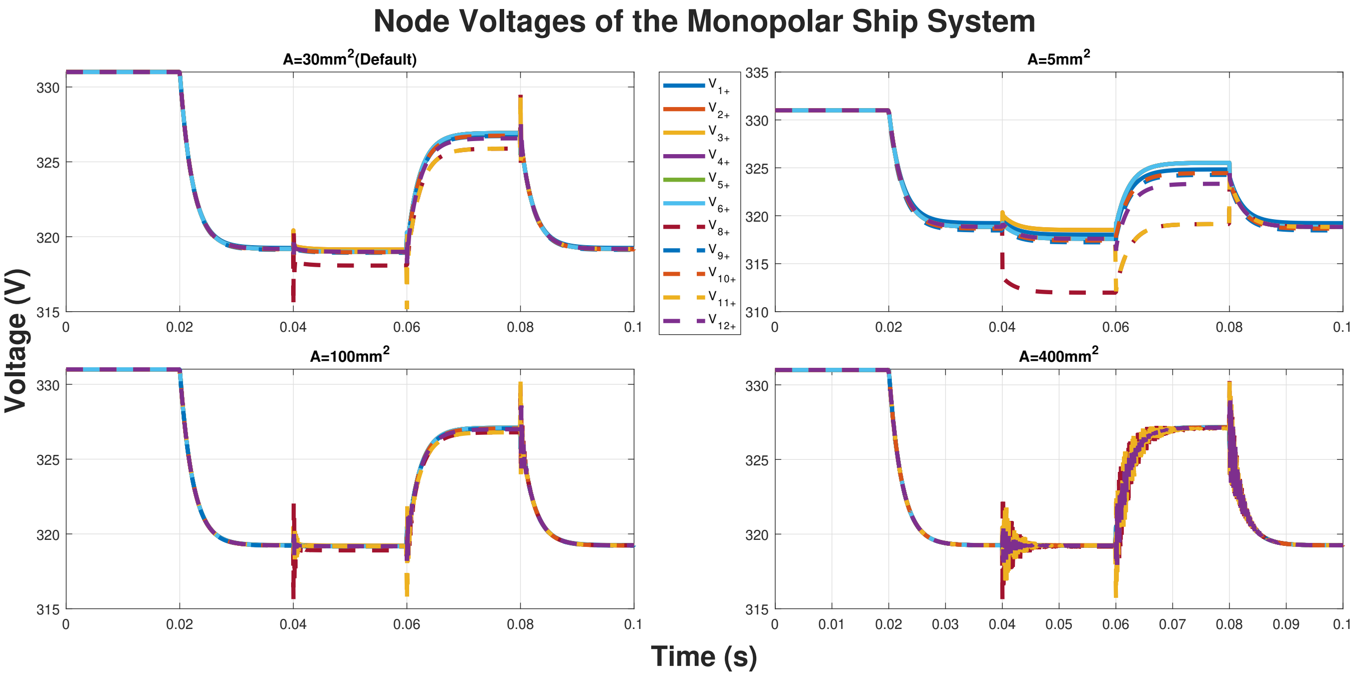

Figure 7.6: Influence of cable cross section variation in the nodevoltages of ship system

Table 7.3: Inference from the analysis carried out for the cable cross section variation

Cross Section (mm^2)	Stability	Node Voltage	Line current	Oscillation
A=5	Most stable	Slight decrease	Decrease in positive and negative peak amplitude of oscillation	Least oscillation
A=100	Increased stability compared-case 3	Increase compared to default	Slight increase compared to default	Increased oscillation compared-case-1
A=400	Least stability	Increase compared to A=100mm^2	Slight increase compared to A=5mm^2	Most oscillation

7.1.4. Source converter capacitance

In this analysis now the capacitance of the source converter is varied, the rest of the parameter's values are maintained as it is in the default condition. The main reason for doing this analysis is to study the influence that power electronic converter has on the cable and system performance. The power electronic converter connected to the source is considered as source converter. The nodes at which source converters are connected to are node 2 and 4 in neighbourhood and node 2 till 6 in the ship distribution system. The default case source converter capacitance value is taken as 400(μF) for both the distribution system. The source converter capacitance value that is taken for this analysis is 100,500, and 700(μF).

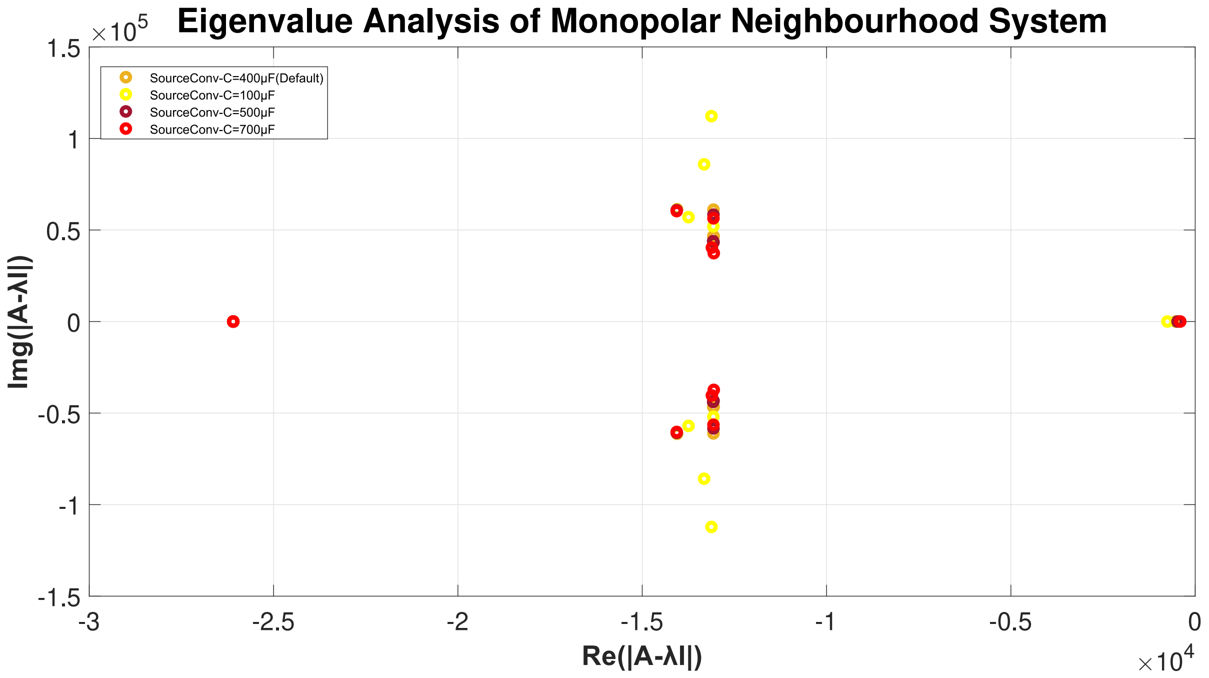

Figure 7.7: Influence of source converter capacitance variation in the eigenvalue plots of neighbourhood system

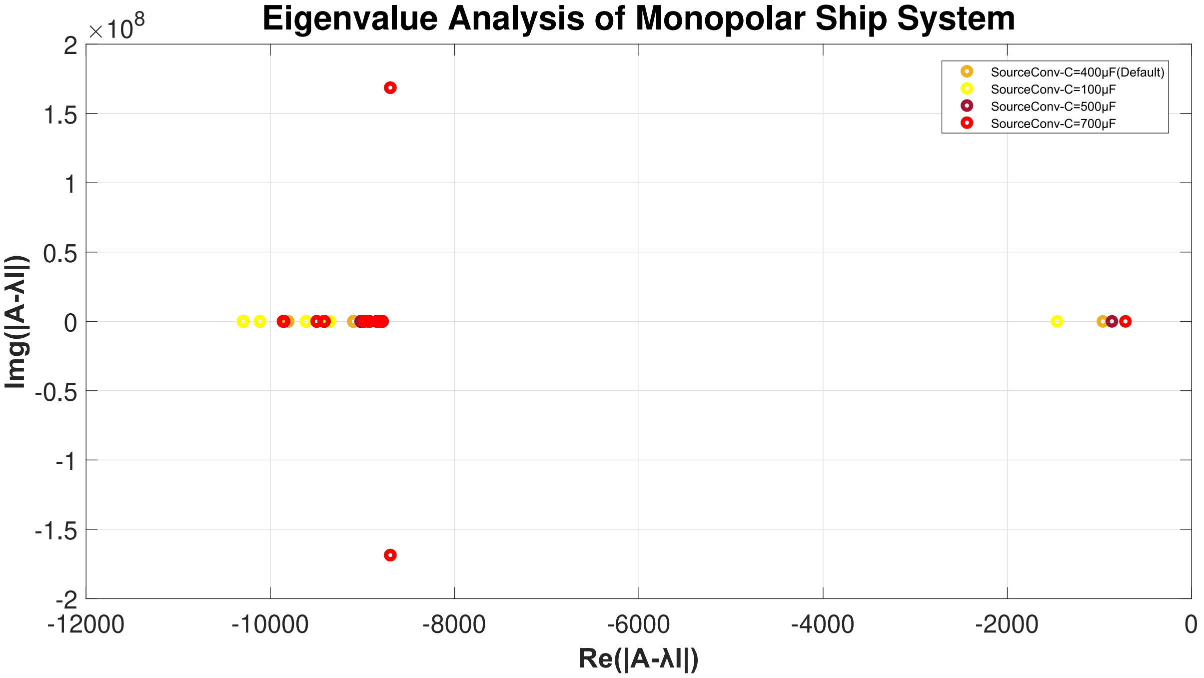

Figure 7.8: Influence of source converter capacitance variation in the eigenvalue plots of ship system

For these source converter capacitance values, the variation in the node voltages, oscillations, line currents and stability of the system is analysed. First, it can be seen in the stability analysis plots that are shown in Fig 7.7 and Fig 7.8. It shows that as the source converter capacitance value is increased, the poles of the distribution system derived from their characteristic equation lie closer to the jω axis. The amplitude of oscillation present in the system increases and these oscillations affects the stability of the distributions system. The influence of the source converter capacitance variation in node voltages and the line currents plots can be seen in the appendixB. There is more visible oscillation present as the source converter capacitance value is increased. There is more oscillation present in the lines connected to the source node as the source converter capacitance value is decreased. Also, more oscillations are seen to be present in other lines not connected to source as the converter capacitance value is increased. So it is inferred that, as the source converter capacitance is decreased this leads to the distribution systems become more stable and less oscillations are present. The equilibrium node voltage and line current achieved by the distribution system is not affected by the source converter capacitance variation. A summary table of the findings from the stability and sensitivity analysis carried out for the source converter capacitance is shown in table 7.4 below.

Table 7.4: Inference from the analysis carried out for the source converter capacitance variation

Source Converter Capacitance (μF)	**Stability**	**Node Voltage**	**Line current**	**Oscillation**
C=100	**Most stable**	**Not affected**	**Not affected**	**Least oscillation**
C=500	**Increased stability compared-case 3**	**Not affected**	**Not affected**	**Increased oscillation compared - case 1**
C=700	**Least stability**	**Not affected**	**Not affected**	**Most oscillation**

7.1.5. Load converter capacitance

The capacitance of the load converter is varied, the rest of the parameter's values are maintained as it is in the default condition. The power electronic converter connected to the load is considered as load converter. The nodes at which load converters are connected to are node 3 and 5 in neighbourhood and node 8 till 12 in the ship distribution system. The default case load converter capacitance value is taken as 400(μF) for both the distribution system. The load converter capacitance value that is taken for this analysis is 100,500, and 700(μF).

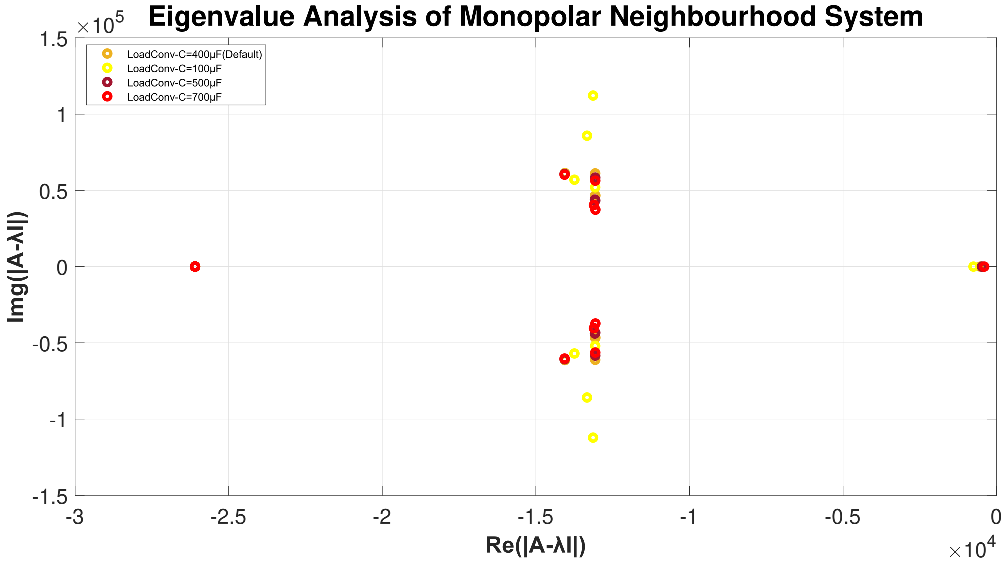

Figure 7.9: Influence of load converter capacitance variation in the eigenvalue plots of neighbourhood system

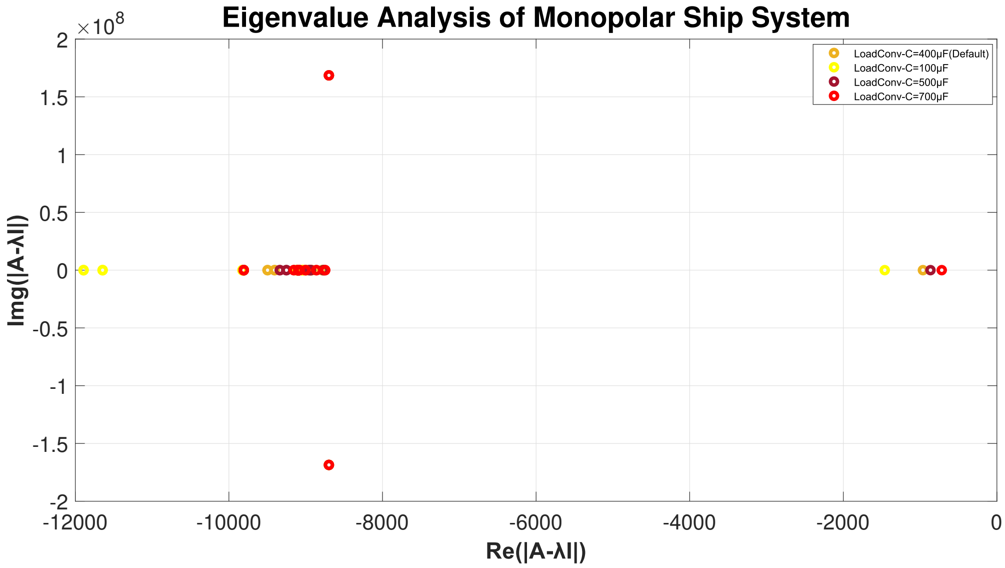

Figure 7.10: Influence of load converter capacitance variation in the eigenvalue plots of ship system

The variation in the node voltages, oscillations, line currents and stability of the system are analysed for these set load converter capacitance values. It can be seen in the stability analysis plots that are shown in Fig 7.9 and Fig 7.10. As the load converter capacitance value is increased the poles of the distribution system derived from their characteristic equation lie closer to the jω axis. The system oscillations generated due to this affects the stability of the distributions system and their amplitude of oscillation increases as the load converter capacitance value is increased. The influence of the load converter capacitance variation in node voltages and the line currents plots can be seen n the appendix B. There is more oscillation present in the lines connected to the load node as the load converter capacitance value is decreased. Also, more oscillations are seen to be present in other lines not connected to load as the converter capacitance value is increased. The positive and negative peak amplitude of oscillation in these plots is seen to be increasing due to this trend. It is inferred through this analysis that as the load converter capacitance is decreased this leads to the distribution systems become more stable and fewer oscillations are present. The equilibrium node voltages and line currents achieved are not affected by the load converter capacitance variation. A summary table of the findings from the stability and sensitivity analysis carried out for the load converter capacitance is shown in table 7.5 below.

Table 7.5: Inference from the analysis carried out for the load converter capacitance variation

Load Converter Capacitance (μF)	**Stability**	**Node Voltage**	**Line current**	**Oscillation**
C=100	**Most stable**	**Not affected**	**Not affected**	**Least oscillation**
C=500	**Increased stability compared-case 3**	**Not affected**	**Not affected**	**Increased oscillation compared - case 1**
C=700	**Decreased stability**	**Not affected**	**Not affected**	**Most oscillation**

7.1.6. Droop Impedance

The impedance of the droop converter is varied, the rest of the parameter's value is maintained as it is in the default condition. The converter input current is set up through the equ (4.3)-(4.4). The droop impedance (Zd) is inversely proportional to the reference input current of the converter. For the default case, the droop impedance is taken as $1(\Omega)$ in both the distribution system. The droop impedance value that is taken for this analysis are 0.5,8.3, and $20(\Omega)$ for neighbourhood and 0.5,8.3, and $10(\Omega)$ for the ship distribution system.

The variation in the node voltages, oscillations, line currents and stability of the system are analysed for these set droop impedance values. It can be seen in the stability analysis plots that are shown in Fig 7.11 and Fig 7.12. As droop impedance value is increased the poles of the distribution system derived from their characteristic equation lie closer to the jω axis. The system oscillations generated due to this affects the stability of the distributions system and their amplitude of oscillation increases as the droop impedance value is increased. The influence of the droop impedance variation in node voltages and the line currents plots can be seen in Fig 7.13-7.16. There is a greater rise and drop in node voltages as the droop impedance value is increased. Also, there is a slight rise in the line currents achieved by the system as the droop impedance value is increased. It is inferred through this analysis that as the droop impedance is increased above the permissible droop impedance value this leads to the distribution systems become less stable and more oscillations are present. A summary table of the findings from the stability and sensitivity analysis carried out for the droop impedance is shown in table 7.6 below.

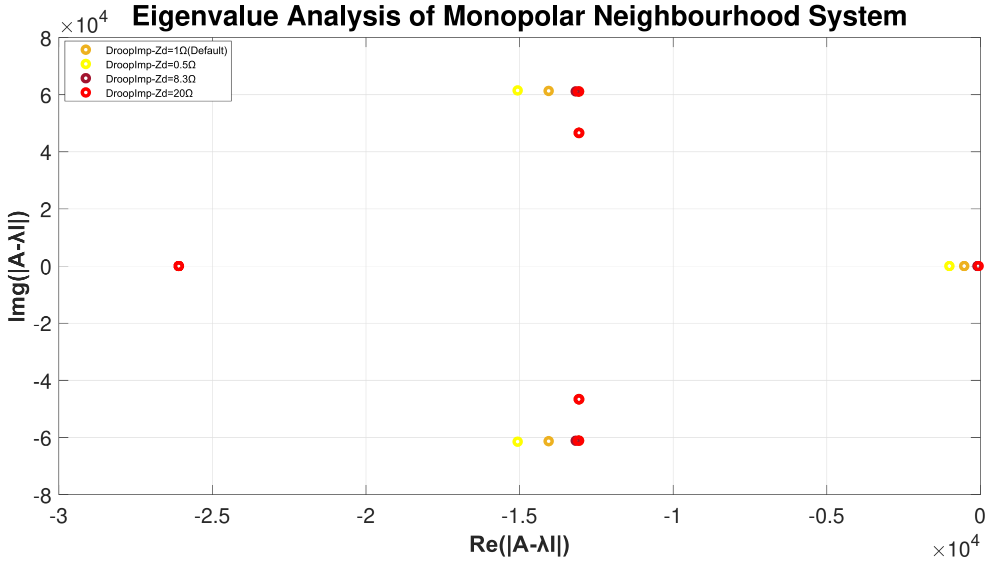

Figure 7.11: Influence of droop impedance variation in the eigenvalue plots of neighbourhood system

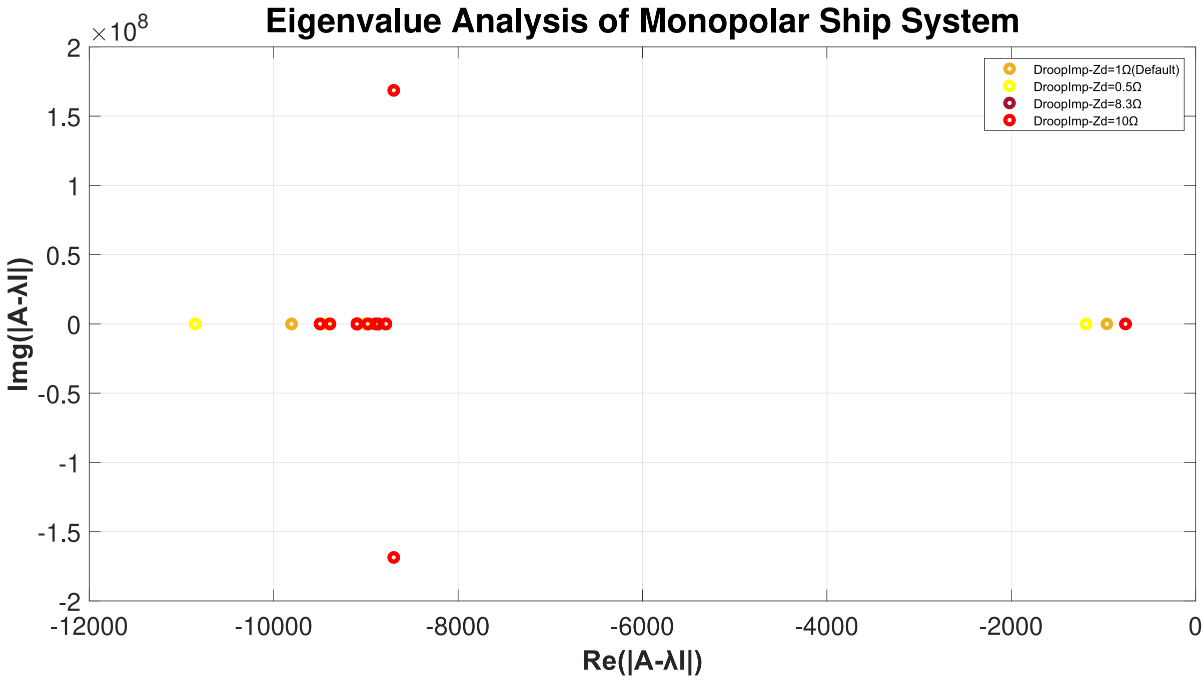

Figure 7.12: Influence of droop impedance variation in the eigenvalue plots of ship system

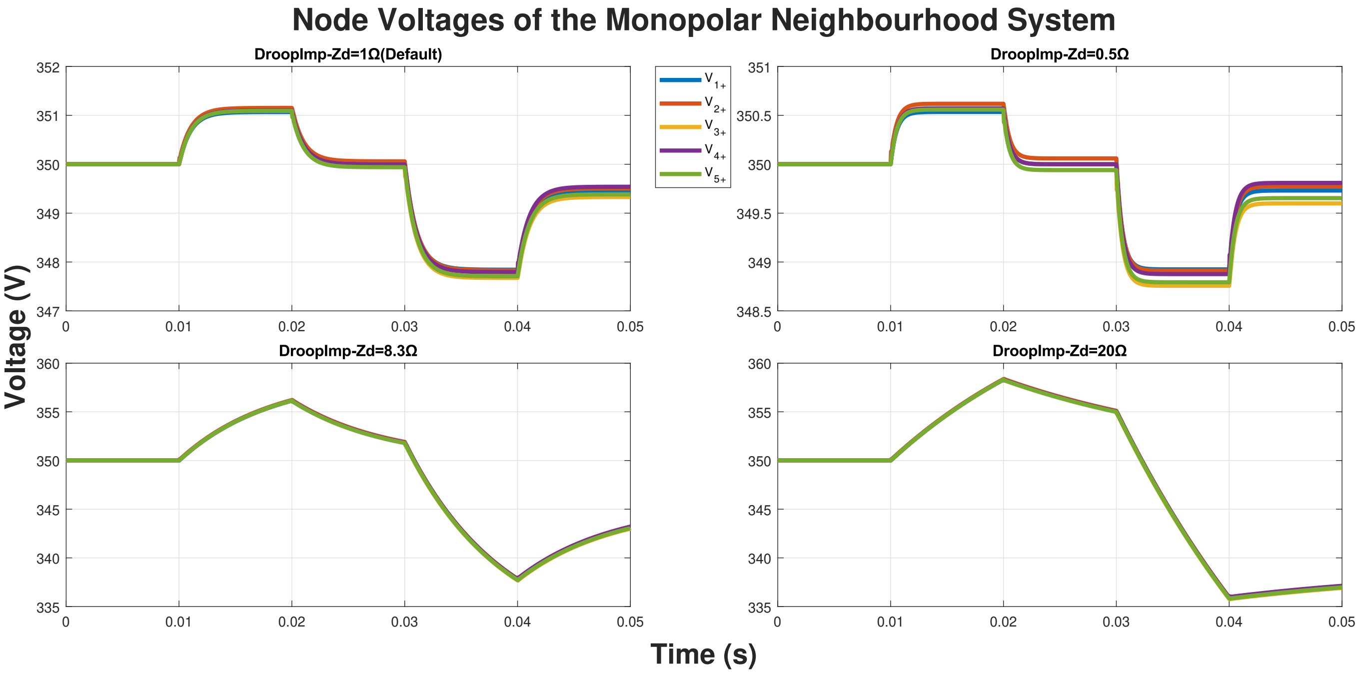

Figure 7.13: Influence of droop impedance variation in the node voltage plots of neighbourhood system

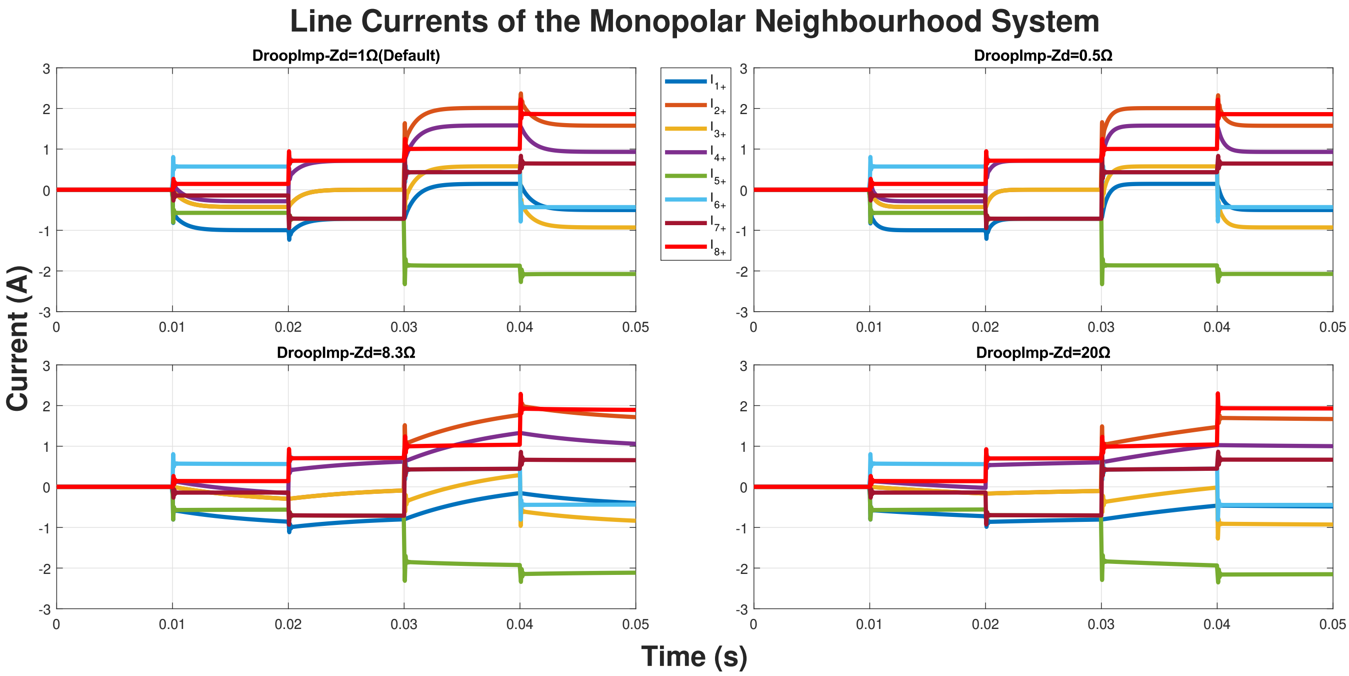

Figure 7.14: Influence of droop impedance variation in the line current plots of neighbourhood system

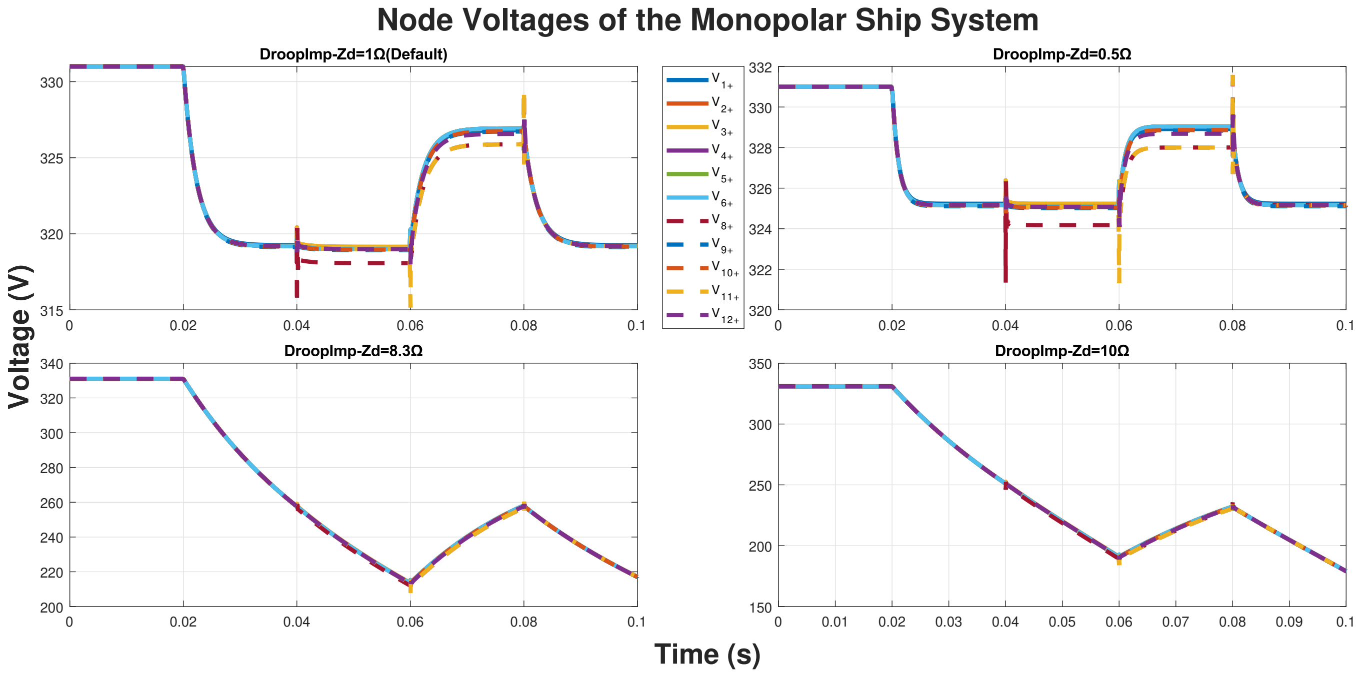

Figure 7.15: Influence of droop impedance variation in the node voltage plots of ship system

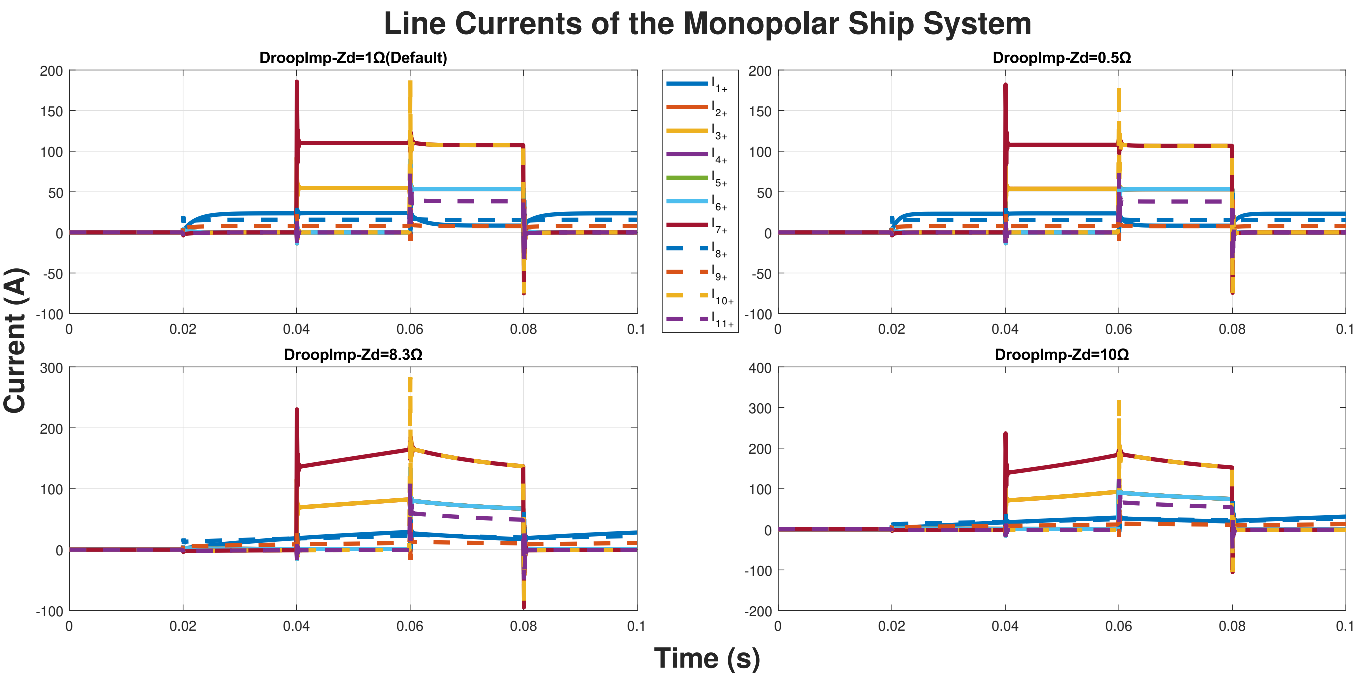

Figure 7.16: Influence of droop impedance variation in the line current plots of ship system

Table 7.6: Inference from the analysis carried out for the droop impedance variation

Impedance(Ω)	Stability	Node Voltage	Line current	Oscillation
Zd=0.5	**Most stable**	**Increase in equilibrium voltage**	**Slight decrease**	**Least oscillation**
Zd=8.3	**Increased Stability compared -Zd=10**	**Decrease in voltage drop and rise compared -Zd=10**	**Decrease compared-Zd=10**	**Increased oscillation compared-Zd=0.5**
Zd=20(Neighbourhood) Zd=10(Ship)	**Decreased stability**	**Increase in voltage drop and rise-Badly designed**	**Slight increase**	**Most oscillation**

7.1.7. Cable length

In this analysis, the length of the cable is varied and the rest of the parameter's value is maintained as it is in the default condition. Usually the length of all the cables in the neighbourhood distribution system is taken as 100m and for the ship distribution system the cable length values are shown in table4.3. The cable length for this analysis is varied and studied for three different cable length configurations in order to properly assess the influence of cable length in the performance and stability of the system. In the neighbourhood system each of the cable length values chosen for this analysis are 50,200 500(m). For the ship distribution system as there are different lines with different cable length involved, so the cable variation is tabularised and shown in table7.7 below.

Table 7.7: Ship distribution system cable length configurations

Cable length(m)	Default	Configuration1	Configuration2	Configuration3
Line1-6	5	25	50	75
Line 7,10	15	75	150	225
Line 8,9	7	35	70	105
Line11	10	50	100	150

The cable length is directly involved in all the line parameters of the cable, as the line parameters other than resistance are all being considered as per meter values. So the line parameters (R,L,C,G) values are increasing as the cable length value increases. First the influence of the cable length on the stability of the distribution system can be seen in Fig 7.17,7.18. As the cable length is increased the poles of the distribution system derived from their characteristic equation lie closer to the jω axis. The system oscillations generated due to this affects the stability of the distributions system and their amplitude of oscillation increases as the cable length is increased. The influence of the cable length variation in node voltages plots can be seen in Fig 7.19,7.20.As the cable length increase the line resistance, the equilibrium node voltage achieved by the system tend to have a deeper rise and drop during different time instances. The influence of the cable length variation on the line current plot can be seen in the appendix B. The amplitude of oscillation, the positive peak amplitude and the negative peak amplitude of oscillation that is present in the line current and the node voltage's plots tends to increase as the cable length increases. Finally, it is inferred through these plots from the analysis, that as the cable length is decreased this leads to the distribution systems become more stable, more stable equilibrium node voltage is achieved, and fewer oscillations are present. A summary table of the findings from the stability and sensitivity analysis carried out for the cable length variation is shown in table7.8 below.

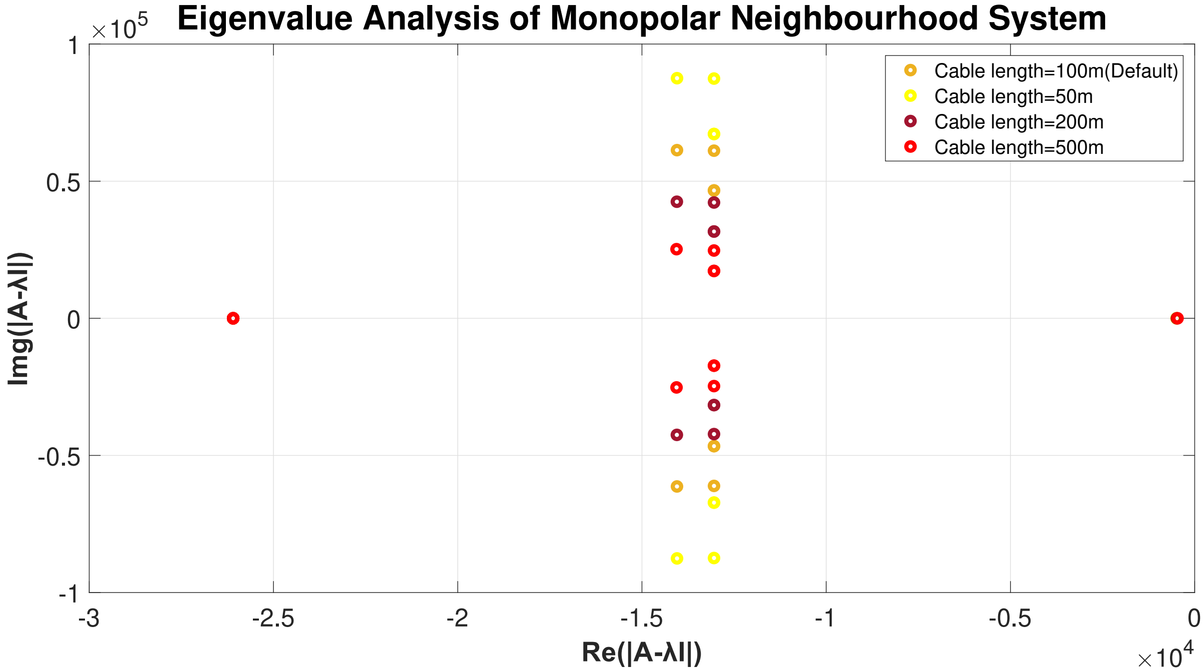

Figure 7.17: Influence of cable length variation in the eigenvalue plots of neighbourhood system

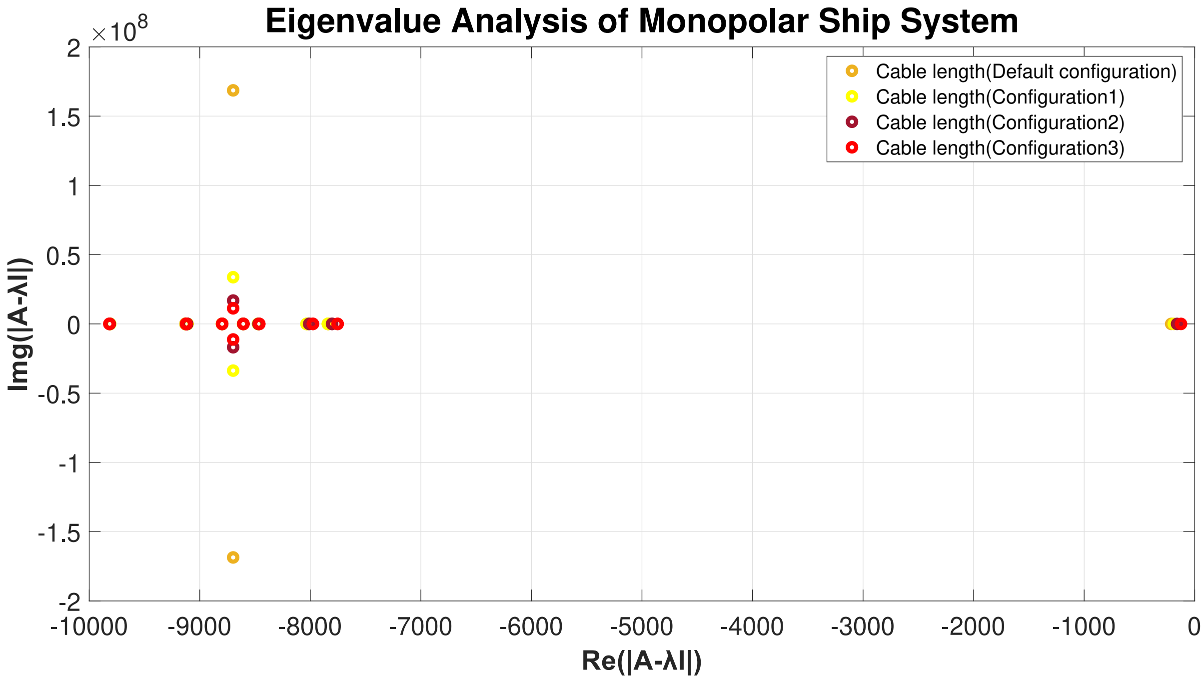

Figure 7.18: Influence of cable length variation in the eigenvalue plots of ship system

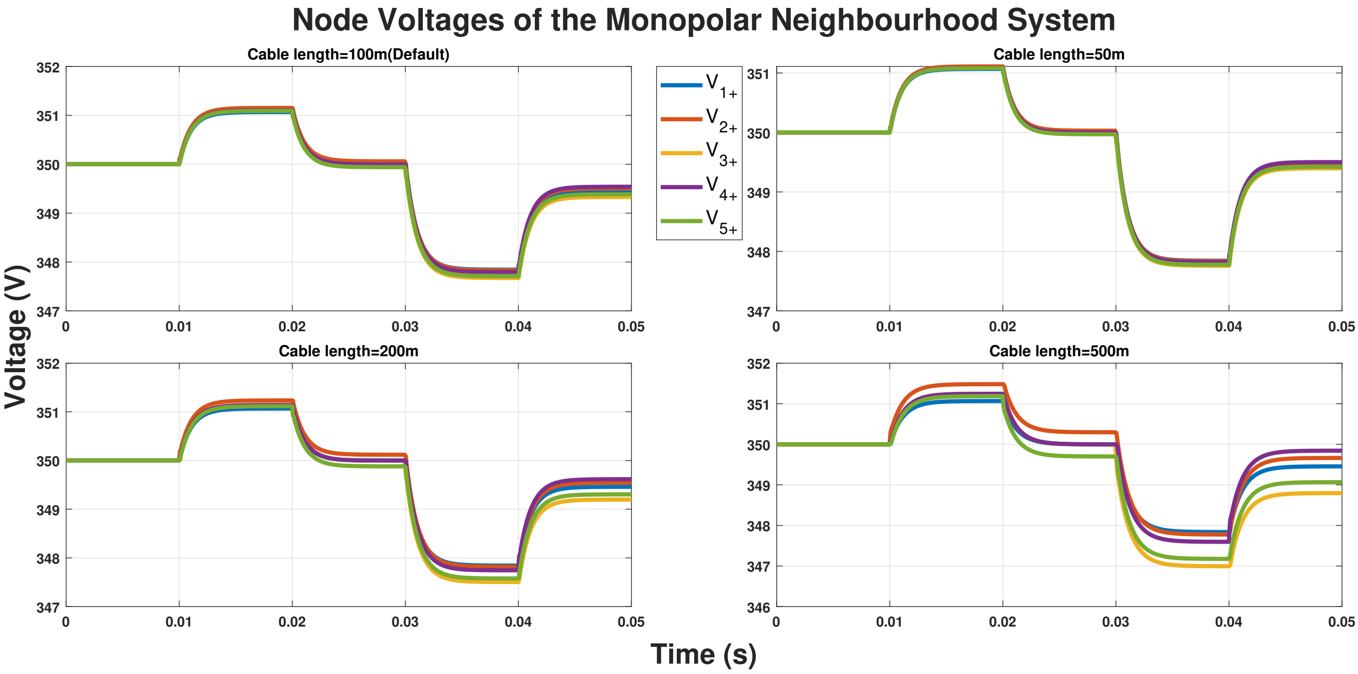

Figure 7.19: Influence of cable length variation in the node voltage plots of neighbourhood system

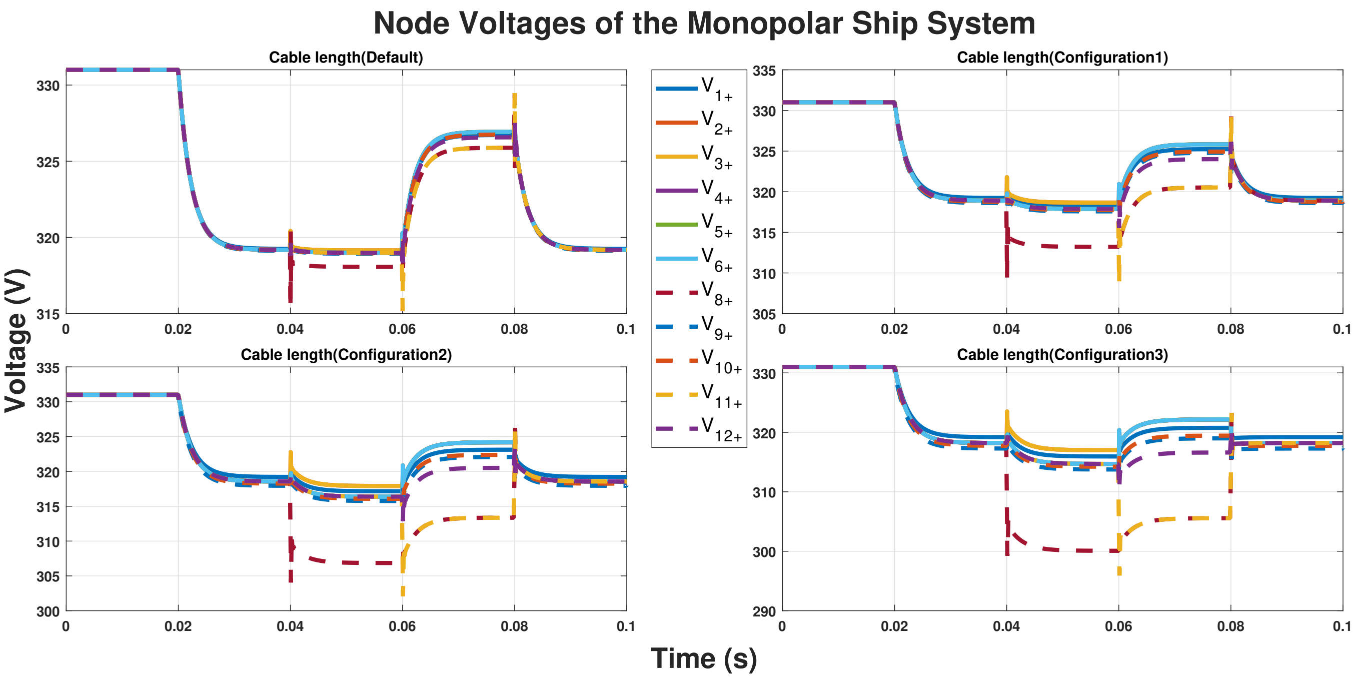

Figure 7.20: Influence of cable length variation in the node voltage plots of ship system

Table 7.8: Inference from the analysis carried out for the cable length variation

Cable length(m)	Stability	Node Voltage	Line current	Oscillation
Config 1	**Increased stability compared to config 2**	**Decrease in Voltage rise and drop**	**Not affected**	**Least oscillation**
Config 2	**Decreased stability compared to config 1**	**Increase voltage rise and drop - compared default case**	**Not affected**	**Increased oscillation compared to config 1**
Config 3	**Least stable**	**Increase voltage rise and drop - compared to config 2**	**Not affected**	**Most oscillation**

7.2. Sensitivity and stability analysis: Bipolar system

The sensitivity and stability analysis is carried out again in the bipolar configuration of the neighbourhood distribution system and ship distribution system. In this analysis, each of the active parameter's values is set to be varied individually and the general trend of the system performance and stability is observed. This observation is tabulated only for the active parameters for which there is a difference in the observation from the analysis carried out for the monopolar configuration. Again, only the positive pole quantities of the bipolar system are assessed.

7.2.1. Cable capacitance

In this analysis, the capacitance of the cable is varied, the rest of the active parameter's value is maintained as it is in the default condition. This stability and sensitivity analysis carried out for the cable capacitance variation in both ship and neighbourhood bipolar distribution systems. The default case line capacitance or cable capacitance value is taken as 45(nF/Km) for both the distribution system. The capacitance value that is taken for this analysis is 20,100, and 300(nF/Km). For these set capacitance values the node voltages, oscillations, line currents and stability of the system are analysed. It was seen earlier in a monopolar configuration that the line capacitance variation didn't have any effect on the system performance and the stability of the distribution system. But in the bipolar configuration, the line capacitance variation is seen to have an effect on the stability of the distribution system. As shown in Fig7.21 and 7.22 it can be seen that as the capacitance value is increased the magnitude of the poles derived from their characteristic equation decreases leading to decrease in system damping and the oscillation increases.Mainly the pole closest to the jw axis is due to the droop controlled converter. Zooming into these poles in the stability plots, it can be seen that the poles derived for the highest capacitance value is seen to be closest and the least capacitance's poles is seen to be further away from the jw-axis. So, as the line capacitance value increases the poles are seen to lie closer to the $j\omega$ axis. The system oscillations generated affects the stability of the distributions system and their amplitude of oscillation increases as the line capacitance value is decreased. The influence of the line capacitance variation in node voltages and the line currents plots can be seen in the appendixB. So, it is inferred through these plots, that as the line capacitance is increased this leads to the distribution systems become less stable, the system damping is reduced and the oscillation present in the system increases. A summary table of the findings from the stability and sensitivity analysis carried out for the cable capacitance variation is shown in table 7.9 below.

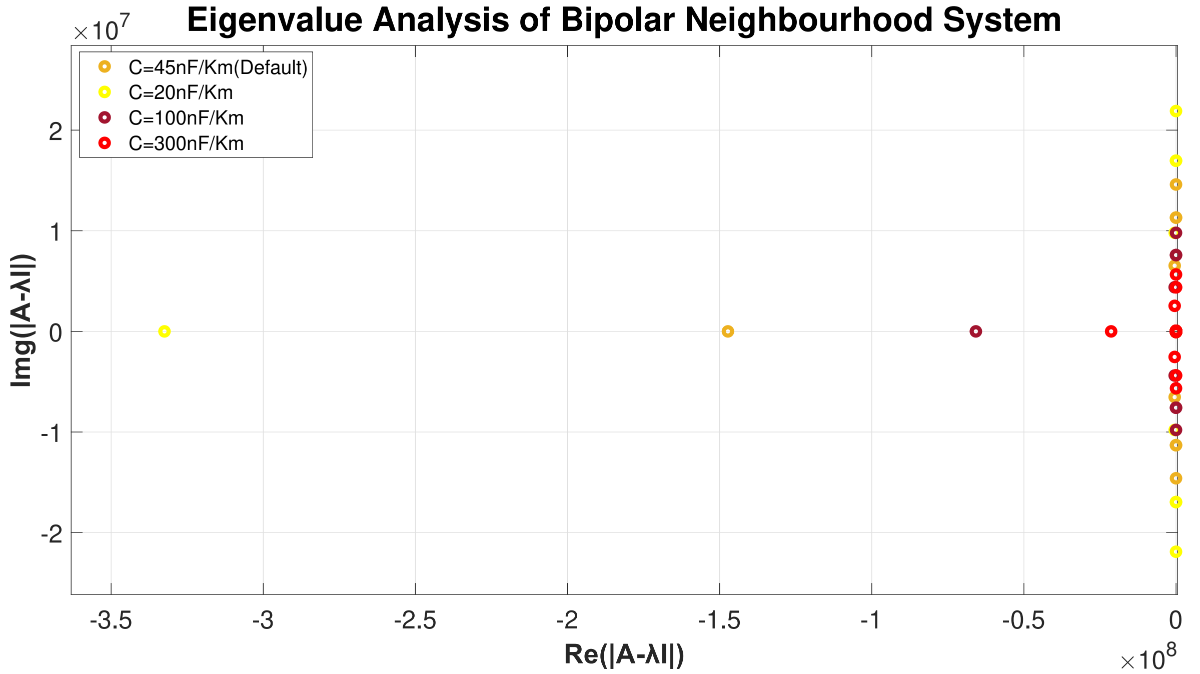

Figure 7.21: Influence of cable capacitance variation in the eigenvalue plots of neighbourhood system

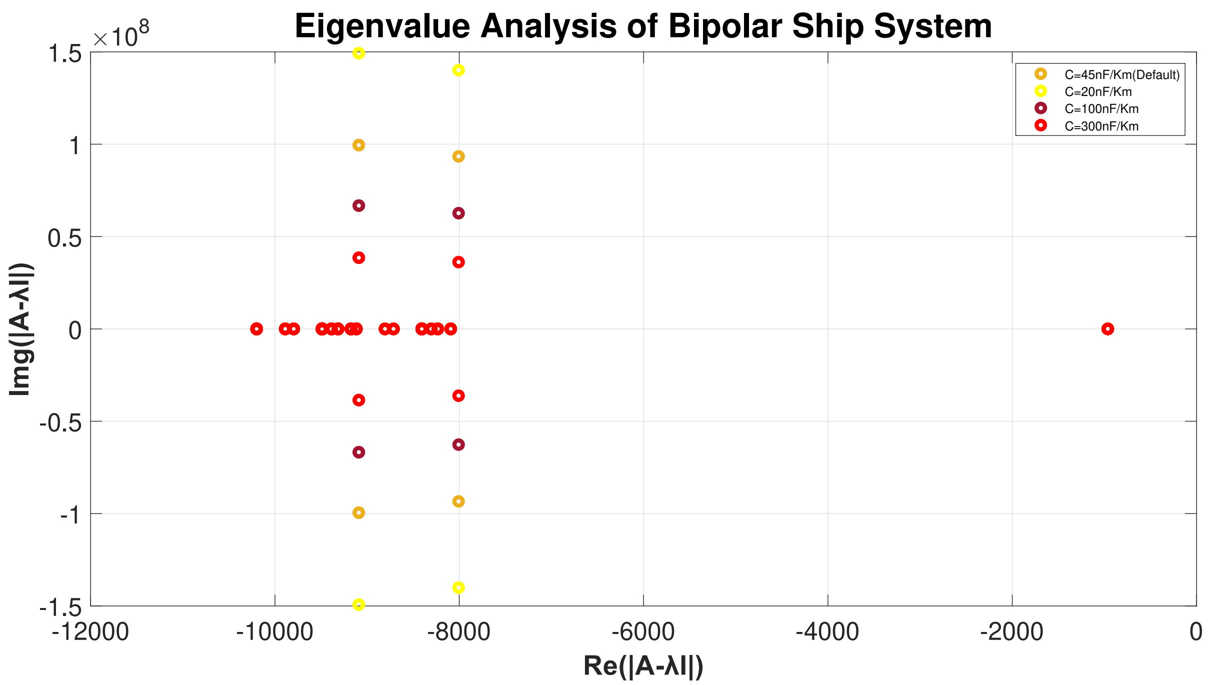

Figure 7.22: Influence of cable capacitance variation in the eigenvalue plots of ship system

Table 7.9: Inference from the analysis carried out for the cable capacitance variation

Capacitance(nF/Km)	Stability	Node Voltage	Line current	Oscillation
C=20	Increased stability compared to default	Not affected	Not affected	Least oscillation
C=100	Decreased stability compared - case 1	Not affected	Not affected	Increased oscillation compared - case 1
C=300	Least stable	Not affected	Not affected	Most oscillation

7.2.2. Rest of the Active parameters

The sensitivity and stability analysis is carried out for the rest of the active parameters namely cable cross-section, inductance, length, droop impedance, source and load converter capacitance. The positive pole quantities of the distribution system under bipolar configuration are analysed thoroughly. But there were no changes in the general trend seen in the performance and stability of the distribution system when the active parameters are varied. The plots of the positive pole quantities in both the configurations seem to be similar in the node voltage and the line currents plots. In the stability graphs, there could be seen an increased number of poles plotted, that is due to the increased number of nodes and lines present in the bipolar system in comparison to the monopolar distribution system. The rest of the active parameter variation in the sensitivity and stability analysis seems to be similar to the monopolar configuration.so in order to avoid repetition, further analysis and explanation on these analysis carried out are not described again.

7.3. Short circuit analysis

The pole to pole and pole to neutral fault analysis is performed on both the neighbourhood and ship distribution system. Here the cable's active parameters that are expected to have an influence on the system performance and the line current during short circuit are taken into consideration. These active parameters are varied throughout this analysis and the resulting plots are further analysed to study their influence. These active parameters are cable resistance, cable inductance, cable capacitance, cable cross-section(indirectly resistance) and cable length. The general trend of the system performance and line current achieved during short circuit due to this cable's active parameter variation is observed. This observation is tabulated for each of the active parameters individually. During this analysis, few active parameters values are varied above and below the rated/permissible values for a LV cable. This is done in order to deeply assess the general trend and influence each of the cable's active parameter has on the system performance and the line current during short circuit. The generated results from this study would support in better assessment of cable's active parameters influence on the short circuit current and designing the LVDC cables.

7.3.1. Cable Inductance

In this analysis, first the inductance of the cable is varied, the rest of the active parameter's values are maintained as it is in the default condition. This inductance value is varied in both the ship and neighbourhood bipolar distribution system. The default case inductance value is taken as 32(μH/Km) for both the distribution system. To get the general trend of how the inductance variation would affect the system performance and line currents achieved during short circuit. The inductance value is increased and decreased with respect to the default case value. This analysis is done for both the pole to pole and pole to neutral fault. The inductance value that is taken for this analysis are 1.2,12, and 100(μH/Km). For these set inductance values the node voltages, line currents are analysed separately for both these short circuit faults.

First variation can be seen in the line currents plots of the pole to pole and pole to neutral faults for both the distribution systems. As the inductance values are increased, the peak short circuit current reached by the lines connected to faulted node also increases. The oscillations present in both the line currents and node voltages plots increase with the inductance increase. This trend is seen to be similar for both the pole to pole and pole to line fault. The influence of the inductance variation in the line currents plots for both the pole to pole and pole to neutral faults can be seen in Fig 7.23-7.26 . The peak magnitude of the short circuit current achieved by both the distribution system after each of the faults occurs is noted and presented with the inference from the analysis in table 7.11 and 7.10. In the pole to pole fault there is a greater rise of peak magnitude of the short circuit current as the inductance value is increased compared to the pole to neutral fault.

For the node voltages plots, only the oscillation present in the plots increases as the inductance is increased. The decay curve during the fault instance and the equilibrium node voltage achieved after the fault are not affected and remains similar throughout, when the inductance is increased. The influence of the inductance variation in the node voltage plots for both the pole to pole and pole to neutral faults can be seen in the appendixB . So, it is inferred through these plots, that as the cable inductance value is decreased this leads to the peak short circuit current reached by the lines connected to faulted node for both the faults to decrease and also the oscillations present in the system decreases. This inductance variation has no distinct effect on the decay curve and equilibrium node voltage achieved by the distribution system. A summary table of the findings from this short circuit analysis carried out for the cable inductance variation is shown table 7.11 and 7.10 below.

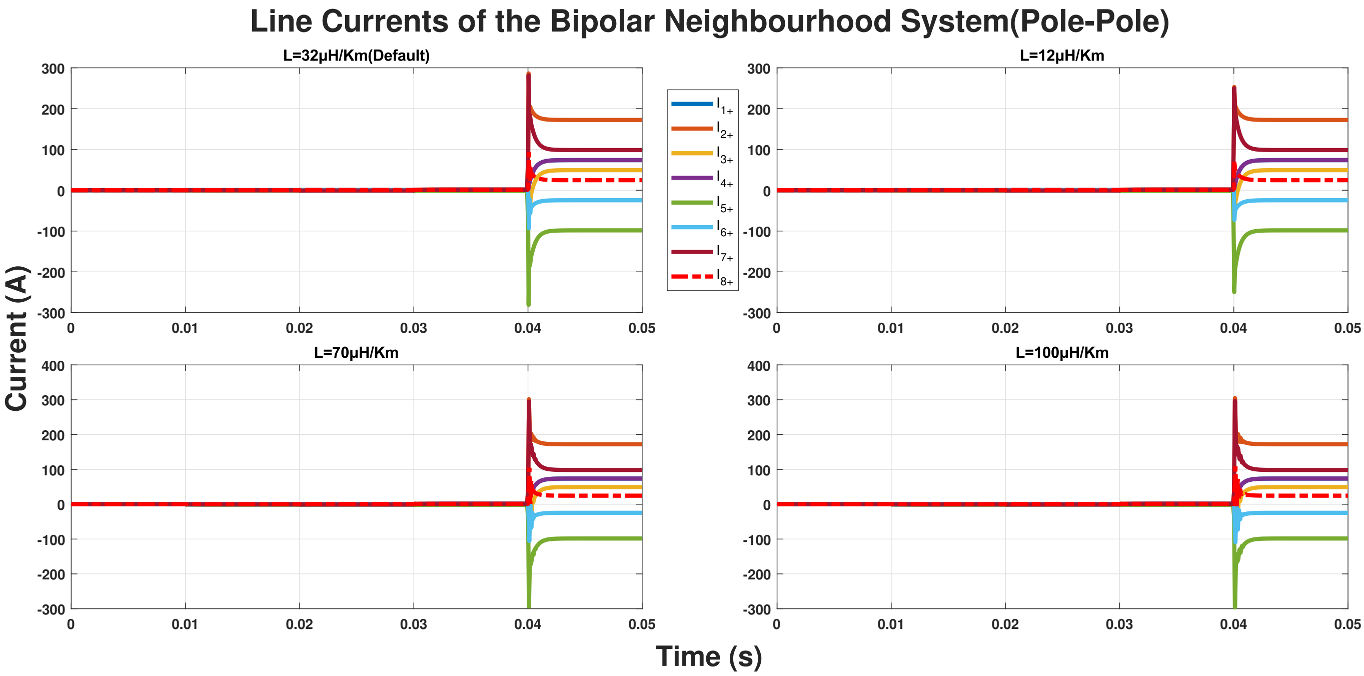

Figure 7.23: Influence of cable inductance variation in the pole to pole fault line current plots of neighbourhood system

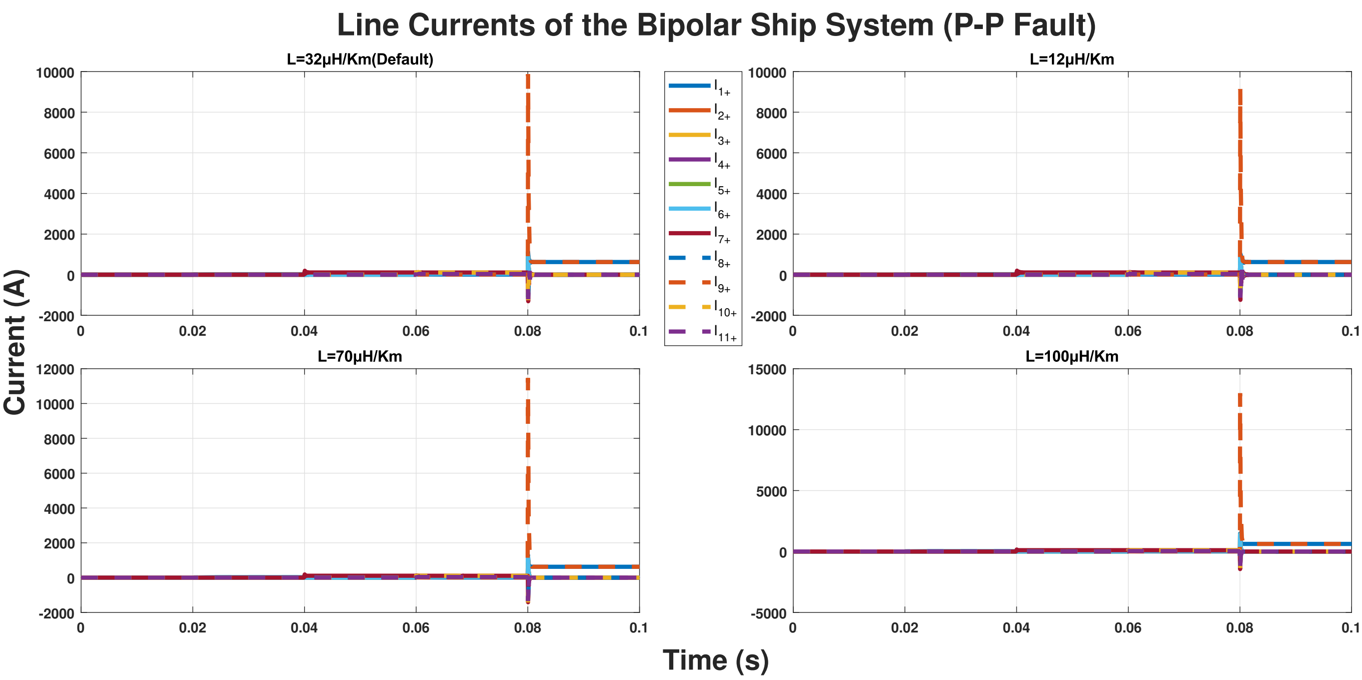

Figure 7.24: Influence of cable inductance variation in the pole to pole fault line current plots of ship system

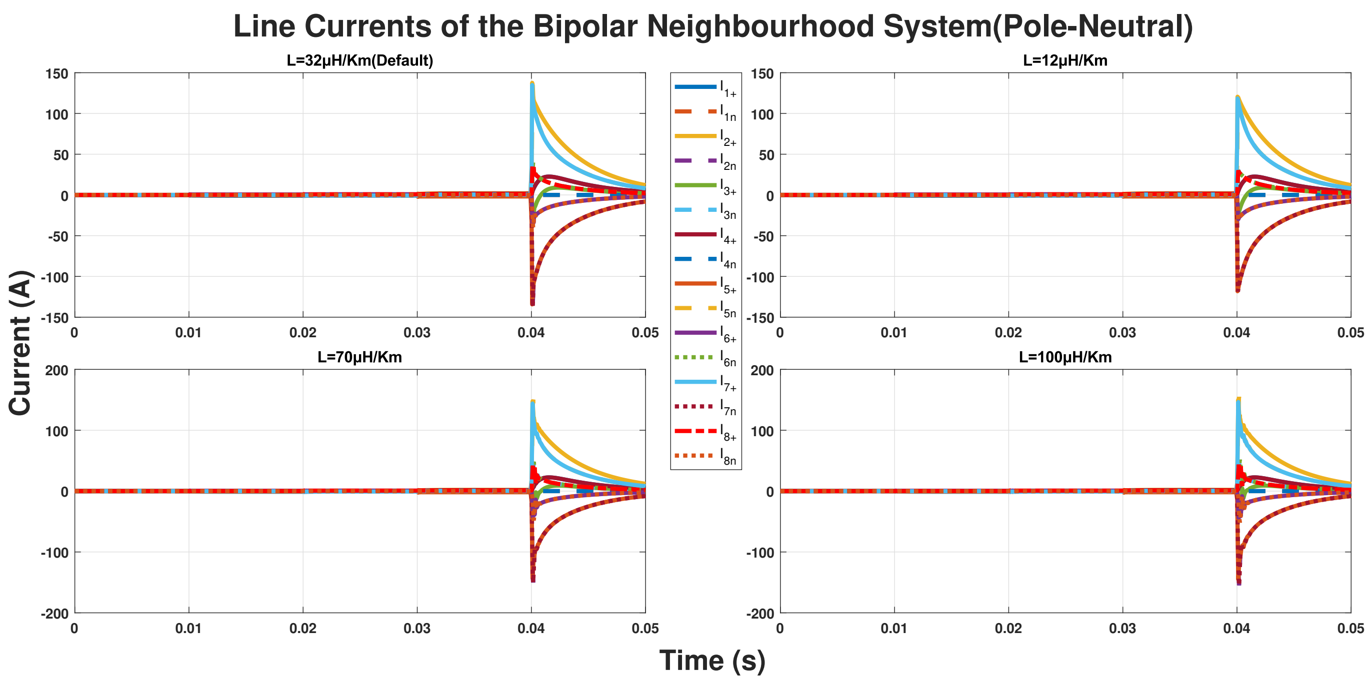

Figure 7.25: Influence of cable inductance variation in the pole to neutral fault line current plots of neighbourhood system

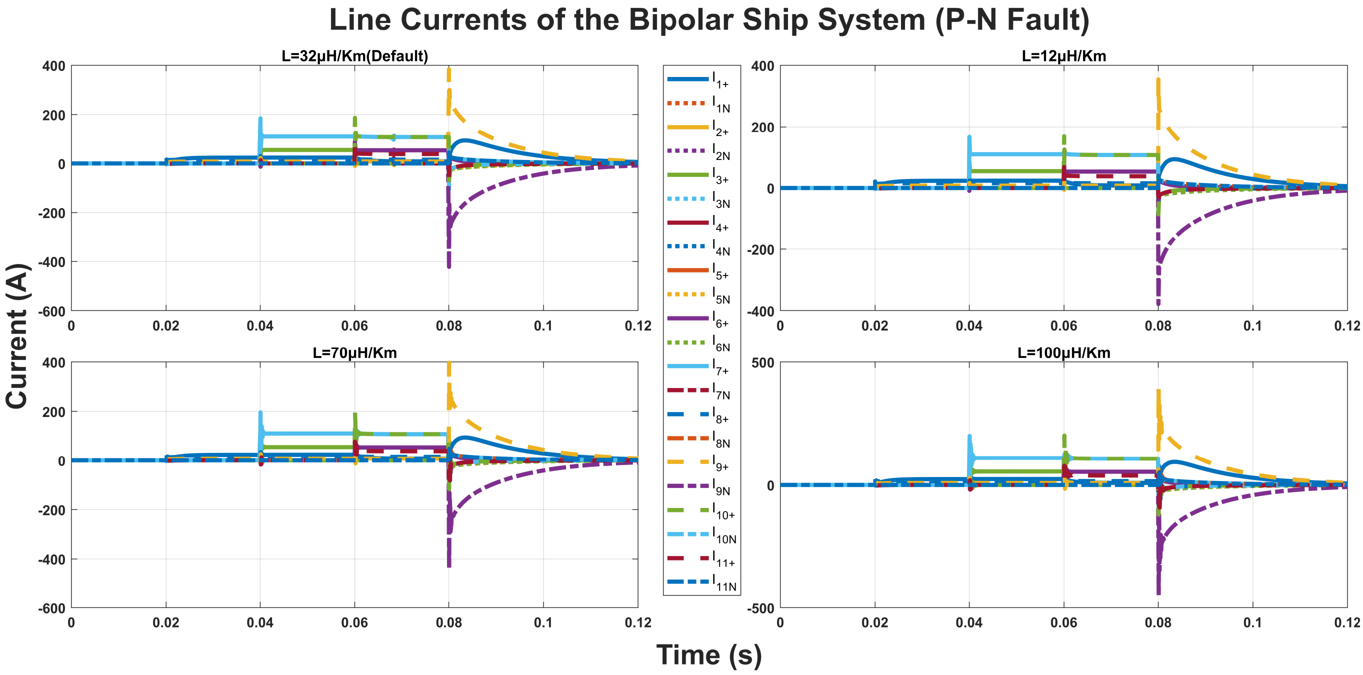

Figure 7.26: Influence of cable inductance variation in the pole to neutral fault line current plots of ship system

Table 7.10: Inference from the pole to neutral fault analysis carried out for the cable inductance variation

Cable inductance (μH/km)	Node voltage	Line current (PeakIsc (A))	Oscillations
L=12	Not affected	Lower peak short circuit current reached compared to case2. Neigh: L2+=119.9 L5+=-118.7 L7+=119 Ship:L9+=354.1	Lower oscillations present:node voltage and line current plots compared to case2.
L=70	Not affected	Higher peak short circuit current reached compared to case1. Neigh: L2+=150.3 L5+=-150.3 L7+=143.9 Ship: L9+=396.6	Higher oscillations present: node voltage and line current plots compared to case1.
L=100	Not affected	Highest peak short circuit current reached compared to all cases Neigh: L2+=154.8 L5+=-154.8 L7+=145.6 Ship:L9+=400.2	Highest oscillations present: node voltage and line current plots compared to allcases.

Table 7.11: Inference from the pole to pole fault analysis carried out for the cable inductance variation

Cable inductance (μH/km)	Node voltage	Line current (PeakIsc (A))	Oscillations
L=12	Not affected	Lower peak short circuit current reached compared to case2. Neigh L2+=253.4 L5+=-249.7 L7+=253.1 Ship L9+=9141	Lower oscillations present:node voltage and line current plots compared to case2.
L=70	Not affected	Higher peak short circuit current reached compared to case1. Neigh L2+=291.2 L5+=-294.7 L7+=290.7 Ship L9+=11460	Higher oscillations present: node voltage and line current plots compared to case1.
L=100	Not affected	Highest peak short circuit current reached compared to all cases Neigh L2+=296.9 L5+=-296 L7+=296.7.1 Ship L9+=12990	Highest oscillations present: node voltage and line current plots compared to allcases.

7.3.2. Cable capacitance

In this analysis, the capacitance of the cable is varied, the rest of the active parameter's values are maintained as it is in the default condition. This capacitance value is varied in both the ship and neighbourhood bipolar distribution system. The default case line capacitance or cable capacitance value is taken as 45(nF/Km) for both the distribution system. To get the general trend of how the capacitance variation would affect the system performance and line currents achieved during short circuit. The capacitance value is increased and decreased with respect to the default case value. This analysis is done for both the pole to pole and pole to neutral fault. The capacitance value that is taken for this analysis are 20,100, and 300(nF/Km). For these set cable capacitance values the node voltages, line currents are analysed separately for both these short circuit faults.

In the line currents plots of the pole to pole and pole to neutral faults for both the distribution systems, no variation can be seen. As the capacitance values are increased, the peak short circuit current reached by the lines connected to faulted node remains same throughout the analysis. The oscillations present in both the line currents and node voltages plots also remain same with the cable capacitance increase. This trend is seen to be similar for both the pole to pole and pole to line fault. The influence of the capacitance variation in the line currents and node voltage plots for both the pole to pole and pole to neutral faults can be seen in Fig7.27-7.30 and in the appendixB. So, it is inferred through these plots, that as the cable capacitance value is decreased this leads to the peak short circuit current reached by the lines connected to faulted node for both the faults remain the same and the oscillations present in the system remain similar throughout. This capacitance variation has no distinct effect on the decay curve and equilibrium node voltage achieved by the distribution system.

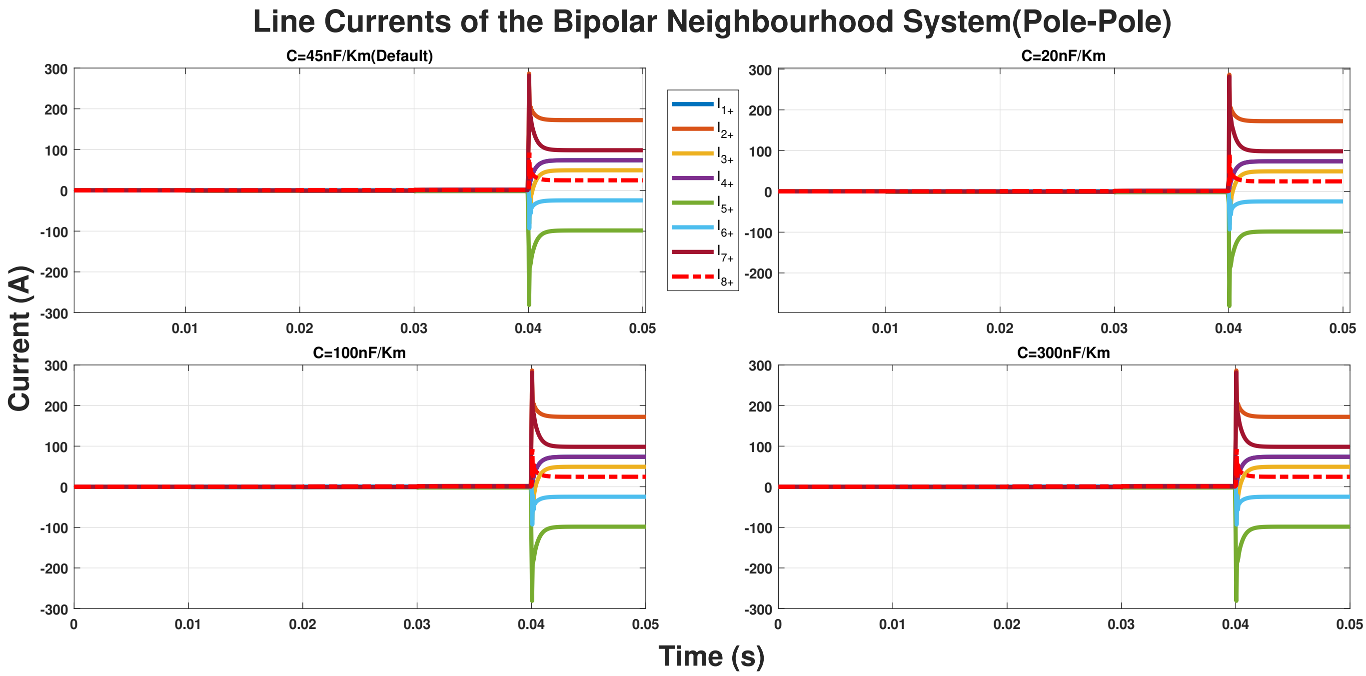

Figure 7.27: Influence of cable capacitance variation in the pole to pole fault line current plots of neighbourhood system

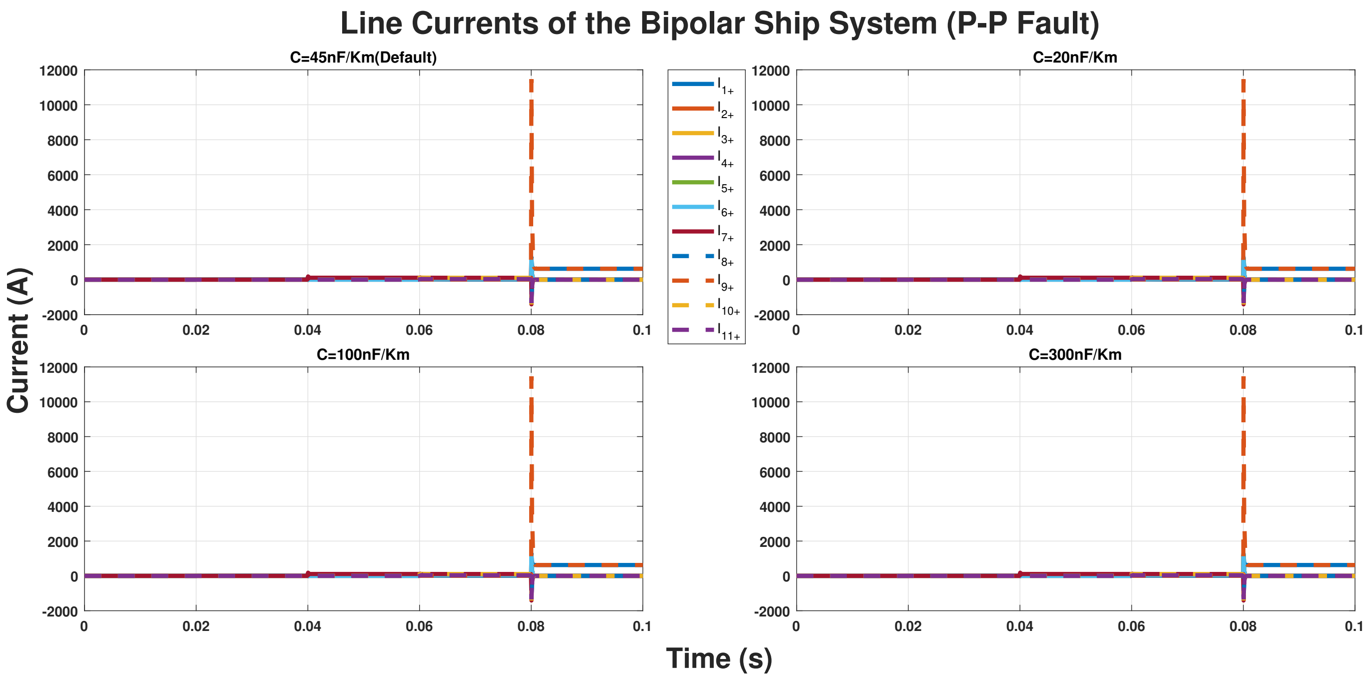

Figure 7.28: Influence of cable capacitance variation in the pole to pole fault line current plots of ship system

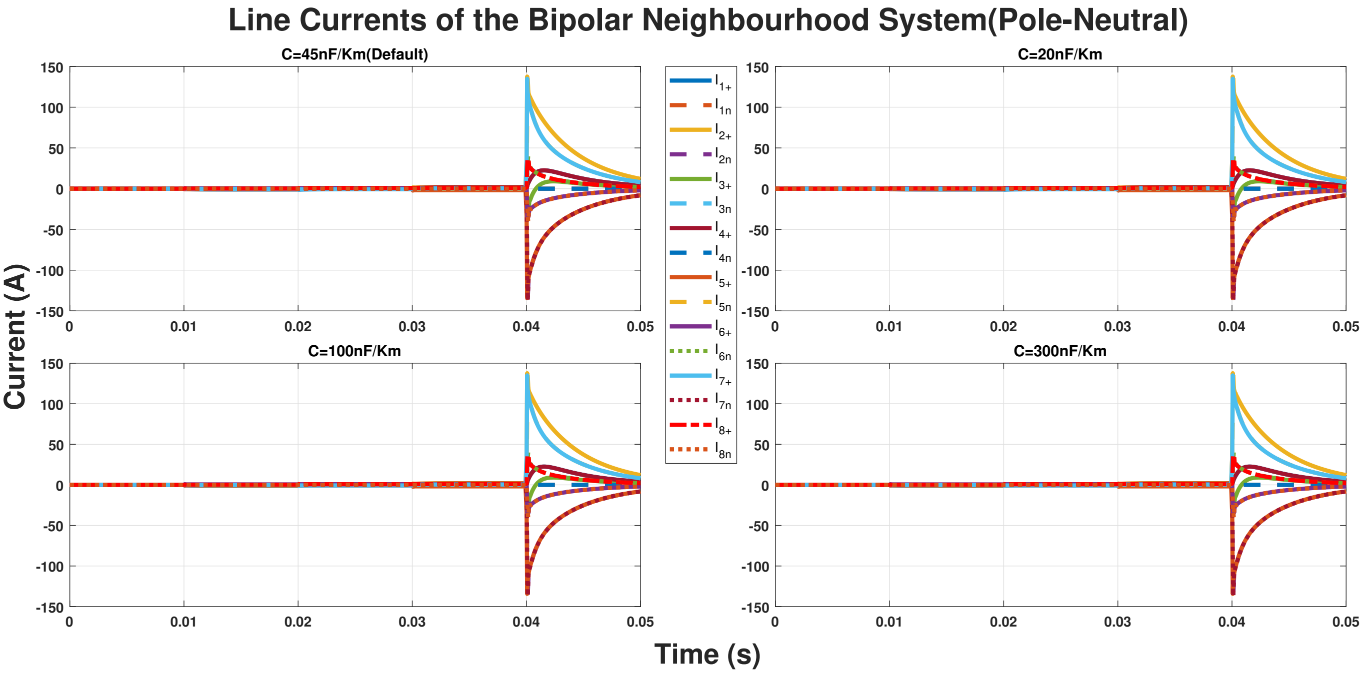

Figure 7.29: Influence of cable capacitance variation in the pole to neutral fault line current plots of neighbourhood system

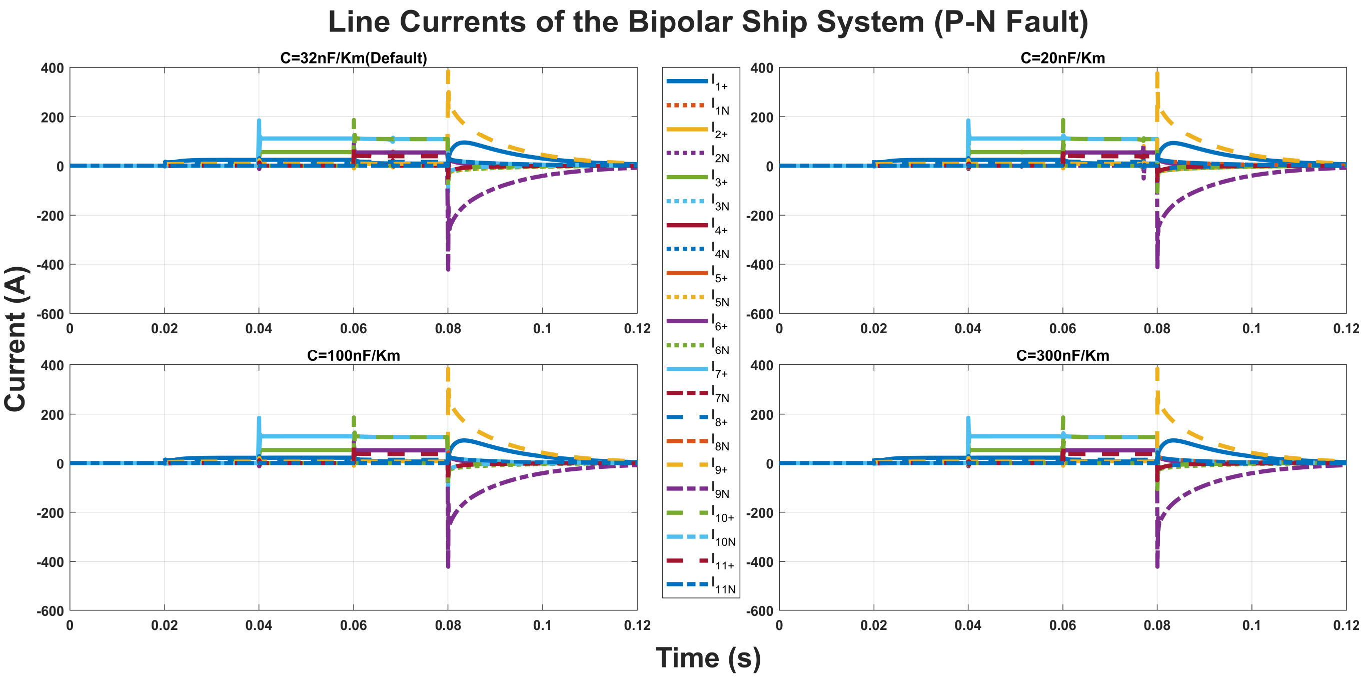

Figure 7.30: Influence of cable capacitance variation in the pole to neutral fault line current plots of ship system

7.3.3. Cable Cross section

In this analysis, first the cross section of the cable is varied, the rest of the active parameter's values are maintained as it is in the default condition. This cross section value is varied in both the ship and neighbourhood bipolar distribution system. As the resistance of the cable is calculated using the formula shown in equ (5.11), varying the cross-section area of the cable is indirectly varying the cable resistance. The default case cross-section value is taken as 20(mm2) for neighbourhood and 30(mm2) for the ship distribution system respectively. To get the general trend of how the cross section variation would affect the system performance and line currents achieved during short circuit. The cross section value is increased and decreased with respect to the default case value. This analysis is done for both the pole to pole and pole to neutral fault. The cross-section value that is taken for this analysis is 5,100, and 400(mm2). For these set cross section values the node voltages, line currents are analysed separately for both these short circuit faults.

First variation can be seen in the line currents plots of the pole to pole and pole to neutral faults for both the distribution systems. As the cross section values are increased, the peak short circuit current reached by the lines connected to faulted node also increases. The oscillations present in both the line currents and node voltages plots increase with the cross section increase. This trend is seen to be similar for both the pole to pole and pole to line fault. The influence of the cross section variation in the line currents plots for both the pole to pole and pole to neutral faults can be seen in Fig7.31-7.34. The peak magnitude of the short circuit current achieved by both the distribution system after each of the faults occurs is noted and presented with the inference from the analysis in table 7.12and 7.13. In the pole to pole fault there is a greater rise of peak magnitude of the short circuit current as the cross section value is increased compared to the pole to neutral fault. For the node voltages plots, the equilibrium node voltage achieved after the fault and oscillation present in the plots increases as the cross section is increased. The influence of the cross section variation in the node voltage plots for both the pole to pole and pole to neutral faults can be seen in Fig 7.35-7.38 . So, it is inferred through these plots, that as the cable cross section value is decreased this leads to the peak short circuit current reached by the lines connected to faulted node to decrease, the equilibrium node voltage achieved after the fault decreases and also the oscillations present in the system decreases for both the faults. A summary table of the findings from this short circuit analysis carried out for the cable cross section variation is shown table7.12 and 7.13 below.

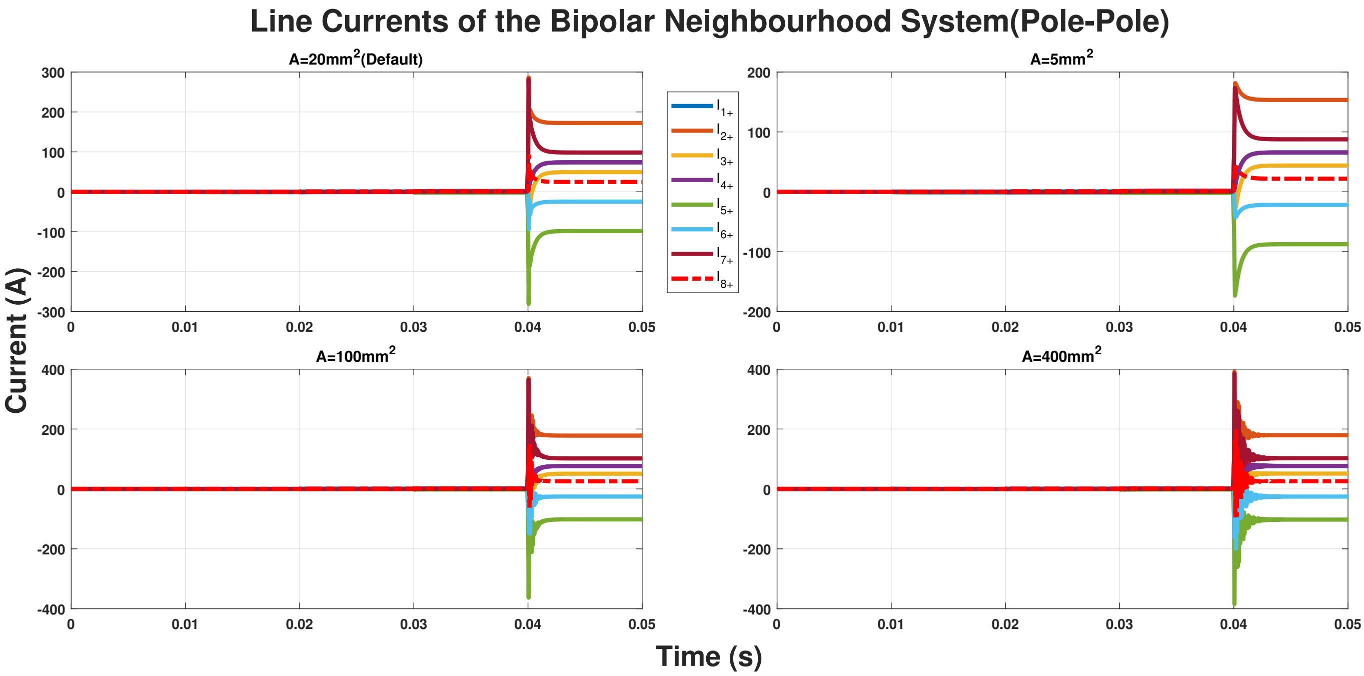

Figure 7.31: Influence of cable cross section variation in the pole to pole fault line current plots of neighbourhood system

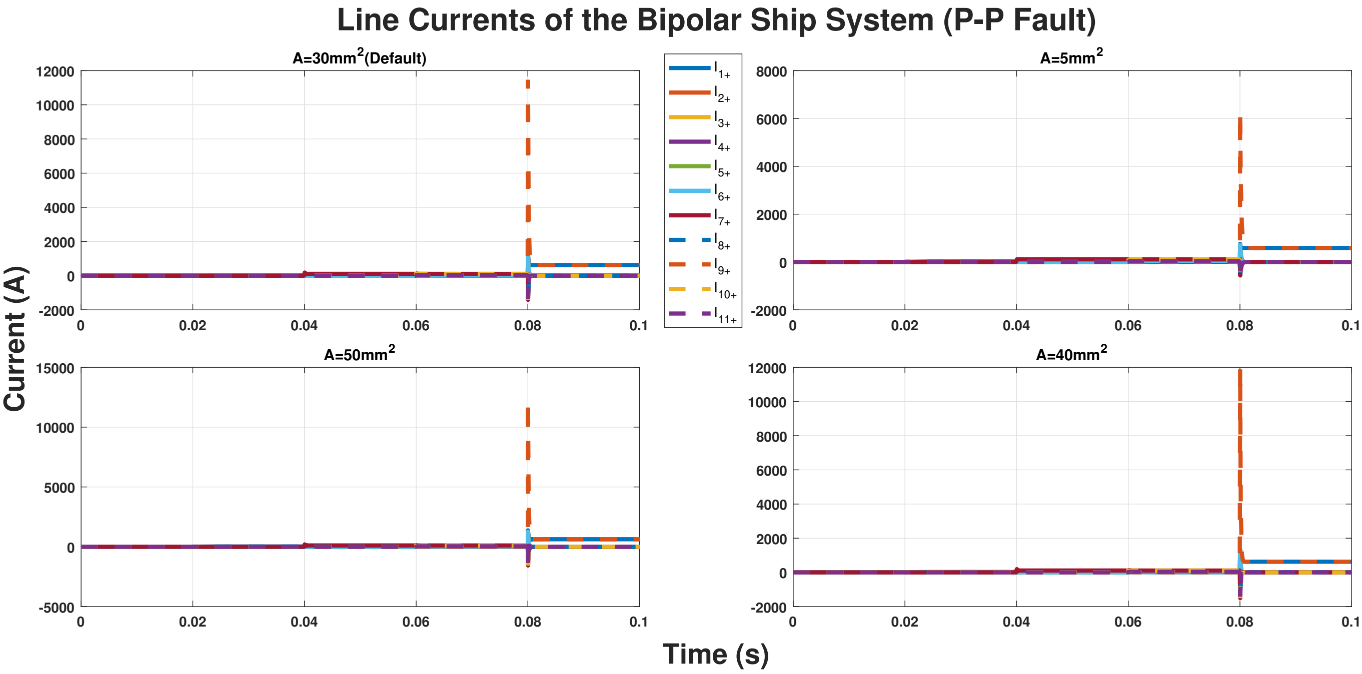

Figure 7.32: Influence of cable cross section variation in the pole to pole fault line current plots of ship system

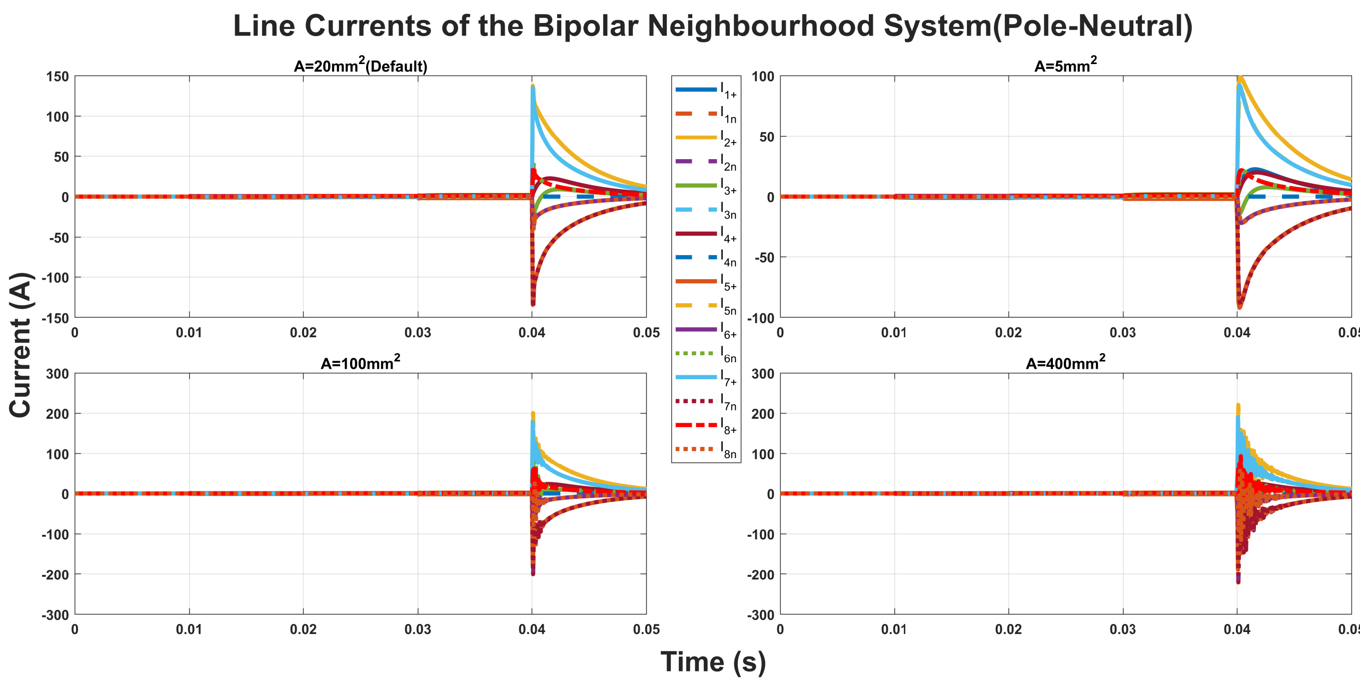

Figure 7.33: Influence of cable cross section variation in the pole to neutral fault line current plots of neighbourhood system

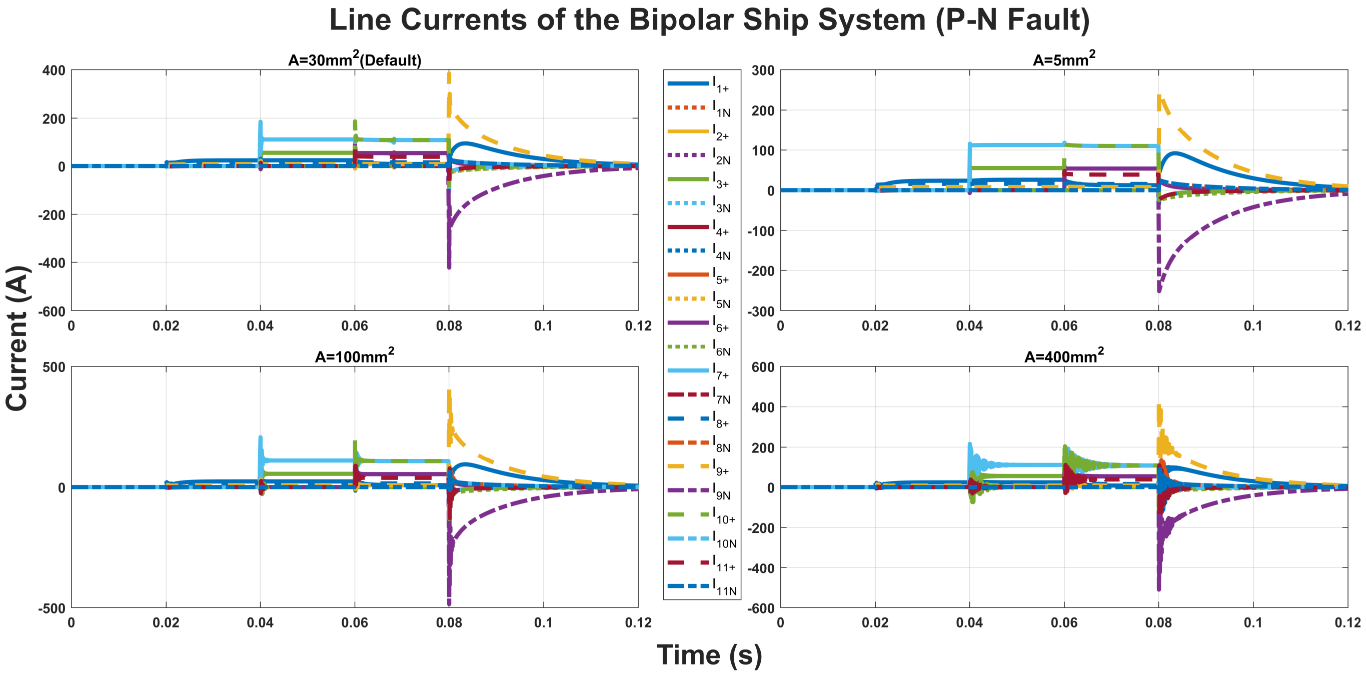

Figure 7.34: Influence of cable cross section variation in the pole to neutral fault line current plots of ship system

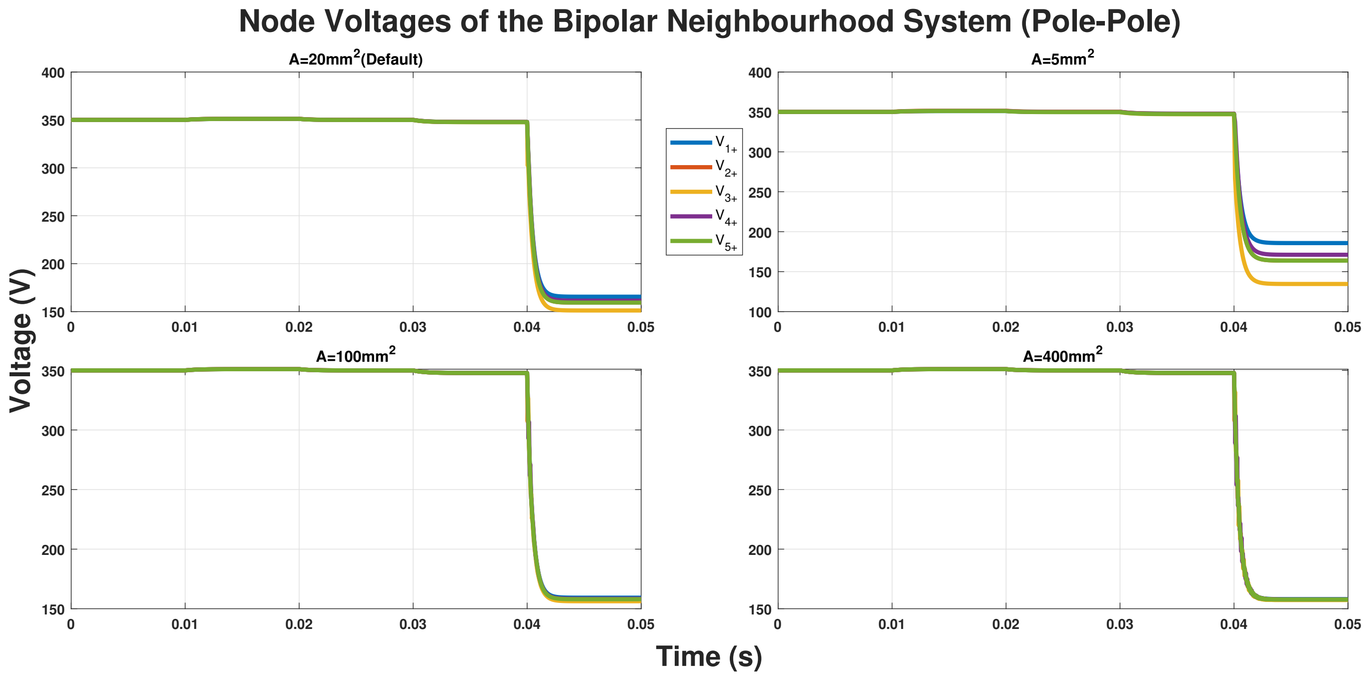

Figure 7.35: Influence of cable cross section variation in the pole to pole fault node voltage plots of neighbourhood system

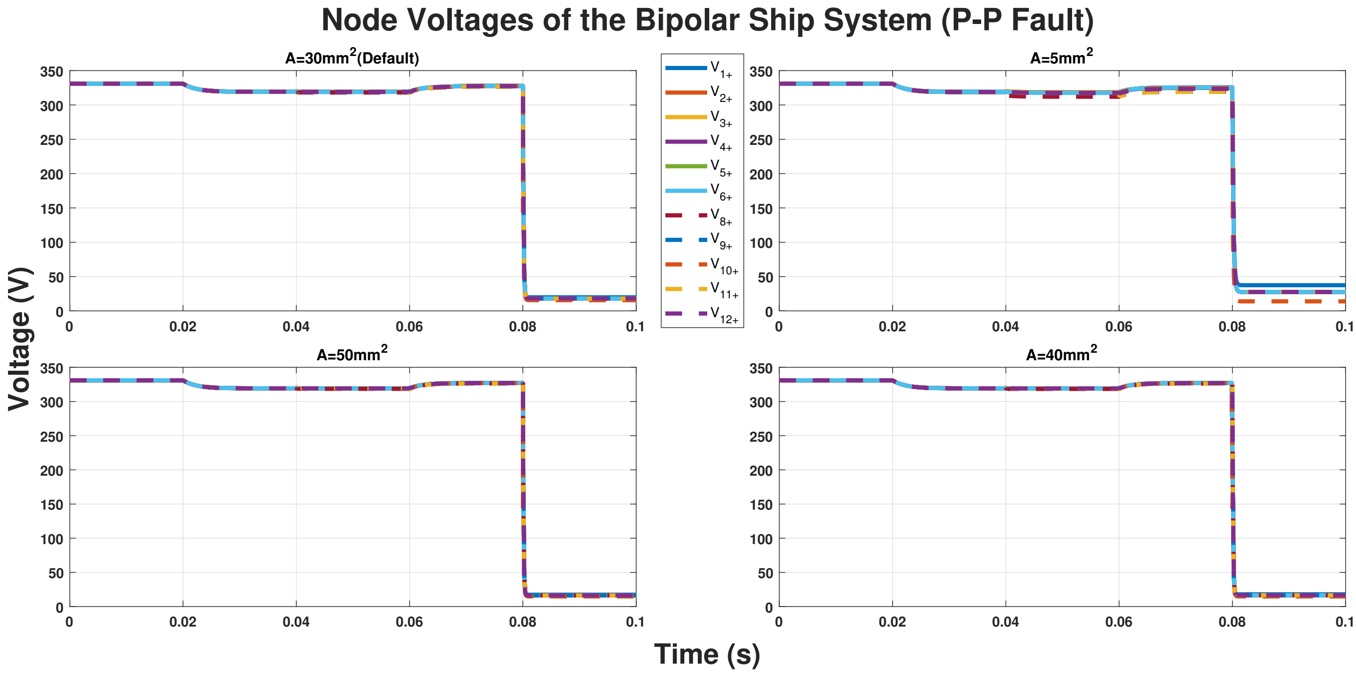

Figure 7.36: Influence of cable cross section variation in the pole to pole fault node voltage plots of ship system

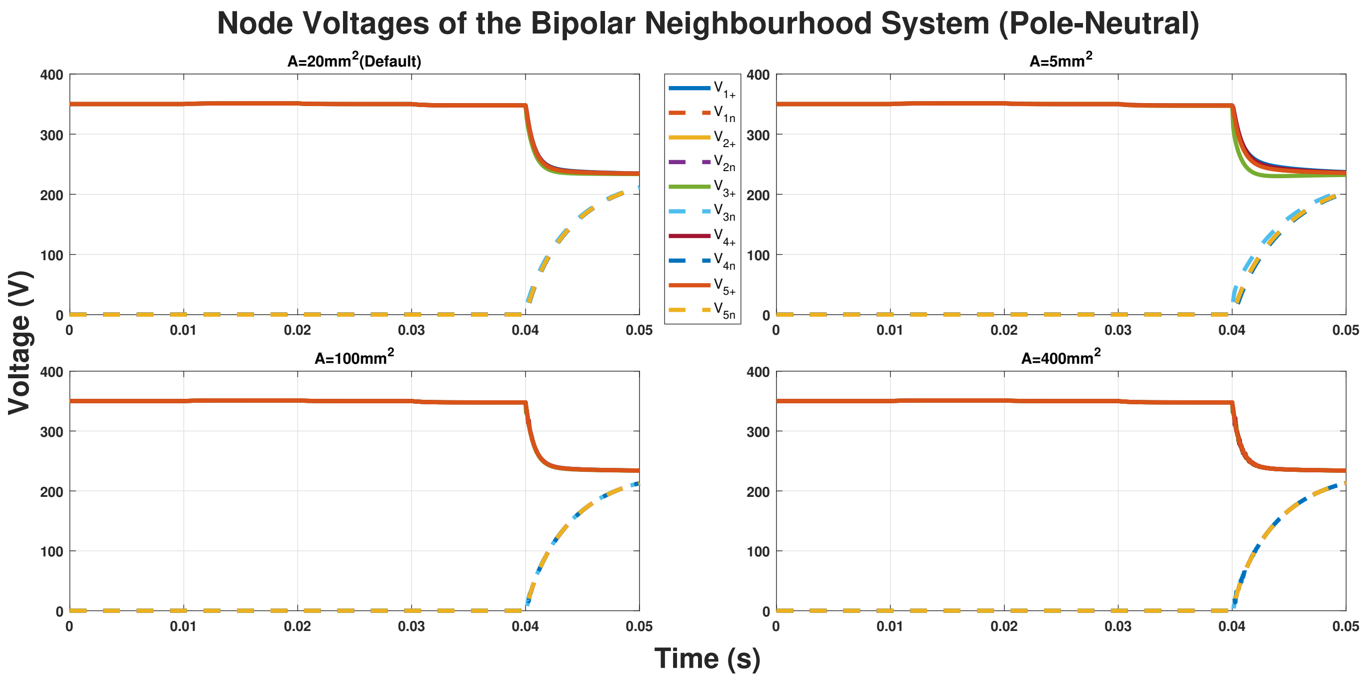

Figure 7.37: Influence of cable cross section variation in the pole to neutral fault node voltage plots of neighbourhood system

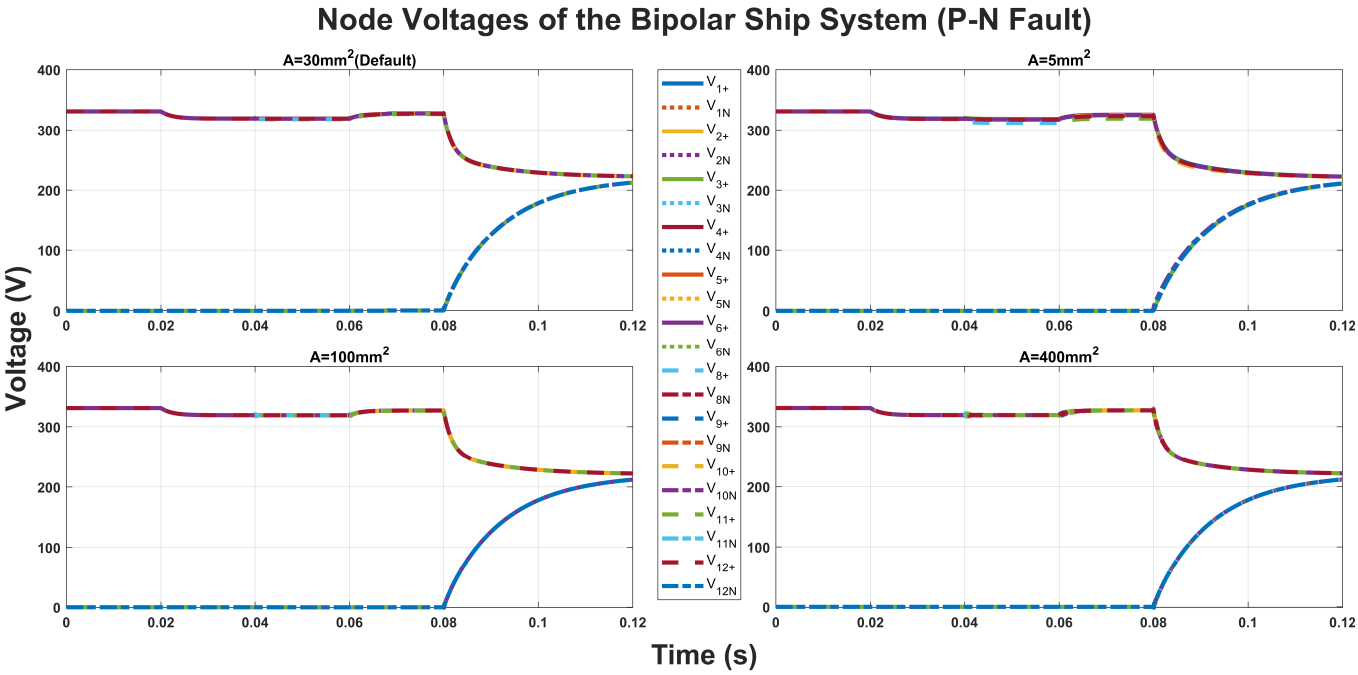

Figure 7.38: Influence of cable cross section variation in the pole to neutral fault node voltage plots of ship system

Table 7.12: Inference from the pole to pole fault analysis carried out for the cable cross section variation

Cable cross section (mm^2)	Node voltage	Line current (PeakIsc (A))	Oscillations
Neighbourhood system: A=5 Ship system:A=5	Equilibrium node voltage achieved after fault occurrence decreases compared - case2. Neigh: V3+= 134.6 Ship:V10+=13.92	Lower peak short circuit current reached compared to case2. Neigh: L2+=180 L5+=-173.3 L7+=170.8 Ship:L9+=6272	Lower oscillations present:node voltage and line current plots compared to case2.
A=100 A=40	Equilibrium node voltage achieved after fault occurrence increases compared - case1. Neigh: V3+=156.3 Ship:V10+=14.79	Higher peak short circuit current reached compared to case1. Neigh: L2+=370.2 L5+=-363.2 L7+=364.3 Ship:L9+=11930	Higher oscillations present: node voltage and line current plots compared to case1.
A=400 A=50	Equilibrium node voltage achieved after fault occurrence highest compared - all cases. Neigh: V3+=157.7 Ship:V10+=16.3	Highest peak short circuit current reached compared to all cases Neigh: L2+=391.9 L5+=-384.4 L7+=385.7 Ship:L9+=12230	Highest oscillations present: node voltage and line current plots compared to allcases.

Table 7.13: Inference from the pole to neutral fault analysis carried out for the cable cross section variation

Cable cross section (mm^2)	Node voltage	Line current (PeakIsc (A))	Oscillations
A=5	**Equilibrium node voltage achieved after fault occurrence decreases compared - case2. Neigh: V3+= 232.2 V3n= 206.7 Ship: V10+=222.4 V10n=211.9**	**Lower peak short circuit current reached compared to case2. Neigh: L2+=98.05 L5+=-91.16 L7+=91.89 Ship:L9+=252.8**	**Lower oscillations present:node voltage and line current plots compared to case2.**
A=100	**Equilibrium node voltage achieved after fault occurrence increases compared - case1. Neigh: V3+=234.1 V3n= 212.9 Ship: V10+=224.2 V10n=212**	**Higher peak short circuit current reached compared to case1. Neigh: L2+=200.7 L5+=-200.7 L7+=171.7 Ship:L9+=424.3**	**Higher oscillations present: node voltage and line current plots compared to case1.**
A=400	**Equilibrium node voltage achieved after fault occurrence highest compared - all cases. Neigh: V3+=234.6 V3n= 213.3 Ship: V10+=224.6 V10n=212.1**	**Highest peak short circuit current reached compared to all cases Neigh: L2+=220.8 L5+=-220.8 L7+=183.6 Ship:L9+=439.6**	**Highest oscillations present: node voltage and line current plots compared to allcases.**

7.3.4. Cable length

In this analysis, first the length of the cable is varied, the rest of the active parameter's values are maintained as it is in the default condition. This cable length value is varied in both the ship and neighbourhood bipolar distribution system. The length of all the cables in the neighbourhood distribution system is taken as 100m and for the ship distribution system the cable length values are already shown in table4.3. The cable length for this analysis is varied and studied for three different cable length configurations in order to properly assess the influence of cable length in the system performance and line currents achieved during short circuit. The cable length value is increased and decreased with respect to the default case value. This analysis is done for both the pole to pole and pole to neutral fault. In the neighbourhood system each of the cable length values chosen for this analysis are 50,200 500(m). For the ship distribution system as there are different lines with different cable length involved, so the cable length variation utilized for the previous sensitivity and stability analysis shown in table7.7 is considered for this analysis. For these set cable length values the node voltages, line currents are analysed separately for both these short circuit faults.

First variation can be seen in the line currents plots of the pole to pole and pole to neutral faults for both the distribution systems. As the cable length values are increased, the peak short circuit current reached by the lines connected to faulted node also decreases. This is due to the cable's active parameters also increasing as the cable length increases. The oscillations present in both the line currents and node voltages plots decreases with the cable length increase. This trend is seen to be similar for both the pole to pole and pole to line fault. The influence of the cable length variation in the line currents plots for both the pole to pole and pole to neutral faults can be seen in Fig7.39-7.42. The peak magnitude of the short circuit current achieved by both the distribution system after each of the faults occurs is noted and presented with the inference from the analysis in table7.14 and 7.15. In the pole to pole fault there is a greater drop of peak magnitude of the short circuit current as the cable length value is increased compared to the pole to neutral fault. For the node voltages plots, the equilibrium node voltage achieved after the fault and the oscillation present in the plots decreases as the cable length is increased. The influence of the cable length variation in the node voltage plots for both the pole to pole and pole to neutral faults can be seen in Fig7.43-7.46. So, it is inferred through these plots, that as the cable length value is increased this leads to the peak short circuit current reached by the lines connected to faulted node to decrease, the equilibrium node voltage achieved after the fault decreases and also the oscillations present in the system decreases for both the faults. A summary table of the findings from this short circuit analysis carried out for the cable length variation is shown table7.14 and 7.15. below.

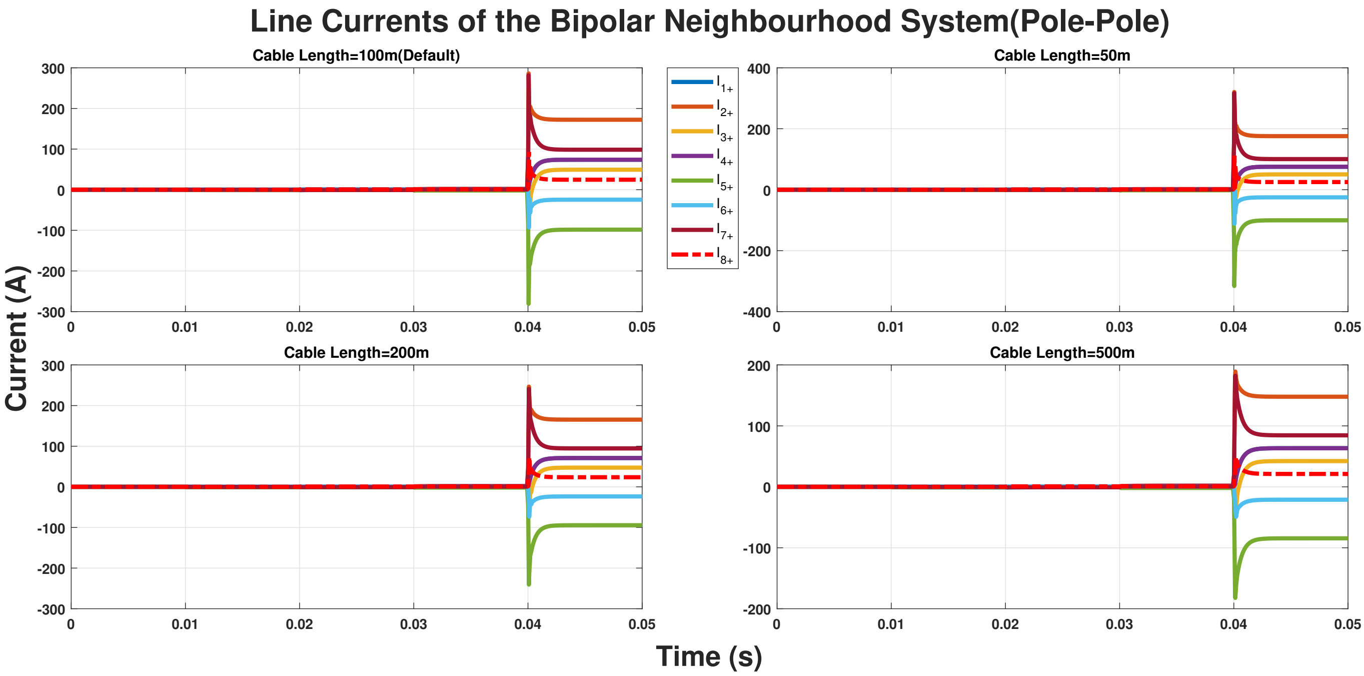

Figure 7.39: Influence of cable length variation in the pole to pole fault line current plots of neighbourhood system

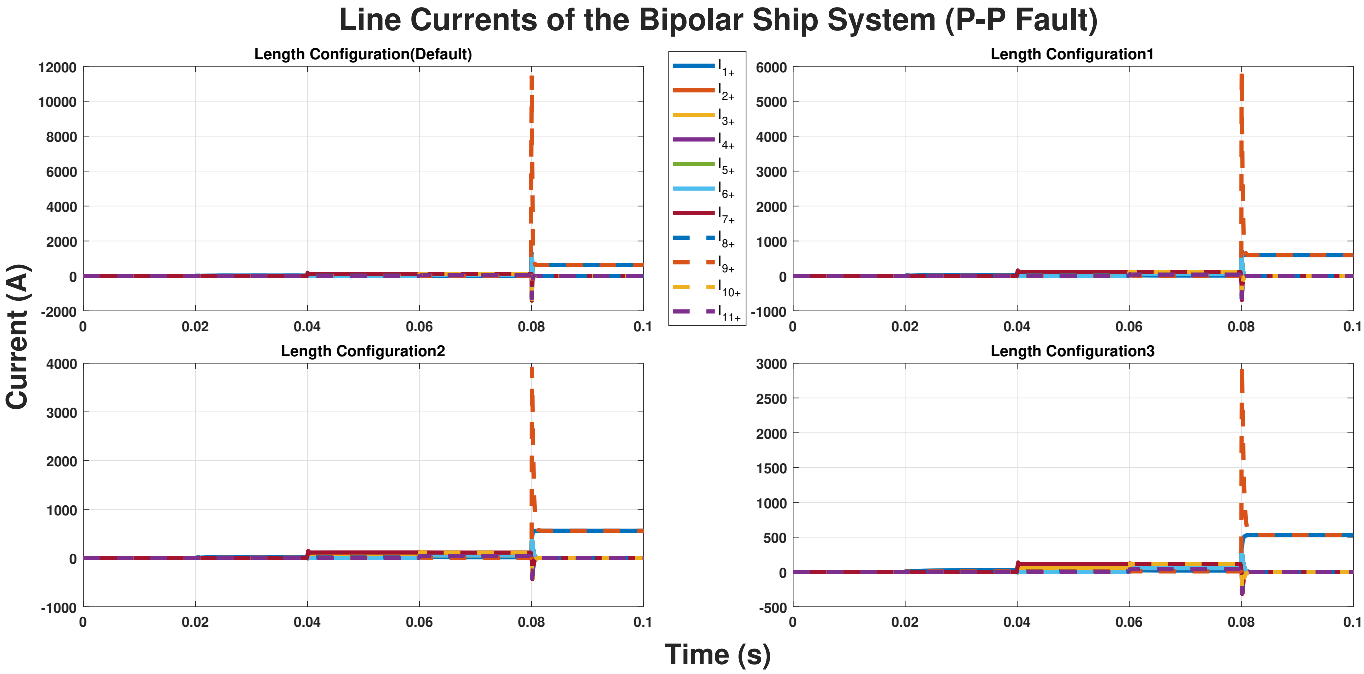

Figure 7.40: Influence of cable length variation in the pole to pole fault line current plots of ship system

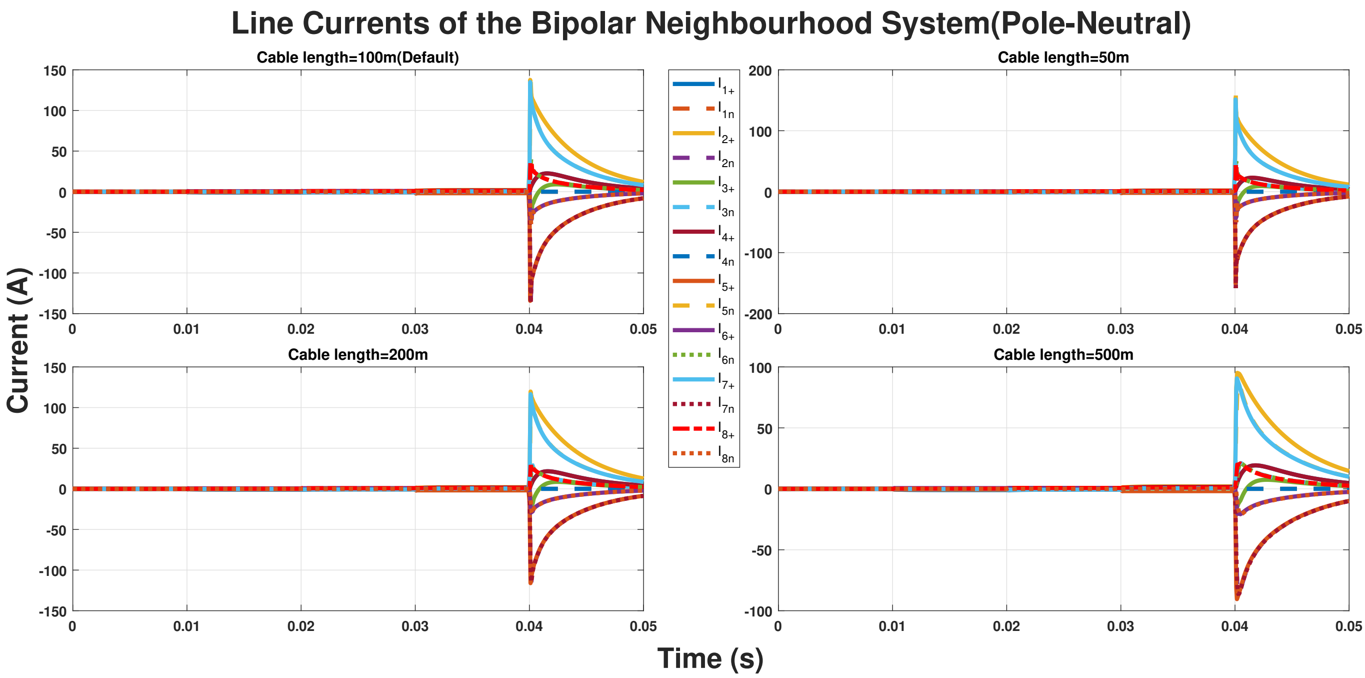

Figure 7.41: Influence of cable length variation in the pole to neutral fault line current plots of neighbourhood system

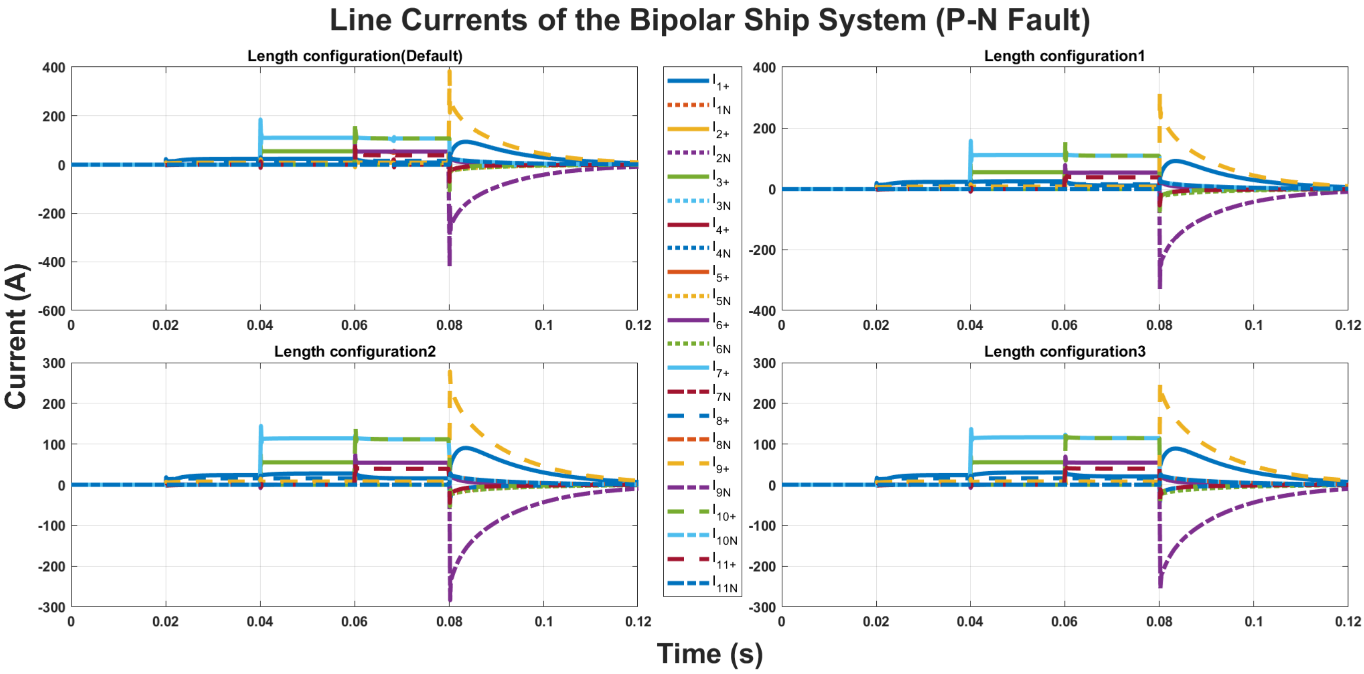

Figure 7.42: Influence of cable length variation in the pole to neutral fault line current plots of ship system

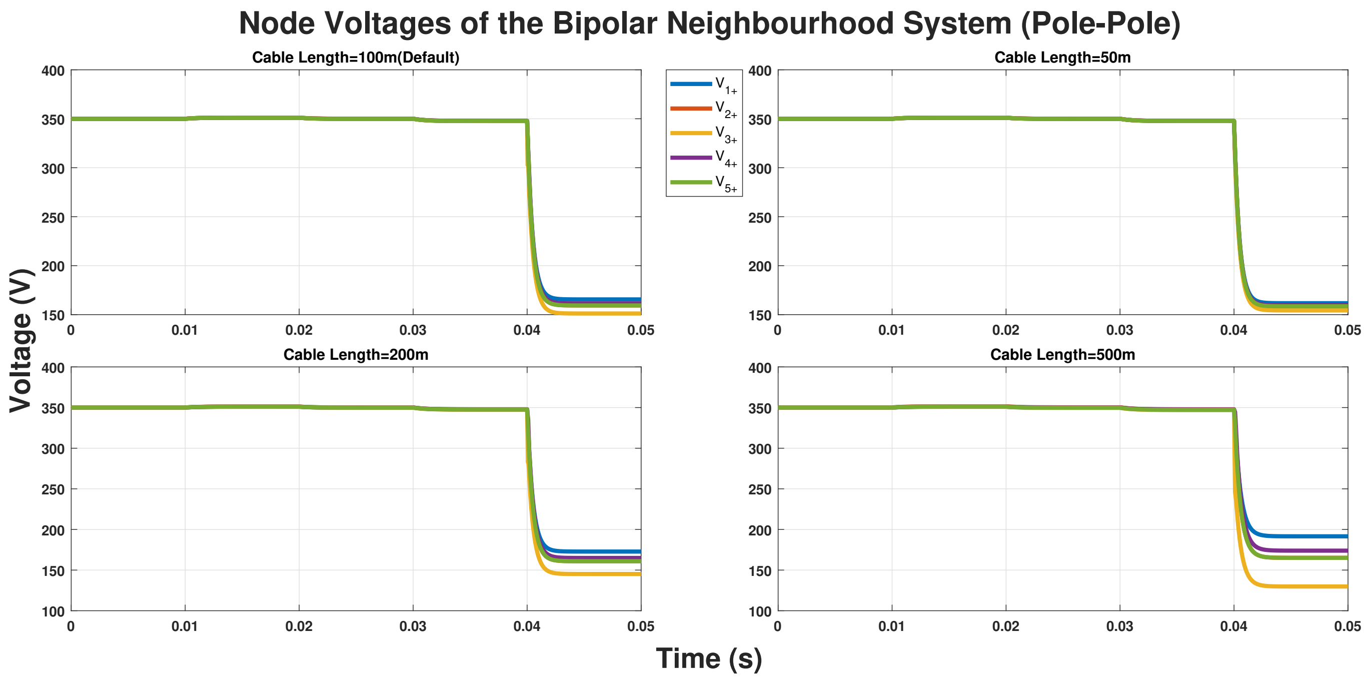

Figure 7.43: Influence of cable length variation in the pole to pole fault node voltage plots of neighbourhood system

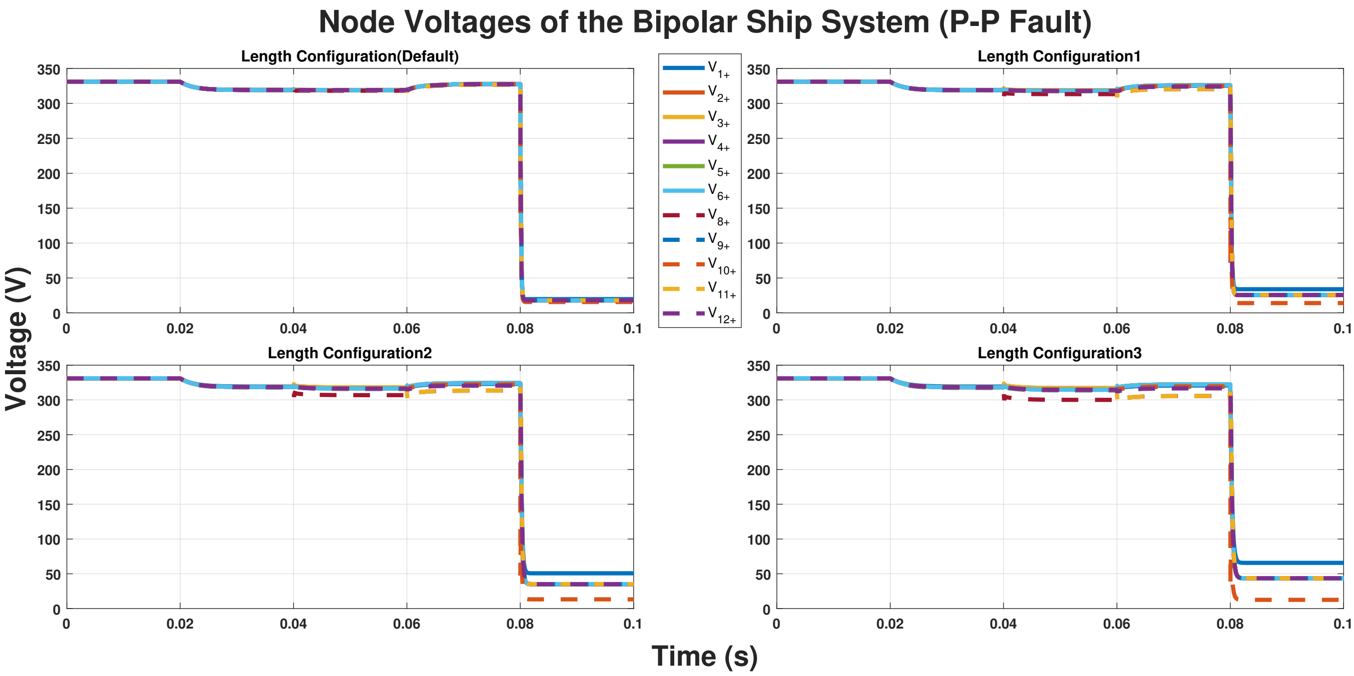

Figure 7.44: Influence of cable length variation in the pole to pole fault node voltage plots of ship system

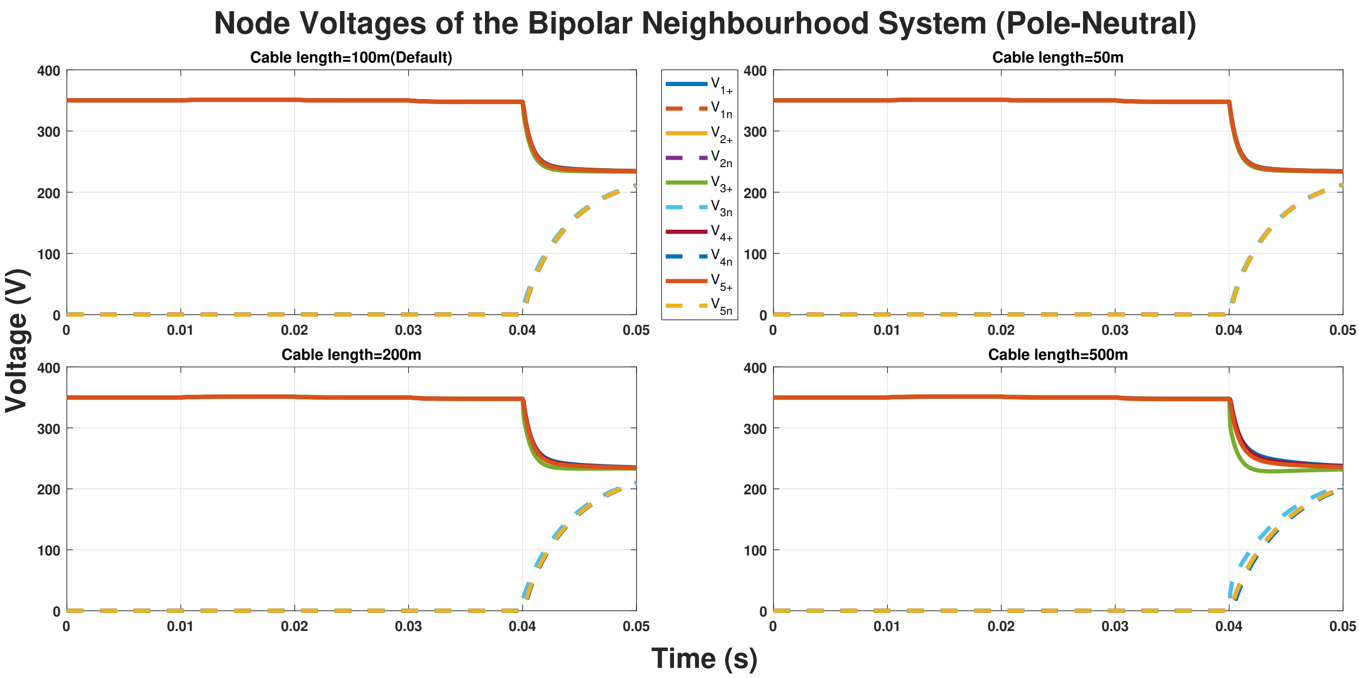

Figure 7.45: Influence of cable length variation in the pole to neutral fault node voltage plots of neighbourhood system

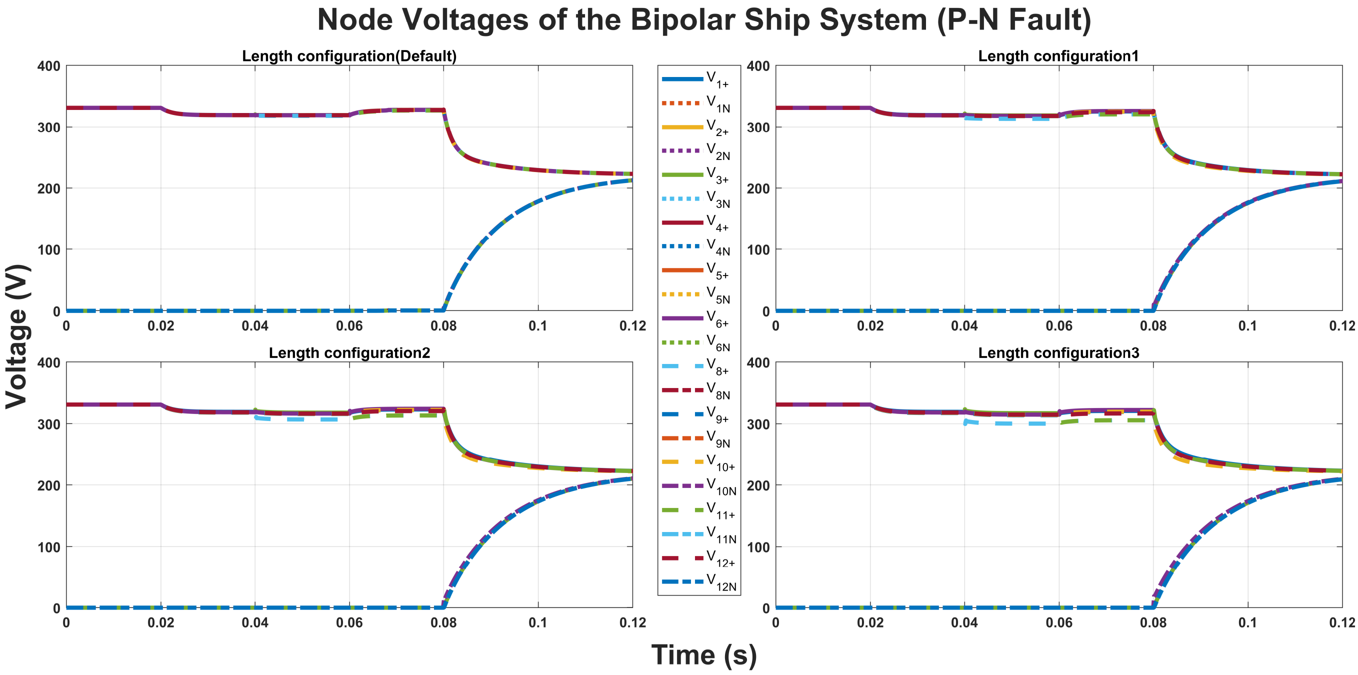

Figure 7.46: Influence of cable length variation in the pole to neutral fault node voltage plots of ship system

Table 7.14: Inference from the pole to pole fault analysis carried out for the cable length variation

Cable Length (m)	Node voltage	Line current (PeakIsc (A))	Oscillations
Neighbourhood system: Length=50 Ship system: Configuration 1	Equilibrium node voltage achieved after faultoccurrence increases compared- case2. Neigh: V3+= 154.3 Ship:V10+=14.05	Higher peak short circuit current reached compared to case2. Neigh: L2+=316.8 L5+=-316.1 L7+=312.8 Ship:L9+=5805	Higher oscillations present: node voltage and line current plots compared to case2.
Length=200 Configuration2	Equilibrium node voltage achieved after faultoccurrence decreases compared - case1. Neigh: V3+=145.2 Ship:V10+=13.26	lower peak short circuit current reached compared to case1. Neigh: L2+=246.6 L5+=-240.6 L7+=244.2 Ship:L9+=3862	lesser oscillations present: node voltage and line current plots compared to case1.
Length=500 Configuration3	Equilibrium node voltage achieved after fault occurrence lowest compared- all cases. Neigh: V3+=129.8 Ship:V10+=12.55	lowest peak short circuit current reached compared to all cases Neigh: L2+=189.2 L5+=-182.3 L7+=185.3 Ship:L9+=2983	Lowest oscillations present: node voltage and line current plots compared to all cases.

Table 7.15: Inference from the pole to neutral fault analysis carried out for the cable length variation

Cable Length (m)	Node voltage	Line current (PeakIsc (A))	Oscillations
Neighbourhood system: Length=50 Ship system: Configuration 1	Equilibrium node voltage achieved after faultoccurrence increases compared - case2. Neigh: V3+= 234.2 V3n= 212.2 Ship: V10+=222.4 V10n=211.2	Higher peak short circuit current reached compared to case2. Neigh: L2+=157.5 L5+=-158.2 L7+=151.2 Ship:L9+=312.4	Higher oscillations present: node voltage and line current plots compared to case2.
Length=200 Configuration2	Equilibrium node voltage achieved after faultoccurrence decreases compared- case1. Neigh: V3+=233.2 V3n=208.6 Ship: V10+=222.1 V10n=210.2	lower peak short circuit current reached compared to case1. Neigh: L2+=119.7 L5+=-114.6 L7+=116.5 Ship:L9+=278.4	lesser oscillations present: node voltage and line current plots compared to case1.
Length=500 Configuration3	Equilibrium node voltage achieved after faultoccurrence lowest compared- all cases. Neigh: V3+=231.7 V3n= 205.2 Ship: V10+=221.6 V10n=209.2	lowest peak short circuit current reached compared to all cases Neigh: L2+=94.87 L5+=–90.49 L7+=90.61 Ship:L9+=253.4	Lowest oscillations present: node voltage and line current plots compared to all cases.

7.4. Accuracy Analysis

7.4.1. Description

This accuracy analysis is performed to validate the accuracy of the model by breaking the distribution system lines into smaller sections and simulating it. The results obtained from these broken down models are compared to analyse the accuracy of the state space approach based dynamic models. This modelling approach, takes a non-transient model with a lumped element representation of the distribution line parameters. So this model neglects the frequency dependent effects and propagation delay present in the system . For that reason, it is necessary to analyse the accuracy of these models utilized in this thesis. As mentioned in several literature [12][15][16]the propagation delay can be neglected by the distribution system, if the length of the distribution lines in the system are smaller than the signal wavelength. For this analysis a sample 2 node 1line distribution system is formulated through the dynamic modelling approach. The frequency of the signal in this distribution system is assessed to be 3MHz. The system lines are broken down into smaller sections (Smaller than the wavelength)and the resulting accuracy analysis results are compared with the dynamic model results.

7.4.2. Analysis

In this approach, the 2 node 1 line sample bipolar system formulated is set as the default dynamic model. The rest of the broken down models results are compared with this default case results inorder to assess the accuracy of the dynamic model. The length of the lines or cable is set to be 100m and the cable cross section is 30 mm2. The length of the distribution lines is broken into smaller sections compared to the wavelength, in order to neglect the frequency dependent effects and propagation delay present in the system and making the system results more accurate. This Bipolar neighbourhood system is broken down in terms of four cases, as shown in the table 7.16 below.

In any case the first node is connected to a droop source and the last node of the bipolar system is connected to a load node. The converters are set to be connected only to these two nodes (i.e source and load node). At 20ms is the only time instance where the load is turned on and takes in 1500 W. For the rest of the time it is switched off. These conditions and smaller system is mainly considered to reduce the simulation time as the line divisions increases. For these set conditions all the four cases are simulated and the results of the node voltages and line current plots are shown in Fig7.47 and 7.48.

In this accuracy analysis, it can be seen from the plots that as the line division increases, at the instance when the load is turned on the amplitude of oscillations present in both the node voltage and line currents plots increases. This is due to increase in line division, even slightest of variation in the system causes increase in the system oscillation. The oscillations present in the line current plots can be seen more significantly, analysing that further. It is seen that the oscillation period after the load is turned on also increases as the line division increases. The accuracy of the dynamic model that has utilised lumped element pi lines (non transient), through these plots it can be assessed that the results obtained are from the dynamic models are closely accurate, when compared to the results of the system with greater line division that has neglected the frequency dependent effects and propagation delay due to its lines being shorter than wavelength. Only when the load is turned on the initial oscillation set by these systems are different, but the equilibrium node voltage and line currents achieved are same. Based on these results it can be adjudged that the dynamic models is a largely accurate model. The main cable length is 100m here, which is a short cable that could have led to lesser differences. When longer cable lengths are divided in to very short lines (greater line divisions) then the system oscillation and performance is expected to be different for each of the load variation and the difference would be significantly higher[8] and[90]. Also the simulation time for these models will be significantly higher. So then, the accuracy of the dynamic model results could be lower as the system oscillation and performance will be varied, when compared to system with longer cables.

Table 7.16: Bipolar Distribution system line breakdown case details

Case	Division	Nodes	Lines	Length per line (m)
Default	1	2	1	100
Case1	10	11	10	10
Case2	50	51	50	2
Case 3	100	101	100	1

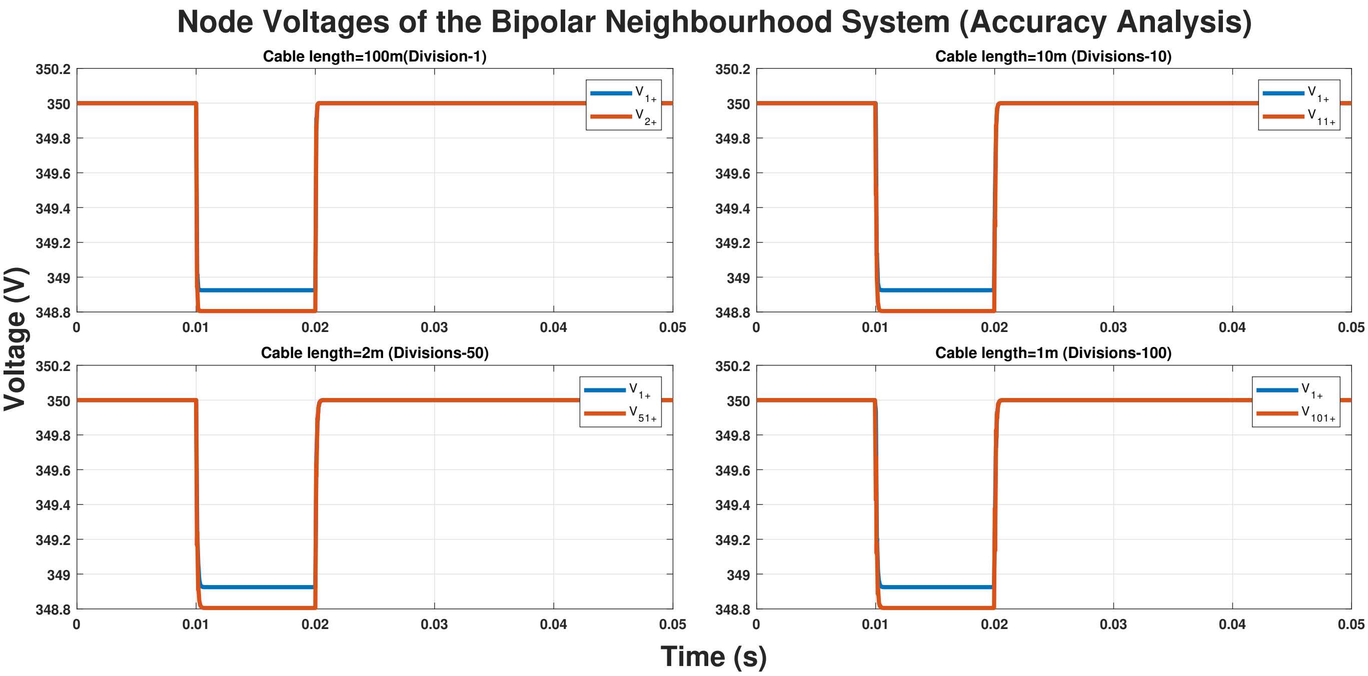

Figure 7.47: Node voltage plots of sample system resulting from the accuracy analysis

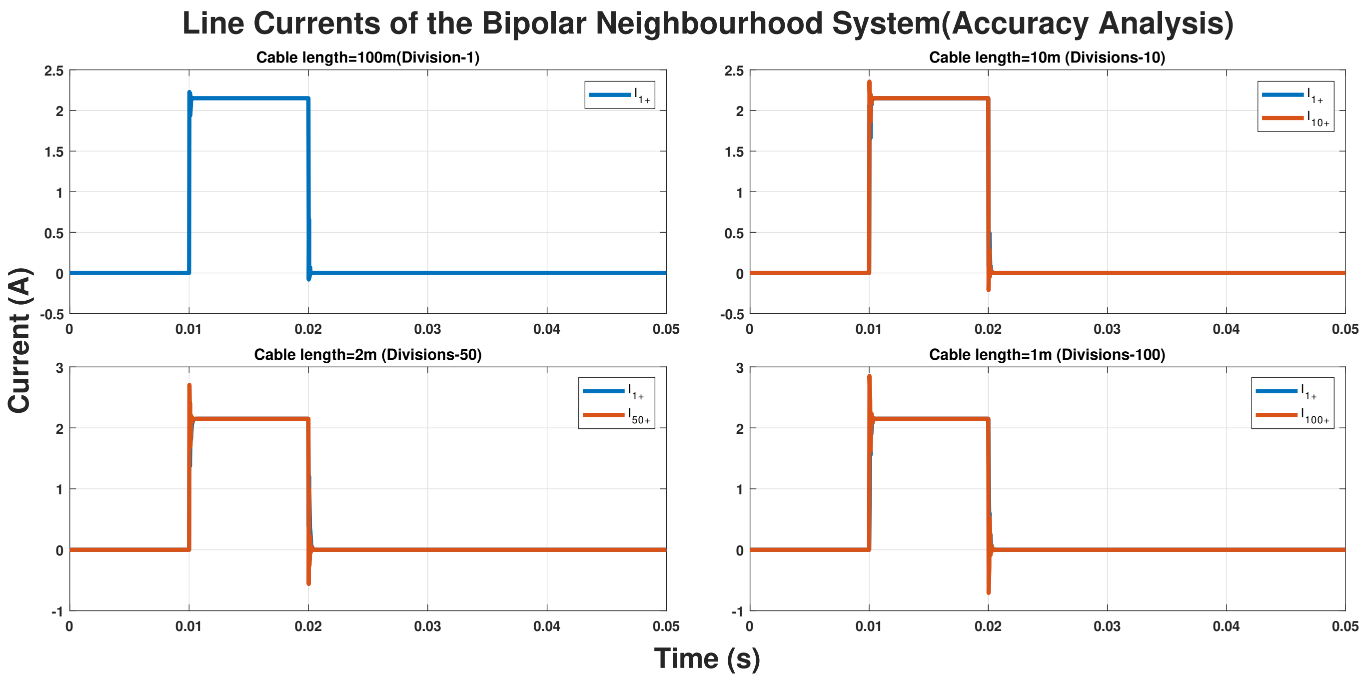

Figure 7.48: Line current plots of bipolar system resulting from the accuracy analysis

7.4.3. Short circuit studies

The short circuit studies are also performed on these distribution system models in order to assess the cable division's influence in the peak short circuit current reached by the system. The pole-pole fault occurs on the node that is present right in the middle of the source and the load node. The lines that are connected to that faulted node are specially assessed and the peak short circuit current reached by these lines are noted down. For ex: if the sample system has 50nodes and 49 lines, then the fault is set to occur at node 25(median) and the lines connected to this node (line 24 and 25) are assessed during fault occurrence. The converters are set to be connected only to these three nodes (i.e source, load and faulted node).

The load is turned on and takes in 1500 W during the time period 20ms till 50ms. For the rest of the time instances it is turned off. The pole to pole fault is considered to occur at t=30ms. The calculated equivalent resistance of these systems is 2.16 Ω. The pole to pole fault procedure followed is already explained in sec6.2.1. The bipolar distribution system division is same as it was previously mentioned in table7.16. The only difference is that the default case lines are now broken down into two divisions having three nodes and two lines in order to accommodate the faulted node.

The resulting plots from the pole to pole fault analysis for the node voltage and line current are shown in Fig7.49 and fig 7.50 below. It can be seen from the node voltage plots that after the pole to pole fault occurrence, the equilibrium node voltage achieved by the droop node and the faulted node decreases as the line division increases. The last node and the faulted node have the same node voltages with very slight difference can be seen in the plots when it's zoomed in. From the line current plots it can be seen that after the pole to pole fault occurs, the peak short circuit current magnitude achieved by the lines connected to the faulted node increases as the line division increases. The magnitude of peak short circuit current reached for the default case(Divisions-2) is 233.8 A and for the fifty divisions case the peak short circuit current reached is 244 A. This difference generates the error percentage of the dynamic model calculated to be 10.2 % for the short circuit studies. Based on this analysis it can be inferred that greater the line divisions shorter than the signal wavelength, higher would be the magnitude of short circuit current reached by the system in turn lowering the equilibrium node voltage achieved after the fault instance.

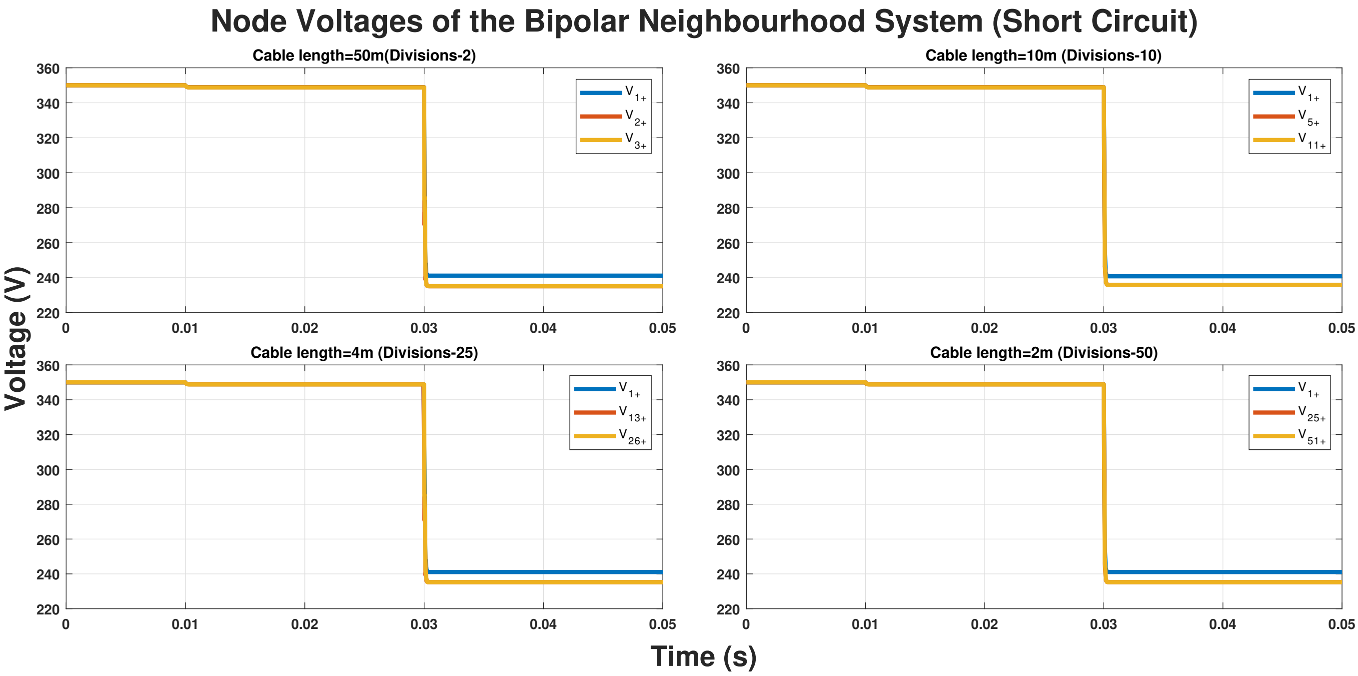

Figure 7.49: Node voltage plots of bipolar system resulting from the pole to pole fault analysis

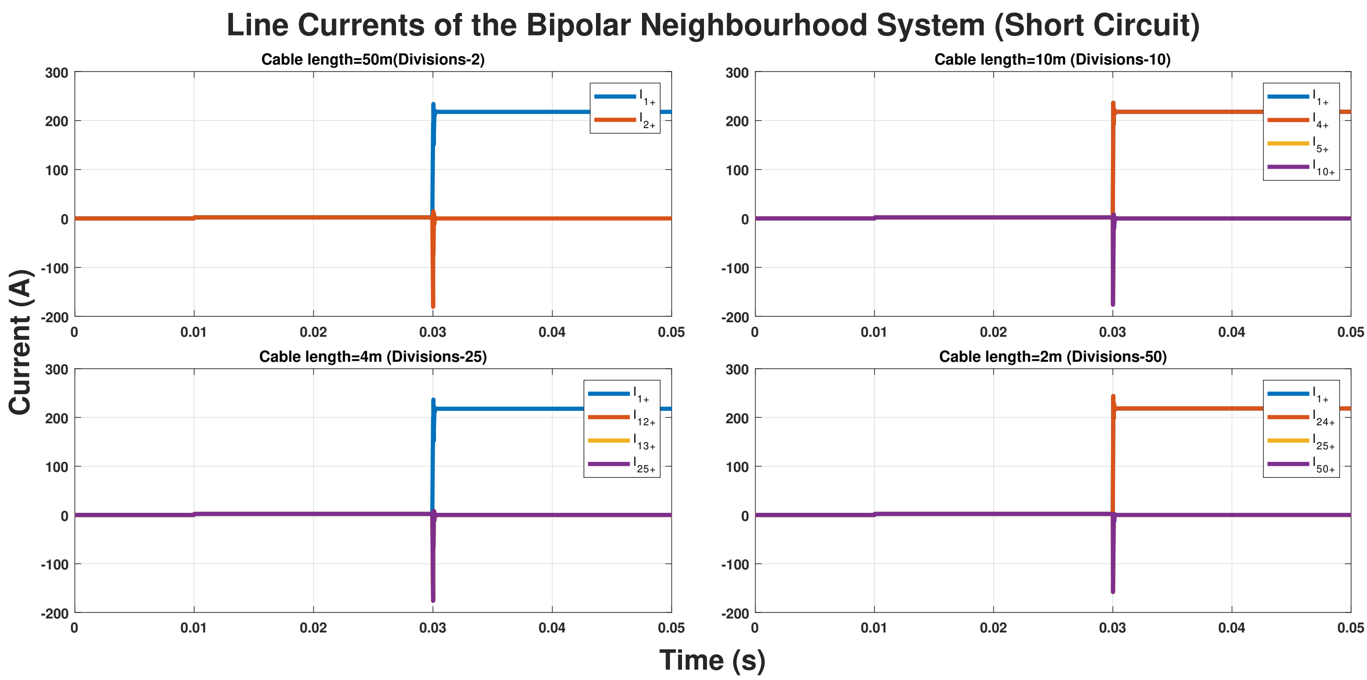

Figure 7.50: Line current plots of bipolar system resulting from the pole to pole fault analysis

7.5. Summary

In this chapter all the results from the different analyses i.e the sensitivity, stability, short circuit and accuracy analysis that is performed in both neighbourhood and ship distribution system were discussed. The influence of cable's active parameter's variation on the system performance and stability was analysed and conclusions are drawn based on the results obtained. Also to validate the accuracy of the dynamic distribution system models, the results from the accuracy analysis performed was discussed. The results from all these analyses mentioned above would surely help in better assessment and designing of the LVDC cables and it supports in formulating the ideal LVDC cable characteristics, as all the active parameters are varied to get this comprehensive outlook.

8 Inference

8.1. Conclusion

The main objective of this thesis is to formulate the optimal characteristics of the LVDC cables based on the outcomes of the different analyses performed during the thesis. The results generated from the sensitivity, stability and short circuit analyses performed is collectively analysed and then the optimal characteristics of the LVDC cables are defined.

The two LVDC state space based dynamic distribution system model namely: a neighbourhood distribution system and a ship distribution system in their monopolar and bipolar configuration are firstly formulated. Then the LVDC cables are incorporated as lines into these models. The Matlab environment was utilized for formulating and simulating the complete LVDC distribution system models. The sensitivity, stability, short circuit and accuracy analyses are performed on the formulated distribution system model. The conclusion of this thesis can be drawn by answering the following research questions.

1. How does the performance and the stability of the LVDC neighbourhood and ship distribution systems gets influenced when each of the active cable and system (system parameters which has influence on the cable) parameters are varied individually?

The inference derived from the sensitivity and stability analysis performed on the DC distribution models, when the active parameters are varied are entailed as follows. The performance of the distribution system (i.e. the node voltage and line current) and the stability of the distribution system (i.e. eigenvalue plots)are closely looked upon to formulate the inference.

- Firstly , as the cable inductance value is decreased this leads to the distribution systems become more stable and fewer oscillations are present. This inductance variation has no distinct effect on the equilibrium node voltage and line current achieved by the distribution system.
- Secondly, as the cable cross-section value is decreased the cable resistance increases and this leads to the distribution systems become more stable, node voltage decreases and fewer oscillations are present.
- Thirdly as the line capacitance is increased this leads to the distribution systems become less stable, the oscillation present in the system increases.
- Fourthly, as the load and source converter capacitance is decreased this leads to the distribution systems become more stable and fewer oscillations are present. The equilibrium node voltages and line currents achieved are not affected by the load and source converter capacitance variation.
- Fifthly as the droop impedance is increased, this leads to the distribution systems become less stable and more oscillations are present. The equilibrium node voltages decreases and the rise and drop of oscillating line currents increases as the as the droop impedance is increased.

- Finally, as the cable length is decreased this leads to the distribution systems become more stable, more stable equilibrium node voltage is achieved, and fewer oscillations are present. As the cable length is decreased this leads the rise and drop of the oscillating line current and the node voltages achieved by the system to decrease and become more stable with less oscillation.

2. How influential are each of the cable‘s active parameters on limiting the effect of the short circuit in the distribution systems modelled?

Based on the results obtained from the pole to pole and pole to neutral fault analysis (SCA) is performed on both the neighbourhood and ship distribution system. The cable’s active parameters variation is seen to have an influence on the system performance and the line current during short circuit condition. It is seen through the result that it could also limit the effect of short circuit on the distribution system. The general trend of the system performance and line current achieved during short circuit due to this cable’s active parameter variation is observed.

- Firstly as the cable inductance value is decreased this leads to the peak short circuit current reached by the lines connected to faulted node for both the faults to decrease and also the oscillations present in the system decreases. This inductance variation has no distinct effect on the decay curve and equilibrium node voltage achieved by the distribution system.
- Secondly as the cable capacitance value is decreased this leads to the peak short circuit current reached by the lines connected to faulted node for both the faults remains same and the oscillations present in the system remain similar throughout This capacitance variation has no distinct effect on the decay curve and equilibrium node voltage achieved by the distribution system.
- Thirdly as the cable cross section value is decreased this leads to the peak short circuit current reached by the lines connected to faulted node to decrease, the equilibrium node voltage achieved after the fault decreases and also the oscillations present in the system decreases for both the faults.
- Finally as the cable length value is increased this leads to the peak short circuit current reached by the lines connected to faulted node to decrease, the equilibrium node voltage achieved after the fault decreases and also the oscillations present in the system decreases for both the faults.

3. How should the optimal LVDC cable’s active parameters look in order to provide the ideal performance expected by the users? Also comment on the accuracy of the dynamic models utilised for the simulation.

After collectively assessing each of the active cable parameters variation’s influence on the performance, oscillations and stability of the distribution system. Based on the results from the sensitivity, stability, short circuit and accuracy analyses, the optimal characteristics of the formulated LVDC cable should be as follows to

- Firstly the cable inductance rating needs to be lowered in the cable design to get better cable performance and higher system protection with improved stability.
- Secondly, the cable resistance needs to be increased in order to get better cable performance and higher system protection with improved stability.
- Thirdly, the cable capacitance needs to be lowered in the cable design to get better cable performance and higher system protection with improved stability.
- Finally, in the case of cable length, it needs to be short to get better system performance and when it’s long it provides better system protection. The pathway to formulate this optimal LVDC cable is presented in section 8.2.

The accuracy of the dynamic model that has utilised lumped element pi lines (non transient), through these plots it can be assessed that the results obtained are from the dynamic models are closely accurate, when compared to the results of the system with greater line division that has neglected the frequency dependent effects and propagation delay due to its lines being shorter than wavelength. Only when the load is turned on the initial oscillation set by these systems are different, but the equilibrium node voltage and line currents achieved are same.

8.2. LVDC Cable optimal characteristics

The optimal LVDC cable's active parameters need to follow a certain trend, to provide the ideal performance expected by the system user. Here the ideal performance means set better system performances and provide better system stability throughout the operation. Also the cable's active parameters has the ability to influence the system to generate lower short circuit peak magnitude in order to protect the system during fault. In order to achieve these optimal characteristics the cable's active parameters needs to follow a certain trend. This certain trend has been formulated by analysing all the results from the stability, sensitivity, accuracy and the short circuit analysis performed during this thesis. The cable inductance, capacitance needs to be lower and the cable resistance needs to be increased in order to get better cable performance and higher system protection with improved stability. But in the case of cable length, it needs to be short to get better system performance and when it's long it provides better system protection. In the upcoming paragraphs, the pathway to formulate this optimal LVDC cable is explained.

Firstly the cable inductance being one among the influential active parameter, its rating needs to be lowered in the cable design to get better cable performance and higher system protection with improved stability. This conclusion is solely based on studying the results derived from the different analyses carried out in this thesis. To achieve lower cable inductance several pathways are available, these pathways are further discussed here. The cable inductance of a single core cable is defined in equ(5.15)[86] the effective self-inductance of the cable can be reduced by reducing the thickness of the outer sheath and increasing the area of the conductor present in the cable. This would lead to the reduction of self-inductance of the single core cable. For the multiconductor cable the inductance is defined in equ(5.16)[86], the inductance of the cable can be reduced by reducing the equidistant spacing between the conductors and increasing the geometric radius of conductor present in the cable. Following this, would reduce the inductance of the cable. The cable needs to be shorter in length, minimising the separation between the conductors and this reduces the cable inductance. For a Bipolar two line system, when the twisting arrangements of cables are used. It is seen to reduce the inductance of the cable as the magnetic field of cables is reduced leading to reduction in inductance [31].

Secondly, the cable resistance needs to be increased in order to get better cable performance and higher system protection with improved stability. To achieve higher cable resistance several pathways are available, these pathways are further discussed here. The resistance of the cable is given by equ(5.11)[86]., the cross section area of the cable needs to be reduced to get higher resistance as they both are inversely proportional to each other. The cross section area of the cable can be reduced by reducing the equidistant spacing between the conductor by having a tightly packed cable with reduced separation distance between the conductors. Also decreasing the thickness of the external sheath of the cable could help in reducing the cable area and increasing the cable resistance. When the length of the cable is longer it is directly proportional to the resistance increasing the cable resistance. By replacing the conductor material of the cable with the conductor having higher resistivity increases the cable resistance. Also, decreasing the thickness of the insulation layer will lead to decrease in the cross section area leading to increase in the resistance of the cable[31].

Finally, the cable capacitance needs to be lowered in the cable design to get better cable performance and higher system protection with improved stability. To achieve lower cable capacitance several pathways are available, these pathways are further discussed here. Firstly, the capacitance of the single core cable is defined in equ (5.12)[8]. The capacitance of these cables can be reduced by increasing the thickness of the cable sheath, having shorter cable length, utilising certain insulation material for the cable with lower relative permittivity and reducing the radius of the conductor material used in the cable will lead to the cable capacitance rating to be reduced. Secondly, the pole-pole capacitance of multi conductor cable is defined in equ(5.13)[12]. The capacitance of these cables can be reduced by increasing the spacing between the conductors, having shorter cable length, utilising certain insulation material for the cable with lower relative permittivity and reducing the radius of the conductor material used in the cable will lead to the cable capacitance rating to be reduced[8]. The insulation layer also influences the cable capacitance, as the thickness of the layer increases the cable capacitance gets reduced[90].

These were the pathway to formulate an optimal LVDC cable, where the optimal characteristics of the LVDC cable were defined based on the results from different analyses conducted during this thesis.

8.3. Future Scope

This thesis work could be further taken forward by carrying out research on these recommended parts presented below.

- The influence of the damping factor of the cable in the performance and the stability of the system could be further researched.As the increase in damping factor of the cable would reduce the oscillations present in the system[31]. Also the damping factor unites all the active parameters of the cable and the results produced based on the damping factor of the cable would be a significant additions.
- Based on the LVDC optimal characterstics section presented in the thesis, the optimal LVDC cable can be formulated on COMSOL. For different cable configuration the FEM simulations could be performed to assess the electric field distribution under different test conditions(i.e Moisture ingress and introducing elliptical voids in the cable).The electric field distribution analysis would be significant in assessing the stability of the cable and cable failure occurrence of the formulated LVDC cable[9].

Bibliography

[1] *Global electricity demand to increase 57% by 2050*, Sep. 2018. [Online]. Available: https://about.bnef.com/blog/global-electricity-demand-increase-57-2050/.

[2] M. Larsson, "Global Energy Transformation-A Roadmap to 2050," Tech. Rep., 2018. DOI: 10.1057/9780230244092.

[3] A. Shekhar, E. Kontos, A. R. Mor, L. Ramírez-Elizondo, and P. Bauer, "Refurbishing existing mvac distribution cables to operate under dc conditions," in *2016 IEEE International Power Electronics and Motion Control Conference (PEMC)*, 2016, pp. 450–455. DOI: 10.1109/EPEPEMC.2016.7752039.

[4] P. B. Aditya Shekhar, Laura Ramírez-Elizondo, "Grid capacity and efficiency enhancement by operating medium voltage AC cables as DC links with modular multilevel converters," Ph.D. dissertation, 2017.

[5] A. Clerici and L. Paris, "HVDC conversion of HVAC lines to provide substantial power upgrading," vol. 6, no. 1, pp. 324–333, 1991.

[6] R. Asad and A. Kazemi, "A Quantitative Analysis of Effects of Transition from AC to DC System , on Storage and Distribution Systems," 2012.

[7] prof.dr.ir. P. Bauer, "From DC building to a DC distribution and transmission :" *Tudelft*, no. June, 2017.

[8] G.Raju, *Electromagnetic Field Theory and Transmission Lines*, 2nd. Pearson, 2003, ISBN: 9788131701713.

[9] D. Antoniou, A. Tzimas, and S. M. Rowland, "DC utilization of existing LVAC distribution cables," *2013 IEEE Electrical Insulation Conference, EIC 2013*, no. June, pp. 518–522, 2013. DOI: 10.1109/EIC.2013.6554302.

[10] G. Liu, Y. Liu, S. Jiang, H. Li, Y. Zhao, and T. Xiong, "The comparison of full link energy efficiency between low voltage ac and dc distribution power system," in *2019 IEEE Sustainable Power and Energy Conference (iSPEC)*, 2019, pp. 2385–2390. DOI: 10.1109/iSPEC48194.2019.8975141.

[11] B. Kruizinga, "Low voltage underground power cable system: Degradation Mechanism and the path to diagnostics," Ph.D. dissertation, 2017, ISBN: 9789038642499.

[12] C. R. Paul, *Analysis of Multiconductor Transmission Lines*, 2nd ed. Wiley Series in Microwave Optical Engineering, 2007.

[13] N. H. V. D. Blij, L. M. Ramirez-elizondo, M. T. J. Spaan, and P. Bauer, "A State-Space Approach to Modelling DC Distribution Systems," vol. 33, no. 1, pp. 943–950, 2018.

[14] T. Dhaene and D. de Zutter, "Selection of lumped element models for coupled lossy transmission lines," *IEEE Transactions on Computer-Aided Design of Integrated Circuits and Systems*, vol. 11, no. 7, pp. 805–815, 1992. DOI: 10.1109/43.144845.

[15] J. Han, Y.-s. Oh, G.-h. Gwon, D.-u. Kim, and C.-h. Noh, "Modeling and Analysis of a Low-Voltage DC Distribution System," 2015, pp. 713–735. DOI: 10.3390/resources4030713.

[16] X. Zhang, "Analysis and selection of transmission line models used in power system transient simulations," vol. 17, no. 4, pp. 239–246, 1995.

[17] International Electrotechnical Commission, "INTERNATIONAL STANDARD Voltage level classification," *IEC*, 2009.

[18] V.Kamaraju, *Electrical Power Distribution Systems*. McGraw Hill, 2014, ISBN: 9780070151413.

[19] A. A. Sallam and O. P. Malik, *Electric distribution systems*. 2018, pp. 1–604, ISBN: 9781119509332. DOI: 10.1002/9781119509332.

[20] P. Waeckerlé, "Potential of using Low Voltage Direct Current in local distribution network to improve the overall efficiency," p. 76, 2011. [Online]. Available: https://www.diva-portal.org/smash/get/diva2:470829/FULLTEXT01.pdf..

[21] A. Agustoni, E. Borioli, M. Brenna, G. Simioli, E. Tironi, and G. Ubezio, "LV DC distribution network with distributed energy resources: Analysis of possible structures," *IEE Conference Publication*, vol. 5, no. 2005-11034, pp. 49–53, 2005, ISSN: 05379989. DOI: 10.1049/cp:20051292.

[22] E. Borioli, M. Brenna, R. Faranda, and G. Simioli, "A comparison between the electrical capabilities of the cables used in LV AC and DC power lines," *2004 11th International Conference on Harmonics and Quality of Power*, pp. 408–413, 2004. DOI: 10.1109/ichqp.2004.1409390.

[23] G. V. D. Broeck, "Voltage control of bipolar DC distribution systems," Ph.D. dissertation, KU Leuven, 2019.

[24] L. Mackay, "Steps towards the universal direct current distribution system," Ph.D. dissertation, TU Delft, 2018, ISBN: 9789461869050. DOI: 10.4233/uuid.

[25] A. Tzimas, D. Antoniou, and S. M. Rowland, "Low voltage DC cable insulation challenges and opportunities," *Annual Report - Conference on Electrical Insulation and Dielectric Phenomena, CEIDP*, pp. 696–699, 2012, ISSN: 00849162. DOI: 10.1109/CEIDP.2012.6378876.

[26] M. M. Hirschler, *Electrical Insulating Materials : International Issues*. ASTM Symposium on Electrical Insulating Materials: International Issues (1999ASTM Symposium on Electrical Insulating Materials: International Issues (1999, 2000, ISBN: 0803126131.

[27] T. Andritsch, A. Vaughan, and G. C. Stevens, "Novel insulation materials for high voltage cable systems," *IEEE Electrical Insulation Magazine*, vol. 33, no. 4, pp. 27–33, 2017, ISSN: 08837554. DOI: 10.1109/MEI.2017.7956630.

[28] D. Antoniou, "Transition from AC to DC LV Distribution Networks," 2015.

[29] B. Kruizinga, P. A. Wouters, and E. F. Steennis, "Comparison of polymeric insulation materials on failure development in low-voltage underground power cables," *34th Electrical Insulation Conference, EIC 2016*, no. June, pp. 444–447, 2016. DOI: 10.1109/EIC.2016.7548633.

[30] S. Kulkarni, "Fault Location and Characterization in AC and DC Power Systems," p. 304, 2012. [Online]. Available: http://hdl.handle.net/2152/22121.

[31] A. William, *Electrical Power Cable Engineering, Third Edition*. 2012, ISBN: 9781439856451.

[32] D. Enescu, P. Colella, and A. Russo, "Thermal assessment of power cables and impacts on cable current rating: An overview," *Energies*, vol. 13, no. 20, 2020, ISSN: 19961073. DOI: 10.3390/en13205319.

[33] A. S. Alghamdi and R. K. Desuqi, "A study of expected lifetime of XLPE insulation cables working at elevated temperatures by applying accelerated thermal ageing," *Heliyon*, vol. 6, no. 1, e03120, 2020, ISSN: 24058440. DOI: 10.1016/j.heliyon.2019.e03120. [Online]. Available: https://doi.org/10.1016/j.heliyon.2019.e03120.

[34] V. Ganguli, Sushil Kumar Kohli, *Power cable technology*. 2016, ISBN: 9781498709101. [Online]. Available: http://library1.nida.ac.th/termpaper6/sd/2554/19755.pdf.

[35] X. H. Wang, Y. H. Song, C. K. Jung, and J. B. Lee, "Tackling sheath problems : Latest research developments in solving operational sheath problems in underground power transmission cables," vol. 77, pp. 1449–1457, 2007. DOI: 10.1016/j.epsr.2006.10.004.

[36] W. Boone, "COPPER IN COMPARISON WITH ALUMINIUM AS COMMON MATERIAL IN CONDUCTORS OF LV AND MV CABLES CONDUCTORS USED IN LV AND MV," June, 23 rd International Conference on Electricity Distribution Paper 0026, 2015, pp. 15–18.

[37] T. D. Eish, F. M. H. Youssef, and S. S. El-Dessouky, "Effect of temperature rise and water contamination on leakage current in underwater used xlpe insulated power cables," in *Conference Record of the 1988 IEEE International Symposium on Electrical Insulation*, 1988, pp. 343–346. DOI: 10.1109/ELINSL.1988.13937.

[38] PacificElectric, *Products & Services□Pacific Electric Wire and Cable Co Ltd*, 2019. [Online]. Available: https://www.pewc.com.tw/en/p2-products-2-3.php (visited on 02/25/2021).

[39] "Ieee draft guide for selecting and testing jackets for power, instrumentation, and control cables," *IEEE P532/D4, October 2020*, pp. 1–45, 2020.

[40] Habia, *Insulations and sheats | Habia Cable*. [Online]. Available: `https://www.habia.com/our-knowledge/materials/insulation-and-sheath/` (visited on 02/25/2021).

[41] "Ieee guide for the design andinstallation of cable systems in substations," *IEEE Std 525-2016 (Revision of IEEE Std 525-2007)*, pp. 1–243, 2016. DOI: `10.1109/IEEESTD.2016.7747734`.

[42] I. Pleşa, P. V. Noţingher, C. Stancu, F. Wiesbrock, and S. Schlögl, "Polyethylene Nanocomposites for Power Cable Insulations," pp. 1–60, 2019. DOI: `10.3390/polym11010024`.

[43] Anixter, *Cable Jacket Types 101 | Anixter*. [Online]. Available: `https://www.anixter.com/en%7B%5C_%7Dus/resources/literature/wire-wisdom/cable-jackets-types-101.html` (visited on 02/25/2021).

[44] GalaxyWire, *Chlorinated Polyethylene (CPE) Insulation/Jacket Material for Wire and Cable | Galaxy*, 2015. [Online]. Available: `https://www.galaxywire.com/custom-wire-cable/jacket-insulation/cpe-chlorinated-polyethylene/` (visited on 02/25/2021).

[45] S. Anand and B. G. Fernandes, "Reduced-Order Model and Stability Analysis of Low-Voltage DC Microgrid," vol. 60, no. 11, pp. 5040–5049, 2013.

[46] N. Van der Blij, "DC Distribution Systems Modeling , Stability , Control & Protection," Ph.D. dissertation, 2020, ISBN: 9789463841528. DOI: `10.4233/uuid`.

[47] K. Smith, S. Galloway, and G. Burt, "A Review of Design Criteria for Low Voltage DC Distribution Stability," 2016.

[48] F. Ghazanfar, "Modeling of LVDC Distribution System: An Assessment of Control, Power Quality, and DC Faults," Ph.D. dissertation, POLITECNICO DI MILANO, 2019.

[49] P. Salonen, P. Nuutinen, P. Peltoniemi, and J. Partanen, "Protection scheme for an lvdc distribution system," in *CIRED 2009 - 20th International Conference and Exhibition on Electricity Distribution - Part 1*, 2009, pp. 1–4. DOI: `10.1049/cp.2009.1053`.

[50] J. V. Euler-chelpin and J. V. Euler-chelpin, "Distribution Grid Fault Location An Analysis of Methods for Fault Location in LV and MV Power Distribution Grids," Ph.D. dissertation, 2018.

[51] Y. Norouzi, C. Frohne, V. Gauler, *et al.*, "IDENTIFICATION AND CLASSIFICATION OF FAULTS IN DC CABLE SYSTEMS," 2017.

[52] R. Guarnotta, "Optimal Power Flow and Pricing Mechanism for Bipolar DC Distribution Grids," *Delft University of Technology*, 2016.

[53] L. Mackay, T. Hailu, L. Ramirez-Elizondo, and P. Bauer, "Towards a DC distribution system-opportunities and challenges," *2015 IEEE 1st International Conference on Direct Current Microgrids, ICDCM 2015*, pp. 215–220, 2015. DOI: `10.1109/ICDCM.2015.7152041`.

[54] T. Dragicevic, J. Vasquez, J. Guerrero, and D. Škrlec, "Advanced LVDC Electrical Power Architectures and Microgrids," *IEEE Electrification Magazine*, vol. 2, no. 1, pp. 54–65, 2014, ISSN: 2325-5897.

[55] G. Makarabbi, V. Gavade, R. Panguloori, and P. Mishra, "Compatibility and performance study of home appliances in a DC home distribution system," *2014 IEEE International Conference on Power Electronics, Drives and Energy Systems, PEDES 2014*, 2014. DOI: `10.1109/PEDES.2014.7042151`.

[56] E. Rodriguez-Diaz, M. Savaghebi, J. C. Vasquez, and J. M. Guerrero, "An overview of low voltage DC distribution systems for residential applications," *5th IEEE International Conference on Consumer Electronics - Berlin, ICCE-Berlin 2015*, pp. 318–322, 2015. DOI: `10.1109/ICCE-Berlin.2015.7391268`.

[57] M. T. M. Alhashimi, Y. Jawad, K. Nukhailawi, and A. T. Ali, "Review on Electrical Wiring (Types , Sizes and Installation)," no. December 2019, 2019.

[58] Stijn Cole, "STEADY-STATE AND DYNAMIC MODELLING OF VSC HVDC SYSTEMS FOR POWER SYSTEM," Ph.D. dissertation, Katholieke Universiteit Leuven, 2010, ISBN: 9789460182396.

[59] D. Petropoulos, "Transient Analysis of DC Distribution Grids," Ph.D. dissertation, TU Delft, 2016.

[60] B. Mao, B. Zhang, J. Wang, *et al.*, "Dynamic Modelling for Distribution Networks Containing Dispersed Generations and Energy Storage Devices," no. October 2010, 2016. DOI: 10.1109/POWERCON.2010.5666158.

[61] D. Santos-martin, "Simplified Modeling of Low Voltage Distribution Networks for PV Voltage Impact Studies," Tech. Rep. January 2015, 2016. DOI: 10.1109/TSG.2015.2500620.

[62] J. C. Boemer and M. Gibescu, "Dynamic Models for Transient Stability Analysis of Transmission and Distribution Systems with Distributed Generation : an overview," *IEEE Bucharest Power Tech Conference*, 2010. DOI: 10.1109/PTC.2009.5282177.

[63] A. Bazoune, *Transfer function approach to modeling Dynamic Systems*. 2012.

[64] G. Shahgholian and A. Fattollahi, "Improving Power System Stability Using Transfer Function : A Comparative Analysis," Tech. Rep. 5, 2017, pp. 1946–1952.

[65] D. J. Pagano, E. Lenz, and V. Stramosk, "Modeling and Stability Analysis of Islanded DC Microgrids under Droop Control," Tech. Rep. X, 2014, pp. 1–11. DOI: 10.1109/TPEL.2014.2360171.

[66] T. G. Hailu, L. Mackay, and L. M. Ramirez-elizondo, "Voltage Weak DC Distribution Grids," *Electric Power Components and Systems*, vol. 45, no. 10, pp. 1091–1105, 2017, ISSN: 1532-5008. DOI: 10.1080/15325008.2017.1319436. [Online]. Available: https://doi.org/10.1080/15325008.2017.1319436.

[67] Q. Shafiee, T. Dragicevic, J. C. Vasquez, and J. M. Guerrero, "Modeling , Stability Analysis and Active Stabilization of Multiple DC-Microgrid Clusters," no. Lvdc, pp. 1284–1290, 2014.

[68] F. Barakou, "Transient Modeling and Sensitivity Analysis of Cable System Parameters," 2016.

[69] M. T. Dat, G. Van Den Broeck, and J. Driesen, "Modeling the dynamics of a DC distribution grid integrated of renewable energy sources," *IECON Proceedings (Industrial Electronics Conference)*, no. February, pp. 5559–5564, 2014. DOI: 10.1109/IECON.2014.7049350.

[70] M. T. Dat, G. Van den Broeck, and J. Driesen, "Modeling the dynamics of a dc distribution grid integrated of renewable energy sources," in *IECON 2014 - 40th Annual Conference of the IEEE Industrial Electronics Society*, 2014, pp. 5559–5564. DOI: 10.1109/IECON.2014.7049350.

[71] P. Li, H. Yu, C. Wang, *et al.*, "State-space model generation of distribution networks for model order reduction application," in *2013 IEEE Power Energy Society General Meeting*, 2013, pp. 1–5. DOI: 10.1109/PESMG.2013.6672287.

[72] John, *How to get the state-space model of a dynamic system*, 2019. [Online]. Available: https://x-engineer.org/graduate-engineering/signals-systems/control-systems/state-space-model-dynamic-system/ (visited on 02/25/2021).

[73] Y. Tang, "Distribution System Modeling, Analysis and Design with High Penetration of Photovoltaic Generation," Ph.D. dissertation, 2017, p. 192, ISBN: 9781339714219. [Online]. Available: http://ezproxy.rice.edu/login?url=https://search.proquest.com/docview/1793408092?accountid=7064%7B%5C%%7D0Ahttp://sfxhosted.exlibrisgroup.com/rice?url%7B%5C_%7Dver=Z39.88-2004%7B%5C&%7Drft%7B%5C_%7Dval%7B%5C_%7Dfmt=info:ofi/fmt:kev:mtx:dissertation%7B%5C&%7Dgenre=dissertations+%7B%5C%%7D26+theses%7B%5C&%7Dsid=ProQ:ProQuest+Di.

[74] N. H. van der Blij, L. M. Ramirez-Elizondo, M. T. Spaan, and P. Bauer, "A state-space approach to modelling DC distribution systems," *IEEE Transactions on Power Systems*, vol. 33, no. 1, pp. 949–950, 2018, ISSN: 08858950. DOI: 10.1109/TPWRS.2017.2691547.

[75] F. Cecati, "Stability Analysis and Control of a Distribution Grid with High Penetration of Wind Energy," 2016.

[76] S. Yadav, N. H. Van Der Blij, and P. Bauer, "Modeling and stability analysis of radial and zonal architectures of a bipolar dc ferry ship," in *2021 IEEE Electric Ship Technologies Symposium (ESTS)*, 2021, pp. 1–8. DOI: 10.1109/ESTS49166.2021.9512334.

[77] A. Thiyagarajan, S. G. Praveen Kumar, and A. Nandini, "Analysis and comparison of conventional and interleaved DC/DC boost converter," *2nd International Conference on Current Trends in Engineering and Technology, ICCTET 2014*, pp. 198–205, 2014. DOI: 10.1109/ICCTET.2014.6966287.

[78] A. A. Aboushady, K. H. Ahmed, S. J. Finney, and B. W. Williams, “Linearized large signal modeling, analysis, and control design of phase-controlled series-parallel resonant converters using state feedback,” *IEEE Transactions on Power Electronics*, vol. 28, no. 8, pp. 3896–3911, 2013, ISSN: 08858993. DOI: 10.1109/TPEL.2012.2231700.

[79] K. Jha and S. Mishra, “Large-signal linearization of a boost converter,” *2010 IEEE Energy Conversion Congress and Exposition, ECCE 2010 - Proceedings*, pp. 4140–4144, 2010. DOI: 10.1109/ECCE.2010.5617739.

[80] F. L. Luo, “Small signal investigation of energy factor and mathematical modeling for power DC/DC converters,” *7th International Power Engineering Conference, IPEC2005*, vol. 2005, pp. 1–6, 2005. DOI: 10.1109/ipec.2005.207021.

[81] C.-c. Li, T.-h. Tseng, and P.-h. Huang, “New Eigenvalue Method for Power System Stability Analysis,” vol. 733, pp. 888–891, 2013. DOI: 10.4028/www.scientific.net/AMR.732-733.888.

[82] P. Kundur, *Power system stability and control*. 2007.

[83] Z. Jin, L. Meng, and J. M. Guerrero, “Constant power load instability mitigation in DC shipboard power systems using negative series virtual inductor method,” *Proceedings IECON 2017 - 43rd Annual Conference of the IEEE Industrial Electronics Society*, vol. 2017-Janua, pp. 6789–6794, 2017. DOI: 10.1109/IECON.2017.8217186.

[84] L. Chua, D. Charles, and K. Ernest, *Linear and Nonlinear Circuits*. McGraw Hill, 1987, ISBN: 0070108986.

[85] S. Maniktala, *DC- DC Converter Design and Magnetics*. Science direct, 2012, pp. 61–121, ISBN: 9780123865335. DOI: 10.1016/B978-0-12-386533-5.00002-4.

[86] L. Grigsby, *Electric Power Generation, Transmission and Distribution*. 2007, p. 500, ISBN: 9780849392924.

[87] “Ieee recommended practice for conducting short-circuit studies and analysis of industrial and commercial power systems,” *IEEE Std 3002.3-2018*, pp. 1–184, 2019. DOI: 10.1109/IEEESTD.2019.8672198.

[88] J. C. Das, “Arc-flash hazard calculations in LV and MV DC systems - Part I: Short-circuit calculations,” *IEEE Transactions on Industry Applications*, vol. 50, no. 3, pp. 1687–1697, 2014, ISSN: 00939994. DOI: 10.1109/TIA.2013.2288416.

[89] S. Cleva Power, *Deep cycle rechargeable lithium ion battery 48v 3kwh lifepo4 battery 60ah*. [Online]. Available: http://m.clevapowerbattery.com/showroom/deep-cycle-rechargeable-lithium-ion-battery-48v-3kwh-lifepo4-battery-60ah.html.

[90] P. C. Magnusson, G. C. Alexander, V. K. Tripathi, and A. Weisshaar, *Transmission Lines and Wave Propagation*, 4th. 2000, ISBN: 0849302692.

A

Derivation

In this appendix, the bipolar configuration of a 3 node 2 line state equation derivation is explained. The monopolar configuration is easier to derive in comparison to Bipolar. This approach explained here can be easily reproduced to derive the state equation numerically for any DC distribution system designed, if the steps are followed properly.

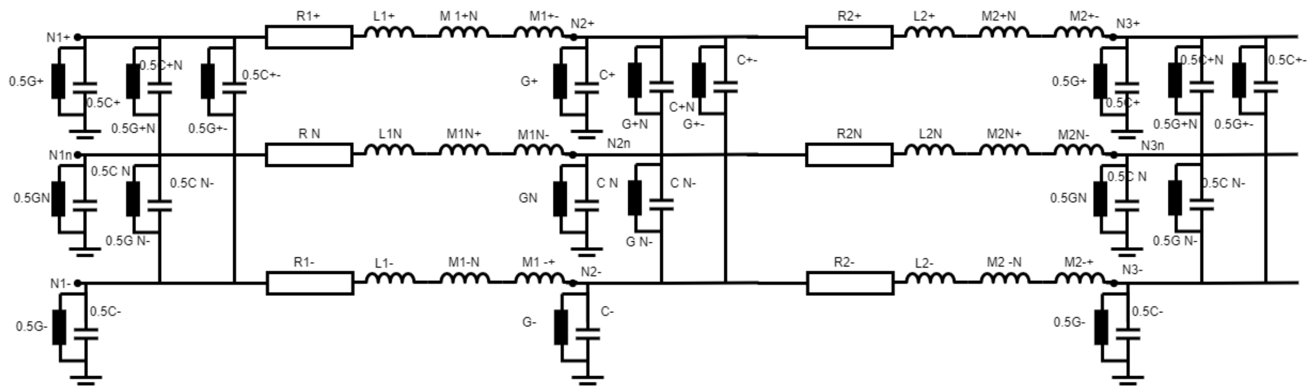

Figure A.1: Three node,two line Bipolar DC system

The state equation is usually defined in the state space approach by the equ (A.1)shown below.

$$\dot{x} = \mathbf{A} \cdot x + \mathbf{B} \cdot u \tag{A.1}$$

First step, in this approach is to define the incidence matrix of the DC distribution system. The incidence matrix of the 3 node, 2 line bipolar system is given by equ (A.2)

$$\Gamma = \begin{bmatrix} 1 & 0 & 0 & -1 & 0 & 0 & 0 & 0 \\ 0 & 1 & 0 & 0 & -1 & 0 & 0 & 0 \\ 0 & 0 & 1 & 0 & 0 & -1 & 0 & 0 \\ 0 & 0 & 0 & 1 & 0 & 0 & 0 & 0 \\ 0 & 0 & 0 & 0 & 1 & 0 & -1 & 0 \\ 0 & 0 & 0 & 0 & 0 & 1 & 0 & -1 \end{bmatrix}_{[(l_{1+}\cdots l_{2-}),(n_{1+}\cdots n_{3-})]} \tag{A.2}$$

The second step is to choose the state variables of the DC distribution system, that would return as output from solving the state equation of the system. Here in this system, the state variables are taken as U_n (voltage at each node) and I_l (current at each distribution line) present in the DC distribution system.

The net current(I_{net}) flowing into each node is given by equ(A.3) and the voltage over the inductance present in each distribution line(U_L) is given by equ(A.4).

$$I_{net} = C\frac{dU_n}{dt} = C\dot{U}_n \tag{A.3}$$

$$U_L = L\frac{dI_l}{dt} = L\dot{I}_l \tag{A.4}$$

Applying KCL at Node 1+

$$\begin{aligned} I_{n1+} = {} & C_{1+}\dot{U}_{n1+} + C_{1+N}(\dot{U}_{n1+} - \dot{U}_{n1N}) + C_{1+-}(\dot{U}_{n1+} - \dot{U}_{n1-}) + G_{1+}U_{n1+} \\ & + G_{1+N}(U_{n1+} - U_{n1N}) + G_{1+-}(U_{n1+} - U_{n1-}) + I_{l1+} \end{aligned} \tag{A.5}$$

Applying KCL at Node 1N

$$\begin{aligned} I_{n1N} = {} & C_{1N}\dot{U}_{n1N} + C_{1N+}(\dot{U}_{n1N} - \dot{U}_{n1+}) + C_{1N-}(\dot{U}_{n1N} - \dot{U}_{n1-}) + G_{1N}U_{n1N} \\ & + G_{1N+}(U_{n1N} - U_{n1+}) + G_{1N-}(U_{n1N} - U_{n1-}) + I_{l1N} \end{aligned} \tag{A.6}$$

Applying KCL at Node 1-

$$\begin{aligned} I_{n1-} = {} & C_{1-}\dot{U}_{n1-} + C_{1-N}(\dot{U}_{n1-} - \dot{U}_{n1N}) + C_{1-+}(\dot{U}_{n1-} - \dot{U}_{n1+}) + G_{1-}U_{n1-} \\ & + G_{1-N}(U_{n1-} - U_{n1N}) + G_{1-+}(U_{n1-} - U_{n1+}) + I_{l1-} \end{aligned} \tag{A.7}$$

Converting the KCL applied at Node 1 into Matrix form

$$\begin{aligned} & \begin{bmatrix} C_{1+} + C_{1+N} + C_{1+N} & -C_{1+N} & -C_{1+-} \\ -C_{1N+} & C_{1N} + C_{1N+} + C_{1N-} & -C_{1N-} \\ -C_{1-+} & -C_{1-N} & C_{1-} + C_{1-N} + C_{1-+} \end{bmatrix} \begin{bmatrix} \dot{U}_{n1+} \\ \dot{U}_{n1N} \\ \dot{U}_{n1-} \end{bmatrix} = \\ & \begin{bmatrix} I_{n1+} \\ I_{n1N} \\ I_{n1-} \end{bmatrix} - \begin{bmatrix} I_{l1+} \\ I_{l1N} \\ I_{l1-} \end{bmatrix} - \begin{bmatrix} G_{1+} + G_{1+N} + G_{1+N} & -G_{1+N} & -G_{1+-} \\ -G_{1N+} & G_{1N} + G_{1N+} + G_{1N-} & -G_{1N-} \\ -G_{1-+} & -G_{1-N} & G_{1-} + G_{1-N} + G_{1-+} \end{bmatrix} \begin{bmatrix} U_{n1+} \\ U_{n1N} \\ U_{n1-} \end{bmatrix} \end{aligned} \tag{A.8}$$

Applying KCL at Node 2+

$$\begin{aligned} I_{l1+} + I_{n2+} = {} & C_{2+}\dot{U}_{n2+} + C_{2+N}(\dot{U}_{n2+} - \dot{U}_{n2N}) + C_{2+-}(\dot{U}_{n2+} - \dot{U}_{n2-}) + G_{2+}U_{n2+} \\ & + G_{2+N}(U_{n2+} - U_{n2N}) + G_{2+-}(U_{n2+} - U_{n2-}) + I_{l2+} \end{aligned} \tag{A.9}$$

Applying KCL at Node 2N

$$\begin{aligned} I_{l1N} + I_{n2N} = {} & C_{2N}\dot{U}_{n2N} + C_{2N+}(\dot{U}_{n2N} - \dot{U}_{n2+}) + C_{2N-}(\dot{U}_{n2N} - \dot{U}_{n2-}) + G_{2N}U_{n2N} \\ & + G_{2N+}(U_{n2N} - U_{n2+}) + G_{2N-}(U_{n2N} - U_{n2-}) + I_{l2N} \end{aligned} \tag{A.10}$$

Applying KCL at Node 2-

$$\begin{aligned} I_{l1-} + I_{n2-} = {} & C_{2-}\dot{U}_{n2-} + C_{2-N}(\dot{U}_{n2-} - \dot{U}_{n2N}) + C_{2-+}(\dot{U}_{n2-} - \dot{U}_{n2+}) + G_{2-}U_{n2-} \\ & + G_{2-N}(U_{n2-} - U_{n2N}) + G_{2-+}(U_{n2-} - U_{n2+}) + I_{l2-} \end{aligned} \tag{A.11}$$

Converting the KCL applied at Node 2 into Matrix form

$$\begin{aligned} & \begin{bmatrix} C_{2+} + C_{2+N} + C_{2+N} & -C_{2+N} & -C_{2+-} \\ -C_{2N+} & C_{2N} + C_{2N+} + C_{2N-} & -C_{2N-} \\ -C_{2-+} & -C_{2-N} & C_{2-} + C_{2-N} + C_{2-+} \end{bmatrix} \begin{bmatrix} \dot{U}_{n2+} \\ \dot{U}_{n2N} \\ \dot{U}_{n2-} \end{bmatrix} = \\ & \begin{bmatrix} I_{n2+} \\ I_{n2N} \\ I_{n2-} \end{bmatrix} - \begin{bmatrix} I_{l2+} - I_{l1+} \\ I_{l2N} - I_{l1N} \\ I_{l2-} - I_{l1-} \end{bmatrix} - \begin{bmatrix} G_{2+} + G_{2+N} + G_{2+N} & -G_{2+N} & -G_{2+-} \\ -G_{2N+} & G_{2N} + G_{2N+} + G_{2N-} & -G_{2N-} \\ -G_{2-+} & -G_{2-N} & G_{2-} + G_{2-N} + G_{2-+} \end{bmatrix} \begin{bmatrix} U_{n2+} \\ U_{n2N} \\ U_{n2-} \end{bmatrix} \end{aligned} \tag{A.12}$$

Applying KCL at node 3+

$$I_{l2+} + I_{n3+} = C_{3+}\dot{U}_{n3+} + C_{3+N}(\dot{U}_{n3+} - \dot{U}_{n3N}) + C_{3+-}(\dot{U}_{n3+} - \dot{U}_{n3n}) + G_{3+}U_{n3+} + G_{3+N}(U_{n3+} - U_{n3N}) + G_{3+-}(U_{n3+} - U_{n3-}) \tag{A.13}$$

Applying KCL at Node 3N

$$I_{l2N} + I_{n3N} = C_{3N}\dot{U}_{n3N} + C_{3N+}(\dot{U}_{n3N} - \dot{U}_{n3+}) + C_{3N-}(\dot{U}_{n3N} - \dot{U}_{n3-}) + G_{3N}U_{n3N} + G_{3N+}(U_{n3N} - U_{n3+}) + G_{3N-}(U_{n3N} - U_{n3-}) \tag{A.14}$$

Applying KCL at Node 3-

$$I_{l2-} + I_{n3-} = C_{3-}\dot{U}_{n3-} + C_{3-N}(\dot{U}_{n3-} - \dot{U}_{n3N}) + C_{3-+}(\dot{U}_{n3-} - \dot{U}_{n3+}) + G_{3-}U_{n3-} + G_{3-N}(U_{n3-} - U_{n3N}) + G_{3-+}(U_{n3-} - U_{n3+}) \tag{A.15}$$

Converting the KCL applied at Node 3 into Matrix form

$$\begin{bmatrix} C_{3+} + C_{3+N} + C_{3+N} & -C_{3+N} & -C_{3+-} \\ -C_{3N+} & C_{3N} + C_{3N+} + C_{3N-} & -C_{3N-} \\ -C_{3-+} & -C_{3-N} & C_{3-} + C_{3-N} + C_{3-+} \end{bmatrix} \begin{bmatrix} \dot{U}_{n3+} \\ \dot{U}_{n3N} \\ \dot{U}_{n3-} \end{bmatrix} = \begin{bmatrix} I_{n3+} \\ I_{n3N} \\ I_{n3-} \end{bmatrix} - \begin{bmatrix} I_{l2+} \\ I_{l2N} \\ I_{l2-} \end{bmatrix} - \begin{bmatrix} G_{3+} + G_{3+N} + G_{3+N} & -G_{3+N} & -G_{3+-} \\ -G_{3N+} & G_{3N} + G_{3N+} + G_{3N-} & -G_{3N-} \\ -G_{3-+} & -G_{3-N} & G_{3-} + G_{3-N} + G_{3-+} \end{bmatrix} \begin{bmatrix} U_{n3+} \\ U_{n3N} \\ U_{n3-} \end{bmatrix} \tag{A.16}$$

Applying KVL between Node1+ and Node 2+

$$U_{n1+} - R_{l1+}I_{l1+} - L_{l1+}\dot{I}_{l1+} - U_{n2+} - M_{1+N}\dot{I_{l1n}} - M_{1+-}\dot{I_{l1-}} = 0 \tag{A.17}$$

Applying KVL between Node1N and Node 2N

$$U_{n1N} - R_{l1N}I_{l1N} - L_{l1N}\dot{I}_{l1N} - U_{n2N} - M_{1N+}\dot{I_{l1+}} - M_{1N-}\dot{I_{l1-}} = 0 \tag{A.18}$$

Applying KVL between Node1- and Node 2-

$$U_{n1-} - R_{l1-}I_{l1-} - L_{l1-}\dot{I}_{l1-} - U_{n2-} - M_{1-+}\dot{I_{l1+}} - M_{1-N}\dot{I_{l1N}} = 0 \tag{A.19}$$

Converting the KVL applied between Node 1 and Node 2 into Matrix form

$$\begin{bmatrix} L_{l1+} & M_{1+N} & M_{1+-} \\ M_{1N+} & L_{l1N} & M_{1N-} \\ M_{1-+} & M_{1-N} & L_{l1-} \end{bmatrix} \begin{bmatrix} \dot{I}_{l1+} \\ \dot{I}_{l1N} \\ \dot{I}_{l1-} \end{bmatrix} = \begin{bmatrix} U_{n1+} - U_{n2+} \\ U_{n1N} - U_{n2N} \\ U_{n1-} - U_{n2-} \end{bmatrix} - \begin{bmatrix} R_{l1+} & 0 & 0 \\ 0 & R_{l1N} & 0 \\ 0 & 0 & R_{l1-} \end{bmatrix} \begin{bmatrix} I_{l1+} \\ I_{l1N} \\ I_{l1-} \end{bmatrix} \tag{A.20}$$

Applying KVL between Node2+ and Node 3+

$$U_{n2+} - R_{l2+}I_{l2+} - L_{l2+}\dot{I}_{l2+} - U_{n3+} - M_{2+N}\dot{I_{l2n}} - M_{2+-}\dot{I_{l2-}} = 0 \tag{A.21}$$

Applying KVL between Node2N and Node 3N

$$U_{n2N} - R_{l2N}I_{l2N} - L_{l2N}\dot{I}_{l2N} - U_{n3N} - M_{2N+}\dot{I_{l2+}} - M_{2N-}\dot{I_{l2-}} = 0 \tag{A.22}$$

Applying KVL between Node2- and Node 3-

$$U_{n2-} - R_{l2-}I_{l2-} - L_{l2-}\dot{I}_{l2-} - U_{n3-} - M_{2-+}\dot{I_{l2+}} - M_{2-N}\dot{I_{l2N}} = 0 \tag{A.23}$$

Converting the KVL applied between Node 2 and Node 3 into Matrix form

$$\begin{bmatrix} L_{l2+} & M_{2+N} & M_{2+-} \\ M_{2N+} & L_{l2N} & M_{2N-} \\ M_{2-+} & M_{2-N} & L_{l2-} \end{bmatrix} \begin{bmatrix} \dot{I}_{l2+} \\ \dot{I}_{l2N} \\ \dot{I}_{l2-} \end{bmatrix} = \begin{bmatrix} U_{n2+} - U_{n3+} \\ U_{n2N} - U_{n3N} \\ U_{n2-} - U_{n3-} \end{bmatrix} - \begin{bmatrix} R_{l2+} & 0 & 0 \\ 0 & R_{l2N} & 0 \\ 0 & 0 & R_{l2-} \end{bmatrix} \begin{bmatrix} I_{l2+} \\ I_{l2N} \\ I_{l2-} \end{bmatrix} \tag{A.24}$$

Next step is combining all the KCL applied matrix together and rearranging them in terms of state variable. Based on the number of nodes (N) and the total number of conductors(K) present, here C_{NK} and G_{NK} gives the sum of all capacitance or conductance that is connected to the particular node and the conductor. For example C_{11} gives the sum of all capacitances connected to the +conductor (1) present at node 1.

$$
\begin{bmatrix} \dot{U}_{n1+} \\ \dot{U}_{n1N} \\ \dot{U}_{n1-} \\ \dot{U}_{n2+} \\ \dot{U}_{n2N} \\ \dot{U}_{n2-} \\ \dot{U}_{n3+} \\ \dot{U}_{n3N} \\ \dot{U}_{n3-} \end{bmatrix}
=
\begin{bmatrix}
C_{11} & -C_{1+N} & -C_{1+-} & 0 & 0 & 0 & 0 & 0 & 0 \\
-C_{1N+} & C_{22} & -C_{1N-} & 0 & 0 & 0 & 0 & 0 & 0 \\
-C_{1-+} & -C_{1-N} & C_{33} & 0 & 0 & 0 & 0 & 0 & 0 \\
0 & 0 & 0 & C_{44} & -C_{2+N} & -C_{2+-} & 0 & 0 & 0 \\
0 & 0 & 0 & -C_{2N+} & C_{55} & -C_{2N-} & 0 & 0 & 0 \\
0 & 0 & 0 & -C_{2-+} & -C_{2-N} & C_{66} & 0 & 0 & 0 \\
0 & 0 & 0 & 0 & 0 & 0 & C_{77} & -C_{3+N} & -C_{3+-} \\
0 & 0 & 0 & 0 & 0 & 0 & -C_{3N+} & C_{88} & -C_{3N-} \\
0 & 0 & 0 & 0 & 0 & 0 & -C_{3-+} & -C_{3-N} & C_{99}
\end{bmatrix}^{-1}
(
\begin{bmatrix} I_{n1+} \\ I_{n1N} \\ I_{n1-} \\ I_{n2+} \\ I_{n2N} \\ I_{n2-} \\ I_{n3+} \\ I_{n3N} \\ I_{n3-} \end{bmatrix}
$$

$$
-
\begin{bmatrix}
G_{11} & -G_{1+N} & -G_{1+-} & 0 & 0 & 0 & 0 & 0 & 0 \\
-G_{1N+} & G_{22} & -G_{1N-} & 0 & 0 & 0 & 0 & 0 & 0 \\
-G_{1-+} & -G_{1-N} & G_{33} & 0 & 0 & 0 & 0 & 0 & 0 \\
0 & 0 & 0 & G_{44} & -G_{2+N} & -G_{2+-} & 0 & 0 & 0 \\
0 & 0 & 0 & -G_{2N+} & G_{55} & -G_{2N-} & 0 & 0 & 0 \\
0 & 0 & 0 & -G_{2-+} & -G_{2-N} & G_{66} & 0 & 0 & 0 \\
0 & 0 & 0 & 0 & 0 & 0 & G_{77} & -G_{3+N} & -G_{3+-} \\
0 & 0 & 0 & 0 & 0 & 0 & -G_{3N+} & G_{88} & -G_{3N-} \\
0 & 0 & 0 & 0 & 0 & 0 & -G_{3-+} & -G_{3-N} & G_{99}
\end{bmatrix}
\begin{bmatrix} U_{n1+} \\ U_{n1N} \\ U_{n1-} \\ U_{n2+} \\ U_{n2N} \\ U_{n2-} \\ U_{n3+} \\ U_{n3N} \\ U_{n3-} \end{bmatrix}
$$

$$
-
\begin{bmatrix}
1 & 0 & 0 & -1 & 0 & 0 & 0 & 0 \\
0 & 1 & 0 & 0 & -1 & 0 & 0 & 0 \\
0 & 0 & 1 & 0 & 0 & -1 & 0 & 0 \\
0 & 0 & 0 & 1 & 0 & 0 & 0 & 0 \\
0 & 0 & 0 & 0 & 1 & 0 & -1 & 0 \\
0 & 0 & 0 & 0 & 0 & 1 & 0 & -1
\end{bmatrix}
\begin{bmatrix} I_{l1+} \\ I_{l1N} \\ I_{l1-} \\ I_{l2+} \\ I_{l2N} \\ I_{l2-} \\ I_{l3+} \\ I_{l3N} \\ I_{l3-} \end{bmatrix}
)
\tag{A.25}
$$

Then, combining all the KVL applied matrix together and rearranging them in terms of state variable.

$$
\begin{bmatrix} \dot{I}_{l1+} \\ \dot{I}_{l1N} \\ \dot{I}_{l1-} \\ \dot{I}_{l2+} \\ \dot{I}_{l2N} \\ \dot{I}_{l2-} \end{bmatrix}
=
\begin{bmatrix}
L_{l1+} & M_{1+N} & M_{1+-} & 0 & 0 & 0 \\
M_{1N+} & L_{l1N} & M_{1N-} & 0 & 0 & 0 \\
M_{1-+} & M_{1-N} & L_{l1-} & 0 & 0 & 0 \\
0 & 0 & 0 & L_{l2+} & M_{2+N} & M_{2+-} \\
0 & 0 & 0 & M_{2N+} & L_{l2N} & M_{2N-} \\
0 & 0 & 0 & M_{2-+} & M_{2-N} & L_{l2-}
\end{bmatrix}^{-1}
(
\begin{bmatrix}
1 & 0 & 0 & -1 & 0 & 0 & 0 & 0 \\
0 & 1 & 0 & 0 & -1 & 0 & 0 & 0 \\
0 & 0 & 1 & 0 & 0 & -1 & 0 & 0 \\
0 & 0 & 0 & 1 & 0 & 0 & 0 & 0 \\
0 & 0 & 0 & 0 & 1 & 0 & -1 & 0 \\
0 & 0 & 0 & 0 & 0 & 1 & 0 & -1
\end{bmatrix}
$$

$$
\begin{bmatrix} U_{n1+} \\ U_{n1N} \\ U_{n1-} \\ U_{n2+} \\ U_{n2N} \\ U_{n2-} \\ U_{n3+} \\ U_{n3N} \\ U_{n3-} \end{bmatrix}
-
\begin{bmatrix}
R_{l1+} & 0 & 0 & 0 & 0 & 0 \\
0 & R_{l1N} & 0 & 0 & 0 & 0 \\
0 & 0 & R_{l1-} & 0 & 0 & 0 \\
0 & 0 & 0 & R_{l2+} & 0 & 0 \\
0 & 0 & 0 & 0 & R_{l2N} & 0 \\
0 & 0 & 0 & 0 & 0 & R_{l2-}
\end{bmatrix}
\begin{bmatrix} I_{l1+} \\ I_{l1N} \\ I_{l1-} \\ I_{l2+} \\ I_{l2N} \\ I_{l2-} \end{bmatrix}
)
\tag{A.26}
$$

Finally Combining (A.25) and (A.26)

$$
\begin{bmatrix} \dot U_{n1+} \\ \dot U_{n1N} \\ \dot U_{n1-} \\ \dot U_{n2+} \\ \dot U_{n2N} \\ \dot U_{n2-} \\ \dot U_{n3+} \\ \dot U_{n3N} \\ \dot U_{n3-} \\ \dot I_{l1+} \\ \dot I_{l1N} \\ \dot I_{l1-} \\ \dot I_{l2+} \\ \dot I_{l2N} \\ \dot I_{l2-} \end{bmatrix} =
$$

$$
\begin{bmatrix}
\frac{G_{11}}{C_{11}} & \frac{G_{1+N}}{C_{1+N}} & \frac{G_{1+-}}{C_{1+-}} & 0 & 0 & 0 & 0 & 0 & 0 & \frac{-1}{C_{11}} & \frac{1}{C_{1+N}} & \frac{1}{C_{1+-}} & 0 & 0 & 0 \\
\frac{G_{1N+}}{C_{1N+}} & \frac{G_{22}}{C_{22}} & \frac{G_{1N-}}{C_{1N-}} & 0 & 0 & 0 & 0 & 0 & 0 & \frac{1}{C_{1N+}} & \frac{-1}{C_{22}} & \frac{1}{C_{1N-}} & 0 & 0 & 0 \\
\frac{G_{1-+}}{C_{1-+}} & \frac{G_{1-N}}{C_{1-N}} & \frac{G_{33}}{C_{33}} & 0 & 0 & 0 & 0 & 0 & 0 & \frac{1}{C_{1-+}} & \frac{1}{C_{1-N}} & \frac{-1}{C_{33}} & 0 & 0 & 0 \\
0 & 0 & 0 & \frac{G_{44}}{C_{44}} & \frac{G_{2+N}}{C_{2+N}} & \frac{G_{2+-}}{C_{2+-}} & 0 & 0 & 0 & \frac{1}{C_{44}} & \frac{-1}{C_{2+N}} & \frac{-1}{C_{2+-}} & \frac{-1}{C_{44}} & \frac{1}{C_{2+N}} & \frac{1}{C_{2+-}} \\
0 & 0 & 0 & \frac{G_{2N+}}{C_{2N+}} & \frac{G_{55}}{C_{55}} & \frac{G_{2N-}}{C_{2N-}} & 0 & 0 & 0 & \frac{-1}{C_{2N+}} & \frac{1}{C_{55}} & \frac{-1}{C_{2N-}} & \frac{1}{C_{2N+}} & \frac{-1}{C_{55}} & \frac{1}{C_{2N-}} \\
0 & 0 & 0 & \frac{G_{2-+}}{C_{2-+}} & \frac{G_{2-N}}{C_{2-N}} & \frac{G_{66}}{C_{66}} & 0 & 0 & 0 & \frac{-1}{C_{2-+}} & \frac{-1}{C_{2-N}} & \frac{1}{C_{66}} & \frac{1}{C_{2-+}} & \frac{1}{C_{2-N}} & \frac{-1}{C_{66}} \\
0 & 0 & 0 & 0 & 0 & 0 & \frac{G_{77}}{C_{77}} & \frac{G_{3+N}}{C_{3+N}} & \frac{G_{3+-}}{C_{3+-}} & 0 & 0 & 0 & \frac{1}{C_{77}} & \frac{-1}{C_{3+N}} & \frac{-1}{C_{3+-}} \\
0 & 0 & 0 & 0 & 0 & 0 & \frac{G_{3N+}}{C_{3N+}} & \frac{G_{88}}{C_{88}} & \frac{G_{3N-}}{C_{3N-}} & 0 & 0 & 0 & \frac{-1}{C_{3N+}} & \frac{1}{C_{88}} & \frac{-1}{C_{3N-}} \\
0 & 0 & 0 & 0 & 0 & 0 & \frac{G_{3-+}}{C_{3-+}} & \frac{G_{3-N}}{C_{3-N}} & \frac{G_{99}}{C_{99}} & 0 & 0 & 0 & \frac{-1}{C_{3-+}} & \frac{-1}{C_{3-N}} & \frac{1}{C_{99}} \\
\frac{1}{L_{l1+}} & \frac{1}{M_{1+N}} & \frac{1}{M_{1+-}} & \frac{-1}{L_{l1+}} & \frac{-1}{M_{1+N}} & \frac{-1}{M_{1+-}} & 0 & 0 & 0 & \frac{-R_{l1+}}{L_{l1+}} & \frac{-R_{l1+N}}{M_{1+N}} & \frac{-R_{l1+-}}{M_{1N-}} & 0 & 0 & 0 \\
\frac{1}{M_{1N+}} & \frac{1}{L_{l1N}} & \frac{1}{M_{1+-}} & \frac{-1}{M_{1N+}} & \frac{-1}{L_{l1N}} & \frac{-1}{M_{1+-}} & 0 & 0 & 0 & \frac{-R_{l1+}}{M_{1N+}} & \frac{-R_{l1n}}{L_{l1N}} & \frac{-R_{l1-}}{M_{1N-}} & 0 & 0 & 0 \\
\frac{1}{M_{1-+}} & \frac{1}{M_{1-N}} & \frac{1}{L_{l1-}} & \frac{-1}{M_{1-+}} & \frac{-1}{M_{1-N}} & \frac{-1}{L_{l1-}} & 0 & 0 & 0 & \frac{-R_{l1+}}{M_{1-+}} & \frac{-R_{l1n}}{M_{1-N}} & \frac{-R_{l1-}}{L_{l1-}} & 0 & 0 & 0 \\
0 & 0 & 0 & \frac{1}{L_{l2+}} & \frac{1}{M_{2+N}} & \frac{1}{M_{2+-}} & \frac{-1}{L_{l2+}} & \frac{-1}{M_{2+N}} & \frac{-1}{M_{2+-}} & 0 & 0 & 0 & \frac{-R_{l2+}}{L_{l2+}} & \frac{-R_{l2n}}{M_{2+N}} & \frac{-R_{l2-}}{M_{2+-}} \\
0 & 0 & 0 & \frac{1}{M_{2N+}} & \frac{1}{L_{l2N}} & \frac{1}{M_{2N-}} & \frac{-1}{M_{2N+}} & \frac{-1}{L_{l2N}} & \frac{-1}{M_{2N-}} & 0 & 0 & 0 & \frac{-R_{l2+}}{M_{2N+}} & \frac{-R_{l2N}}{L_{l2N}} & \frac{-R_{l2-}}{M_{2N-}} \\
0 & 0 & 0 & \frac{1}{M_{2-+}} & \frac{1}{M_{2-N}} & \frac{1}{L_{l2-}} & \frac{-1}{M_{2-+}} & \frac{-1}{M_{2-N}} & \frac{-1}{L_{l2-}} & 0 & 0 & 0 & \frac{-R_{l2+}}{M_{2-+}} & \frac{-R_{l2n}}{M_{2-N}} & \frac{-R_{l2-}}{L_{l2-}}
\end{bmatrix}
$$

$$
* \begin{bmatrix} U_{n1+} \\ U_{n1N} \\ U_{n1-} \\ U_{n2+} \\ U_{n2N} \\ U_{n2-} \\ U_{n3+} \\ U_{n3N} \\ U_{n3-} \\ I_{l1+} \\ I_{l1N} \\ I_{l1-} \\ I_{l2+} \\ I_{l2N} \\ I_{l2-} \end{bmatrix} +
\begin{bmatrix}
\frac{1}{C_{11}} & \frac{-1}{C_{1+N}} & \frac{-1}{C_{1+-}} & 0 & 0 & 0 & 0 & 0 & 0 \\
\frac{-1}{C_{1N+}} & \frac{1}{C_{22}} & \frac{-1}{C_{1N-}} & 0 & 0 & 0 & 0 & 0 & 0 \\
\frac{-1}{C_{1-+}} & \frac{-1}{C_{1-N}} & \frac{1}{C_{33}} & 0 & 0 & 0 & 0 & 0 & 0 \\
0 & 0 & 0 & \frac{1}{C_{44}} & \frac{-1}{C_{2+N}} & \frac{-1}{C_{2+-}} & 0 & 0 & 0 \\
0 & 0 & 0 & \frac{-1}{C_{2N+}} & \frac{1}{C_{55}} & \frac{-1}{C_{2N-}} & 0 & 0 & 0 \\
0 & 0 & 0 & \frac{-1}{C_{2-+}} & \frac{-1}{C_{2-N}} & \frac{1}{C_{66}} & 0 & 0 & 0 \\
0 & 0 & 0 & 0 & 0 & 0 & \frac{1}{C_{77}} & \frac{-1}{C_{3+N}} & \frac{-1}{C_{3+-}} \\
0 & 0 & 0 & 0 & 0 & 0 & \frac{-1}{C_{3N+}} & \frac{1}{C_{88}} & \frac{-1}{C_{3N-}} \\
0 & 0 & 0 & 0 & 0 & 0 & \frac{-1}{C_{3-+}} & \frac{-1}{C_{3-N}} & \frac{1}{C_{99}} \\
0 & 0 & 0 & 0 & 0 & 0 & 0 & 0 & 0 \\
0 & 0 & 0 & 0 & 0 & 0 & 0 & 0 & 0 \\
0 & 0 & 0 & 0 & 0 & 0 & 0 & 0 & 0 \\
0 & 0 & 0 & 0 & 0 & 0 & 0 & 0 & 0 \\
0 & 0 & 0 & 0 & 0 & 0 & 0 & 0 & 0 \\
0 & 0 & 0 & 0 & 0 & 0 & 0 & 0 & 0
\end{bmatrix}
* \begin{bmatrix} I_{n1+} \\ I_{n1N} \\ I_{n1-} \\ I_{n2+} \\ I_{n2N} \\ I_{n2-} \\ I_{n3+} \\ I_{n3N} \\ I_{n3-} \end{bmatrix} \tag{A.27}
$$

The state equation of the chosen distribution system is derived and shown in (A.27) above. This equation's representation in terms of the state equation is individually represented in equ (A.28)-(A.32).

$$\dot{x} = \begin{bmatrix} \dot{U}_{n1+} \\ \dot{U}_{n1N} \\ \dot{U}_{n1-} \\ \dot{U}_{n2+} \\ \dot{U}_{n2N} \\ \dot{U}_{n2-} \\ \dot{U}_{n3+} \\ \dot{U}_{n3N} \\ \dot{U}_{n3-} \\ \dot{I}_{l1+} \\ \dot{I}_{l1N} \\ \dot{I}_{l1-} \\ \dot{I}_{l2+} \\ \dot{I}_{l2N} \\ \dot{I}_{l2-} \end{bmatrix} \tag{A.28}$$

$$A = \left[\begin{array}{ccccccccccccccc}
\frac{G_{11}}{C_{11}} & \frac{G_{1+N}}{C_{1+N}} & \frac{G_{1+-}}{C_{1+-}} & 0 & 0 & 0 & 0 & 0 & 0 & \frac{-1}{C_{11}} & \frac{1}{C_{1+N}} & \frac{1}{C_{1+-}} & 0 & 0 & 0 \\
\frac{G_{1N+}}{C_{1N+}} & \frac{G_{22}}{C_{22}} & \frac{G_{1N-}}{C_{1N-}} & 0 & 0 & 0 & 0 & 0 & 0 & \frac{1}{C_{1N+}} & \frac{-1}{C_{22}} & \frac{1}{C_{1N-}} & 0 & 0 & 0 \\
\frac{G_{1-+}}{C_{1-+}} & \frac{G_{1-N}}{C_{1-N}} & \frac{G_{33}}{C_{33}} & 0 & 0 & 0 & 0 & 0 & 0 & \frac{1}{C_{1-+}} & \frac{1}{C_{1-N}} & \frac{-1}{C_{33}} & 0 & 0 & 0 \\
0 & 0 & 0 & \frac{G_{44}}{C_{44}} & \frac{G_{2+N}}{C_{2+N}} & \frac{G_{2+-}}{C_{2+-}} & 0 & 0 & 0 & \frac{1}{C_{44}} & \frac{-1}{C_{2+N}} & \frac{-1}{C_{2+-}} & \frac{-1}{C_{44}} & \frac{1}{C_{2+N}} & \frac{1}{C_{2+-}} \\
0 & 0 & 0 & \frac{G_{2N+}}{C_{2N+}} & \frac{G_{55}}{C_{55}} & \frac{G_{2N-}}{C_{2N-}} & 0 & 0 & 0 & \frac{-1}{C_{2N+}} & \frac{1}{C_{55}} & \frac{-1}{C_{2N-}} & \frac{1}{C_{2N+}} & \frac{-1}{C_{55}} & \frac{1}{C_{2N-}} \\
0 & 0 & 0 & \frac{G_{2-+}}{C_{2-+}} & \frac{G_{2-N}}{C_{2-N}} & \frac{G_{66}}{C_{66}} & 0 & 0 & 0 & \frac{-1}{C_{2-+}} & \frac{-1}{C_{2-N}} & \frac{1}{C_{66}} & \frac{1}{C_{2-+}} & \frac{1}{C_{2-N}} & \frac{-1}{C_{66}} \\
0 & 0 & 0 & 0 & 0 & 0 & \frac{G_{77}}{C_{77}} & \frac{G_{3+N}}{C_{3+N}} & \frac{G_{3+-}}{C_{3+-}} & 0 & 0 & 0 & \frac{1}{C_{77}} & \frac{-1}{C_{3+N}} & \frac{-1}{C_{3+-}} \\
0 & 0 & 0 & 0 & 0 & 0 & \frac{G_{3N+}}{C_{3N+}} & \frac{G_{88}}{C_{88}} & \frac{G_{3N-}}{C_{3N-}} & 0 & 0 & 0 & \frac{-1}{C_{3N+}} & \frac{1}{C_{88}} & \frac{-1}{C_{3N-}} \\
0 & 0 & 0 & 0 & 0 & 0 & \frac{G_{3-+}}{C_{3-+}} & \frac{G_{3-N}}{C_{3-N}} & \frac{G_{99}}{C_{99}} & 0 & 0 & 0 & \frac{-1}{C_{3-+}} & \frac{-1}{C_{3-N}} & \frac{1}{C_{99}} \\
\frac{1}{L_{l1+}} & \frac{1}{M_{1+N}} & \frac{1}{M_{1+-}} & \frac{-1}{L_{l1+}} & \frac{-1}{M_{1+N}} & \frac{-1}{M_{1+-}} & 0 & 0 & 0 & \frac{-R_{l1+}}{L_{l1+}} & \frac{-R_{l1+N}}{M_{1+N}} & \frac{-R_{l1+-}}{M_{1N-}} & 0 & 0 & 0 \\
\frac{1}{M_{1N+}} & \frac{1}{L_{l1N}} & \frac{1}{M_{1+-}} & \frac{-1}{M_{1N+}} & \frac{-1}{L_{l1N}} & \frac{-1}{M_{1+-}} & 0 & 0 & 0 & \frac{-R_{l1+}}{M_{1N+}} & \frac{-R_{l1n}}{L_{l1N}} & \frac{-R_{l1-}}{M_{1N-}} & 0 & 0 & 0 \\
\frac{1}{M_{1-+}} & \frac{1}{M_{1-N}} & \frac{1}{L_{l1-}} & \frac{-1}{M_{1-+}} & \frac{-1}{M_{1-N}} & \frac{-1}{L_{l1-}} & 0 & 0 & 0 & \frac{-R_{l1+}}{M_{1-+}} & \frac{-R_{l1n}}{M_{1-N}} & \frac{-R_{l1-}}{L_{l1-}} & 0 & 0 & 0 \\
0 & 0 & 0 & \frac{1}{L_{l2+}} & \frac{1}{M_{2+N}} & \frac{1}{M_{2+-}} & \frac{-1}{L_{l2+}} & \frac{-1}{M_{2+N}} & \frac{-1}{M_{2+-}} & 0 & 0 & 0 & \frac{-R_{l2+}}{L_{l2+}} & \frac{-R_{l2n}}{M_{2+N}} & \frac{-R_{l2-}}{M_{2+-}} \\
0 & 0 & 0 & \frac{1}{M_{2N+}} & \frac{1}{L_{l2N}} & \frac{1}{M_{2N-}} & \frac{-1}{M_{2N+}} & \frac{-1}{L_{l2N}} & \frac{-1}{M_{2N-}} & 0 & 0 & 0 & \frac{-R_{l2+}}{M_{2N+}} & \frac{-R_{l2N}}{L_{l2N}} & \frac{-R_{l2-}}{M_{2N-}} \\
0 & 0 & 0 & \frac{1}{M_{2-+}} & \frac{1}{M_{2-N}} & \frac{1}{L_{l2-}} & \frac{-1}{M_{2-+}} & \frac{-1}{M_{2-N}} & \frac{-1}{L_{l2-}} & 0 & 0 & 0 & \frac{-R_{l2+}}{M_{2-+}} & \frac{-R_{l2n}}{M_{2-N}} & \frac{-R_{l2-}}{L_{l2-}}
\end{array}\right] \tag{A.29}$$

$$x = \begin{bmatrix} U_{n1+} \\ U_{n1N} \\ U_{n1-} \\ U_{n2+} \\ U_{n2N} \\ U_{n2-} \\ U_{n3+} \\ U_{n3N} \\ U_{n3-} \\ I_{l1+} \\ I_{l1N} \\ I_{l1-} \\ I_{l2+} \\ I_{l2N} \\ I_{l2-} \end{bmatrix} \tag{A.30}$$

$$B = \begin{bmatrix} \frac{1}{C_{11}} & \frac{-1}{C_{1+N}} & \frac{-1}{C_{1+-}} & 0 & 0 & 0 & 0 & 0 & 0 \\ \frac{-1}{C_{1N+}} & \frac{1}{C_{22}} & \frac{-1}{C_{1N-}} & 0 & 0 & 0 & 0 & 0 & 0 \\ \frac{-1}{C_{1-+}} & \frac{-1}{C_{1-N}} & \frac{1}{C_{33}} & 0 & 0 & 0 & 0 & 0 & 0 \\ 0 & 0 & 0 & \frac{1}{C_{44}} & \frac{-1}{C_{2+N}} & \frac{-1}{C_{2+-}} & 0 & 0 & 0 \\ 0 & 0 & 0 & \frac{-1}{C_{2N+}} & \frac{1}{C_{55}} & \frac{-1}{C_{2N-}} & 0 & 0 & 0 \\ 0 & 0 & 0 & \frac{-1}{C_{2-+}} & \frac{-1}{C_{2-N}} & \frac{1}{C_{66}} & 0 & 0 & 0 \\ 0 & 0 & 0 & 0 & 0 & 0 & \frac{1}{C_{77}} & \frac{-1}{C_{3+N}} & \frac{-1}{C_{3+-}} \\ 0 & 0 & 0 & 0 & 0 & 0 & \frac{-1}{C_{3N+}} & \frac{1}{C_{88}} & \frac{-1}{C_{3N-}} \\ 0 & 0 & 0 & 0 & 0 & 0 & \frac{-1}{C_{3-+}} & \frac{-1}{C_{3-N}} & \frac{1}{C_{99}} \\ 0 & 0 & 0 & 0 & 0 & 0 & 0 & 0 & 0 \\ 0 & 0 & 0 & 0 & 0 & 0 & 0 & 0 & 0 \\ 0 & 0 & 0 & 0 & 0 & 0 & 0 & 0 & 0 \\ 0 & 0 & 0 & 0 & 0 & 0 & 0 & 0 & 0 \\ 0 & 0 & 0 & 0 & 0 & 0 & 0 & 0 & 0 \\ 0 & 0 & 0 & 0 & 0 & 0 & 0 & 0 & 0 \end{bmatrix} \tag{A.31}$$

$$u = \begin{bmatrix} I_{n1+} \\ I_{n1N} \\ I_{n1-} \\ I_{n2+} \\ I_{n2N} \\ I_{n2-} \\ I_{n3+} \\ I_{n3N} \\ I_{n3-} \end{bmatrix} \tag{A.32}$$

B

Figures

The rest of the figures that are part of the analysis, but doesn't provide more important insights to the analysis are included here in this appendix.

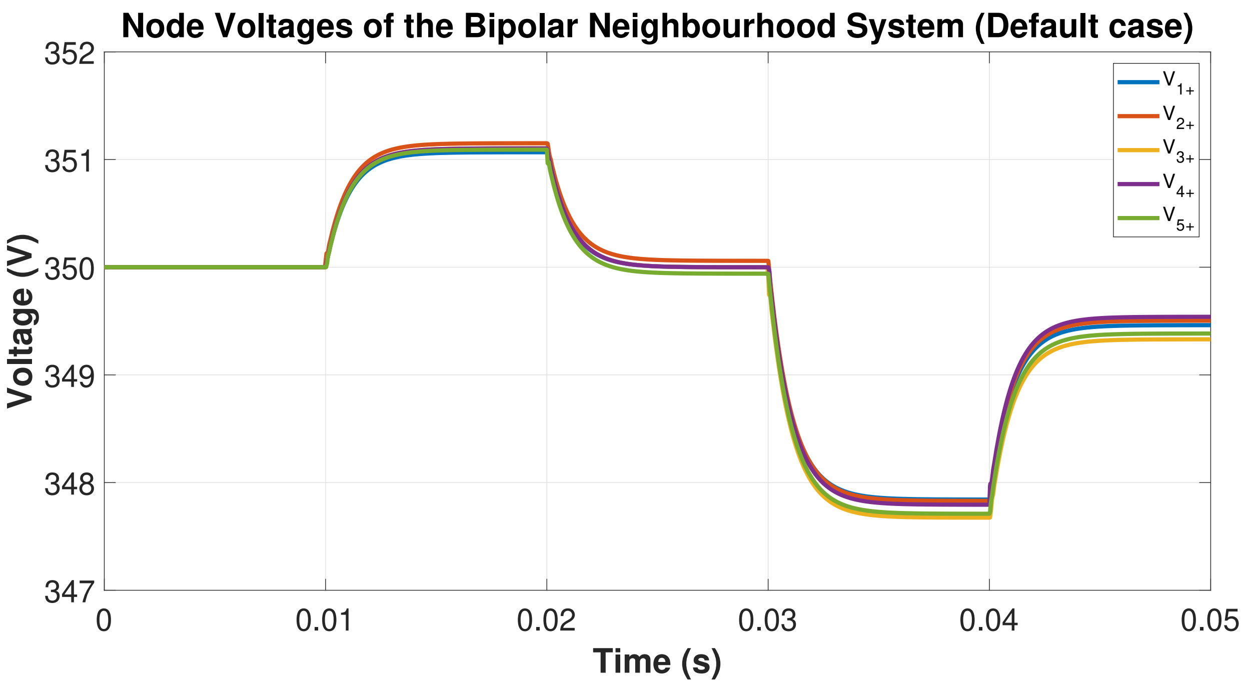

Figure B.1: Node voltage plot of Bipolar neighbourhood system(Default)

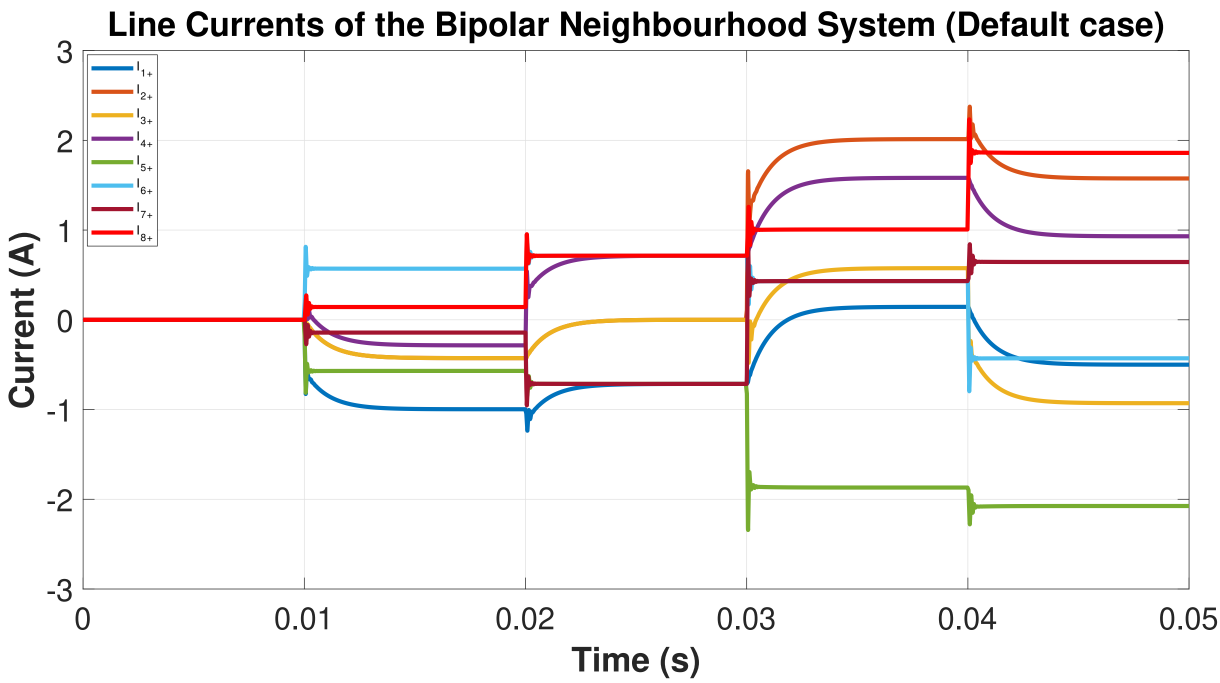

Figure B.2: Line current plot of Bipolar neighbourhood system(Default)

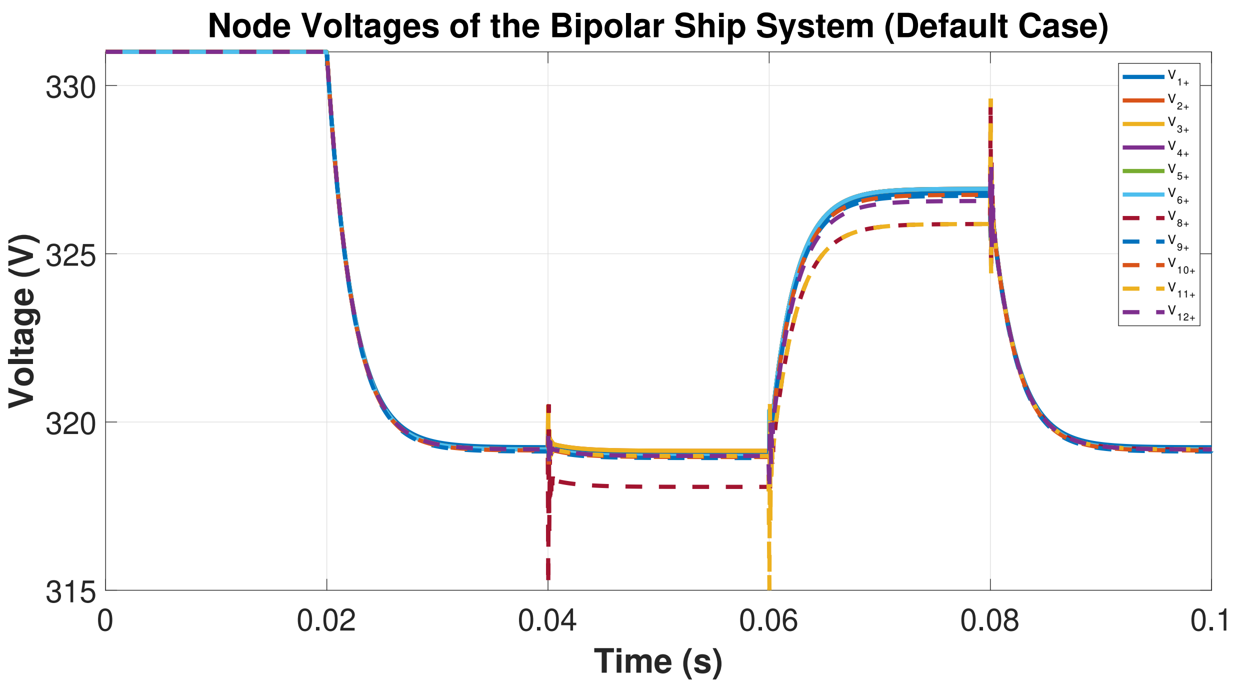

Figure B.3: Node voltage plot of Bipolar ship system(Default)

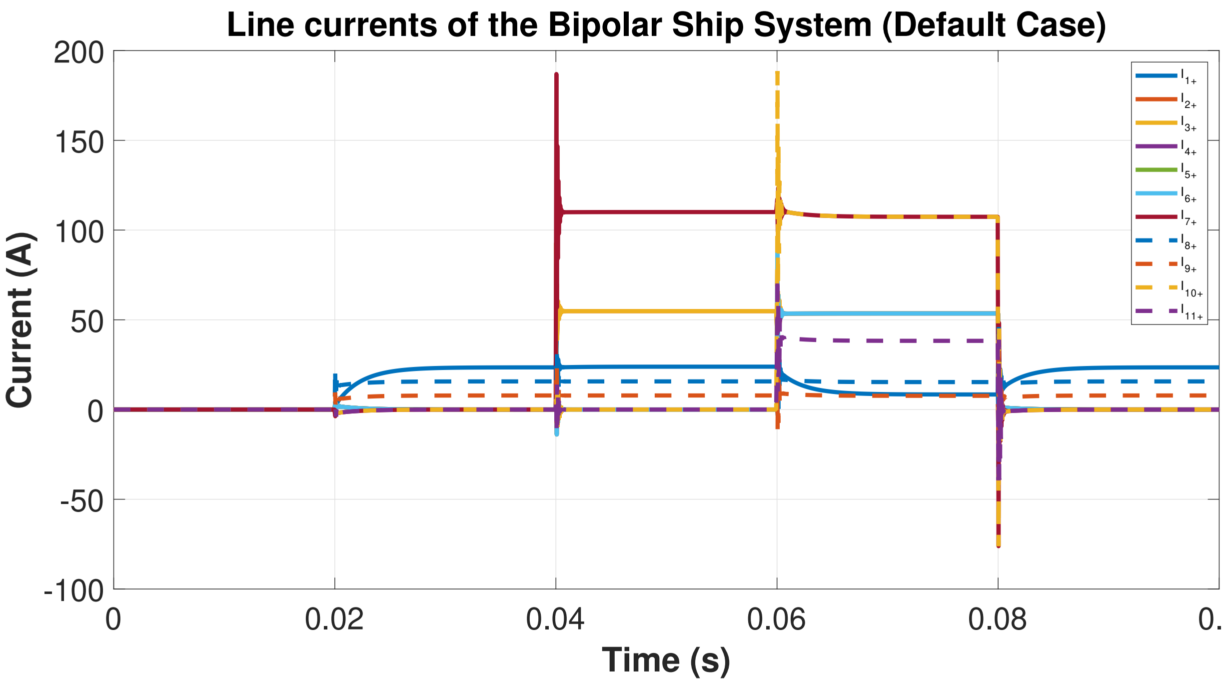

Figure B.4: Line current plot of Bipolar ship system(Default)

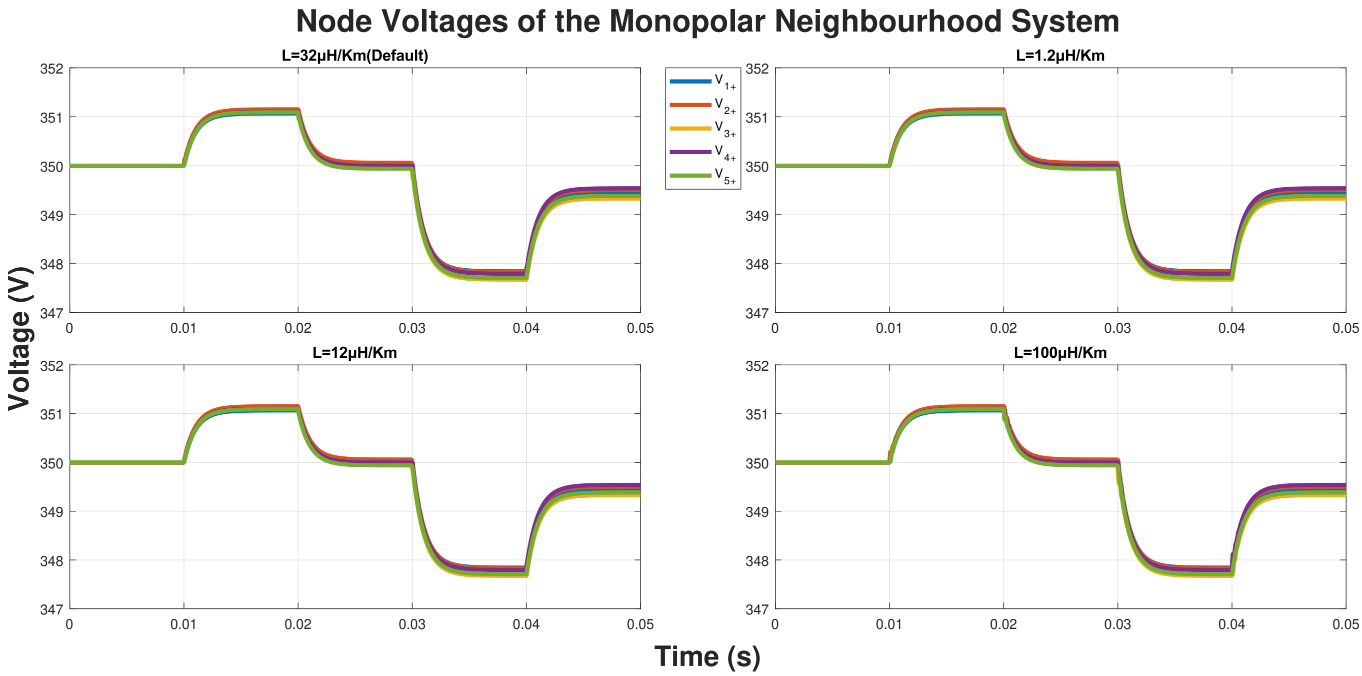

Figure B.5: Influence of cable inductance variation in the Node voltage plots of neighbourhood system

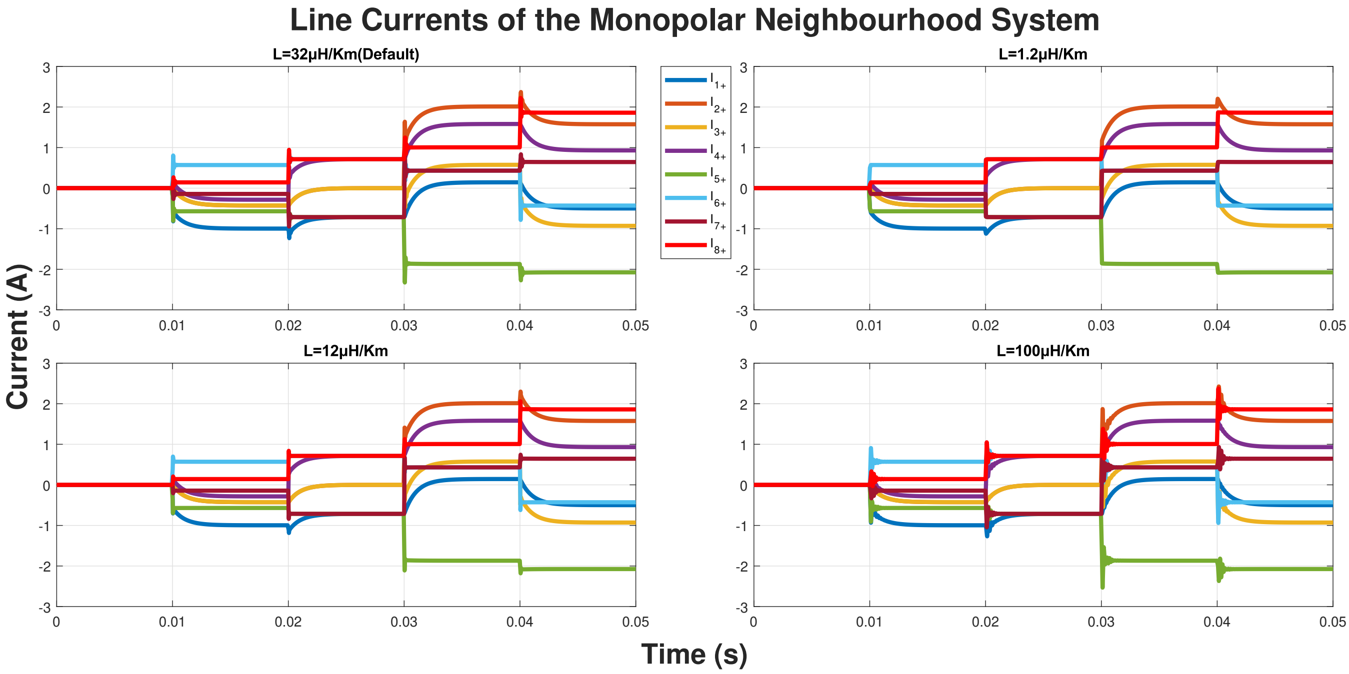

Figure B.6: Influence of cable inductance variation in the Line current plots of neighbourhood system

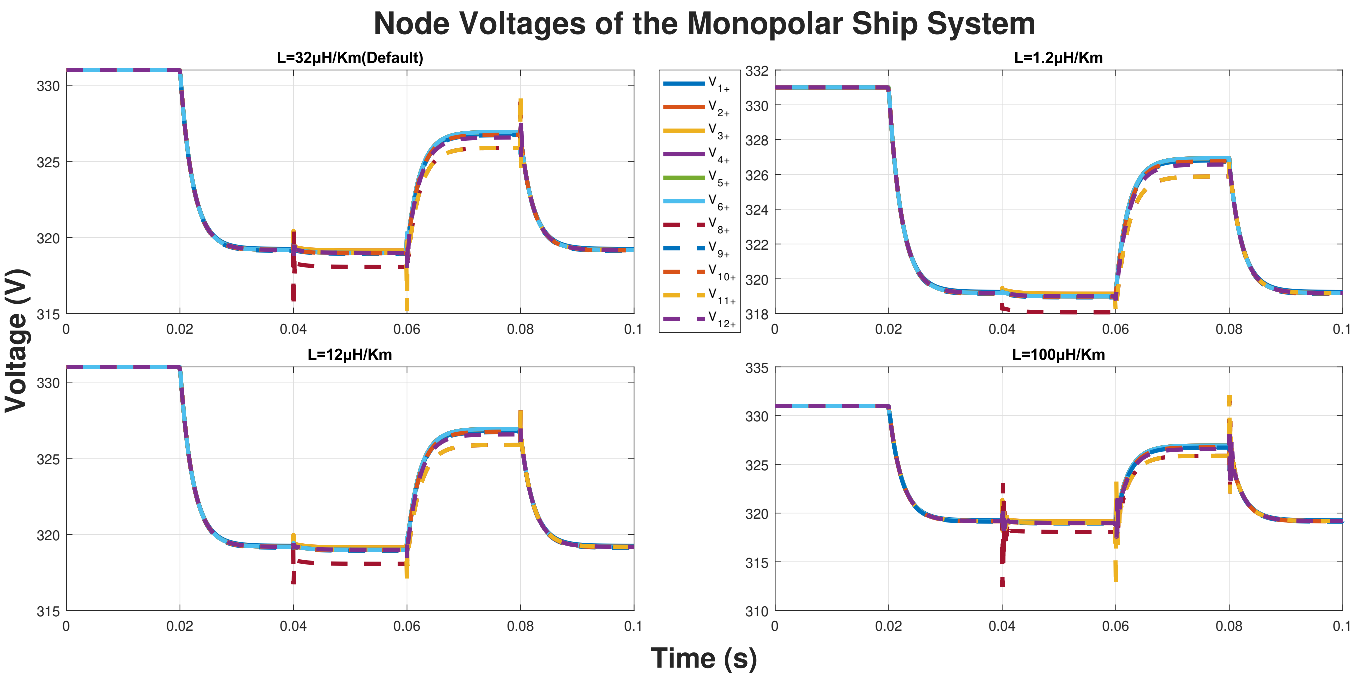

Figure B.7: Influence of cable inductance variation in the Node voltage plots of ship system

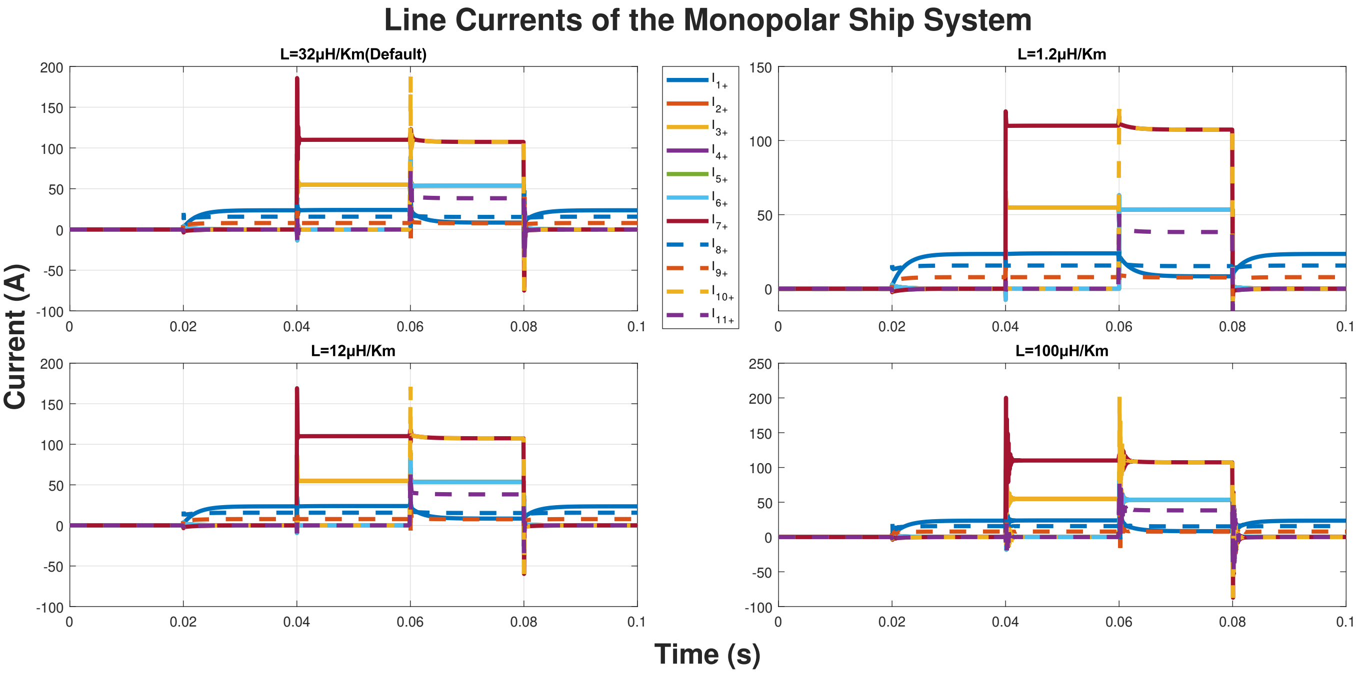

Figure B.8: Influence of cable inductance variation in the Line current plots of ship system

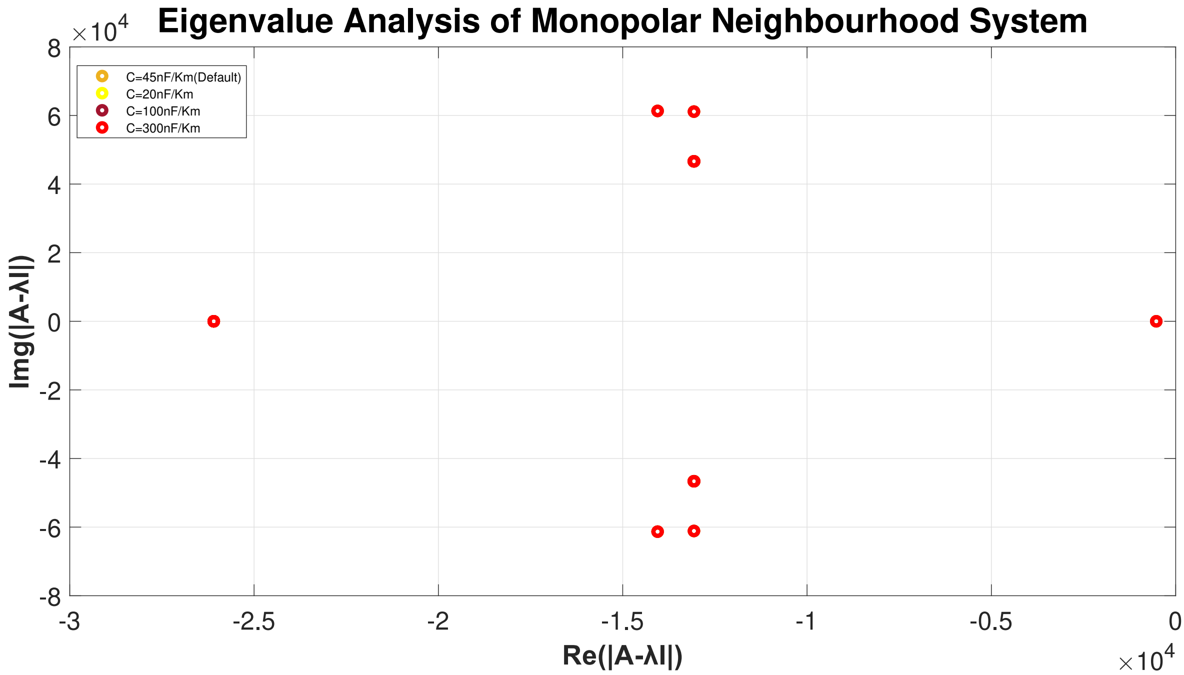

Figure B.9: Influence of cable capacitance variation in the eigenvalue plots of neighbourhood system

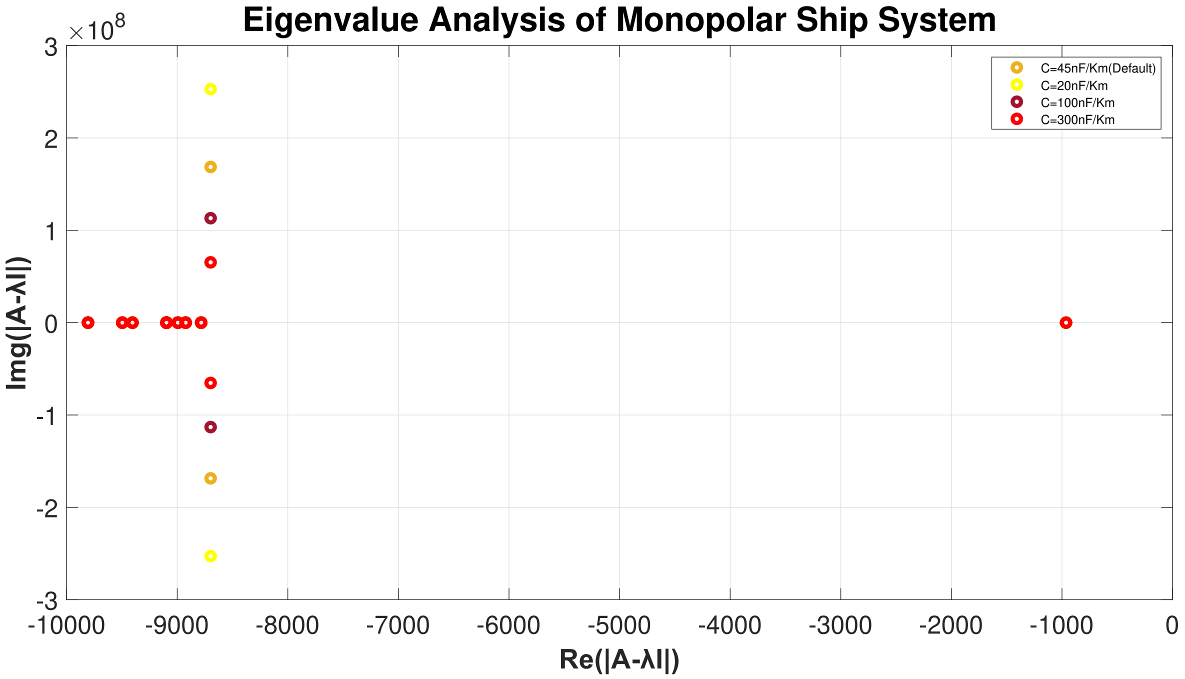

Figure B.10: Influence of cable capacitance variation in the eigenvalue plots of ship system

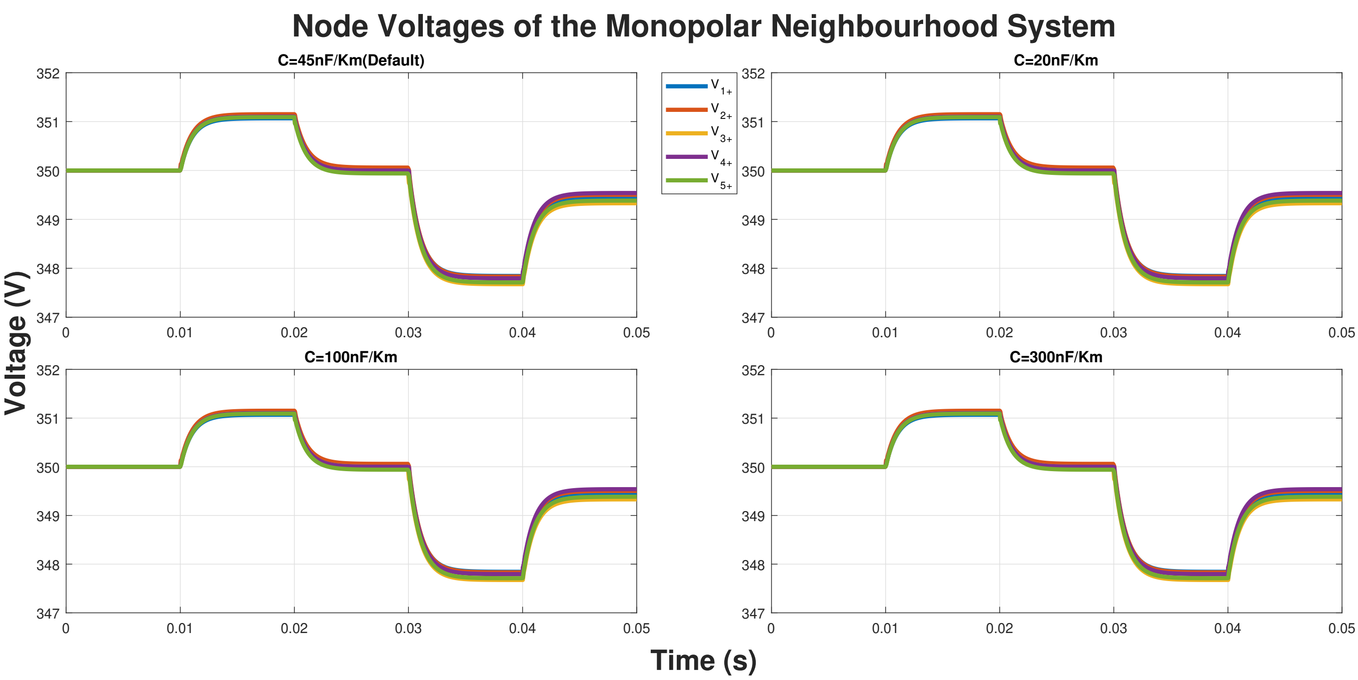

Figure B.11: Influence of cable capacitance variation in the node voltage plots of neighbourhood system

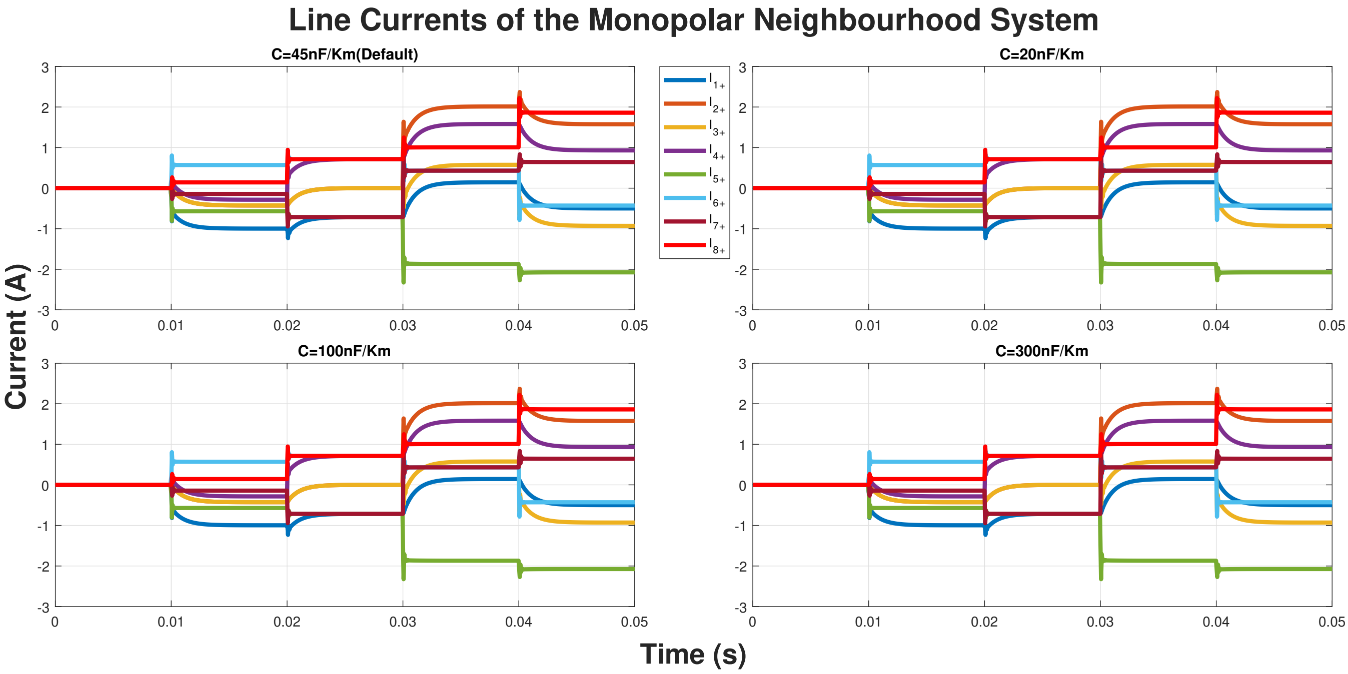

Figure B.12: Influence of cable capacitance variation in the line current plots of neighbourhood system

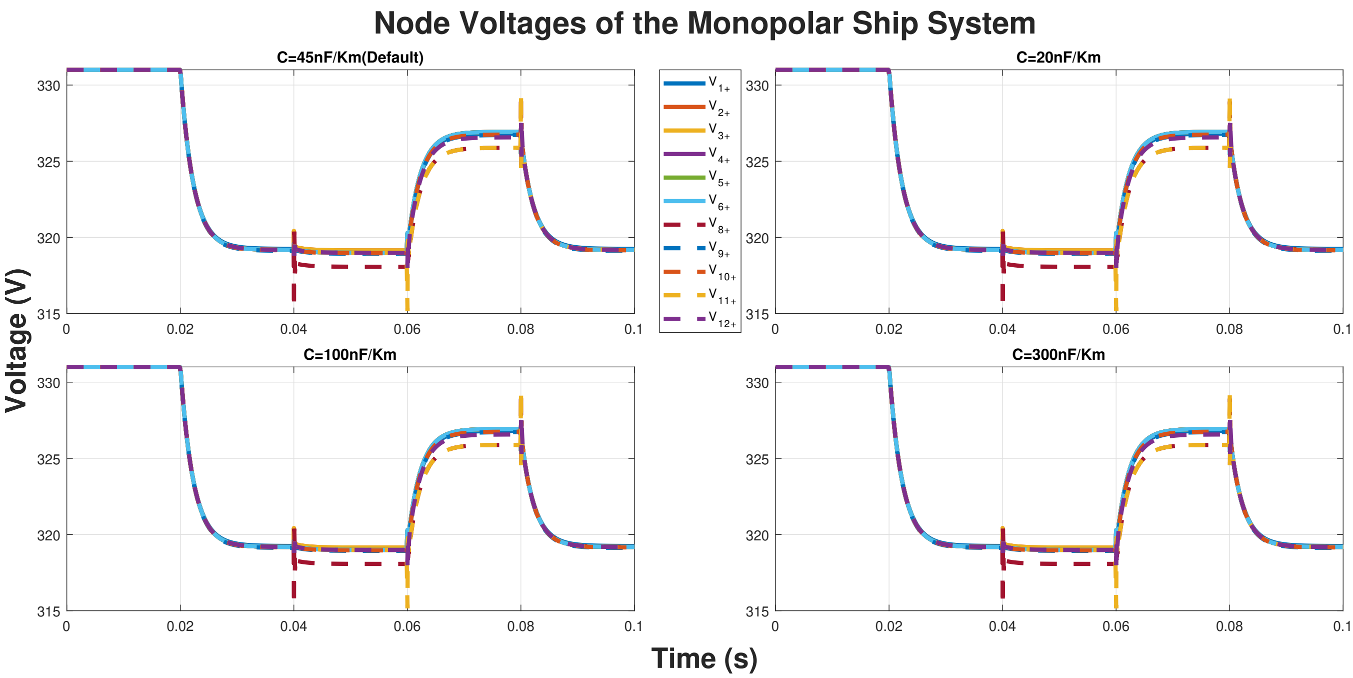

Figure B.13: Influence of cable capacitance variation in the node voltage plots of ship system

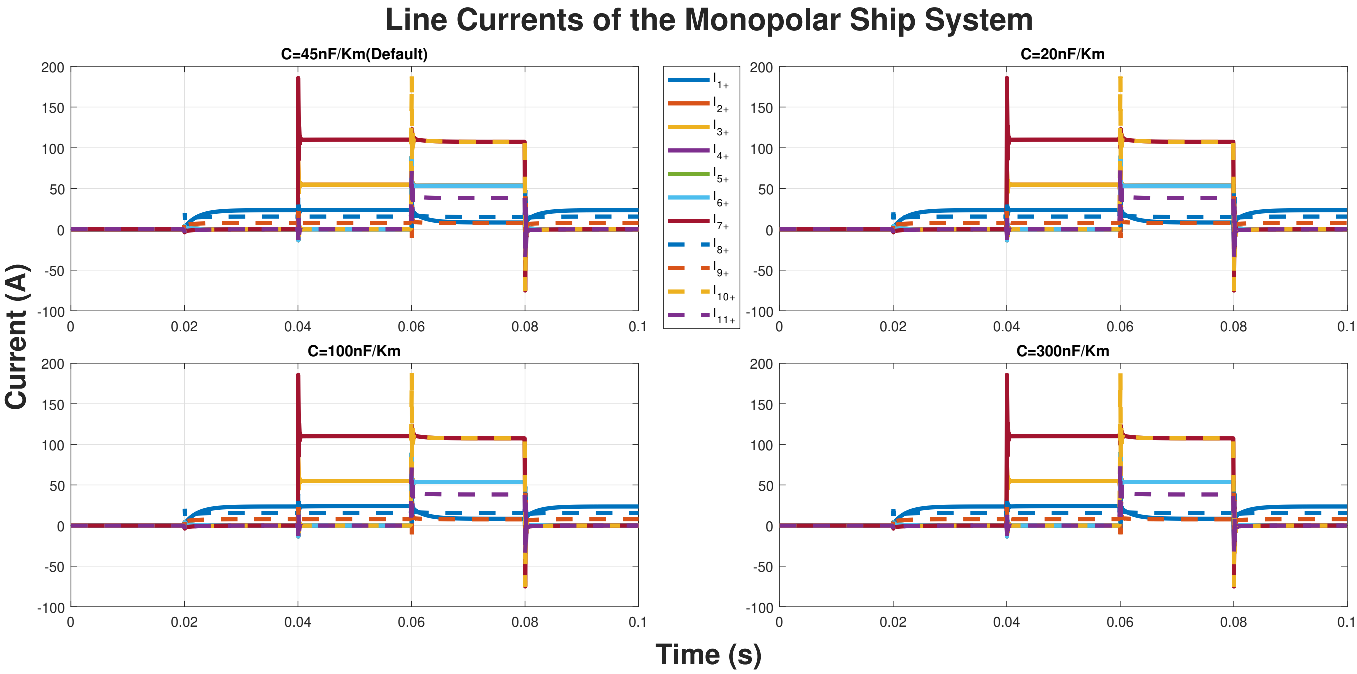

Figure B.14: Influence of cable capacitance variation in the line current plots of ship system

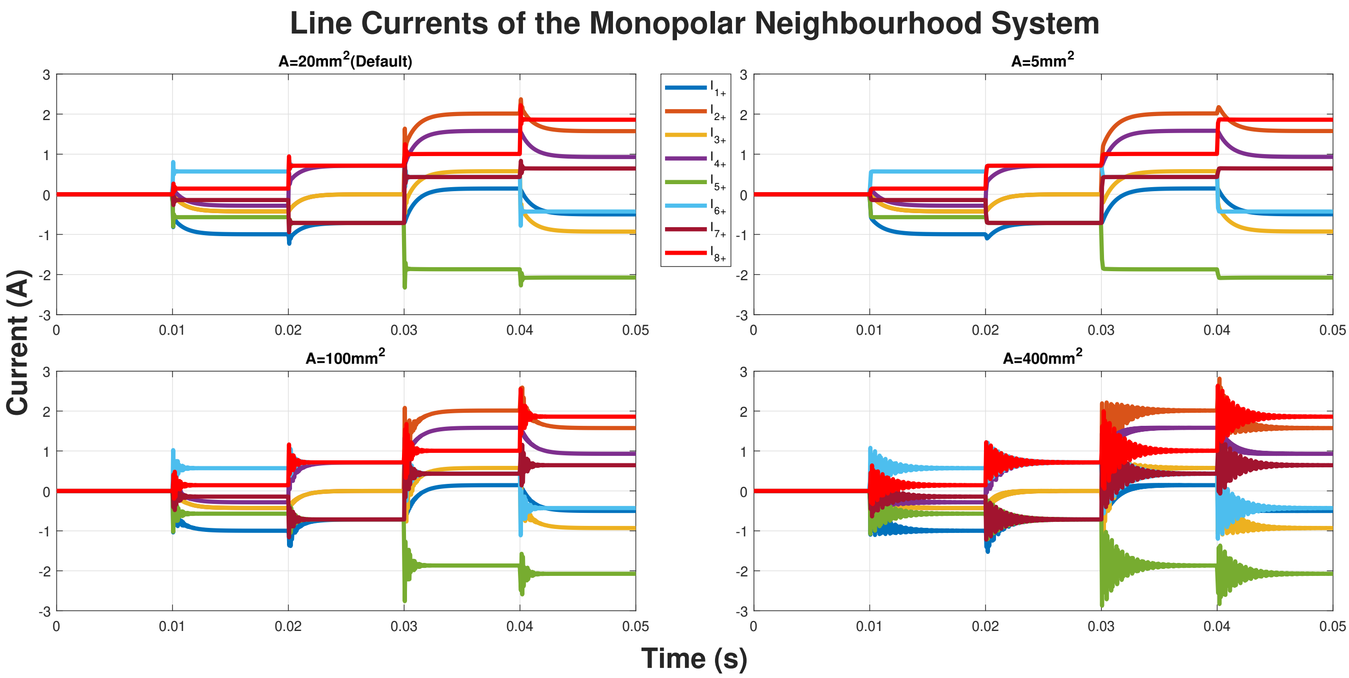

Figure B.15: Influence of cable cross section variation in the line current plots of neighbourhood system

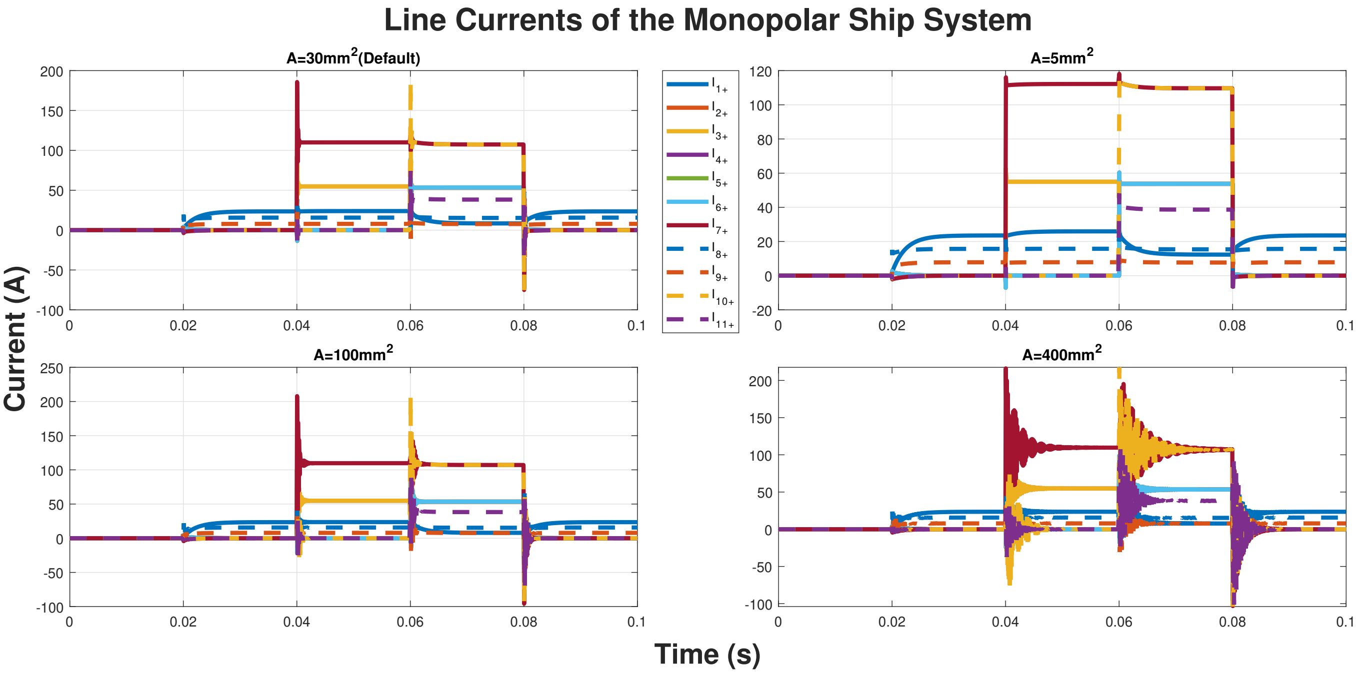

Figure B.16: Influence of cable cross section variation in the line current plots of ship system

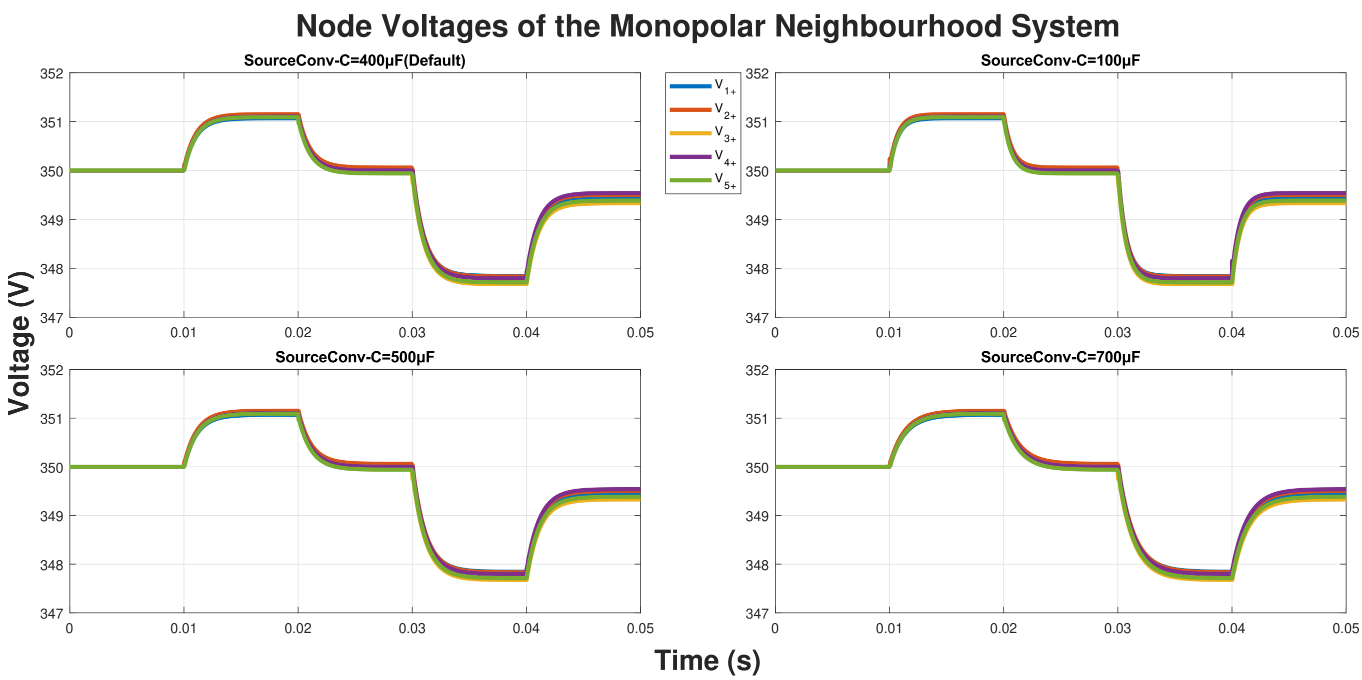

Figure B.17: Influence of source converter capacitance variation in the node voltage plots of neighbourhood system

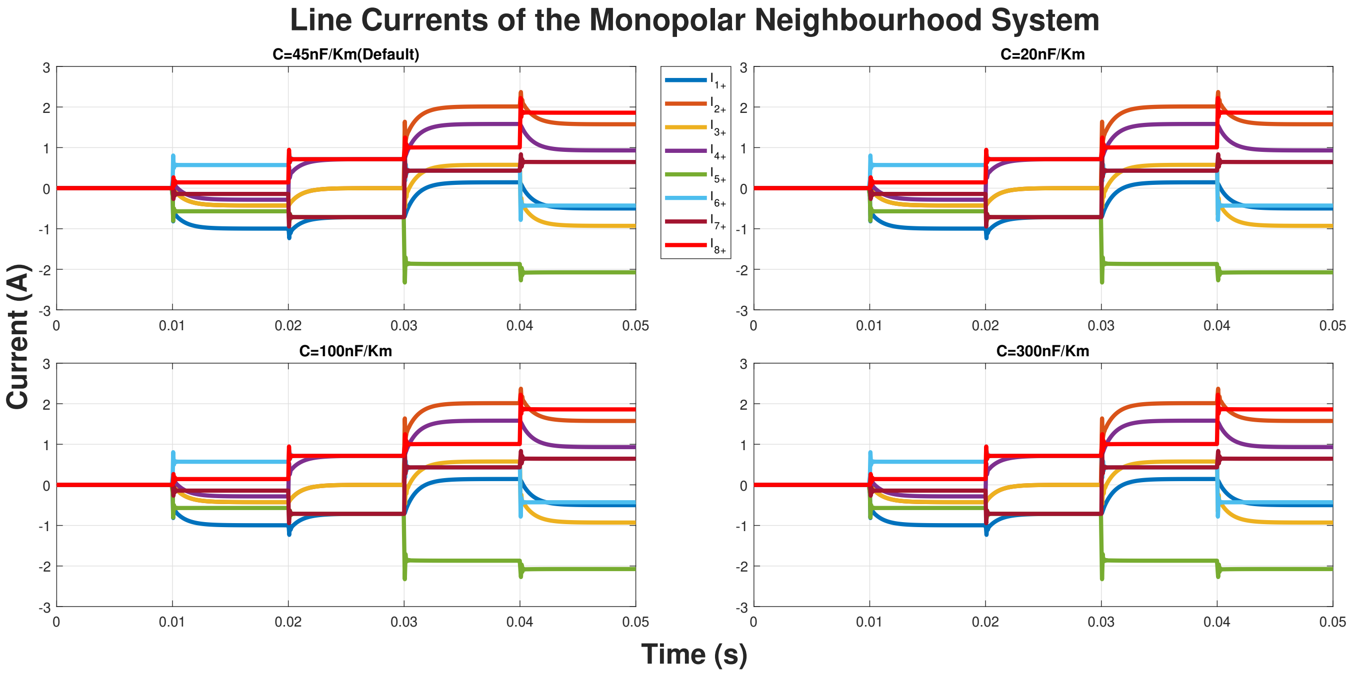

Figure B.18: Influence of source converter capacitance variation in the line currents plots of neighbourhood system

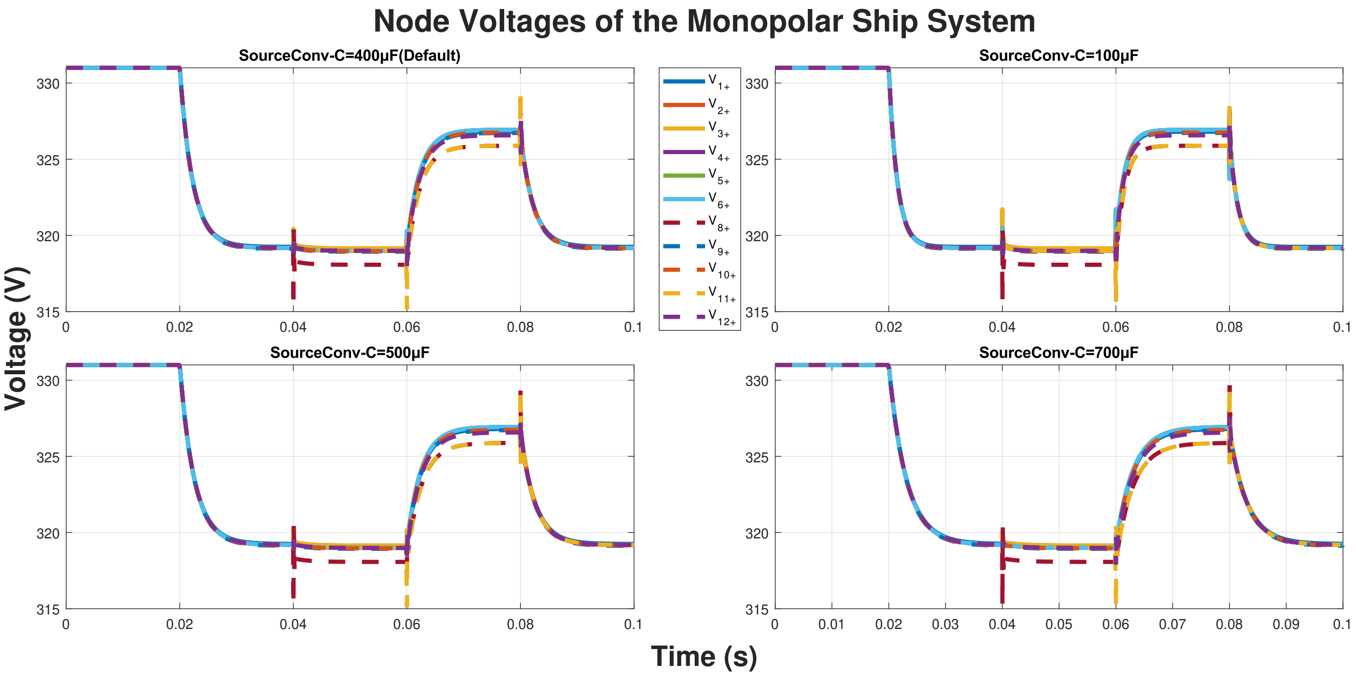

Figure B.19: Influence of source converter capacitance variation in the node voltage plots of ship system

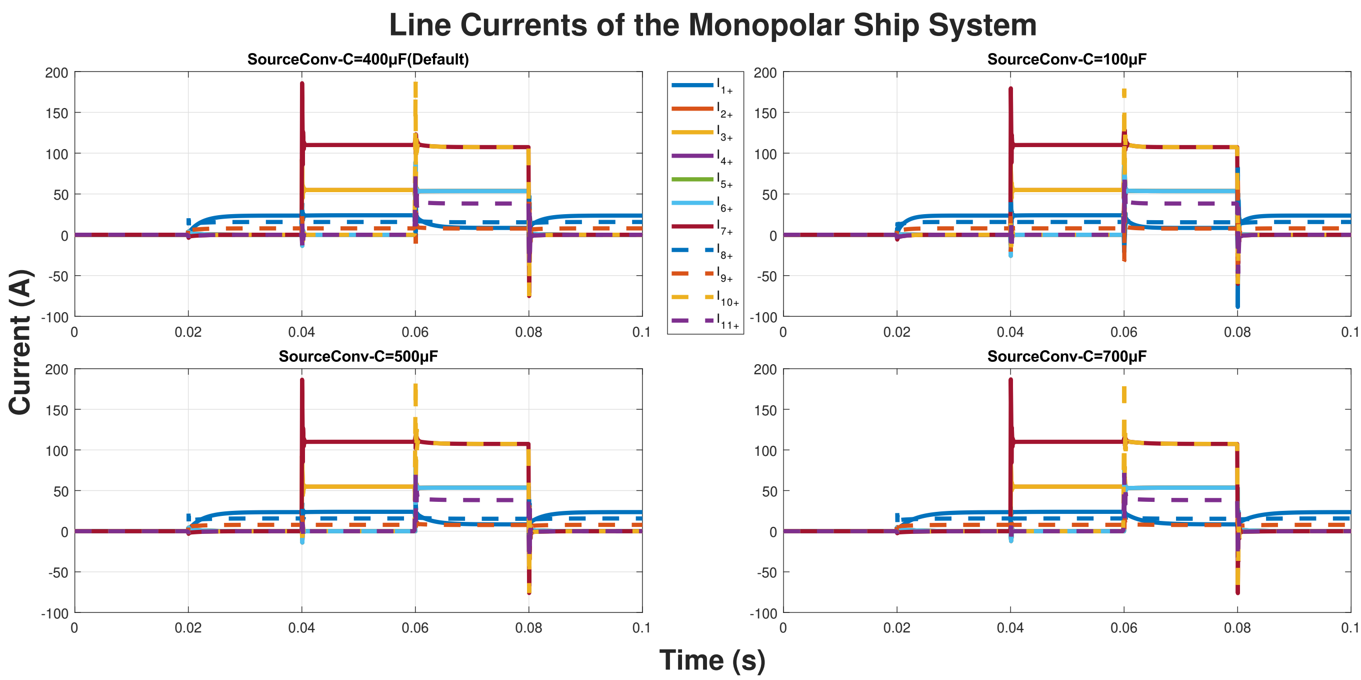

Figure B.20: Influence of source converter capacitance variation in the line currents plots of ship system

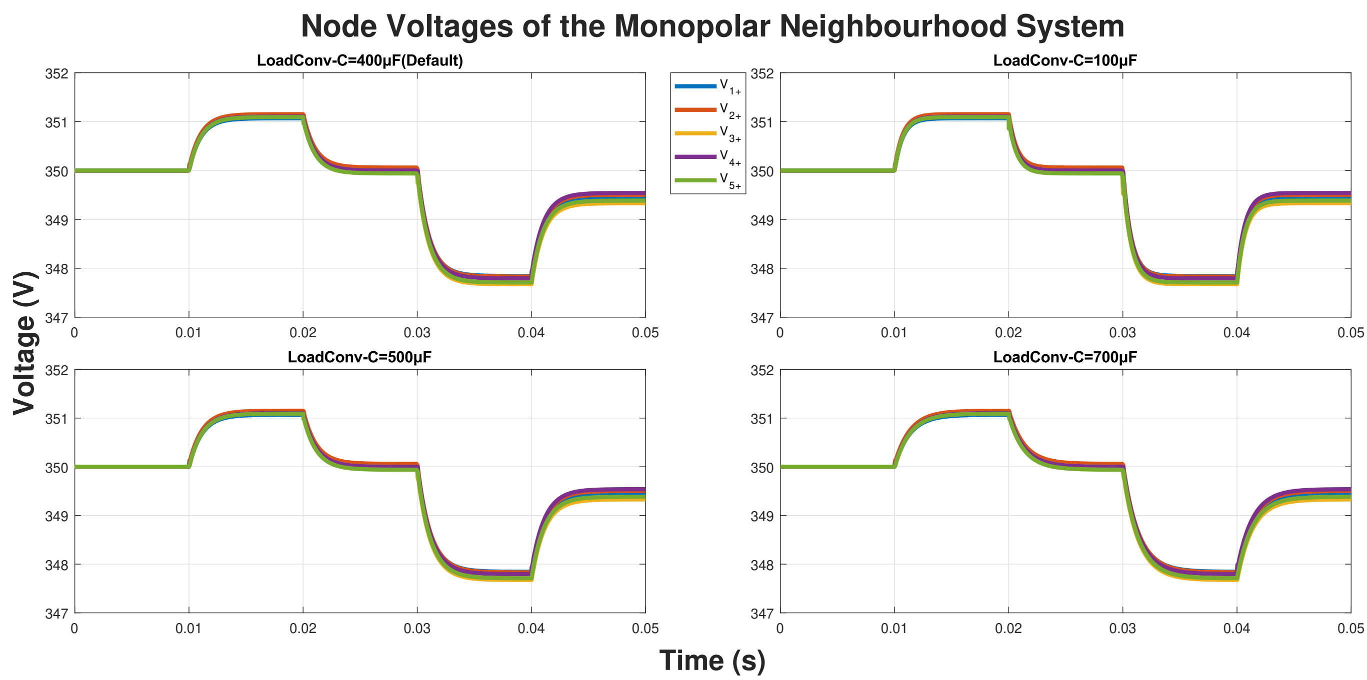

Figure B.21: Influence of load converter capacitance variation in the node voltage plots of neighbourhood system

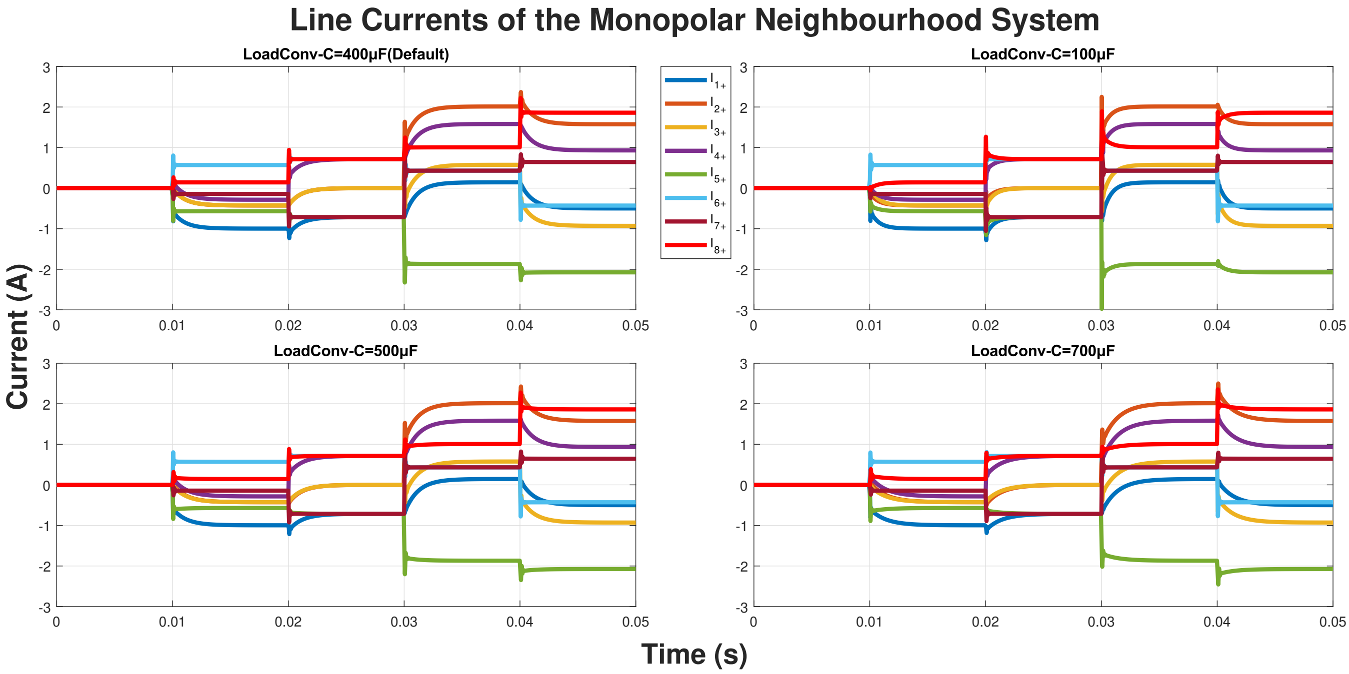

Figure B.22: Influence of load converter capacitance variation in the line current plots of neighbourhood system

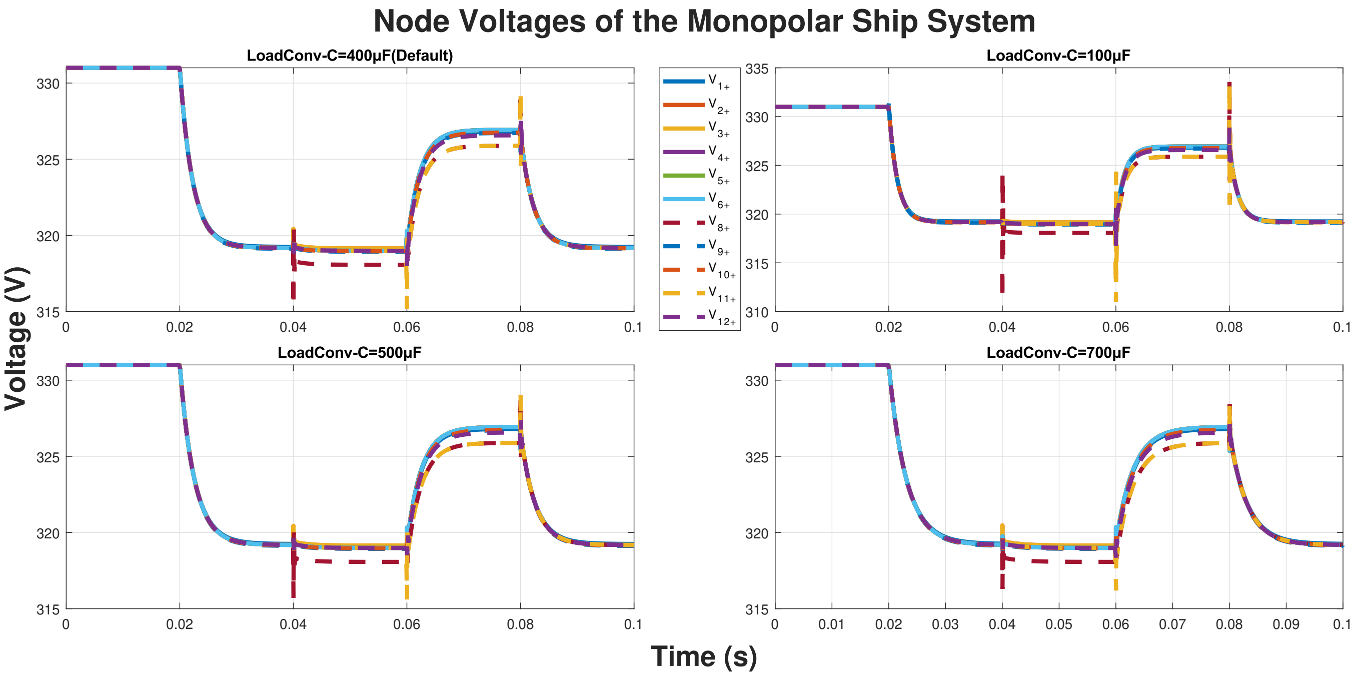

Figure B.23: Influence of load converter capacitance variation in the node voltage plots of ship system

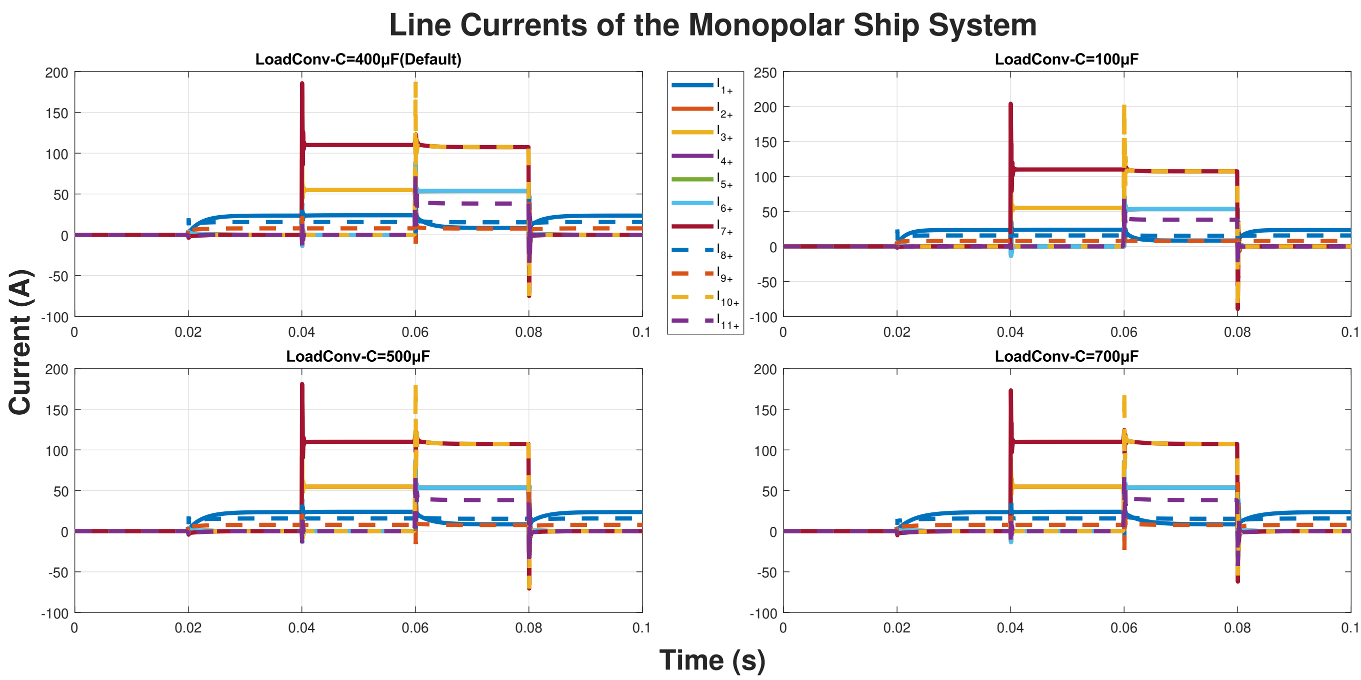

Figure B.24: Influence of load converter capacitance variation in the line current plots of ship system

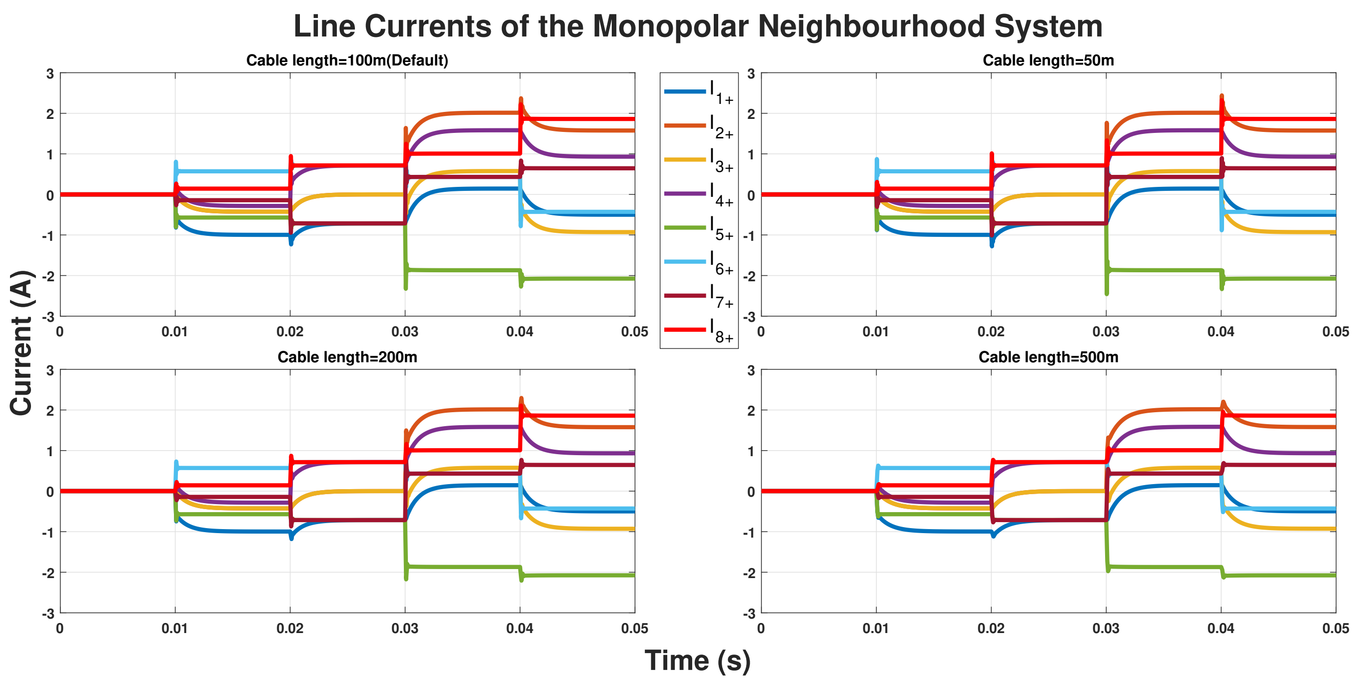

Figure B.25: Influence of cable length variation in the line current plots of neighbourhood system

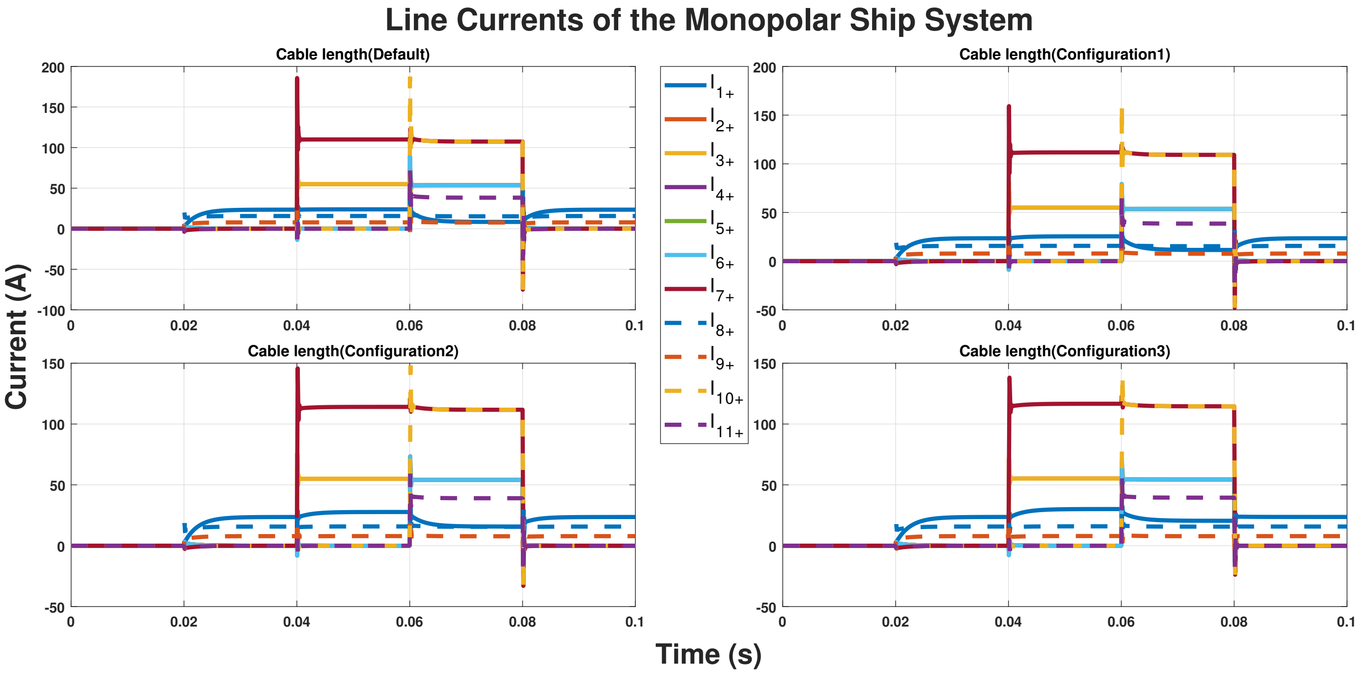

Figure B.26: Influence of cable length variation in the line current plots of ship system

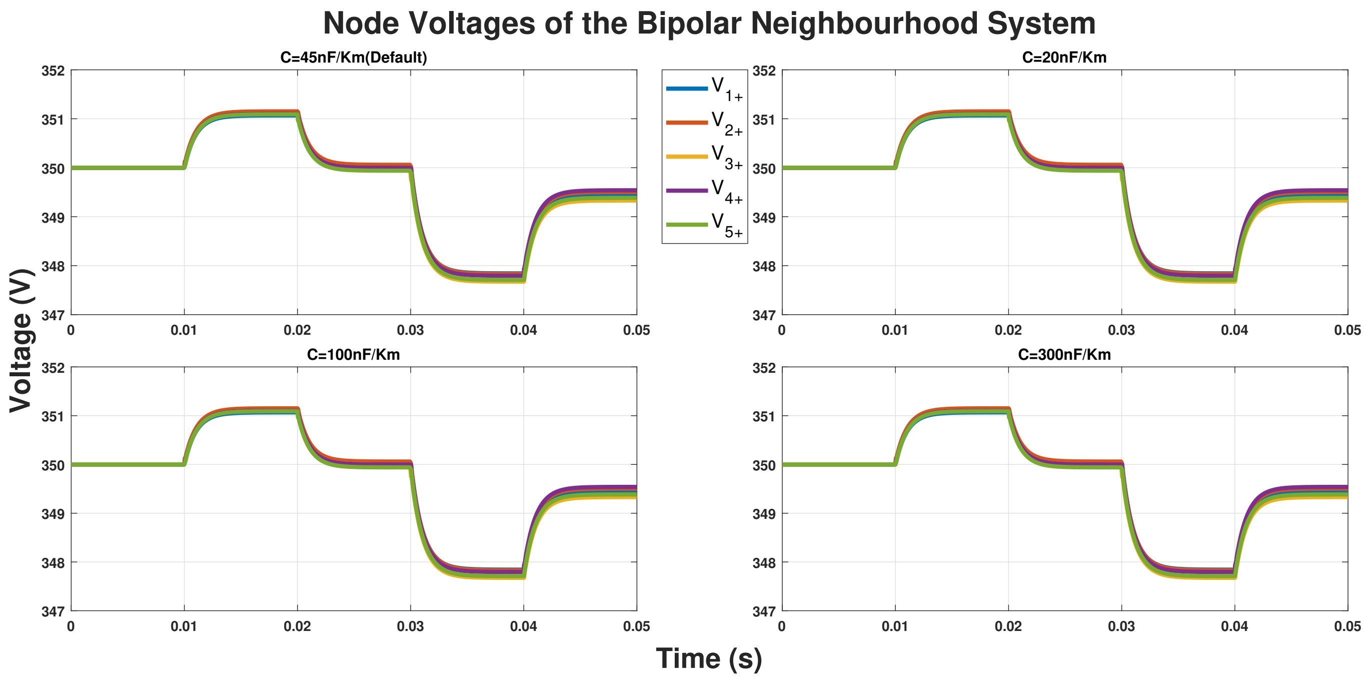

Figure B.27: Influence of cable capacitance variation in the node voltage plots of Bipolar neighbourhood system

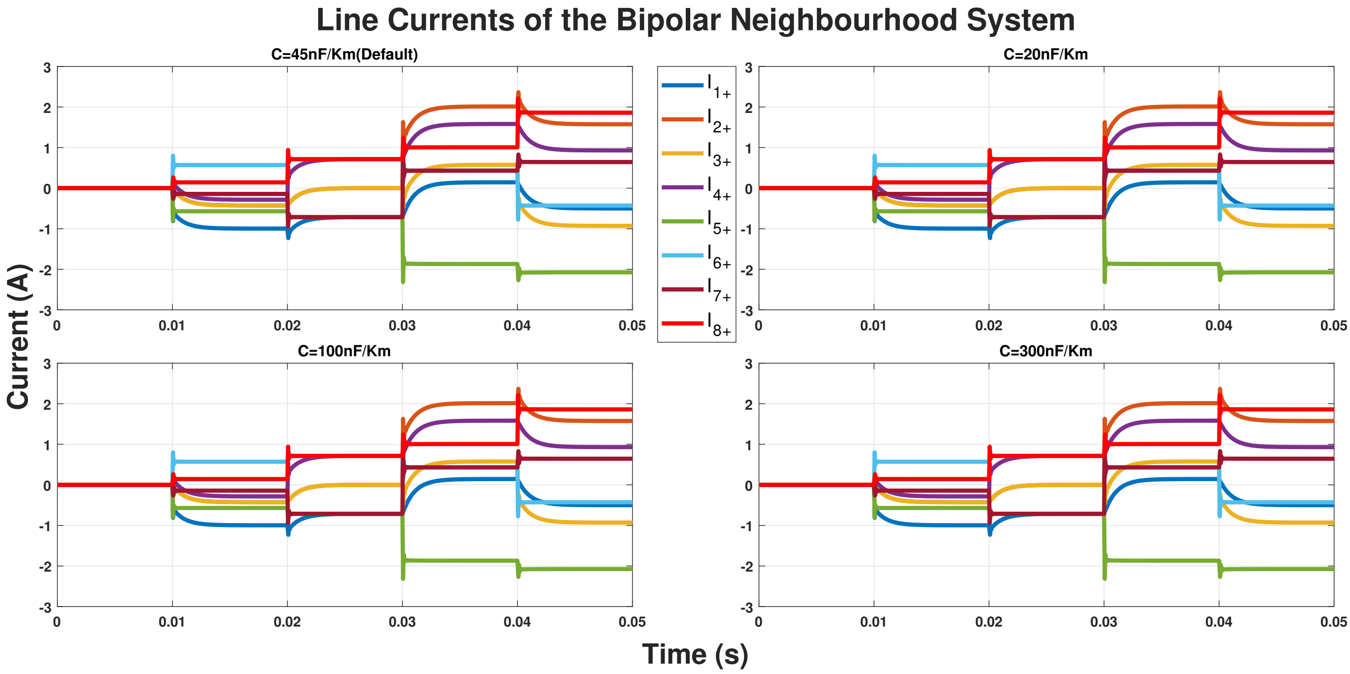

Figure B.28: Influence of cable capacitance variation in the line current plots of Bipolar neighbourhood system

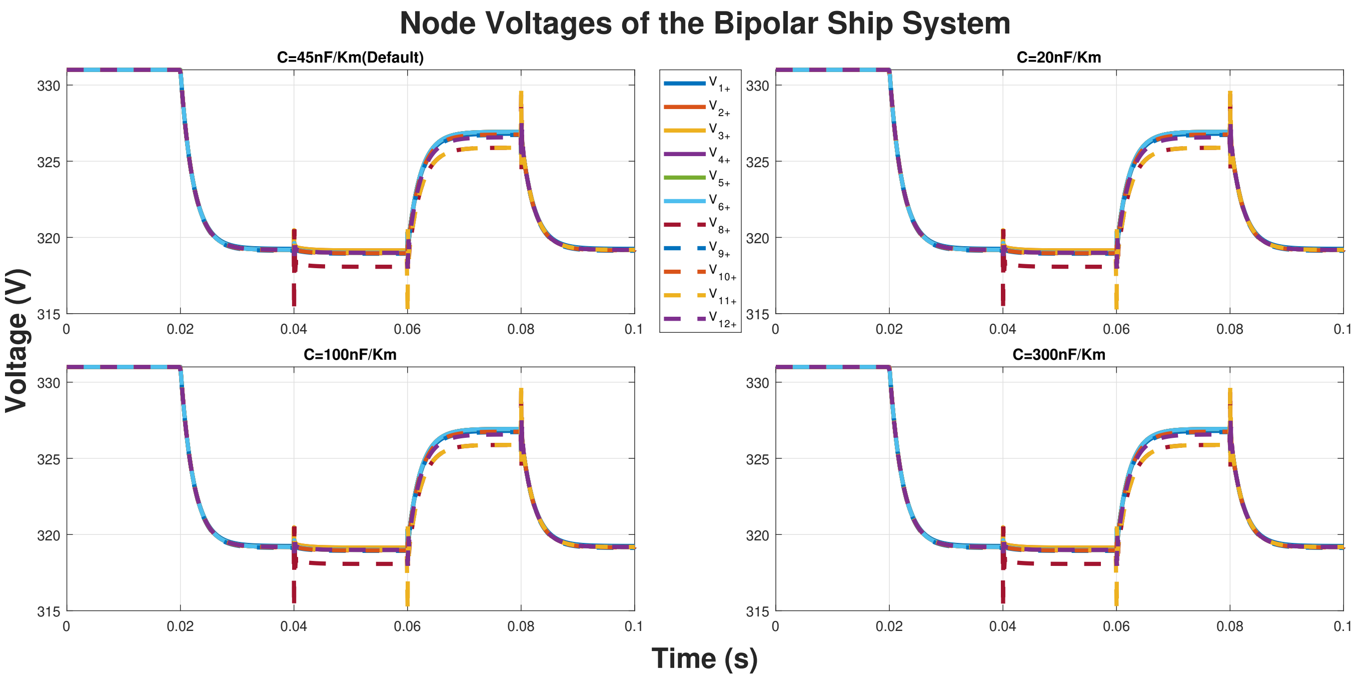

Figure B.29: Influence of cable capacitance variation in the node voltage plots of Bipolar ship system

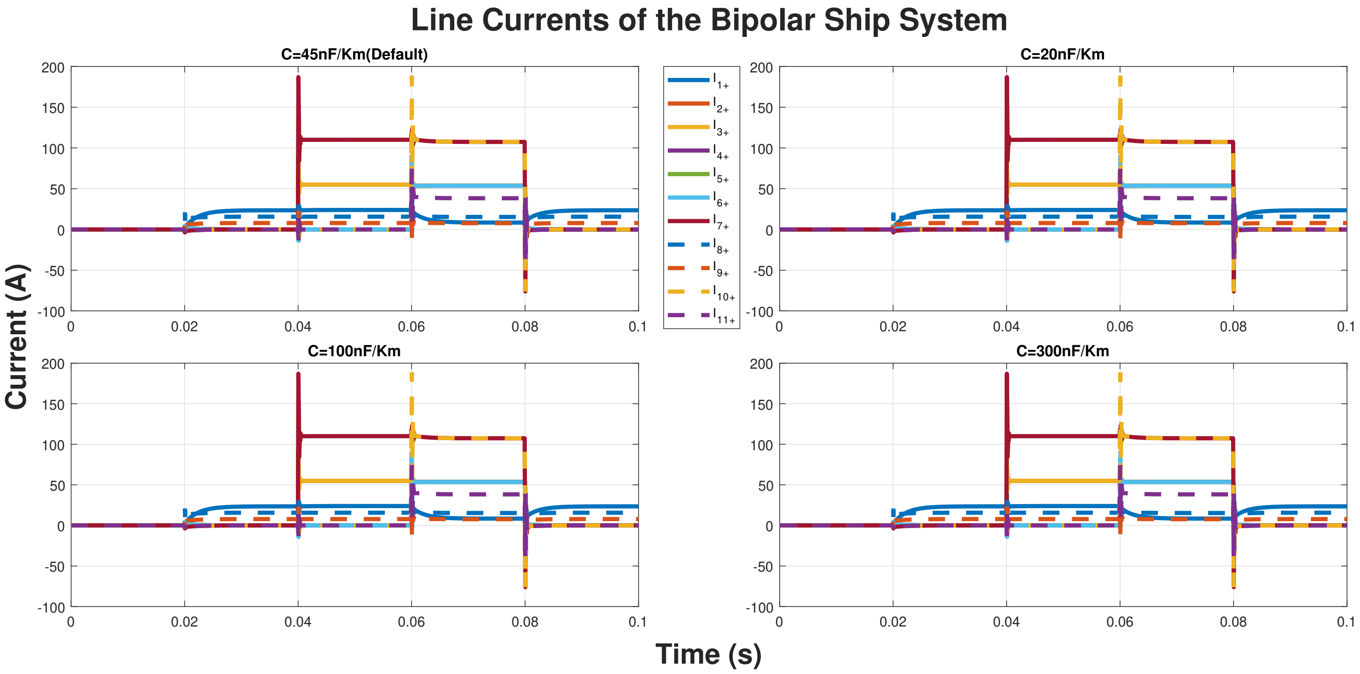

Figure B.30: Influence of cable capacitance variation in the line current plots of Bipolar ship system

B.1. Short circuit analysis

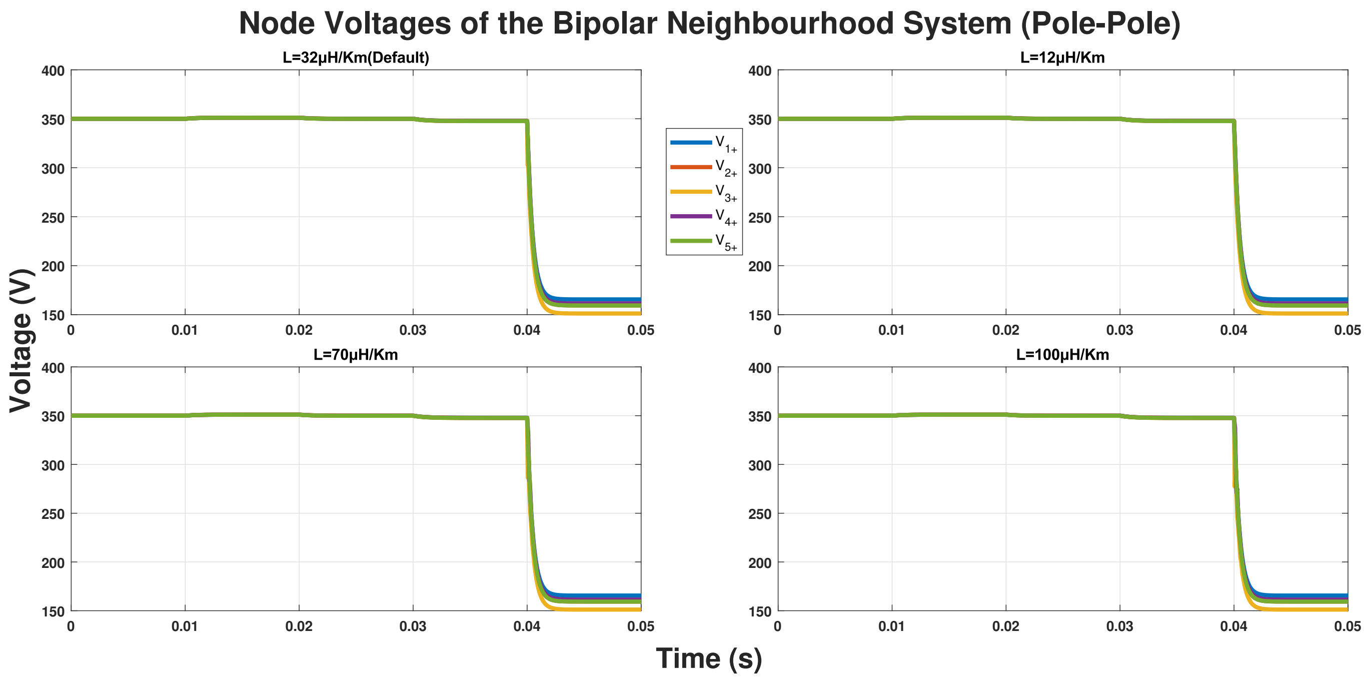

Figure B.31: Influence of cable inductance variation in the pole to pole fault node voltage plots of neighbourhood system

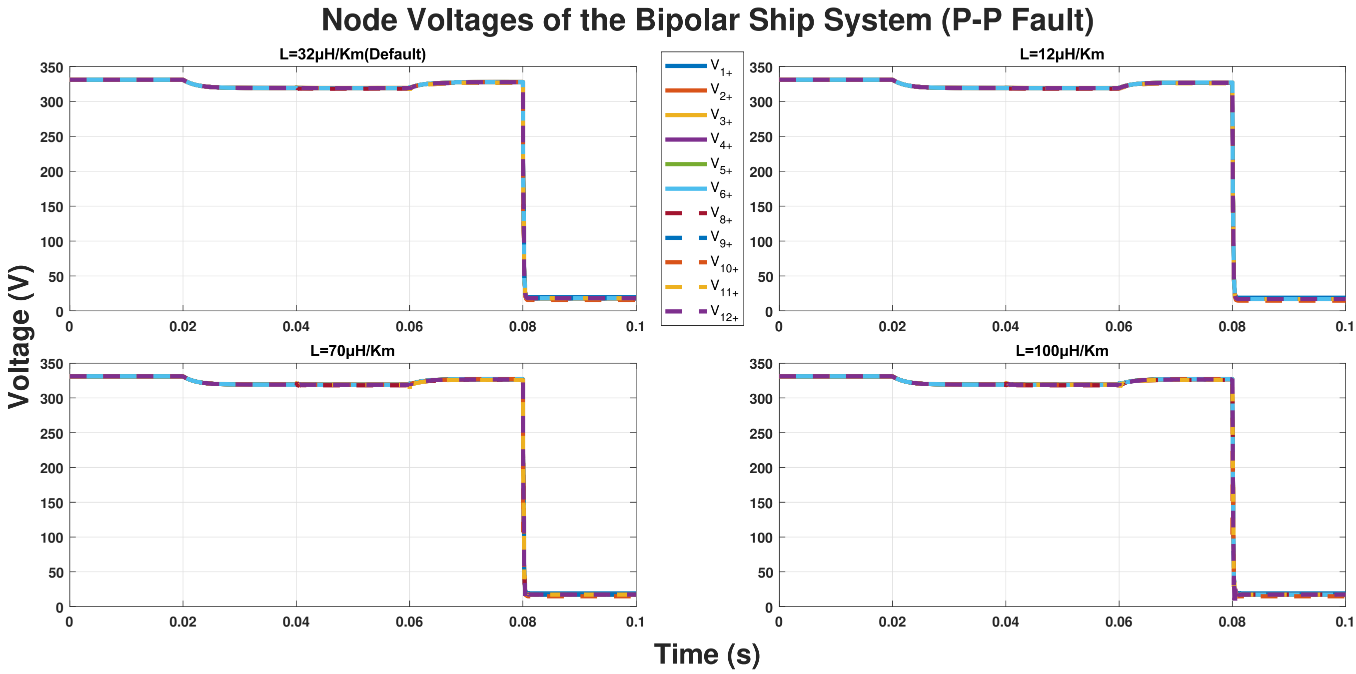

Figure B.32: Influence of cable inductance variation in the pole to pole fault node voltage plots of ship system

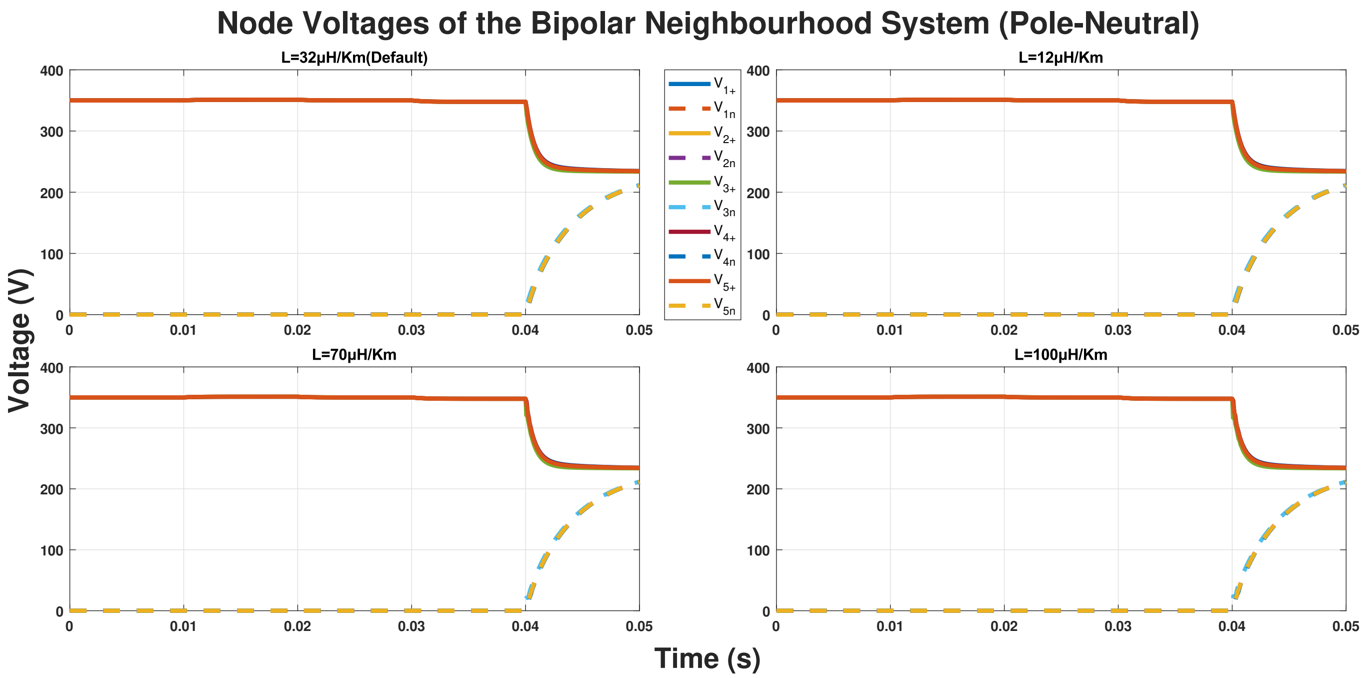

Figure B.33: Influence of cable inductance variation in the pole to neutral fault node voltage plots of neighbourhood system

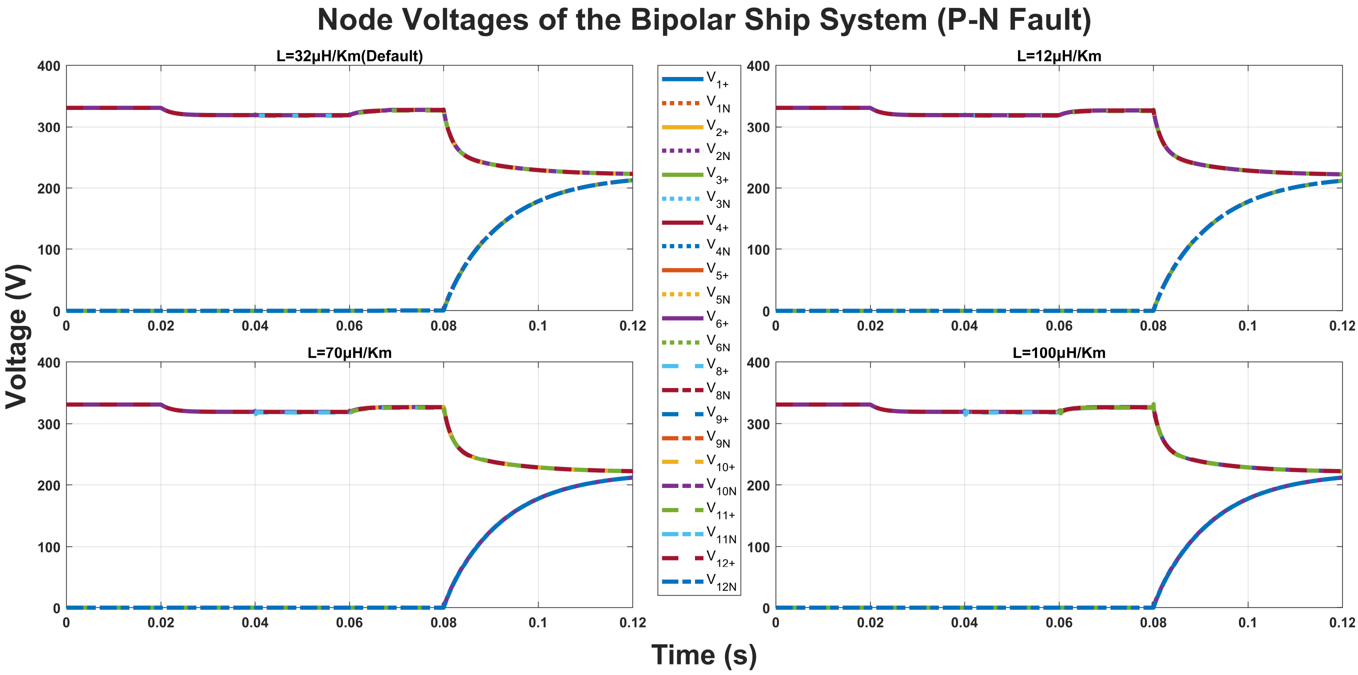

Figure B.34: Influence of cable inductance variation in the pole to neutral fault node voltage plots of ship system

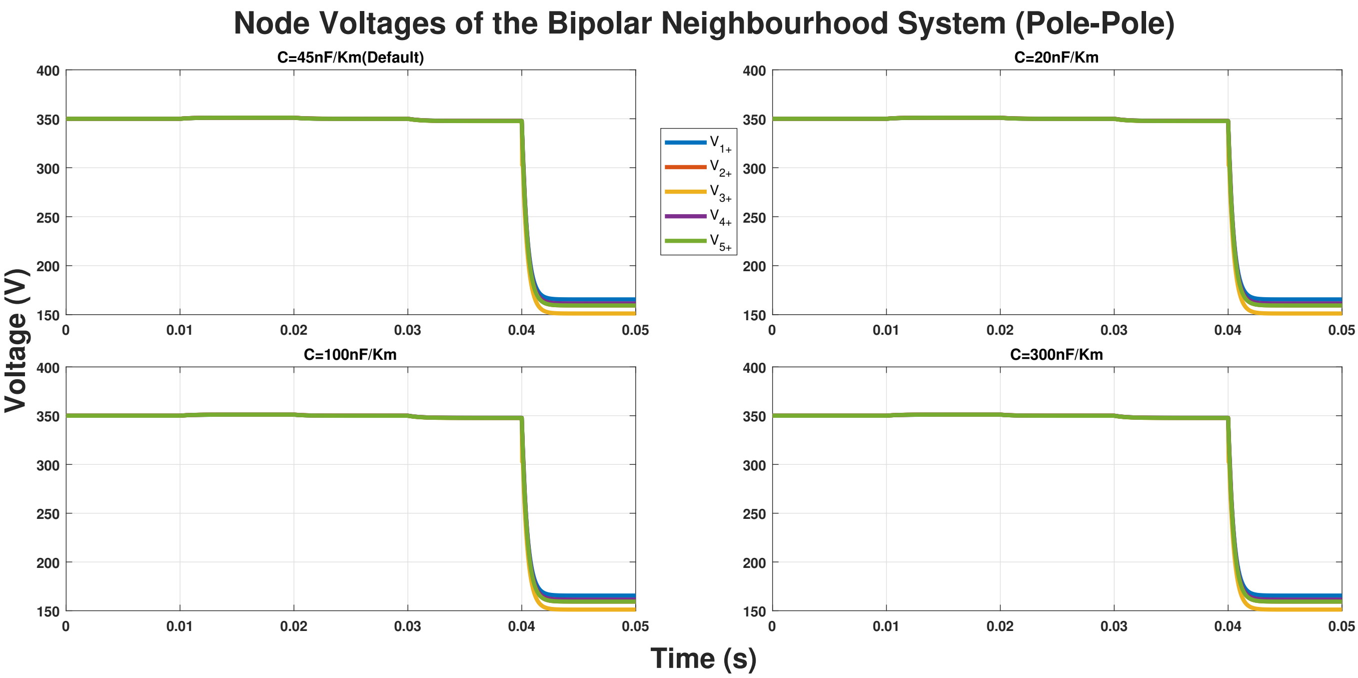

Figure B.35: Influence of cable capacitance variation in the pole to pole fault node voltage plots of neighbourhood system

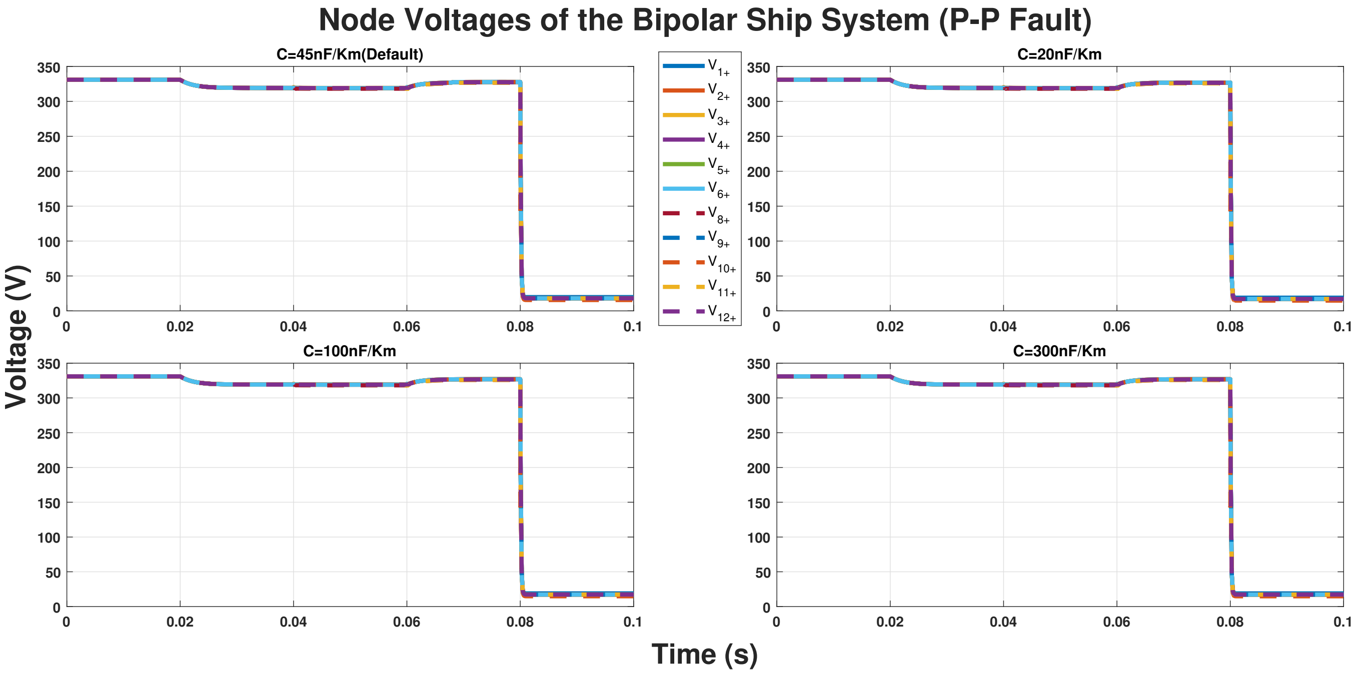

Figure B.36: Influence of cable capacitance variation in the pole to pole fault node voltage plots of ship system

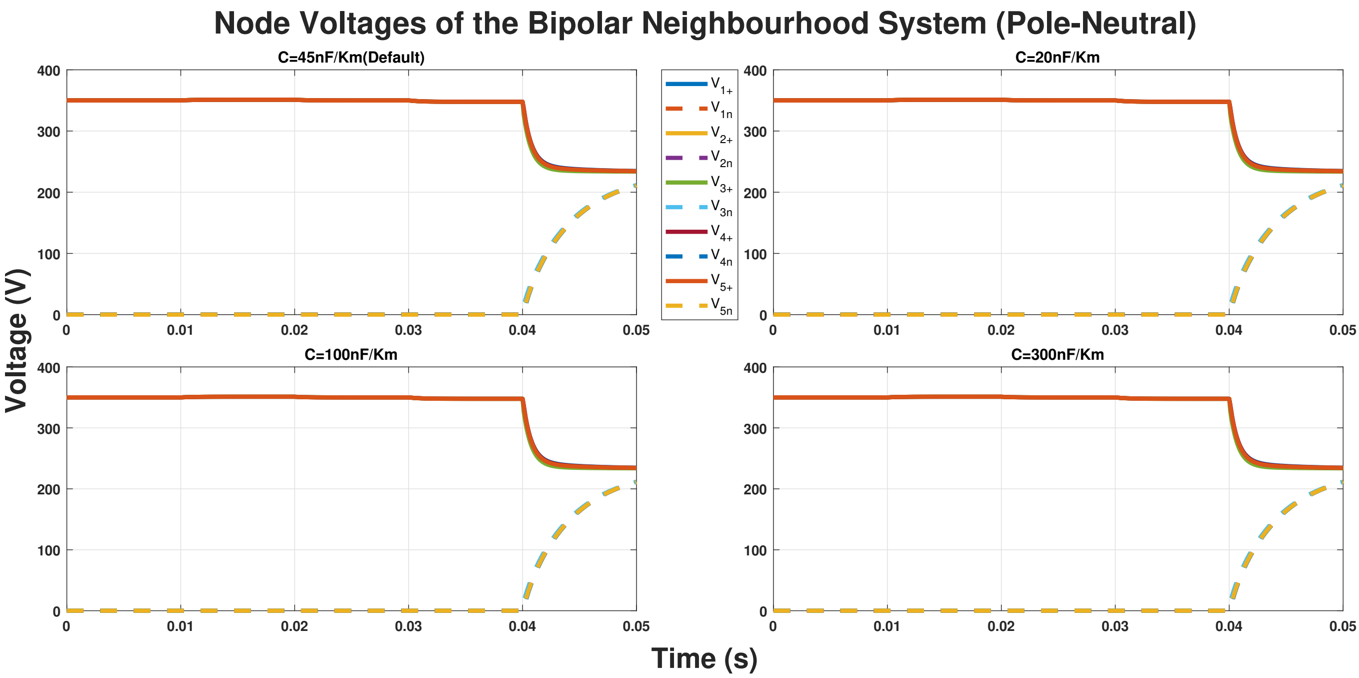

Figure B.37: Influence of cable capacitance variation in the pole to neutral fault node voltage plots of neighbourhood system

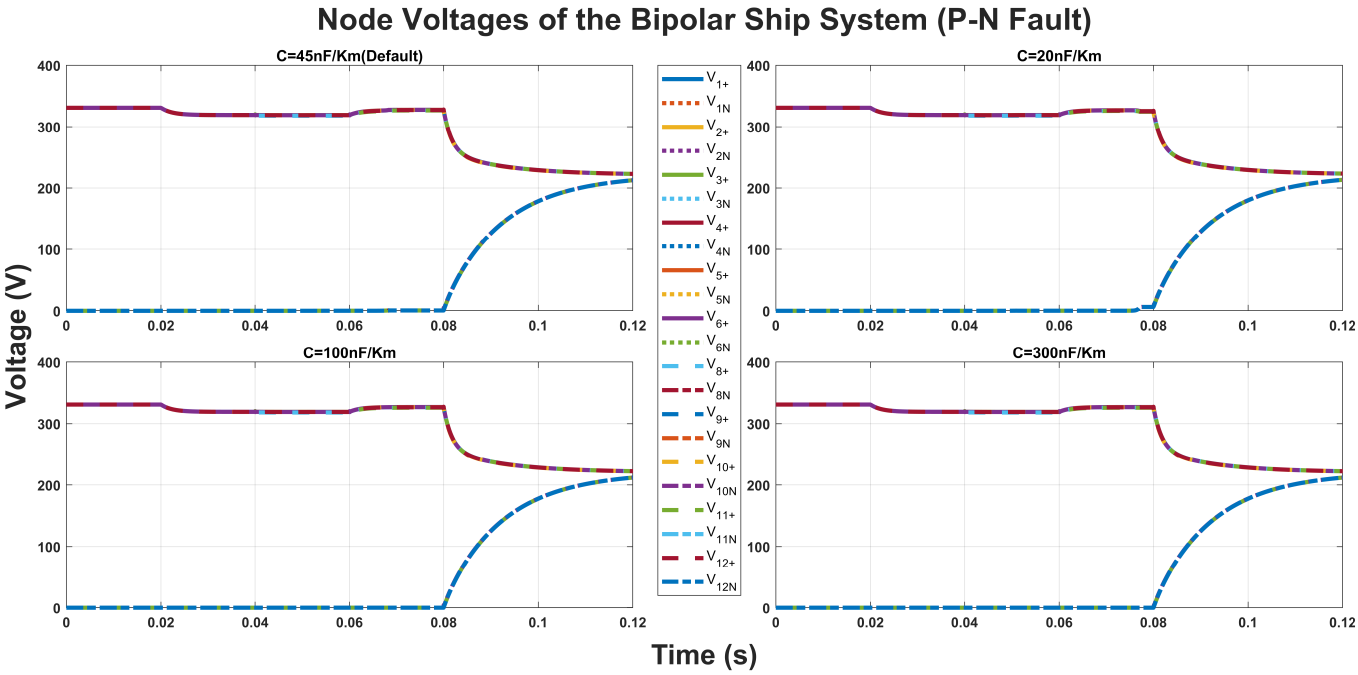

Figure B.38: Influence of cable capacitance variation in the pole to neutral fault node voltage plots of ship system